ResearchOnline@JCU

This file is part of the following reference:

Mumtaz, Saira (2017) *Photochemical synthesis in batch and micro flow reactors*. **PhD thesis, James Cook University.**

Access to this file is available from:

http://researchonline.jcu.edu.au/51976/

JAMES COOK UNIVERSITY
AUSTRALIA

Photochemical Synthesis in Batch and Micro Flow Reactors

PhD Thesis

Saira Mumtaz (M.Phil.)

April 2017

College of Science and Engineering

James Cook University

Supervisor:

Associate Professor Michael Oelgemöller

Dedicated to my Teachers

Abstract

This thesis aimed to discover new photochemical transformations and to develop novel flow chemical processes for photochemical reactions.

Despite being isoelectronic to the highly photoactive phthalimides, isatin derivatives remained unreactive and did not yield any *inter-* or *intramolecular* photoaddition products. The photochemical studies involving benzoylbenzamides resulted in the discovery of new transformations based on Norrish type II or photoinduced electron transfer processes. Visible light mediated photoredox decarboxylation reactions of *N*-phenylglycines with enones were successfully carried out using ruthenium tris(bipyridyl) chloride as a photocatalyst. The developed procedure proceeded efficiently under batch as well as flow conditions and yielded both, open and ring addition products.

The previously established photodecarboxylative addition of carboxylates to *N*-alkylphthal-imides was used as a key step in the synthesis of biologically active compounds such as **AL12**, **AL5** and their analogues. The initially formed photoproducts were readily converted by acid catalyzed dehydration followed by amination. A library of compounds was successfully synthesized following this procedure. The photodecarboxylative addition also served as a key step for aristolactam synthesis. The synthesis route combined photodecarboxylative addition, dehydration and photodehydrohalogenation, with the option of further thermal amination. This 3-4 step methodology was successfully applied to the syntheses of parent aristolactams.

The multistep synthesis of bioactive **AL12** and its analogues could be successfully realized *in-series* under flow conditions. Compared to the stepwise batch protocols, the *in-series* operation prevented time- and resource-demanding isolation steps and gave the final product in high purity and improved yield. Likewise, the cardiovascular active **AKS186** has been synthesized using an advanced, commercially available flow reactor. Following a tandem photochemical-thermal process, the desired **AKS186** product was obtained in in high purity and in good yield, far exceeding the batch process. Selected examples of photodecarboxylative additions of phenyl acetates to phthalimide derivatives were furthermore realized in a concentrated solar trough flow reactor. The simple reactor achieved a threefold concentration of sunlight. Comparison reactions in batch and in direct sunlight failed to initiate any photoreactions even after prolonged exposure.

The monobromination of acetophenone was investigated by request of Takeda pharmaceuticals. The poor solubility of *N*-bromosuccinimide was found to be challenging for flow operations. The best reaction conditions gave moderate conversions in reasonable residence times and in diethyether as a solvent.

The Mallory reaction was investigated in supercritical carbon dioxide during a research stay at NAIST in Japan. While supercritical carbon dioxide is generally not an efficient medium for oxidative reactions, the photoisomerization-oxidative electrocyclization cascade furnished higher yields under microflow $scCO_2$ than under batch conditions.

Declaration

I hereby certify that this material, which I now submit for assessment on the program of study leading to the award of Doctor of Philosophy is entirely my own work, that I have exercised reasonable care to ensure that the work is original, and does not to the best of my knowledge breach any law of copyright, and has not been taken from the work of others save and to the extent that such work has been cited and acknowledged within the text of my work.

Signed: ID No.:   12723742

Date: 14. 04. 2017

Acknowledgements

It is my privilege to present this thesis to you, which is by far the most substantial scientific contribution of my life and it would have been impossible without a pleasant and supportive surrounding, owing to a lot of people around me.

First of all, I would like to express my sincere gratitude to my amazing supervisor, Associate Professor Michael Oelgemöller, for providing me the opportunity and for assisting me in every step. This thesis would not be possible without his inspiring supervision, encouragement and continuous assistance. I am unable to express my thanks for his precious time and valuable suggestions, throughout the course of study. His meaningful and confident smile on every expected result and a critical review of previously published data on every unexpected finding was a prof of his scientific enthusiasm and professional commitment. His critical questioning during our discussions helped me in thinking more logically. Undoubtedly these discussions will benefit my future research as well. His academic conscientiousness and professional ethic has also set an example for my future research. Furthermore, his endless support during the course of writing my thesis is also unforgettable. It was a reasonably long journey which was literary pleasant, mainly because of a motivating, cheering and friendly supervisor.

I am also grateful to Professor Kiyomi Kakiuchi and Assistant Professor Yasuhiro Nishiyama for the support I received during my work and stay at NAIST, Japan. I am thankful to Dr. Cherie Motti (AIMS-biomolecular analysis facility) and Associate Professor Bruce Bowden for giving access and providing assistance in collecting Mass and NMR data. I also thank Professor Peter Junk and Dr. Jun Wang for the X-ray structure analyses.

I have been very fortunate to have a diverse, multicultural and friendly lab group with lovely fellows from around the globe. I am thankful to all of them for making my passage enjoyable and I wish them all the best in their future lives. I am especially thankful to Dr. Devagi Kanakaraju, Alkit Beqiraj and Frances Mükenheim for making things easier for me in my early days of lab.

Financial support from the Australian Research Council and from James Cook University is also gratefully acknowledged. Many thanks are also due to NAIST, Japan for internship grant.

Finally, I am grateful to my homeland, and homeland institutes, to HEC Pakistan for providing initial grant for the project through IRSIP, to Dr. Ashfaq Mahmood Qureshi for suggesting me to choose photochemistry and to my parents and all of my family members for their unconditional love and support during my study.

List of Abbreviations

^{13}C-NMR	carbon nuclear magnetic resonance
^{1}H-NMR	proton nuclear magnetic resonance
acetone-d$_6$	deuterated acetone
Ar	aryl
BET	back electron transfer
Bn	benzyl group
CDCl$_3$	deuterated chloroform
CO$_2$	carbon dioxide
DCM	dichloromethane
d	doublet
dd	doublet of a doublet
ddd	doublet of a doublet of a doublet
DMF	dimethylformamide
DMSO-d$_6$	deuterated dimethyl sulphoxide
eq.	equivalents
EnT	energy transfer
ET	electron transfer
Et	ethyl group
et al.	et alii (and others)
g	gram
H$_2$O	distilled water
H$_2$SO$_4$	sulphuric acid
H$_{arom.}$	aromatic proton
HCl	hydrochloric acid
H$_{olef.}$	olefinic proton
h or hr(s)	hour(s)
hυ	light photon
i-Bu or *i*-butyl	iso butyl group
i-Pr or *i*-propyl	iso propyl group
IUPAC	Internal Union of Pure and Applied Chemistry
J	coupling constant
K$_2$CO$_3$	potassium carbonate
m	multiplet

Me	methyl group
$MgSO_4$	magnesium sulphate
mL	milliliter(s)
mmol	millimole(s)
NaCl	sodium chloride
nm	nanometres
NMR	nuclear magnetic resonance
^oC	degree Celsius
PET	photoinduced electron transfer
Ph	phenyl group
ppm	parts per million
Pr	propyl group
R	rest group
s	singlet
s-Bu or *s*-butyl	secondary butyl group
t	triplet
t-Bu or *t*-butyl	tertiary butyl group
TFA	trifluoroacetic acid
TLC	thin layer chromatography
UV	ultraviolet
π	pi
σ	sigma

Publications

1. S. Josland, **S. Mumtaz**, M. Oelgemöller "Photodecarboxylations in an advanced meso-scale continuous flow photoreactor" *Chem. Eng. Technol.* **2016**, *39*, 81-87.

2. **S. Mumtaz**, C. Sattler, M. Oelgemöller "Solar photochemical manufacturing of fine chemicals: historical background, modern solar technologies, recent applications and future challenges" In: Chemical Processes for a Sustainable Future. T. M. Letcher, J. L. Scott, D. A. Patterson, A. Darrell (eds.), Royal Society of Chemistry: Cambridge, UK, **2015**, pp. 158-191.

3. **S. Mumtaz**, M. Oelgemöller "Bromination of acetophenone in batch and flow" *Report for Takeda Pharmaceutical Co. Ltd*, Osaka (Japan), **2015**.

4. M. Oelgemöller, M. Bolte, T. Goodine, **S. Mumtaz**, P. Malakar, A. Dunkerton, R. Hunter "TropEco Research Award 2014 – The Eradicate Insect-borne Diseases with Sunlight Initiative at JCU" *Sustainability@JCU Newletters* **2014**, *November*.

5. M. Oelgemöller, M. Bolte, T. Goodine, **S. Mumtaz**, P. Malakar, A. Dunkerton, R. Hunter "TropEco Research Award 2014 – The Eradicate Insect-borne Diseases with Sunlight Initiative at JCU" *AITHM Newslett.* **2015**, *April*, 12.

6. M. Oelgemöller, M. Bolte, T. Goodine, **S. Mumtaz**, P. Malakar, A. Dunkerton, R. Hunter "The Eradicate Insect-borne Diseases with Sunlight Initiative at James Cook University in Australia" *EPA Newslett.* **2015**, *88*, 85-90.

Presentations

1. **Poster presentation** "Transforming Organic Synthesis: Automated Production of Fine Chemicals" **S. Mumtaz**, M. Oelgemöller *CBMDT and CBTID Retreat*, Fitzroy Island (Australia), 15.-17. July 2016.

2. **Poster presentation and Best student poster award:** "Transforming Organic Synthesis: Automated Production of Fine Chemicals" **S. Mumtaz**, M. Oelgemöller *North Queensland Festival of Life Sciences 2015*, Townsville (Australia), 5. November 2015.

3. **Poster presentation** "Transforming Organic Synthesis: Automated Production of Fine Chemicals" **S. Mumtaz**, M. Oelgemöller *2015 Australasian Tropical Health Conference – Emerging Priorities in Tropical Health Research*, Palm Cove (Australia), 20.-22. September 2015.

4. **Oral presentation** "Tandem Photochemical-Thermal Continuous Flow Reactions with UV and Sunlight and their Applications in the Synthesis of Potential Pharmaceuticals" S.

Mumtaz, M. Oelgemöller *2015 Gordon Research Conference on Photochemistry,* Easton (USA), 19.-24. July 2015.

5. **Poster presentation** "Photoredox catalysis in flow: Ru-catalyzed, visible light mediated addition phenylglycines to enones" **S. Mumtaz**, M. Oelgemöller *2015 Gordon Research Conference on Photochemistry,* Easton (USA), 19.-24. July 2015.

6. **Poster presentation** "Photodecarboxylations and their Application in Organic Synthesis" **S. Mumtaz**, M. Oelgemöller *North Queensland Festival of Life Sciences 2014*, Townsville (Australia), 4. November 2014.

7. "Photodecarboxylations and their Application in Organic Synthesis" **S. Mumtaz**, M. Oelgemöller *8th Australasian Organometallics Discussion Meeting (OZOM8)*, Magnetic Island (Australia), 22.-25. July 2014.

Curriculum Vitae

Personal data:

Name: Saira Mumtaz

Date of birth: 03.04.1984

Place of birth: Multan (Pakistan)

Academic qualifications:

2013-2016   PhD (Organic Chemistry), James Cook University, College of Science and Engineering, Discipline of Chemistry, Townsville, Australia, with Associate Prof. Michael Oelgemöller

Title: Photochemical Syntheses in Batch and Flow.

2005-2007   M.Phil. (Organic Chemistry), Bahauddin Zakariya University, Institute of Chemical Sciences, Multan, Pakistan

Title: Syntheses and biological testing of some novel 1-and 5-subsituted-2,3-indolinones derived hydrazones.

2003-2005   M.Sc. (Chemistry), Government College University, Department of Chemistry, Lahore, Pakistan

Title: Phytochemical studies of *Eugenia jambolana*and synthesis of 2,2-dimethyl-1, 5-dioxolane.

Professional activities:

2013-2016   Laboratory demonstrator, James Cook University, College of Science and Engineering, Discipline of Chemistry, Townsville, Australia

2012   Guest lecturer, Bahauddin Zakariya University, Institute of Chemical Sciences, Multan, Pakistan

2010-2012   Research assistant, Bahauddin Zakariya University, Institute of Chemical Sciences, Multan, Pakistan, with Assistant Professor Ashfaq Mahmood Qureshi

2008-2010   Research assistant, Bahauddin Zakariya University, Institute of Chemical Sciences, Multan, Pakistan, with Dr. Humayun Pervez

Table of contents

Chapter 1:

Introduction

1. Introduction

1.1 Photochemical principles

Human understanding of photochemistry began in the 17th century, when Jan Ingenhousz blamed sunlight for Joseph Priestley's 'injured air' [1]. In 1834, the crystals of α-santonin were observed to turn yellow and then burst on exposure to sunlight. Thus, the idea was established that light can induce chemical changes in molecules and cause reactions or degradations [2]. According to the IUPAC, photochemistry is 'the branch of chemistry concerned with the chemical effects of light' [3]. As stated by the Grotthus-Draper law, only light which is absorbed by a molecule can cause a photochemical change [4]. This activation by light generates an excited state molecule (**Figure 1.1**). The Stark-Einstein law, however, states that for each photon of light absorbed only one molecule can get activated. This is also known as photo equivalence law [4].

$$S_0 \xrightarrow{h\nu} S_n^*$$

excited state S_n^*

ground state S_0

$\Delta E = S_n^* - S_0$
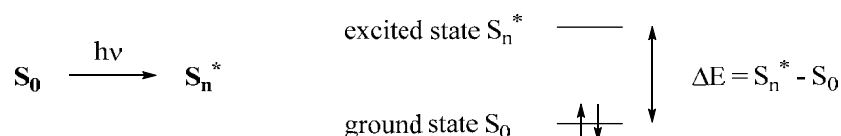
Figure 1.1: Electronic states in photochemical reaction.

For a molecule in the ground state (S_0), the lower (bonding) orbitals remain fully occupied by pairs of electrons and the upper (anti-bonding) orbitals stay unoccupied. After excitation, an electron from the highest occupied molecular orbital (HOMO) promotes to the lowest unoccupied molecular orbital (LUMO). Photochemically excited electrons can exist in the singlet or triplet state. In an excited singlet state (S_n^*) their spins remain paired as shown in **Figure 1.2** [4].

Energy

LUMO

$h\nu$

HOMO

S_0

S_n^*
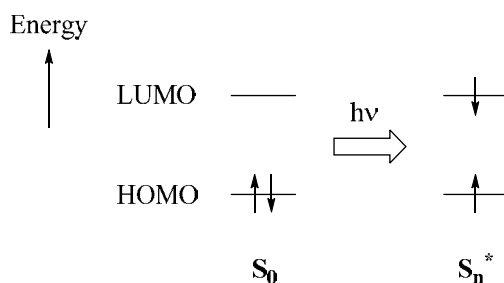
Figure 1.2: Singlet excited state.

In contrast, excited triplet state (T_n^*) have their spins parallel. Direct transmission from excited singlet (S_1) to excited triplet state (T_1) is energetically favoured but forbidden by Wigner's rule.

The excited triplet state can be generated through inter-system crossing (ISC), which allows the excited singlet state to reach the lower energy triplet state (**Figure 1.3**) [4].
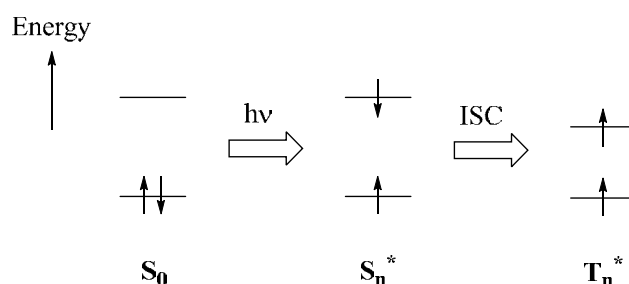
Figure 1.3: Triplet excited state.

When an electron is promoted to the excited state, there are a number of pathways how an excited electron can release energy. The various radiative and non-radiative processes are commonly represented in a Jablonski diagram (**Figure 1.4**) [5]
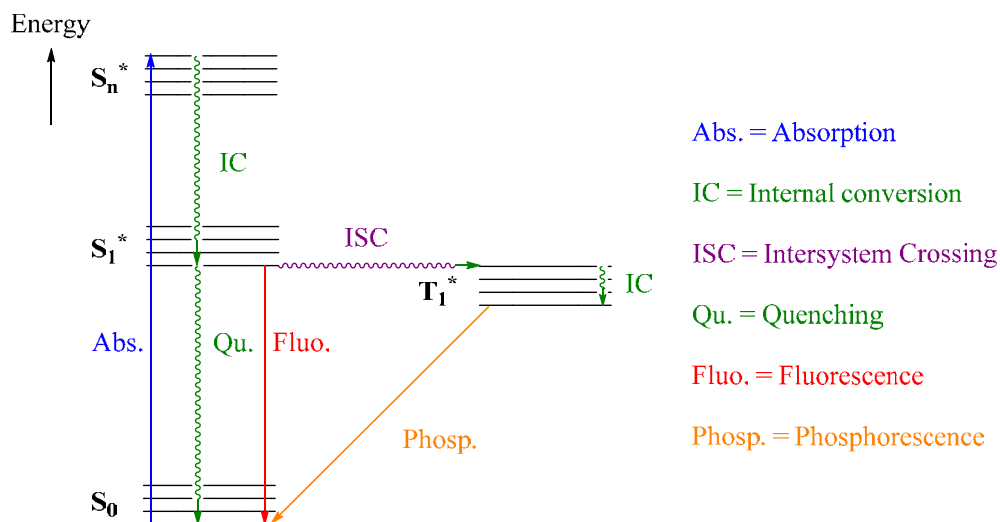
Figure 1.4: Jablonsaki diagram.

Most of the excited states of higher energy decay very rapidly to the lowest lying S_1 or T_1 states. This happens through radiationless decay known as internal conversion (without change of spin: $S_n{\rightarrow}S_1$ or $T_n{\rightarrow}T_1$) or inter system crossing (involving change of spin: $S_1{\rightarrow}T_1$). S_1 and T_1 excited states therefore have special significance in photochemical reactions. They have longer life time as the energy gap between S_1 or T_1 and the ground state S_0 is quite large. A chemical reaction has to compete with radiationless decay to the ground state, and to luminescent decay, *i.e.* fluorescence (no change of spin: $S_1{\rightarrow}S_0 + h\nu$) or phosphorescence (change of state: $T_1{\rightarrow}S_0 + h\nu$) [4].

1.2   Photosensitization and photoinduced electron transfer (PET)

Photosensitization initiates a reaction through the use of a sensitizer (Donor, Do) capable of absorbing light and efficiently populating its triplet state. The energy is subsequently transferred to the desired reactants (Acceptor, Acc). This process allows for the effective generation of triplet states that may not be accessible by direct excitation (**Figure 1.5**) [4]. The triplet energy of the donor must be higher than that of the acceptor.

$$Do\ (S_0) \xrightarrow{\ h\nu\ } Do\ (S_1^*) \xrightarrow{\ ISC\ } Do\ (T_1^*)$$

$$Do\ (T_1^*) \ + \ Acc\ (S_0) \xrightarrow{\ EnT\ } Do\ (S_0) \ + \ Acc\ (T_1^*)$$
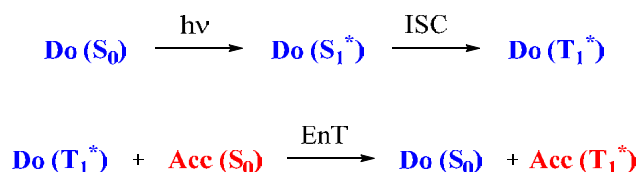
Figure 1.5: Triplet sensitization.

An alternative process is photoinduced electron transfer (PET), *i.e.* the transfer of an electron from an electron donor (Do) to an electron acceptor (Acc) [4]. As a result, radical ion pairs are formed that can undergo further transformations (**Figure 1.6**).
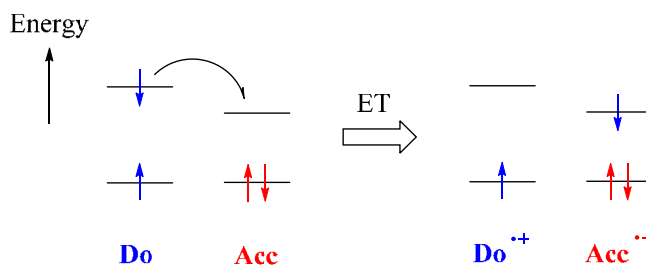
Figure 1.6: Photoinduced electron transfer.

The probability of a photoinduced electron transfer step can be estimated by using the Rehm-Weller equation (**Equation 1.1**) [6, 7], where E_{ox} (Do), and E_{red} (Acc) stands for the oxidation and reduction potentials of the donor and acceptor moieties, respectively. E_∞^* represents the electronic excitation energy and E_{coul} the columbic interaction energy of the products.

$$\Delta G = F(E_{ox}\ (Do) - E_{red}\ (Acc)) + E_{coul} - E_\infty^*$$

Equation 1.1: Rehm-Weller equation.

1.3   Photophysical and electrochemical properties of phthalimides

In their UV spectra, phthalimides exhibit unstructured absorption with maxima around 235 nm ($\pi{\rightarrow}\pi^*$) and 295 nm ($n{\rightarrow}\pi^*$). *N*-Alkylphthalimides show weak fluorescence of low quantum

yield ($\Phi_f < 1 \times 10^{-3}$) at room temperature in ethanol or acetonitrile. Broad structureless phosphorescence at 450 nm with quantum yields (Φ_p) of 0.3-0.7 and triplet lifetimes (τ_p) of 0.7-1.04 s (at -196ºC in alcohol) have been observed in oxygen free conditions. The excited states levels of phthalimide have been controvertibly discussed [8-10].

In DMF and acetonitrile, *N*-methylphthalimide is reversibly reduced to its corresponding radical anion at *ca.* -1.35 V and at *ca.* -1.5 V, respectively [11-13]. The presence of hydrogen donor sites in the *N*-side chain affects the redox potentials by *intra-* and *intermolecular* hydrogen bonding. These were reflected by anodically shifted pre-waves in the cyclic voltammograms of the phthalimide electrophores [14, 15].

From the photophysical and electrochemical data, the possibility of electron transfer processes can be assessed using the Rehm-Weller equation (**Equation 1.1**). For the first excited singlet state ($E^*_\infty = 3.8$ eV), the limiting oxidizing power is *ca.* 2.4 V (*vs.* SCE), whereas for the first excited triplet state ($E^*_\infty = = 3.1$ eV), the limiting oxidation power decreases to *ca.* 1.7 V (*vs.* SCE). For the second triplet state ($E^*_\infty \approx 3.6$ eV), the oxidation power increases by approximately 0.5 V.

Inter- and *intramolecular* quenching of *N*-substituted 4,5-dimethoxyphthalimides by sulfide, amines and alkyl carboxylates have been studied by Griesbeck and Schieffer [16]. Strong *intramolecular* fluorescence quenching was indeed observed for thioethers and tertiary amines. Biczok and Görner studied the photophysical and photoreduction properties of *N*-acetyl- and *N*-benzoylphthalimide [17]. The triplet states of both compounds were efficiently populated but the latter was found short lived. The trimethoxy-derivative of *N*-benzoylphthalimide was not photoactive, whereas the corresponding nitro-analogue showed typical photophysical and photochemical properties of nitrobenzene derivatives.

1.4   Photodecarboxylation reactions of phthalimides

One of the earliest photochemical reactions of phthalimides has been reported by Kanaoka and co-workers. Upon irradiation, *N*-phthalimido-α-amino acids underwent efficient α-photo-decarboxylation [18, 19]. A variety of novel photodecarboxylations of phthalimides have since been discovered as noticeable from numerous summarizing review articles [20-24]. This chapter will thus focus on photodecarboxylations involving phthalimides reported after 1999.

1.4.1   Mechanistic aspects of the photodecarboxylation of phthalimides

The formation of a solvent trapping product (**Scheme 1.1**) upon photoirradiation of *N*-phthaloyl-leucine in acetone suggested the involvement of an azomethine ylide intermediate.

Subsequent cycloaddition of acetone competed with proton transfer to the simple photodecarboxylation product [18]. Further trapping experiments were achieved with a range of carbonyl and alkene dipolarophiles [25-27]. Further confirmation of azomethine ylide intermediates came from laser flash photolysis (LFP) investigations.
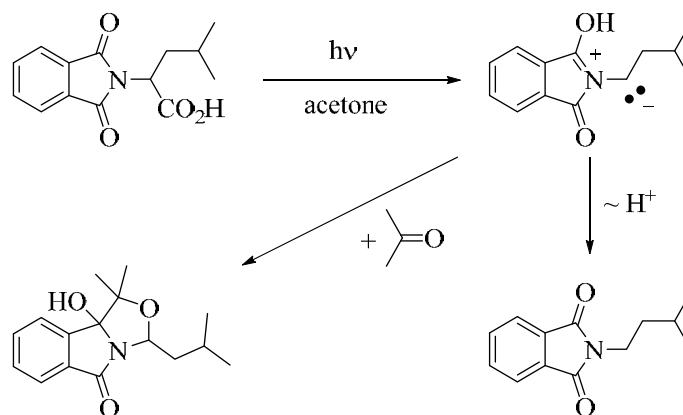
Scheme 1.1: Photoirradiation of *N*-phthaloyl leucine in acetone.

Similar studies on photo-retro-aldol fragmentations of *N*-phthaloyl α- and β-amino alcohols also suggested the formation of azomethine ylide intermediates [28]. *N*-Phthalamido-*β*-hydroxy-α-amino acids can follow both routes for azomethine ylide formation, *i.e.* α-decarboxylation or retro-aldol-cleavage. In acetonitrile, irradiation gave *N*-vinylphthalimide, whereas in the presence of methylacrylate, minor amounts of benzopyrrolizidine adducts were formed in small amounts (**Scheme 1.2**) [29].
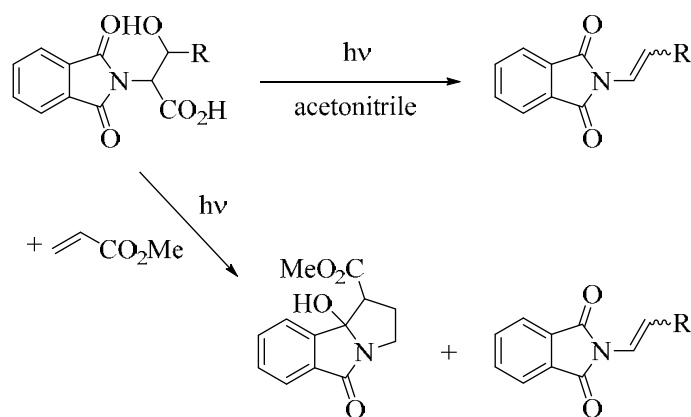
Scheme 1.2: Azomethine ylide formation *via* photodecarboxylation or retro-aldol-cleavage.

Recently, CASPT2//CASSCF calculations on the mechanism of the photodecarboxlation of *N*-phthaloylglycine have been conducted and further supported the involvement of an azomethine ylide intermediate [30].

1.4.2   Intramolecular photodecarboxylative cyclization reactions of phthalimides

Photodecarboxylations, *i.e.* eliminations of carbon dioxide upon irradiation with light, have been intensively studied in preparative photochemistry [31, 32]. These transformations generally employ carboxylate salts and can thus be readily performed in aqueous or largely aqueous solutions, thus avoiding the need of hazardous solvents [33]. Medium- to large-macrocycles have been synthesized through intramolecular photodecarboxylation of *N*-phthaloyl-protected carboxylic acids containing various functional groups (**Scheme 1.3**). Generally, decarboxylations can follow different conformational situations in the ground, electronically excited and radical ion states [34]. Of these two conformational local minima are particularly important: *remote* (where cyclization is disfavored) and *proximate* conformation (where cyclization is feasible).

proximate conformation   *remote* conformation
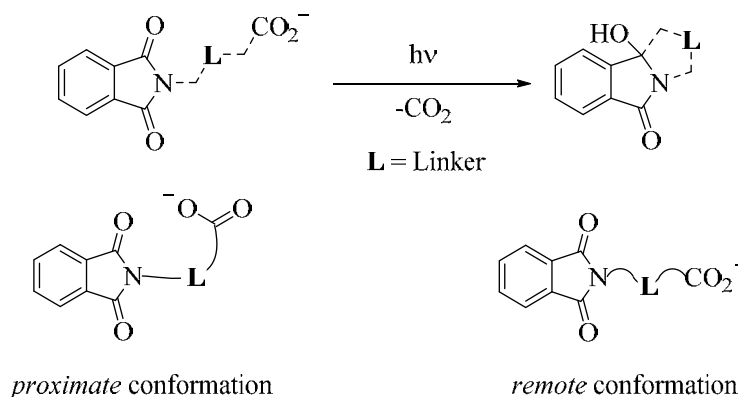
Scheme 1.3: Intramolecular photodecarboxylative cyclizations of *N*-phthaloyl-protected carboxylic acids containing various functional groups.

1.4.2.1 Photodecarboxylative cyclization reactions of phthalimides with carbon-spacers

Photodecarboxylations of potassium salts of ω-phthalimido alkanoates represent an efficient entry to medium- and large-ring compounds. As a representative example, the glutamic monomethyl ester derivative efficiently gave the corresponding benzopyrrolizidine in 82% yield. The diastereoselectivity was found to be low, however, acid-catalyzed epimerization exclusively favored the *cis*-isomer (**Scheme 1.4**) [35].
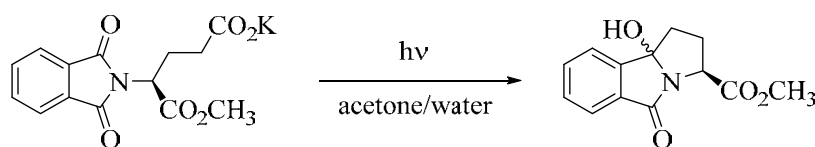
Scheme 1.4: Photodecarboxylative cyclization of *N*-phthloylglutamic acid methyl ester.

Multigram syntheses were achieved using a falling film reactor equipped with a XeCl excimer radiation source. As two representative examples, the glutamic acid and aminoundecanoic acid derivatives furnished the corresponding cyclization products in high yields of 91% and 82%, respectively (**Scheme 1.5**) [36].
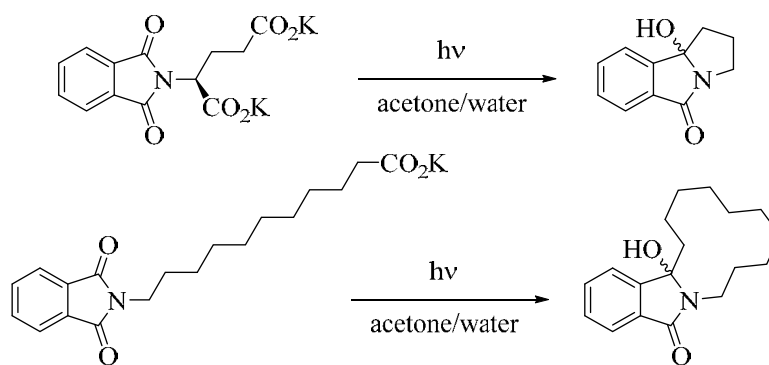
Scheme 1.5: Intramolecular photodecarboxylations of potassium ω-phthalimido carboxylates.

The photodecarboxylation of 3-(*N*-phthalimido)adamantane-1-carboxylic acid under direct and sensitized conditions solely gave *N*-(1-admantyl) phthalimide (**Scheme 1.6**) [37]. The efficiency of the photodecarboxylation could be improved by use of a protic solvent (H_2O) and a base (K_2CO_3). Trapping experiments in the presence of alkene or arenes allowed for further functionalization of the adamantly ring in yields of 20-100%. Electron deficient alkenes reacted most efficiently, yielding novel 1, 3-disubstituted adamantane derivatives.
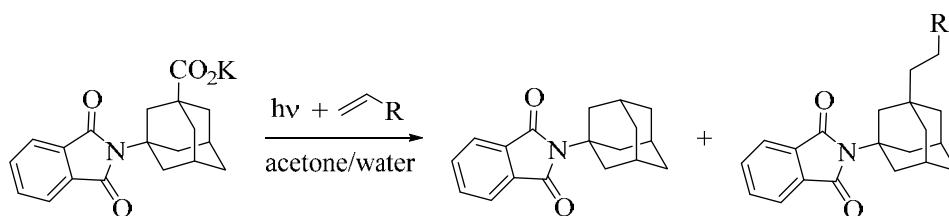
Scheme 1.6: Photodecarboxylation of potassium 3-(*N*-phthalimido)adamantane-1-carboxylate and subsequent trapping.

The outcome of the photodecarboxylation of ω-phthalimido alkynoates depended on the chain lengths and the position of the triple bond (**Scheme 1.7**). Short chain ω-phthalimido alkynoic acids exclusively gave photoreduced products due to their rigid structures. In contrast, long chained ω-phthalimido alkynoic acids furnished the respective ring compounds (**Table 1.1**) [38, 39].
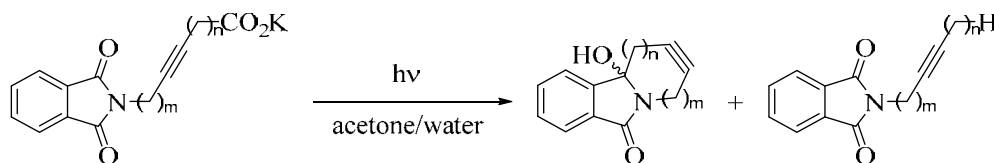
Scheme 1.7: Photodecarboxylations of ω-phthalimido alkynoates.

Table 1.1: Photodecarboxylations of ω-phthalimido alkynoates.

Entry	m	n	Ring size	Yields (%)
A	1	2	7	76
B	1	3	8	70
C	1	10	15	21
D	4	2	10	8
E	6	3	13	33

1.4.2.2 Photodecarboxylative cyclization reactions of phthalimides with heteroatom containing-spacers

Photodecarboxylations of ω-phthalimidoalkoxy acetic acids were carried out in methanol and acetone and yielded the corresponding cyclization products with 74-95% (**Scheme 1.8**). Reactions proceeded faster in methanol than in acetone, indicating that photocyclization operated through an excited singlet state electron transfer. Addition of sodium hydroxide increased the rate of the reaction three-fold by generation of carboxylates that are better electron donors [40].
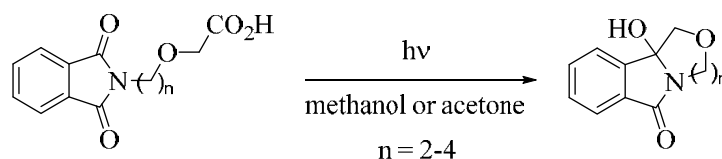
Scheme 1.8: Photodecarboxylation of ω-phthalimidoalkoxy acetic acids.

Photodecarboxylative cyclizations of ω-phthalimido phenoxy carboxylates have likewise been reported. *Ortho*-substitution favored close contact for electron transfer and subsequent cyclization. The yields of the cyclization products critically depended on the linker chain length (**Scheme 1.9**; **Table 1.2**). The methylene-linked derivative furnished the six-membered ring product in a good yield of 75%, whereas the yield decreased slightly to 73% for the ethylene-linked analogue. Further chain elongation resulted in steric overcrowding, poor biradical combination and poor yields even upon extended irradiation [41].
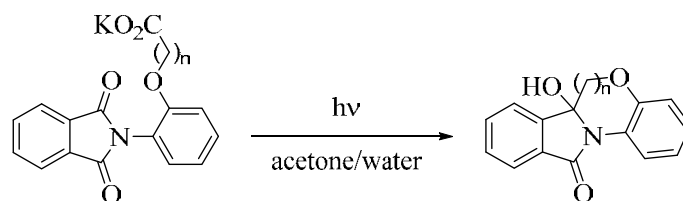
Scheme 1.9: Photodecarboxylative cyclizations of ω-phthalimido-*ortho* phenoxy carboxylates.

Table 1.2: Photodecarboxylative cyclizations of ω-phthalimido-*ortho* phenoxy carboxylates.

Entry	n	Ring size	Time (h)	Yields (%)
a	1	6	1	75
b	3	8	1	42
c	4	9	6	36
d	6	11	10	24
e	9	14	120	12
f	10	15	120	19

In contrast, a steady increase in yields and qualities with increased chain length has been observed for photodecarboxylative cyclizations of ω-phthalimido-*meta*-phenoxy carboxylates. The method furnished a 16-membered macrocyclic product in 48% yield [42]. Photodecarboxylative cyclization reactions of ω-phthalimido-*para*-phenoxy carboxylates were subsequently conducted. Long chain linkers were required to overcome the unfavourable *para*-substitution pattern (**Scheme 1.10**) [43].
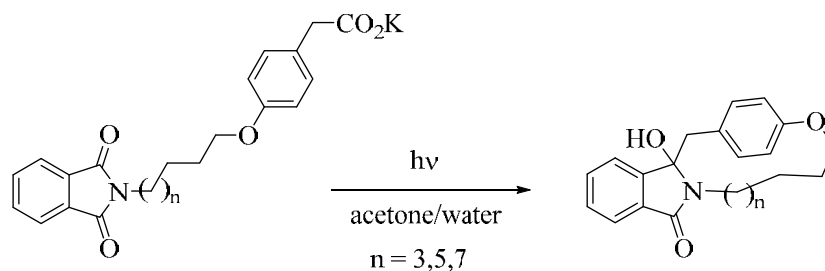
Scheme 1.10: Photodecarboxylative cyclizations of ω-phthalimido-*meta* phenoxy carboxylates.

Photocyclizations of ω-phthalimidoalkylthio acetic acids in methanol have furthermore been studied (**Scheme 1.11**; **Table 1.3**). The reaction mechanism involved intramolecular single electron transfer (SET) from the thioether linker to the triplet excited phthalimide. In selected cases, subsequent dehydration was observed [44].
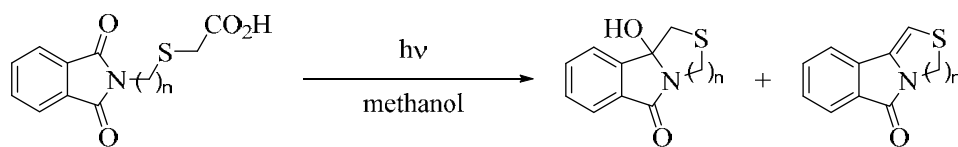
Scheme 1.11: Photocyclizations of ω-phthalimidoalkylthio acetic acids.

Table 1.3: Photocyclizations of ω-phthalimidoalkylthio acetic acids.

Entry	n	Ring size	Conversions (%)
a	2	6	46
b	3	7	80
c	4	8	68
d	6	10	84
e	9	13	80

The same sulphur-containing tricyclic ring systems were obtained from the corresponding ω-phthalimidoalkylthioalkyl carboxylates (**Scheme 1.12**; **Table 1.4**). The transformations proceeded with high efficiencies for terminal thioacetates, whereas low yields were observed for terminal thiopropanoates. For the corresponding acid analogues, cyclic voltammetry studies suggested pre-orientation through hydrogen-bonding prior to photocyclization [45].
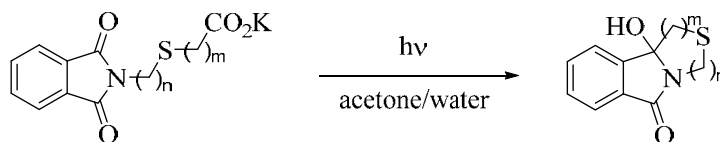
Scheme 1.12: Photocyclizations of ω-phthalimidoalkylthioalkyl carboxylates.

Table 1.4: Photocyclizations of ω-phthalimidoalkylthioalkyl carboxylates.

Entry	n	m	Ring size	Yields (%)
a	1	1	5	95
b	2	1	6	61
c	3	1	7	62
d	4	1	8	66
e	1	2	6	20
f	2	2	7	11
g	3	2	8	15
h	4	2	9	(decomposition)

The synthesis of macrocyclic lactones was achieved in high yields of 77% and 81%, respectively, from the analogous ester-linked precursors. For the valine-derived starting

material, a moderate diastereoselectivity of 60:40 in favor of the *cis*-isomer (with respect to the ^{i}Pr- and hydroxyl-group) was observed [35].
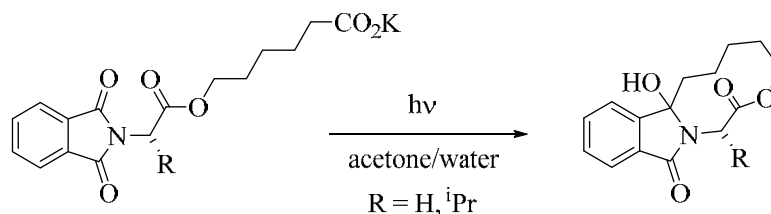
Scheme 1.13: Photodecarboxylative synthesis of macrocyclic lactones.

For the inverted ester-containing starting materials, macrocyclic lactone formation competed with simple decarboxylations. In some cases, distinctive spirocyclopropanes were furthermore obtained (**Scheme 1.14**) [22].
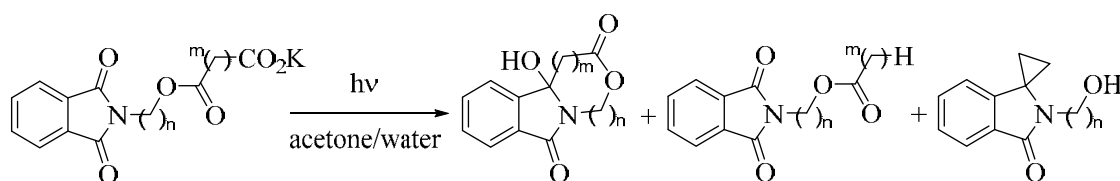
Scheme 1.14: Photodecarboxylations of inverted ester-containing phthalimido carboxylates.

A novel method for the preparation of cyclic peptide mimetics based on SET-promoted photocyclizations of peptides containing *N*-terminal phthalimides and *C*-terminal α-amidocarboxylates has been developed by Yoon and co-workers (**Scheme 1.15**) [46]. The corresponding cyclic peptides were obtained in yields of 18-70%. A comparison of relative photocyclization efficiencies of trimethysilyl- and carboxylate-containing phthalimidopeptides showed that the latter had a 3-fold higher quantum efficiency. ^{n}Bu$_4$NOH was added as a base to convert the carboxylic acids into the corresponding carboxylates.
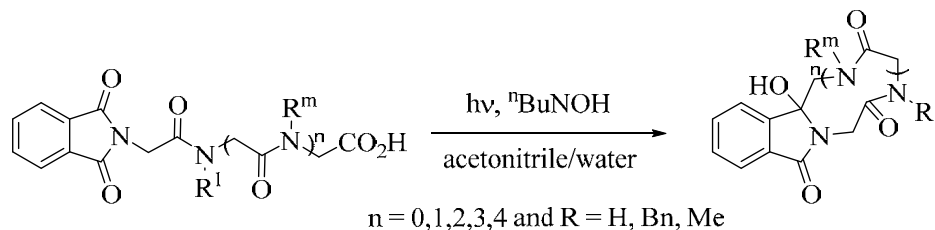
Scheme 1.15: Photocyclizations of peptides containing phthalimides.

Cyclic peptides have also been synthesized from potassium salts of *N*-phthaloyl-protected di-, tri-, tetra- and pentapeptides in a mixture of acetone and water [47]. As the transformation

proceeded, the pH of the reaction mixture increased due to the formation of potassium hydroxide, resulting in side products from hydrolysis of the phthalimides. To minimize these thermal side-reactions, irradiations were conducted in pH 7 buffer, resulting in improved yields and qualities of the cyclization products. Competition between cyclization and simple decarboxylation was observed and depended on several factors including spacer length, geometry and the likeliness of H-bonding between the phthalimide and the amide bonds. In contrast to Yoon *et al.* [46], photoinduced electron transfer from the carboxylate to the triplet excited phthalimide was postulated.

When anthranilic acid was used as linking amino acid, photodecarboxylative cyclizations furnished polycyclic lactams with ring-sizes ranging from 8-16 in yields of 10-81% (**Scheme 1.16**; **Table 1.5**) [48]. The *ortho*-substitution pattern of the anthranilic acid generated a U-shape geometry that resulted in a close proximity between the terminal carboxylate and the phthalimide chromophore, hence favoring cyclization. For longer chain carboxylates, the U-shaped preorientation caused steric overcrowding, thus resulting in a drop in yields.
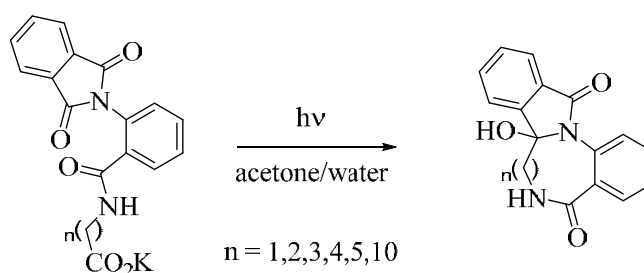
Scheme 1.16: Photocyclizations of anthranilic acid-linked amides.

Table 1.5: Photocyclizations of anthranilic acid-linked amides.

Entry	n	Ring size	Yield (%)
a	1	7	81
b	2	8	75
c	3	9	54
d	4	10	48
e	5	11	38
f	10	16	10

Photodecarboxylations of *N*-phenylphthalimide dipeptide derivatives solely yielded the analogue simple decarboxylation products in yields of 87% and 100%, respectively (**Scheme 1.17**). The *para*-substitution pattern caused special separation and prevented the necessary conformational approach required for photocyclization [37].
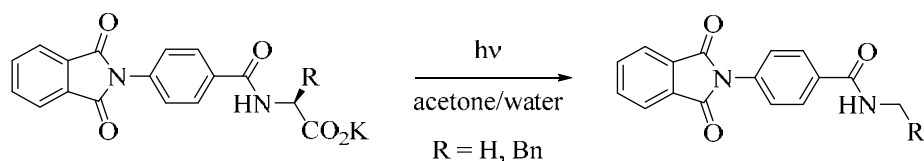
Scheme 1.17: Photodecarboxylations of *N*-phenylphthalimide dipeptide derivatives.

In a related study, photodecarboxylations of *N*-adamantaylphthalimide derived dipeptides were studied. The substitution pattern allowed for some flexibility, hence yielding cyclization as well as simple decarboxylation products (**Scheme 1.18**) [37]. The ring strain inside the initial cyclization products caused partial ring opening.
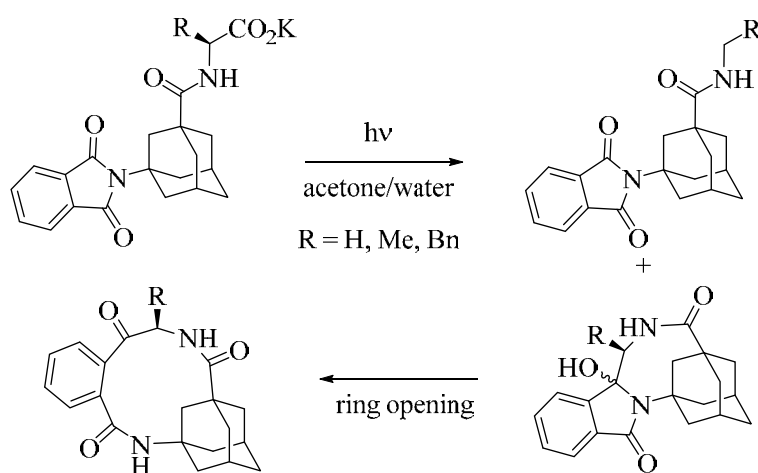
Scheme 1.18: Photodecarboxylations of *N*-adamantaylphthalimide dipeptide derivatives.

1.4.3 Intermolecular photodecarboxylative addition reactions of phthalimides

1.4.3.1 Photodecarboxylative alkylation reactions of phthalimides

Photodecarboxylative additions of potassium carboxylates to phthalimides have been studied extensively as an alternative to thermal Grignard-reactions. The reaction tolerates a variety of branched and unbranched alkyl carboxylates, whereas benzoate salts remain unreactive (**Scheme 1.19**) [49]. When hydroxyl carboxylates were used, the corresponding hydroxyalkylated products were obtained [49]. α-Keto carboxylates behaved differently and gave, depending on the structure of the α-keto carboxylates, acylations, alkylations or ring-extension products [50]. The regioselectivity of the alkylation was studied for unsymmetrically substituted phthalimide analogues and depended on the spin-density of the corresponding radical-ionic intermediate [51]. The photodecarboxylative addition protocol was furthermore extended to electron-deficient carboxylates with online CO_2 monitoring [52].
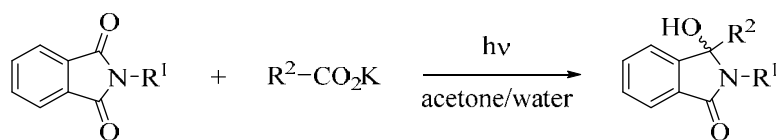
Scheme 1.19: Photodecarboxylative additions of carboxylates to phthalimides.

Simple decarboxylations commonly competed with additions. To suppress this undesired reactions, excess amounts of carboxylates were commonly employed. In case of 2-adamantane carboxylate, however, this pathway became dominant and irradiation in the presence of 1/10 equivalents of *N*-methylphthalimide gave adamantane as the major product in yields of 60-69% (**Scheme 1.20**) [53].
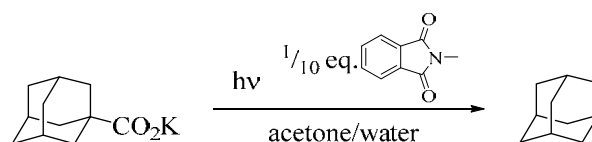
Scheme 1.20: Simple photodecarboxylation of 2-adamantane carboxylate.

A large scale photodecarboxylative addition of potassium isobutyrate to *N*-methylphthalimide was carried out using an advanced falling film reactor equipped with an excimer light source. The reaction could be monitored by GC-analysis or, more rapidly, by recording the pH of the reaction mixture. After 4½ hours of circulation, the reactor produced 5.1 g of the desired alkylation product, corresponding to a yield of 63% [54].

The photodecarboxylative benzylation of phthalimides was developed as a versatile access to pharmaceutically important products. The mechanism was likewise studied and the quantum yields were determined to be high with 30-80%, but depended on the substitution of the arylacetic acids and the pH of the reaction medium [55]. Subsequent dehydration of the product furnished *E/Z*-diastereoisomeric mixtures in high to excellent yields (**Scheme 1.21**) [56].
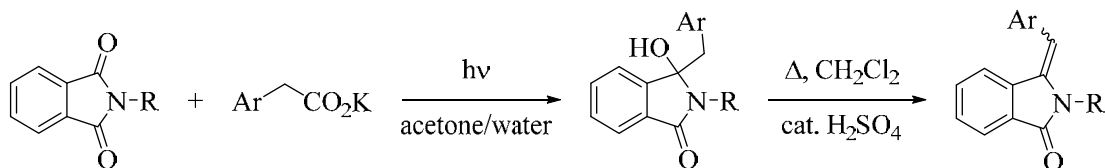
Scheme 1.21: Photodecarboxylative benzylations and subsequent dehydrations.

The versatility of the reaction was further demonstrated by irradiating *N*-methylphthalimide with a range of branched phenyl acetates and longer phenylalkanoates [56]. 1,3-Phenyl lactate

and 2-oxo-3-phenylpropanoate also gave benzylation through subsequent retro-aldol or decarbonylation reactions. In an extension of this work, free phthalimide was reacted with various substituted phenylacetates in an acetone/buffer (pH7) mixture. Subsequent dehydration produced *E/Z*-diastereoisomeric mixtures of 3-arylmethylene-1H-isoindolin-1-ones [57]. The photodecarboxylative addition was consequently applied to the synthesis of biologically active 3-(alkyl and aryl)methylene-1H-isoindolin-1-ones. As an example, the cardiovascular active **AKS186** and its derivatives were successfully synthesized by photoaddition of aryl-substituted alkyl carboxylates to 2-(4-acetoxybenzyl) isoindoline-1,3-dione and acid catalyzed dehydration/deprotection (**Scheme 1.22**) [58].
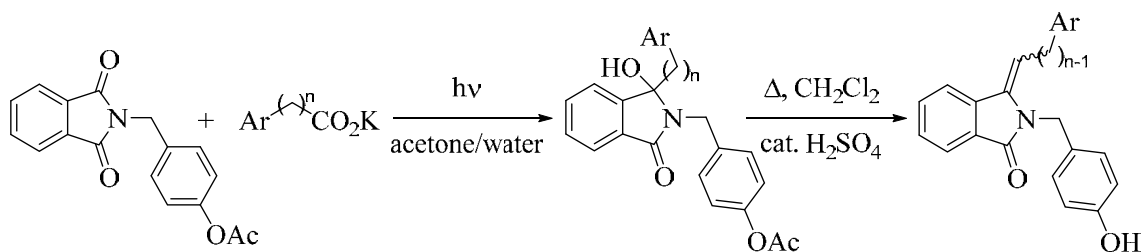
Scheme 1.22: Photoirradiation of 2-(4-acetoxybenzyl)isoindoline-1,3-dione with aryl substituted alkyl carboxylates followed by acid catalyzed dehydration/deprotection.

Likewise, photodecarboxylative additions of potassium alkynoates to *N*-methylphthalimide resulted in the corresponding hydroxyphthalimidines in low yields of 19-26% (**Scheme 1.23**) [39]
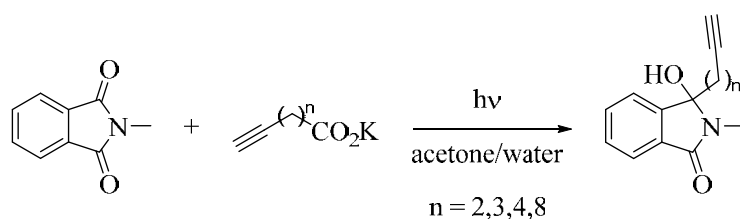
Scheme 1.23: Photodecarboxylative addition of potassium alkynoates to *N*-methylphthalimide.

1.4.3.2 Photodecarboxylative additions of heteroatom containing carboxylates to phthalimides

Substituting carbon-based carboxylates with heteroatom containing carboxylates can either enhance or suppress photoreactivity (**Scheme 1.24**; **Table 1.6**) [41, 45, 50, 56]. Alkoxy- and phenoxyalkyl carboxylates generally furnished the corresponding addition products in acceptable to excellent yields of 21-93%. In contrast, solely α-thioalkyl carboxylates underwent

photoaddition in 57% and 90% yield, whereas the extended β-thioalkyl carboxylate remained unreactive. This difference in reactivity for the latter compounds was explained by a preferred photoinduced electron transfer from the sulfur-atom. For α-thioalkyl carboxylates, the subsequent radical-cation can efficiently eliminate carbon dioxide. For β-thioalkyl carboxylates, back electron transfer operated instead. In contrast, alkoxy- and phenoxyalkyl carboxylates reacted through electron transfer from the carboxylate function. This assumption was supported by the oxidation potentials for the various donors, which increases in the order $R_2S < RCO_2^- < R_2O$.
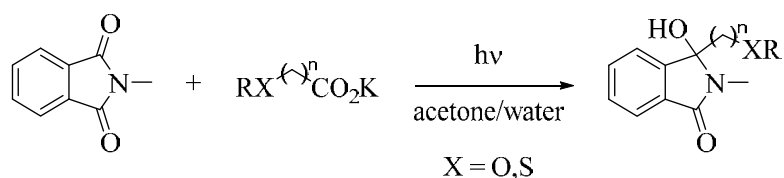
Scheme 1.24: Photodecarboxylative additions to oxoalkyl and thioalkyl carboxylates.

Table 1.6: Photodecarboxylative additions to oxoalkyl and thioalkyl carboxylates.

Entry	R	X	n	Yield (%)
a	CH_3	O	1	57
b	CH_3	O	2	51
c	Ph	O	1	85
d	Ph	O	2	38
e	Ph	O	3	55
f	Ph	O	4	45
g	Ph	O	9	47
h	Ph	O	10	49
i	$2\text{-MeC}_6\text{H}_4$	O	1	93
j	$2\text{-ClC}_6\text{H}_4$	O	1	53
k	$4\text{-ClC}_6\text{H}_4$	O	1	51
l	$2\text{-Me-4-ClC}_6\text{H}_3$	O	1	55
m	$2,4\text{-Cl}_2\text{C}_6\text{H}_3$	O	1	71
n	$2,4,5\text{-Cl}_3\text{C}_6\text{H}_2$	O	1	51
o	1-naphthyl	O	1	21
p	2-naphthyl	O	1	48
q	CH_3	S	1	90
r	Ph	S	1	57
s	CH_3	S	2	no reaction

N, N-Disubstituted α-amino acid salts predominantly underwent photoreduction or acetone trapping when irradiated in the presence of N-methylphthalimide. Solely N-phenyl glycinate furnished additionally the corresponding addition adduct in a moderate yield of 30%. Chemoselectivity was restored for N-acylated α-amino acids salts, which underwent rapid addition in yields of up to 95% (**Scheme 1.25**; **Table 1.7**) [59]. The differences in reactivity were again explained based on the various electron donors. Amines reacted *via* electron transfer from the amino-group, whereas the corresponding amide-derivatives reacted from their terminal carboxylates.
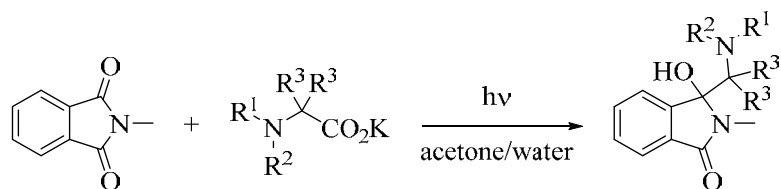
Scheme 1.25: Photodecarboxylative addition of N-acylated α-amino acid salts to N-methylphthalimide.

Table 1.7: Photodecarboxylative addition of N-acylated α-amino acid salts to N-methylphthalimide.

Entry	R^1	R^2	R^3	Yield (%)
a	Ph	H	H	30
b	Ac	Ac	H	71
c	Ac	CH_3	H	73
d	Ac	Ph	H	95
e	Boc	H	H	74
f	Cbz	H	H	56
g	Fmoc	H	H	20
h	Ac	H	CH_3	83
i	Ac	H	$(CH_2)_5$	80

Further proof for this reactivity order came from corresponding ethylation reactions to N-substituted phthalimide derivatives (**Scheme 1.26**; **Table 1.8**) [45, 59, 60].
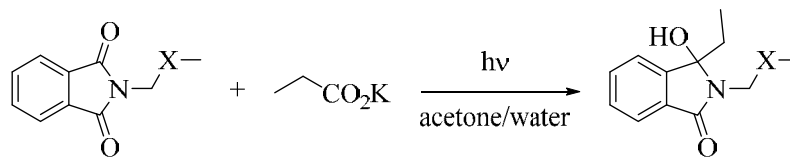
Scheme 1.26: Photodecarboxylative ethylations of N-substituted phthalimide derivatives.

The *N, N*-dimethylated compound showed mainly decomposition, whereas the thioether containing analogue remained entirely photostable. Solely the ether and amide linked derivatives underwent clean photodecarboxylative alkylations and gave the corresponding addition products in acceptable yields of 43-51%.

Table 1.8: Photodecarboxylative ethylations of *N*-substituted phthalimide derivatives.

Entry	X	Yield (%)
A	NCH$_3$	photodecomposition
B	S	no reaction
C	O	51
D	CONH	43
E	CONCH$_3$	51

1.4.4   Miscellaneous reactions

The photodecarboxylation was recently developed into a photoremovable protecting group (PRPG) for the selective liberation of carboxylates and related compounds in high yields (**Scheme 1.27**) [61].
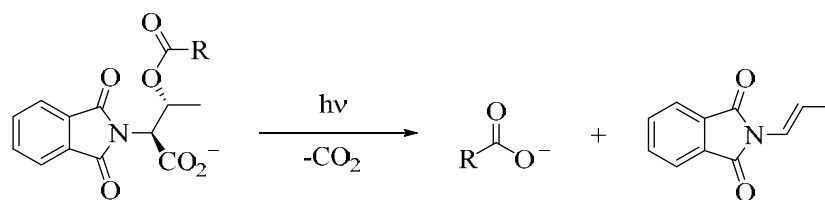
Scheme 1.27: Phthalimide based photoremovable protecting group (PRPG).

The photodecarboxylative release was subsequently coupled to fluorescent fluctuations using substituted phthalimides (**Scheme 1.28**) [62]. These derivatives can thus take on a reporter function.

$$R^1, R^2 = CH_3O \text{ or } R^1 = H; R^2 = NHOAc$$
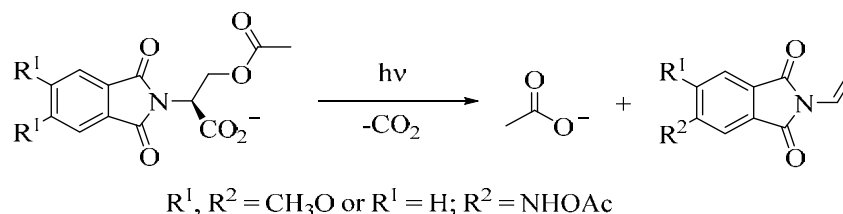
Scheme 1.28: Phthalimide based photoremovable protecting groups (PRPG) with coupled fluorescent fluctuation.

1.5   Photodecarboxylations in advanced photoreactors

Griesbeck *et al.* developed an advanced falling film reactor equipped with a 3 kW XeCl excimer lamp and applied it to a range of photodecarboxylation reactions. The lamp emitted almost monochromatically at 308 nm. The reactor produced multigram quantities of photoproducts in good to high yields (**Figure 1.7**; **Table 1.9**) [36, 54].
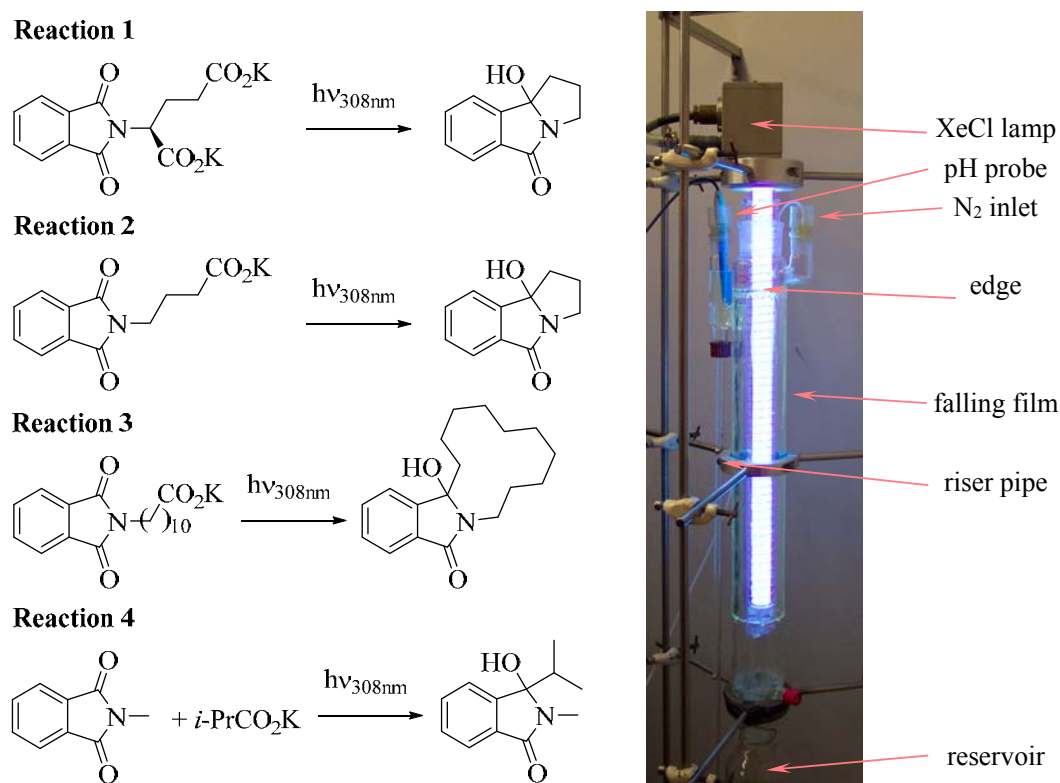
Figure 1.7: Photodecarboxylations in an advanced XeCl falling film reactor.

Table 1.9: Photodecarboxylations in an advanced XeCl falling film reactor.

Reaction	Starting material	Solvent	Time (h)	Yield
1	35.3 g Pht=Glu-OK	2 L acetone	13	17.2 g (91%)
2	6.7 g Pht=Gaba-OK	2 L water/acetone (9:1)	3	21.0 g (82%)
3	18.5 g Pht=Auda-OK	2 L water	4 ½	11.8 g (82%)
4	6.45 g Pht=N-, 30.3 g *i*-PrCO$_2$K	2 L water/acetone (3:1)	4 ¼	5.1 g (63%)

Recently, continuous flow reactors have emerged as advantage platforms for photochemical transformations [63-67]. The thin inner dimensions of microreactor channels or tubes enable high light transparencies, resulting in improved energy- and light-efficiencies. The continuous removal of photoproducts also minimizes photodecompositions or secondary photoprocesses,

thus enabling better product qualities. The irradiation time is easily controlled with the flow rate of the pumping system and larger amounts can be simply produced by supplying larger volumes of reagents.

Photodecarboxylations of phthalimides were subsequently investigated in continuous flow devices. Using the enclosed dwell device, α-photodecarboxylations, photocyclizations and photoadditions were successfully realized (**Figure 1.8**) [68, 69]. Compared to irradiation conducted in conventional chamber photoreactors, shorter reaction times were established to achieve high conversions, even at high concentrations of reagents. This is illustrated for photo-decarboxylative additions to *N*-methylphthalimide. Despite lower light power, the dwell device furnished similar to superior conversions for the same reaction times (**Scheme 1.29**; **Table 1.10**).
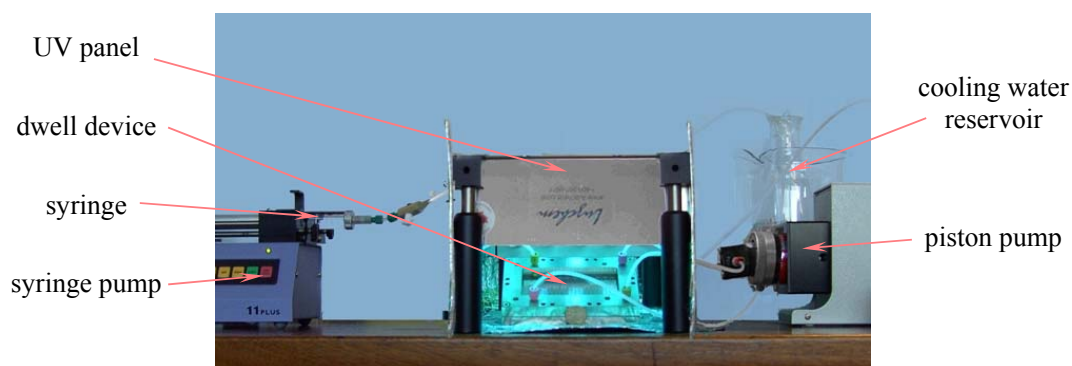
Figure 1.8: Reaction setup for photodecarboxylations in a dwell reactor.
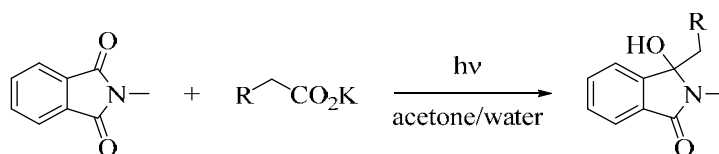
Scheme 1.29: Photodecarboxylative additions used for reactor comparison.

Table 1.10: Photodecarboxylative additions in a dwell device and Rayonet chamber reactor.

Time	Conversion (%) R = Ph		Conversion (%) R = CH$_3$S	
(min)	dwell	Rayonet	dwell	Rayonet
14	83	46	4	2
21	97	93	34	20
40	100	100	66	44
60	100	100	100	86

4,4'-Dimethoxybenzophenone (DMBP) mediated *inter*- and *intramolecular* photodecarboxylation reactions were furthermore realized in the dwell device [70]. All comparison studies demonstrated the superiority of continuous-flow photochemistry over conventional technologies in terms of conversion rates, yields and chemoselectivities. Recently, photodecarboxylations involving phthalimides were carried out in a purpose-designed commercial flow reactor, the Vapourtec UV-150. As an example, the α-photodecarboxylation of phthaloyl glycine achieved a productivity of 1.15 g per hour or 27.6 g per day (**Scheme 1.30**) [71].
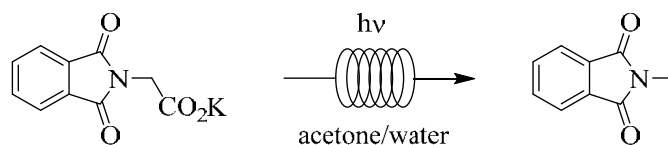
Scheme 1.30: α-Photodecarboxylation of phthaloyl glycine.

1.6   Summary

The understanding of the photophysical and electrochemical properties of phthalimides has led to the development of highly efficient photodecarboxylation reactions. These transformations were likewise applied to the synthesis of macrocyclic compounds and bioactive addition adducts. The generally mild reaction conditions makes these transformations attractive for green chemical applications. The general reaction protocols were successfully transferred to novel photoreactor devices, among these falling film or continuous flow reactors. Despite the relatively poor absorption of acetone within the solar spectrum, sunlight-induced photo-decarboxylations may be realized in sunlight [72].

Chapter 2:

Aims

2.   Aims

This project was broadly aimed at developing new photochemical reactions and technologies.

2.1   Exploratory photochemistry stream

The first stream involved the identification of potentially new photochemical reactions as well as the application of established photoreaction protocols to the synthesis of bioactive compounds. In order to achieve this, it utilized conventional batch photochemical techniques.

- Investigating potentially new photochemical reactions.
  o   Photochemical behavior of isatin.
  o   Photochemistry of benzoylbenzamides.
  o   Visible light mediated photoredox catalysis using $Ru(bpy)_3Cl_2$.
- Synthesis of bioactive compounds through established photodecarboxylations.
  o   Anesthetic **AL12** and **AL5** and analogues using photodecarboxylation as a key step.
  o   Aristolactam using photodecarboxylations and photodehydrohalogenations.

2.2   Photochemical technology development stream

The second technology stream involved the incorporation of continuous flow operations into photochemical syntheses. Selected photochemical protocols from batch processes were transferred to and optimized under microflow conditions. A comparison of batch and flow methods was furthermore desired. Multistep reactions were additionally established using in-series flow protocols. Following a more sustainable approach, outdoor experiments were conducted under solar flow conditions. The industrially important monobromination of acetophenone with *N*-bromosuccinimide (NBS) was furthermore investigated in flow. Likewise, $scCO_2$ was investigated as a sustainable solvent option for flow operation.

- Comparison of batch and flow processes.
- In series photochemical-thermal flow synthesis.
  o   Rapid end-to-end synthesis of **AL12**, **AL5** and their analogues.
  o   Continuous one-flow synthesis of **AKS186**.
- Sustainable flow approaches.
  o   Concentrated solar flow photodecarboxylative additions.
  o   NBS catalyzed brominations of acetophenone.
  o   Microflow photochemistry in $ScCO_2$.

Chapter 3:

Results

3.   Results

3.1   Synthesis of starting materials

3.1.1   Synthesis of 4-amino-*N*-pentenylphthalimide and *N*-alkenylisatin [Experiments 1-5]

N-Alkenylations were carried out following a modified procedure described by Gabriel *et al.* [73], Ding *et al.* [74] or Chen *et al.* [75] by refluxing 4-aminophthalimide (**1**) or isatin (**4**) with the corresponding alkenyl bromides **2** in DMF in the presence of K_2CO_3 and catalytic amounts of KI overnight (**Scheme 1.1** and **Scheme 3.2**). The final products, viscous/dense brownish oils, were obtained in good yields of 81-87% (**Table 1.1**). Their structures were confirmed through ^{1}H-NMR spectroscopy. All compounds showed characteristic triplets for the N-C$\underline{H}_2$ groups in the range of 3.60-3.77 ppm.
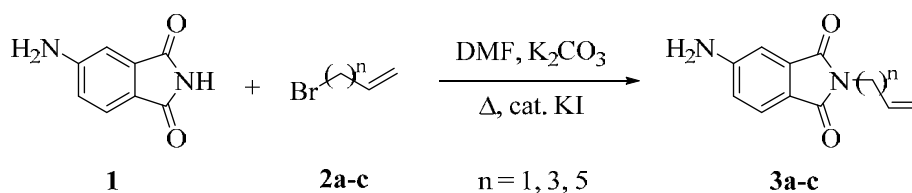
Scheme 3.1: *N*-Alkenylations of 4-aminophthalimide (**1**).
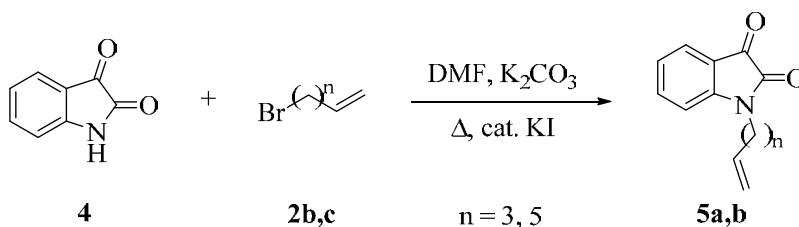
Scheme 3.2: *N*-Alkenylations of isatin (**4**).

Table 3.1: *N*-Alkenylation of aminophthalimide and isatin.

Entry	Imide	n	^{1}H-NMR of NCH$_2$ (ppm)[a]	Yield of 3 or 5 (%)
a	1	1	3.63 (triplet)	85
b	1	3	3.60 (triplet)	87
c	1	5	3.60 (triplet)	85
a	4	3	3.76 (triplet)	81
b	4	5	3.77 (triplet)	83

[a] In CDCl$_3$ or acetone-d$_6$.

The full ^{1}H-NMR spectrum of **3b** is exemplarily shown in **Figure 1.1**. The three aromatic signals are found at 6.92 (dd), 7.03 (d) and 7.59 (d) ppm. The olefinic protons show 3 signals at 4.89-5.03 (2 clustered signals) and 5.80 ppm. The NH$_2$-protons are observed as a broad singlet at 5.89 ppm. The NCH$_2$-group appears as a triplet at 3.56 ppm. The additional methylene-groups are found at 1.63 and 2.12 ppm, the later covered by the solvent peak.
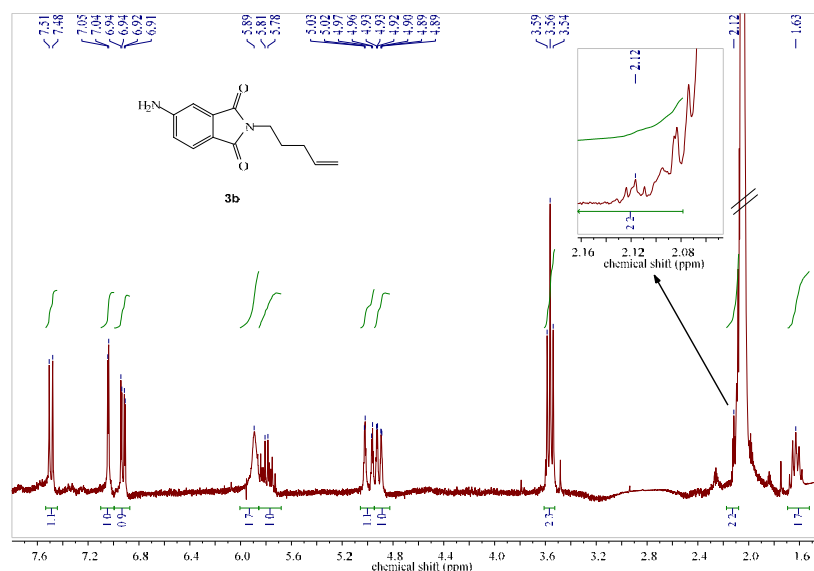
Figure 3.1: ^{1}H-NMR spectrum of 4-amino-*N*-pentenylphthalimide (**3b**) in CDCl$_3$.

3.1.2 Synthesis of 5-{[(*E*)-(5-bromo-2-hydroxy-3-methoxyphenyl)methylidene]amino} - 1*H*-isoindole-1,3(2*H*)-dione [Experiment 6]

Imide **7** was prepared following a modified protocol by Schiff et al. [76]. Refluxing the benzaldehyde derivative **6** with 4-aminophthalimide (**1**) in the presence of catalytic amounts of acetic acid in ethanol for 2 hours (**Scheme 3.3**) furnished 71% of **7** as a pale yellow solid product. A ^{1}H-NMR spectrum was recorded for structural confirmation and showed a characteristic singlet at 9.10 ppm for the imide (-C$\underline{H}$=N-) group.
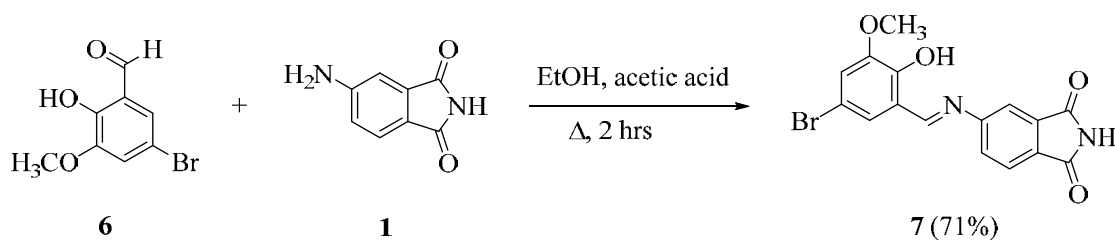
Scheme 3.3: Synthesis of Schiff's base **7** from 4-aminophthalimide (**1**).

3.1.3 Synthesis of 5-{[(*E*)-(5-bromo-2-hydroxy-3-methoxyphenyl)methylidene]amino} - (*N*-pentenyl)-isoindole-1,3(2*H*)-dione [Experiment 7]

N-Pentenylation of Schiff's base **7** was subsequently carried out by following the modified Ding procedure [74]. A mixture of Schiff's base **7** and **2b** was heated overnight in DMF in the presence of K$_2$CO$_3$ (**Scheme 3.4**). The product **8** was obtained in a good yield of 83% as a brown oil. Its structure was confirmed through ^{1}H-NMR spectroscopy which showed a characteristic triplet for the N-C$\underline{\text{H}}_2$ group at 3.65 ppm.
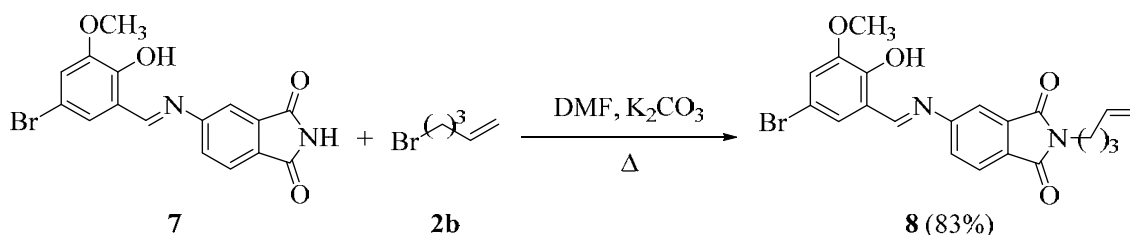
Scheme 3.4: *N*-Pentenylation of Schiff's base **7**.

3.1.4 Synthesis of benzoylbenzamides [Experiments 8-17]

The benzoylbenzamides **11a-e** were prepared following two different routes (**Scheme 3.5** and **Table 3.2**) [77-79]:

(a)   the acid chloride route and

(b)   the EDC coupling route.

For the acid chloride route *ortho*-benzoylbenzoic acid was treated with thionylchloride. The resulting acid chloride was subsequently reacted with various amines and amino acid esters **10a-e** to yield the desired compounds **11a-e** in 63-71% yield as colourless crystalline solids. Alternatively, the *N*-Ethyl-*N′*-(3-dimethylaminopropyl)carbodiimide hydrochloride (EDC) procedure was chosen. Following this procedure, a mixture of the respective amino acid ester and benzoylbenzoic acid was refluxed for a week in DCM with EDC and triethylamine (TEA) to obtain the same products **11a-e** in yields of 75-77%.

Route (a): Acid chloride route
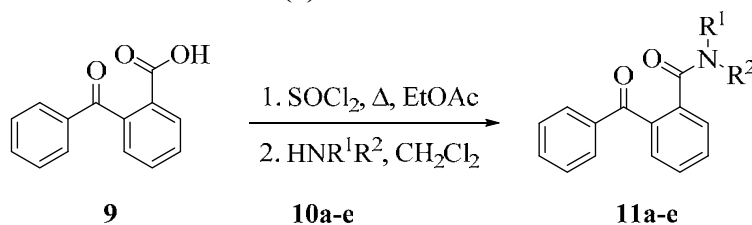
Route (b): EDC route
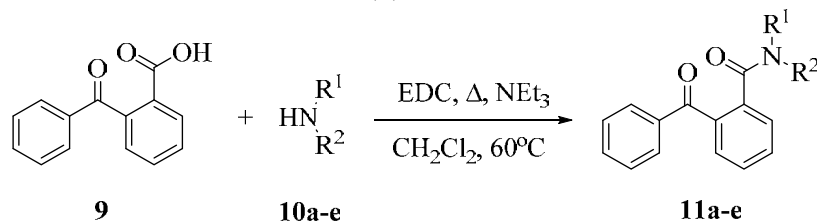
Scheme 3.5: Syntheses of benzoylbenzamide **11a-e**.

The reaction of benzoylbenzoic acid with primary amines and amino acid esters yielded tautomeric cyclic forms of the benzoylbenzamides **11a, c, e** (**Scheme 3.6**) [80]. The amino acid ester derived products furnished pairs of diastereoisomers. In contrast, the secondary amines and amino acid esters furnished pairs of rotamers **11b, d/11'b, d** (**Scheme 3.6**) [81]. As a consequence of these effects, the NMR spectra were highly complex for all coupling products. The ring tautomers **12** showed characteristic singlets for the $\underline{C}$-OH carbon at approx. 90 ppm in their ^{13}C-NMR spectra. The rotamer pairs **11/11'** gave two sets of signals in their ^{1}H-NMR spectra.
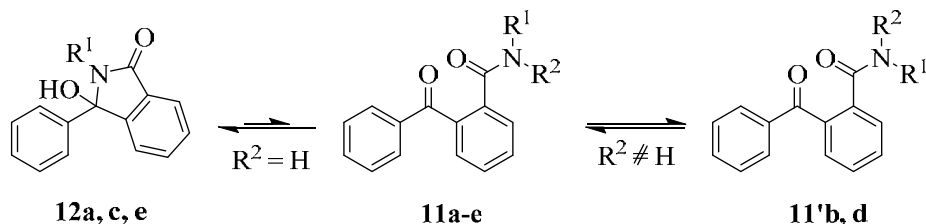
Scheme 3.6: Ring-chain tautomerization and rotamer population of compounds **11a-e**.

Table 3.2: Benzoylbenzoic acid-derived amide synthesis.

Entry	Route	HNR^{1}R^2 (10)	NMR (ppm)[a]	Yield (%)
a	(a)	phenylglycine methyl ester hydrochloride	90.5/90.3 (-$\underline{C}$OH)	71 (9:1[a], **12a**)
b	(a)	*L*-proline methyl ester hydrochloride	dd 4.27/4.58 (C$\underline{H}$CO$_2$Me)	66 (3:1[b], **11b/11'b**)
c	(a)	*L*-methionine methyl ester hydrochloride	90.6/90.4 (-$\underline{C}$OH)	69 (55:45[a], **12c**)[c]
d	(a)	methyl thiazolidine-2-carboxylate hydrochloride	s 5.20/5.62 (C$\underline{H}$CO$_2$Me)	63 (3:1[b], **11d/11'd**)
e	(a)	2-(*tert*-butylthio)ethanamine	90.9 (-$\underline{C}$OH)	65 (**12e**)
a	(b)	phenylglycine methyl ester hydrochloride	90.5/90.3 (-$\underline{C}$OH)	77[d] (**12a**)
b	(b)	*L*-proline methyl ester hydrochloride	dd 4.27/4.58 (C$\underline{H}$CO$_2$Me)	74[d] (**11b/11b'**)

Entry	Route	HNR^{1}R^2 (10)	NMR (ppm)^a	Yield (%)
c	(b)	*L*-methionine methyl ester hydrochloride	90.6/90.4 (-$\underline{C}$OH)	77^d (**12c**)
d	(b)	methyl thiazolidine-2-carboxylate hydrochloride	s 5.20/5.62 (C$\underline{H}$CO$_2$Me)	73^d (**11d, 11d'**)
e	(b)	2-(*tert*-butylthio)ethanamine	90.9 (-$\underline{C}$OH)	74 (**12e**)

^{a} Diasteroisomeric ratio (by integration of the ^{1}H-NMR, ±3%). ^{b} Rotamer ratio (by integration of the ^{1}H-NMR, ±3%). ^{c} Minor amounts (5-10%, by integration of the ^{1}H-NMR, ±3%) of **10** assumed. ^{d} Overall yield of crude reaction mixture.

The ^{1}H-NMR spectrum of the reaction product obtained from the reaction of **9** with *L*-methione methyl ester hydrochloride (**10c**) is depicted in **Figure 3.2**. It shows the presence of a diasteroisomeric mixture of *like*- and *unlike*-**12c**, as evident from two complete sets of signals, in a ratio of approx. 55:45% (determined by integration).
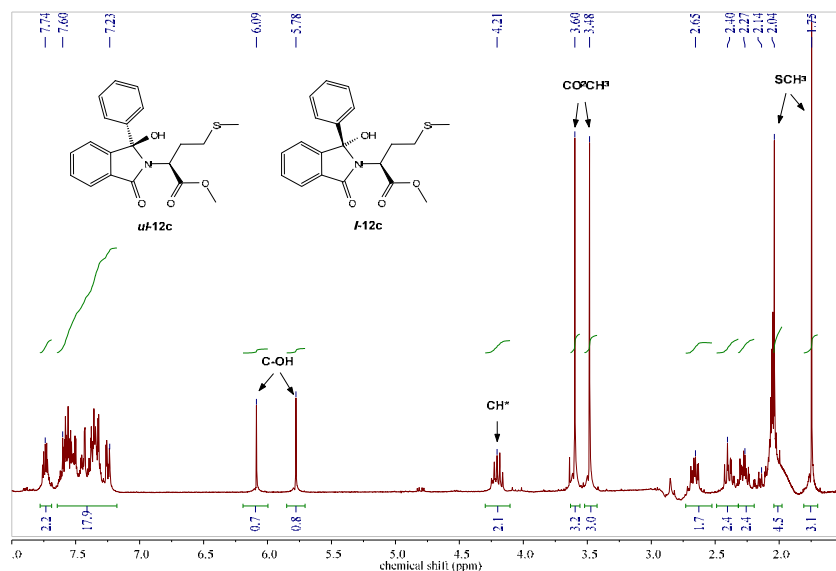
Figure 3.2: ^{1}H-NMR spectrum of a diasteroisomeric mixture of **12c** (in acetone-d$_6$).

In acetone-d$_6$, the main diastereoisomer gives a singlet for the -SCH$_3$-group at 1.76 ppm, a singlet for the methyl ester (-CO$_2$CH$_3$) at 3.60 ppm and a sharp singlet for the characteristic -OH group at 5.78 ppm. The minor diastereoisomer delivers these signals at 2.04, 3.48 and 6.09 ppm, respectively. All other signals are overlapping significantly. An assignment of the diastereoisomers was not attempted. However, the differences in chemical shifts for the terminal -SCH$_3$-groups suggest anisotropy effects by the aromatic rings for one diastereoisomer.

The ^{1}H-NMR spectrum of **11d**, obtained from the reaction of **9** with methyl thiazolidine-2-carboxylate hydrochloride (**10d**) is displayed in **Figure 3.3**. It shows the presence of an *E/Z*-

type mixture of the rotamers **11d** and **11'd**, as evident from two complete sets of signals. The ratio of the rotamers was determined by integration as to 3:1. In analogy to proline derived amides, the *Z*-rotamer **11d** (also called *trans* or *transoid*) was assigned to be the major component [81].
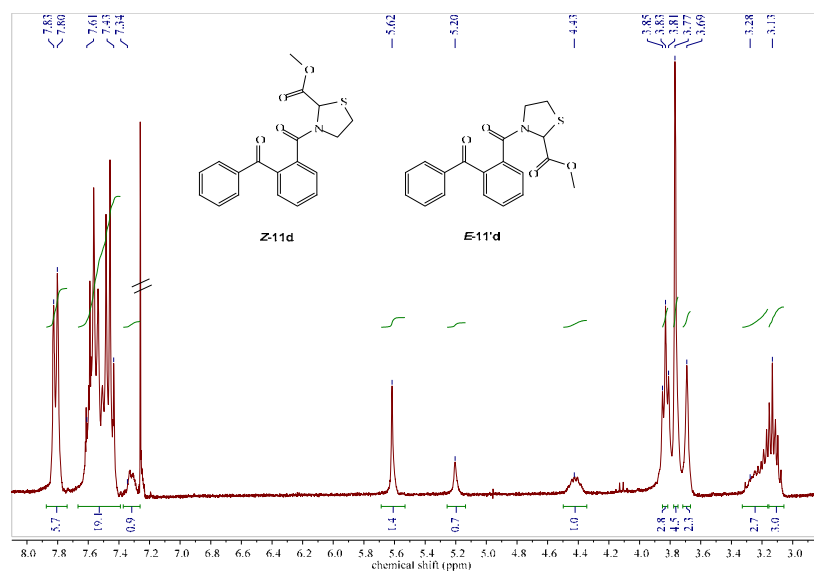
Figure 3.3: ^{1}H-NMR spectrum of a mixture of **11d** and **11'd** after purification (in CDCl$_3$).

The major *Z*-rotamer gives a singlet for the methine (CH*) proton at the chiral center at 5.62 ppm and a singlet for the methyl ester (-CO$_2$CH$_3$) at 3.77 ppm. Two smaller singlets at 5.20 ppm and 3.69 ppm stand for the respective protons of the minor *E*-rotamer **11'd**. The -NCH$_2$group of the minor *E*-form shows a multiplet at 4.43 ppm. For the major *Z*-rotamer, both protons of the -NCH$_2$ group appear as a broad triplet at 3.83 ppm instead. Overlapped signals were observed for the -SCH$_2$ and the aromatics protons. A broad multiplet between 3.0-3.4 ppm represents the -SCH$_2$ group of both *E* and *Z* rotamers. Three separate signals were observed for the aromatic protons: two multiplets at approx. 7.30 ppm (*E*) and between 7.40-7.70 ppm (*E* and *Z*) and a doublet at 7.81 ppm (*E* and *Z*).

The reaction mixture for **12e**, obtained from reaction of **9** and 2-(*tert*-butylthio)ethanamine (**10e**), was subsequently purified by column chromatography. The ^{1}H-NMR spectrum of a pure fraction of **12e** in CDCl$_3$ shows a broad singlet for the -OH group at 5.32 ppm, confirming the presence of the cyclic tautomer form (**Figure 3.4**). The *tert*-butyl hydrogens furnished a large singlet at 1.27 ppm. Likewise, all four hydrogen atoms in the ethylene (-CH$_2$CH$_2$-) bridge give individual signals in the range between 2.20-3.75 ppm. The aromatic groups appear in the region of 7.0-8.0 ppm.
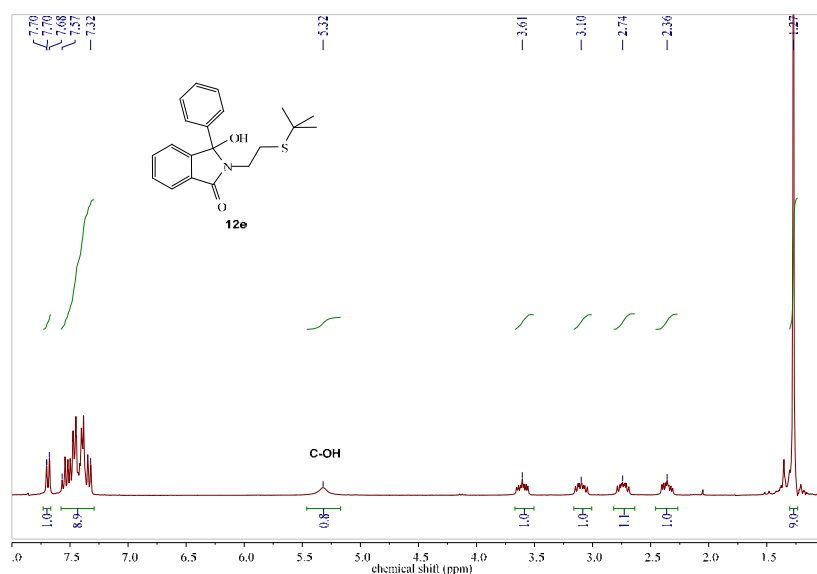
Figure 3.4: ^{1}H-NMR spectrum of the ring tautomer **12e** after purification (in CDCl$_3$).

The ^{13}C-NMR spectrum of **12e** in CDCl$_3$ is likewise shown in **Figure 3.5**. A characteristic peak for the C-OH group, as typically observed in photodecarboxylative additions of carboxylates to phthalimides to form hydroxyisoindolinones [82], is found at 90.9 ppm. The presence of this signal again confirms the cyclic nature of compound **12e**. The remaining, intact C=O group gives a signal at 168.0 ppm. The *tert*-butyl group furnishes two signals at 26.6 for the quaternary carbon and 31.0 ppm for the three equivalent CH$_3$-groups, respectively. Likewise, the ethylene bridge reveals two peaks at 40.4 and 42.6 ppm, respectively. The nine aromatic signals are seen between 122.7 and 149.2 ppm.
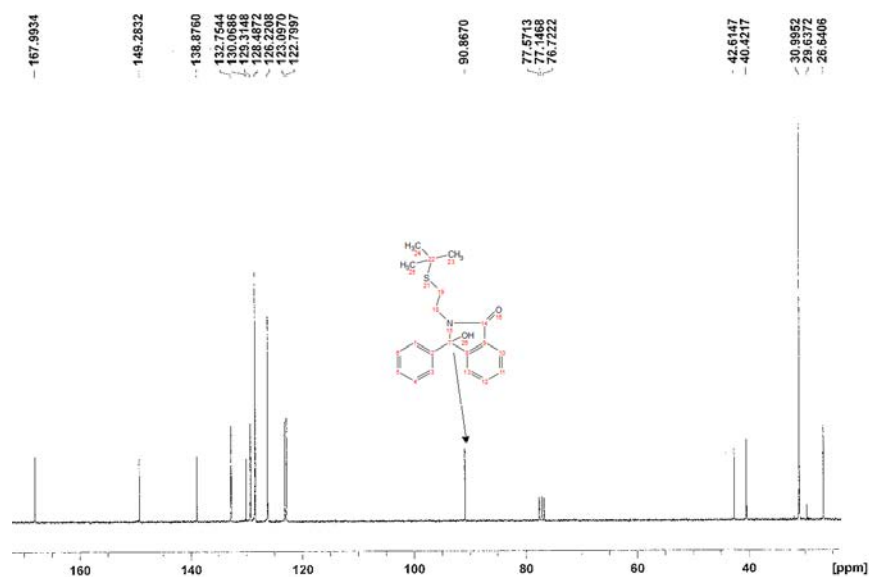
Figure 3.5: ^{13}C-NMR spectrum of the ring tautomer **12e** after purification (in CDCl$_3$).

3.1.5 Synthesis of furanone [Experiment 18]

Furanone was synthesized from furfural (**13**) following a procedure described by Näsman [83].
Hydrogen peroxide was added dropwise to a stirred mixture of furfural, anhydrous sodium
sulfate, *N, N*-dimethylethanolamine (DMAE) and formic acid in dichloromethane (**Scheme
3.7**). After 16 hours of refluxing and subsequent work up, furanone (**14a**) was collected as a
pale yellow oil in a yield of 40%. ^{1}H-NMR analysis of the crude product showed that no further
purification was required.
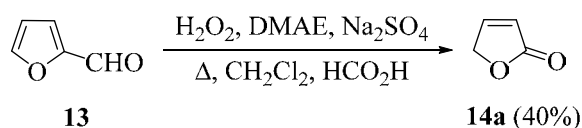
Scheme 3.7: Synthesis of furanone (**14a**) from furfural (**13**).

In CDCl₃, the ^{1}H-NMR spectrum shows three broad signals with poor resolution between 4.5-
8.0 ppm (**Figure 3.6**). The OCH₂-group reveals a narrowly spaced triplet at 4.83 ppm, whereas
the two olefinic =CH–groups occur at 6.05 and 7.56 ppm, respectively.
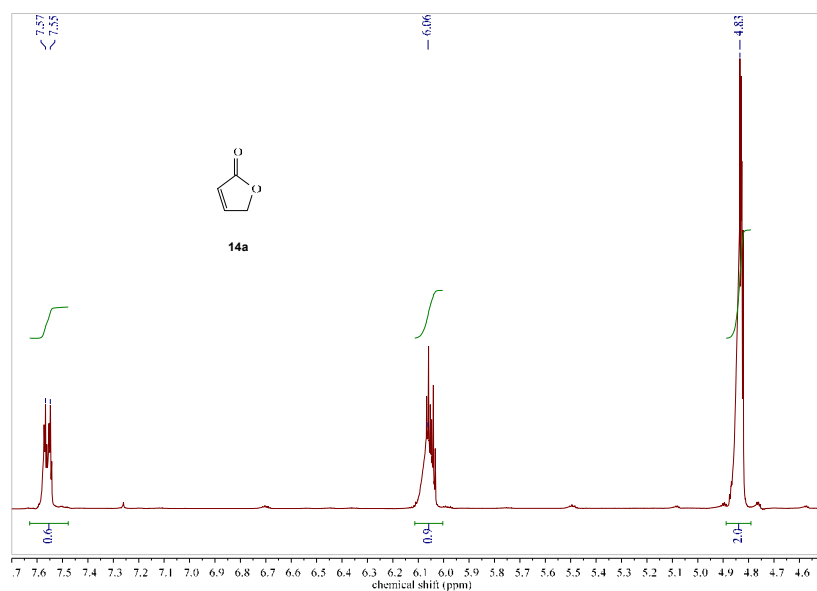
Figure 3.6: ^{1}H-NMR spectrum of furanone (**14a**) (in CDCl₃).

3.1.6 Synthesis of *N*-methylphenylglycine [Experiment 19]

The *N*-methylation of phenyl glycine (**15**) was achieved following a modified procedure by
Gabriel [73]. Phenyl glycine in DMF was initially treated with K₂CO₃, followed by the addition
of methyl iodide and prolonged heating (**Scheme 3.8**). The desired product was obtained as a

colourless oil in a yield of 78%. The structure of **16** was subsequently confirmed by ^{1}H-NMR spectroscopy. In CDCl$_3$, the N-C$\underline{H}_3$ group was observed as a singlet at 2.53 ppm.
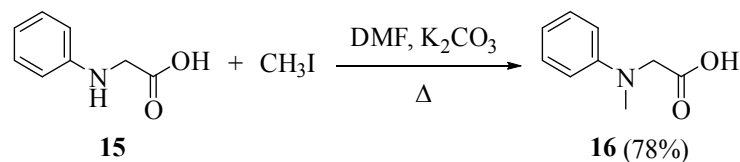
Scheme 3.8: *N*-Methylation of *N*-phenylglycine (**15**).

3.2   Photochemical transformations

3.2.1   Batch set-up

Batch experiments were performed in a Rayonet photochemical chamber reactor (RPR-200; Southern New England Ultraviolet Company, USA) equipped with 16 × 8 W UVA (350 ± 25 nm), UVB (300 ± 25 nm) or cool white (ca. 400-700 nm) fluorescent tubes and a cooling fan. Pyrex (transmission >300 nm) Schlenk flasks with capacities of 60-180 mL were used as reaction vessels. A cold finger was inserted to maintain a reaction temperature below 25°C (**Figure 3.7**). A continuous N$_2$ steam was used for photodecarboxylation reactions, whereas all other reaction mixtures were degassed with N$_2$ for approx. 5 min before capping the reaction vessel. For photodecarboxylations, the reaction was monitored by TLC or a CO$_2$ test using Ba(OH)$_2$. All other photoreactions were monitored by TLC or by ^{1}H-NMR spectroscopy.
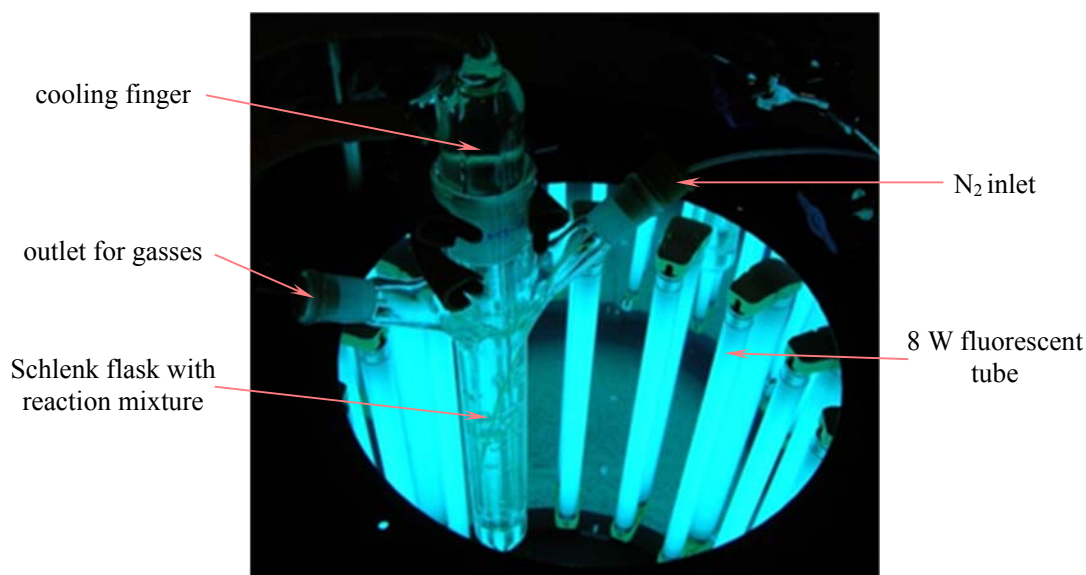
Figure 3.7: Batch chamber photoreactor (Rayonet) with inserted Schlenk flask.

3.2.2   Flow set-ups

Various flow reactors were used during the course of this study. They are described in the following chapter with their key-technical data.

3.2.2.1 In-house capillary reactor

Photoredox catalytic as well as photodecarboxylative additions in continuous flow mode were mainly investigated using a lab built capillary reactor (**Figure 3.8** and **Table 3.3**). The reactor used a fluorinated ethylene propylene (FEP) capillary with an exposed length of 10 m, an inner diameter of 0.8 mm and an internal volume of 5 mL. The capillary was wrapped around a Pyrex body. At its center, the reactor contained a single 8 W fluorescence tube. A small fan was mounted into the base of the reactor column. The whole setup was kept in a light tight box. An additional cooling fan was mounted on the left side of the reactor box. A hanging thermometer allowed for temperature monitoring during operation. A syringe pump was used to transfer the reaction mixture through the capillary tubing. The product solution was collected outside the reactor box in an amber flask.
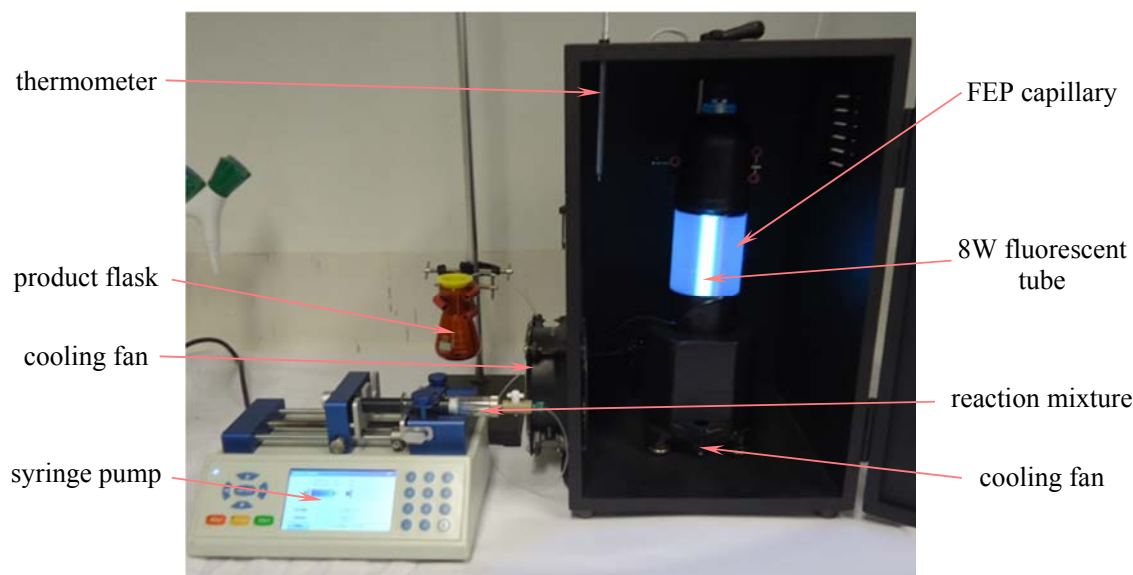
Figure 3.8: In-house capillary reactor.

Table 3.3: Technical data of the in-house capillary reactor.

Tube material	Fluorinated ethylene propylene (FEP)
External diameter	1.58 mm
Internal diameter	0.8 mm
Length of tube	10 m
Volume of tube	5 mL

Pump	Chemyx syringe pump (Model: Fusion 200)
Light source	UVB (300 ± 25 nm)[a] or cool white (ca. 400-700 nm)[b], 8 W each

[a] Used for photodecarboxylative addition reactions. [b] Used for photoredoxreactions.

3.2.2 Vapourtec easy-photochem reactor

The commercially available Vapourtec easy-photochem E-series reactor (**Figure 3.9** and **Table 3.4**) was used for the synthesis of AKS-186. Its integrated setup is highly suitable for exploring tandem photochemical-thermal reactions with automated control of wavelength, flow rate, residence time and reaction temperature. The compact reactor consists of three main components: an easy-Scholar pump with control platform, an E-series cooling module and the UV-150 Photochemical reactor loop. The easy-Scholar unit incorporates three advanced V3 continuous peristaltic pumps that allow operations at flow rates between 0.10 ml·min^{-1} and 10 ml·min^{-1}. The thermal tube reactor cartridge contains a 10 mL perfluoroalkoxy alkane (PFA) reactor coil for optional tandem photochemical-thermal couplings. A reagent and solvent bottle rack is located on the top of the reactor.
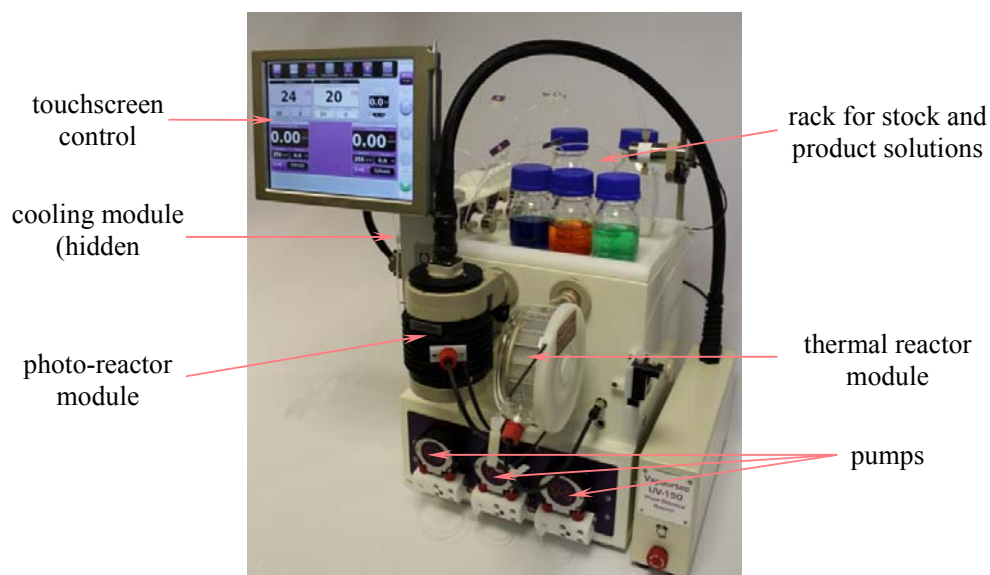
Figure 3.9: Vapourtec easy-photochem module.

The easy-Photochem system is also equipped with an adjustable back-pressure regulator (BPR) and a temperature control module. This cooling unit delivers chilled gas, either nitrogen or compressed air, to the UV-150 irradiation chamber. Within the photochemical module, the reactor room is separated and sealed from the lamp region, thus allowing effective cooling. Depending on the application, the reactor temperature can be varied between -5°C and 80°C.

The UV-150 Photochemical chamber is fitted with a dimmable 150 W medium-pressure pure mercury lamp and a 10 mL fluorinated ethylene propylene (FEP) reactor coil with a wall thickness of 0.15 mm and an internal diameter (ID) of 1.30 mm. The reactor comes with an additional set of three wavelength filters, which can be easily placed between the lamp and the reactor coil. The lamp power can be changed from 75 to 150 W. The whole unit is accompanied by a touchscreen with the necessary control software installed.

For this work, the photoreactor loop was operated with 82 W power to allow for simple cooling with external cooling fans. These kept the temperature inside the photochemical chamber at 32°C. The Type 2 gold filter with a transmittance ranging from 250-390 nm was selected. The temperature of the thermal reactor was set to 50°C.

Table 3.4: Technical data of the Vapourtec easy-photochem reactor.

Tube material	Fluorinated ethylene propylene (FEP)[a] and perfluoroalkoxy alkane (PFA)[b]
External diameter	1.6 mm (FEP)
Internal diameter	1.3 mm (FEP)
Volume of tube	10 mL[a,b]
Pump	three advanced V3 continuous, self-priming, peristaltic pumps
Light source	Medium pressure mercury lamp (type 2 gold filter, 250-390 nm), 82 W
Temperatures	32°C[a], 50°C[b]

[a] Photoreactor loop. [b] Thermal reactor loop.

3.2.2.4 In-house parabolic trough concentrating solar flow reactor

Outdoor photodecarboxylations were studied using an in-house built parabolic trough concentrating solar reactor (**Figure 3.10** and **Table 3.5**). The trough was made from a polished aluminum sheet. A glass tube was positioned in its focal line, which was covered by the reaction capillary. The later consisted of a 27 m long FEP capillary tube with an internal volume of 53 mL. The temperature of the reaction mixture was controlled by flowing tap water through the center of the glass tube. A piston pump was attached to push the reaction mixture through the capillary. A back pressure regulator was used at the outlet to maintain a smooth flow pattern. Reaction and product mixtures were kept in amber flasks underneath the reflector to minimize any reaction outside the capillary. Likewise, the non-exposed tubing was covered with black shrink tube. Illumination data for the days of operations were collected from the photovoltaic station at James Cook University.

Figure 3.10: Parabolic trough concentrating solar flow reactor.

Table 3.5: Technical data of the in-house parabolic trough concentrating solar flow reactor.

Length of internal glass tube	1.2 m
Diameter of glass tube	3 cm
Capillary tube material	Fluorinated ethylene propylene (FEP)
External diameter	3.2 mm
Internal diameter	1.6 mm
Length of tube	27 m
Volume of tube	53 mL
Pump	Ismatec piston pump
Position to sun	manually
Concentrator material	polished aluminum
Concentration factor	3 measured (theoretical= 13)

3.2.2.4 In-house tandem photochemical-thermal continuous flow setup

A lab built three component setup coupled through T-junctions was used for the synthesis of **AL12** and its analogues (**Figure 3.11** and **Table 3.6**). The integrated assembly demonstrates the adoptability and potential of flow chemistry for research based synthesis by overcoming multiple challenges such as solubility, pH, temperature and residence time. Reactant solutions were pumped with syringe pumps at specific positions. Micro-FEP tubing was used for the first and the second loop (each with an I.D. of 0.8 mm, a length of 10 m and an internal volume of 5 mL), whereas a wider tubing diameter was chosen for the third step (I.D. of 1.58 mm, length of 10 m and internal volume of 10 mL). An ultrasonic bath was introduced in the second step

to resolve solubility issues and to prevent precipitation of the dehydration product. An ion exchange resin cartridge was placed between the second and third step to remove excess of acid after the dehydration step. Heating to 80°C was achieved in the third step by employing a water bath. The in-house capillary reactor described in **Chapter3.2.2.1** was used as photochemistry module.
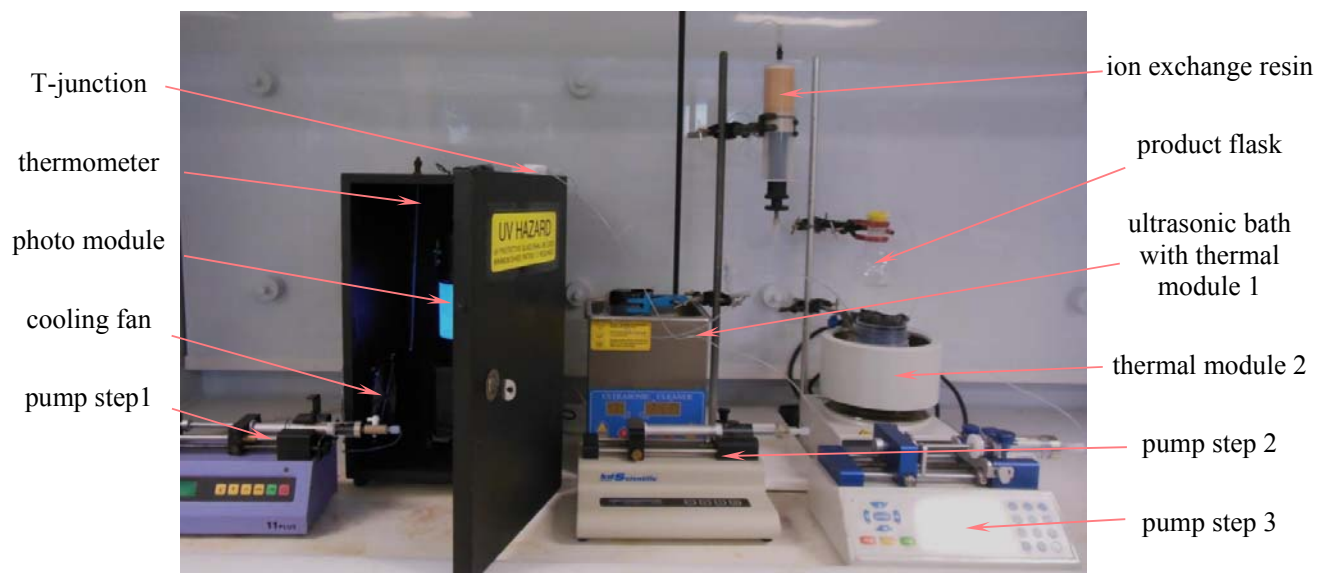
Figure 3.11: Multistep flow reactor setup.

Table 3.6: Technical data of the in-house multistep flow reactor.

Tube material	Fluorinated ethylene propylene (FEP)
External diameter	1.58[a,b]/3.2[c] mm
Internal diameter	0.8[a,b]/1.6[b] mm
Length of tube	10[a,b]/20[c]m
Volume of tube	5[a,b]/10[c] mL
Pumps	Harvard apparatus (Model: 11Plus)[a], kdScientific (Model: KDS-100-CE)[b], Chemyx syringe pump (Model: Fusion 200)[c]
Light source	UVB (300 ± 25 nm; 8 W)[a]

[a] Photo loop. [b] Ultrasonic loop. [c] Thermal heating loop.

3.2.3 Attempted photocyclizations of 4-amino-*N*-alkenylphthalimides and *N*-alkenyl-isatins [Experiments 20-29]

The *N*-alkenyl compounds were dissolved in acetonitrile in a Schlenk flask and irradiated with either UVA or UVB light in a Rayonet chamber reactor. In all cases examined, even prolonged irradiation of up to 54 hours showed no trace of a defined product by TLC or ^{1}H-NMR analysis.

The starting materials were instead recovered in incomplete amounts of 44-63% after this exhaustive irradiation period, suggesting that unselective photodecomposition may have occurred. The results are summarized in **Table 3.7**. Recoveries were not determined for irradiations conducted for 28 hours. In particular, the *N*-alkenylphthalimides **3b** and **c** were exposed to UVA and UVB light for 28 and 48 hours, respectively. Neither of the reactions yielded the anticipated regioisomeric ring-expansion products **17** or **17'** (**Scheme 3.9**). The photoreaction of *N*-alkenylphthalimides **3a** was subsequently not attempted because the suspected photoproduct was considered too strained and thus unstable.
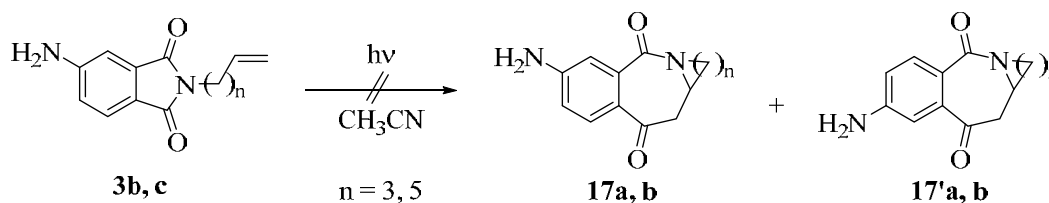
Scheme 3.9: Attempted photocyclizations of **3b** and **c**.

Likewise, acetonitrile solutions of *N*-alkenylisatins **5a** and **5b** were subjected to UVA and UVB irradiation for 28 and 54 hours, respectively. Neither cycloadditions to compounds **18** nor Paternò-Büchi reactions to the oxetanes **19** were observed (**Scheme 3.10**).
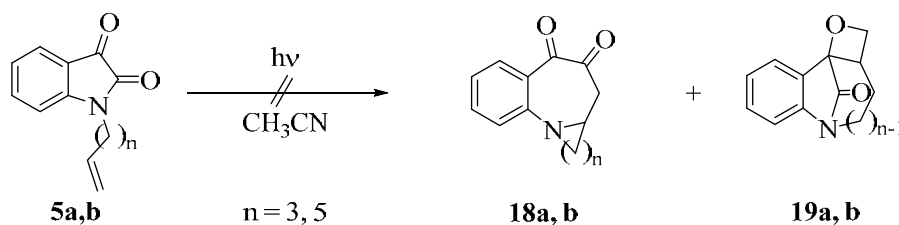
Scheme 3.10: Attempted photocyclizations of *N*-alkenylisatin **5a** and **b**.

Similarly, the *N*-petenyl containing Schiff's base **8**, after dissolving in acetonitrile, was exposed to UVA and UVB radiation for 28 and 54 hours, respectively (**Scheme 3.11**).
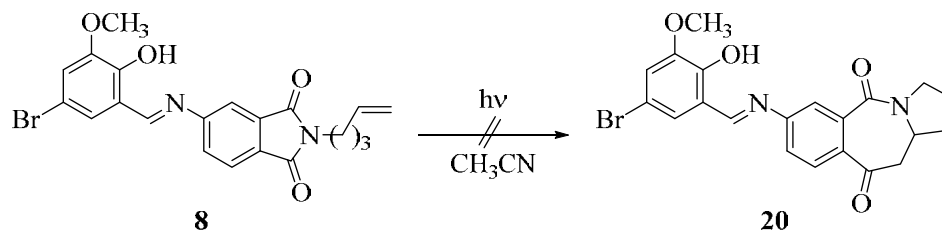
Scheme 3.11: Attempted photocyclization of **8** (regioisomer not shown).

No reaction to the ring-expended cyclization product **20** or its regioisomer (not shown) was again observed and the unreacted starting material was simply recovered

Table 3.7: Attempted intramolecular photocyclizations of **3**, **5** and **8**.

Entry	Imide	Light	Time (hrs)	Recovery (%)
a	3b	UVA	54	44
b		UVB	28	n.d.[a]
c	3c	UVA	54	51
d		UVB	28	n.d.[a]
e	5a	UVA	54	63
f		UVB	28	n.d.[a]
g	5b	UVA	54	57
h		UVB	28	n.d.[a]
i	8	UVA	54	51
j		UVB	28	n.d.[a]

[a] n.d. = not determined.

3.2.4   Attempted intermolecular photodecarboxylative additions of phenylacetates to *N*-methylisatin [Experiments 30-34]

N-Methylisatin (**21**) was irradiated with UVB light for 3 hours in a pH 7 buffer/acetone mixture in the presence of various potassium phenylacetates (**22a-e**), the latter prepared *in situ* from the corresponding carboxylic acid and potassium carbonate. No photodecarboxylative additions to the desired compounds **23** were observed (**Scheme 3.12**). The aldol product **24** of isatin and acetone was instead isolated in yields of 64-75% after column chromatography (**Table 3.8**) [84]. The identity of **24** was confirmed by ^{1}H-NMR spectroscopy [85].
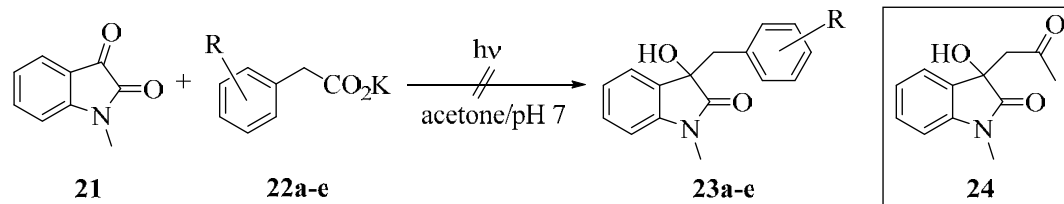
Scheme 3.12: Photoirradiation of *N*-methylisatin (**21**) with phenylacetates (**22a-e**).

Table 3.8: Attempted photodecarboxylative additions to *N*-methylisatin.

Entry	R (22)	Yield of 24 (%)[a]
a	H	70
b	4-CH$_3$	75

Entry	R (22)	Yield of 24 (%)[a]
c	2-CH$_3$	70
d	4-F	71
e	4-Br	64

[a] Isolated yield after column chromatography.

The ^{1}H-NMR spectrum of the aldol product **24** shows a pair of doublets at 2.95 ppm and 3.20 ppm with a ^2J coupling constant of 18 Hz for the methylene (-CH$_2$-) group (**Figure 3.12**). The newly formed -OH group displays a broad singlet at 4.40 ppm. The -COCH$_3$ and -NCH$_3$ groups are found as singlets at 2.18 and 3.30 ppm, respectively. The four aromatic protons give three signals in the range of 6.8 to 7.4 ppm.
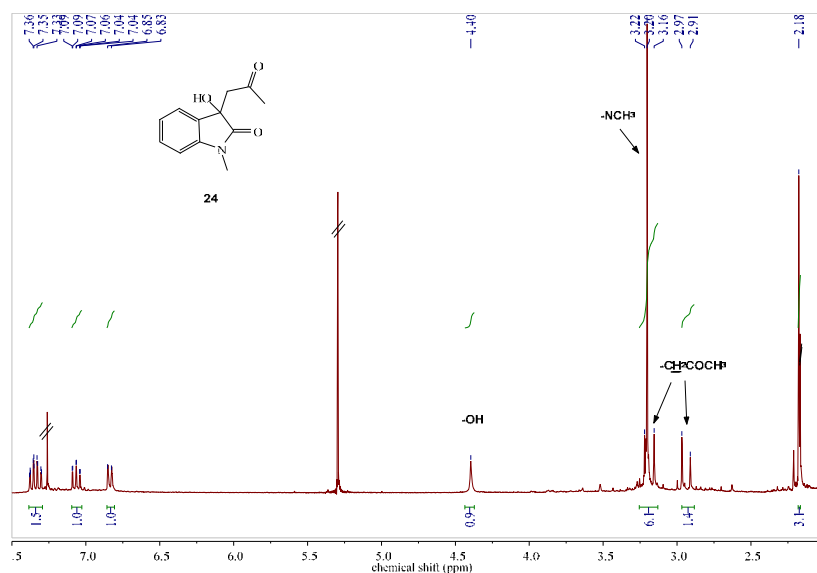
Figure 3.12: ^{1}H-NMR spectrum of the aldol product **24** (in CDCl$_3$).

3.2.5   Photocyclizations of benzoylbenzamides [Experiments 35-39]

Solutions of the respective benzoylbenzamides in acetone were irradiated in Pyrex Schlenk flasks for 4 hours with UVB light. For the ring-tautomeric compounds **12**, it was anticipated that photoreactions may operate from their corresponding open counterparts **11** (**Scheme 3.6**), which would ultimately convert all of the starting materials. For primary amine derived benzoylbenzamides **11a, c** and **e** TLC analyses showed three potential product spots. Column chromatography was subsequently attempted to isolate these suspected products.

As an example, no defined photocyclization products of the open form **11c**, that is neither **25** nor **26**, could be obtained (**Scheme 3.13**). All three fractions collected simply contained the reisolated chain-ring tautomeric forms **11c/12c** of the starting material.
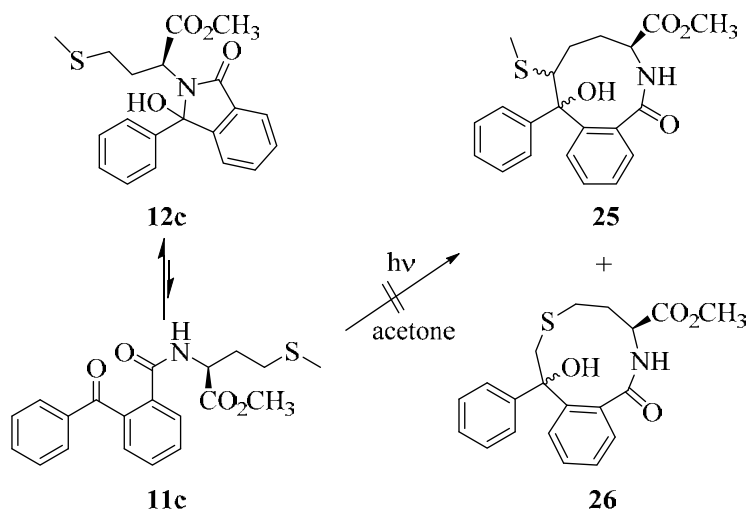
Scheme 3.13: Attempted photocyclization of benzoylbenzamide **11c**.

For the secondary amine derived benzoylbenzamides **11b** and **d**, three new spots appeared during TLC analysis along with the starting material. The reaction mixtures were again separated via column chromatography. In all cases, the first main fraction was found to contain 3-phenylphthalide (**27**). The structure of **27** was unambiguously confirmed by X-ray crystallography (**Figure 3.13**) and NMR spectroscopy.
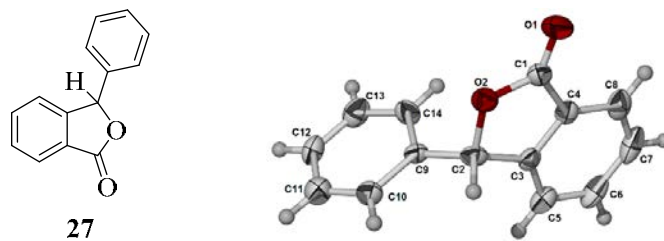
Figure 3.13: Crystal structure of 3-phenylphthalide (**27**).

The ^{1}H-NMR spectrum of 3-phenylphthalide 27 in acetone-d_6 is shown in **Figure 3.14**. The singlet for the characteristic methine -OCHPh group appears at 6.62 ppm, while the multiple aromatic signals emerge between 7.34 ppm and 7.93 ppm, respectively.

^{1}H-NMR and ^{13}C-NMR along with HSQC and HMBC helped in determine the structures of the additional photoproducts obtained by column chromatography. For example, **11/11'b** upon irradiation furnished the regioisomeric cyclization products **28** and **29** in a combined yield of 38% (**Scheme 3.14**). The product ratio was determined by ^{1}H-NMR analysis of the crude product and was found to be approximately 3:1. The major product obtained was **28**, as a pair of diastereoisomers, whereas **29** appeared as a minor product, again as a diasteroisomeric pair.
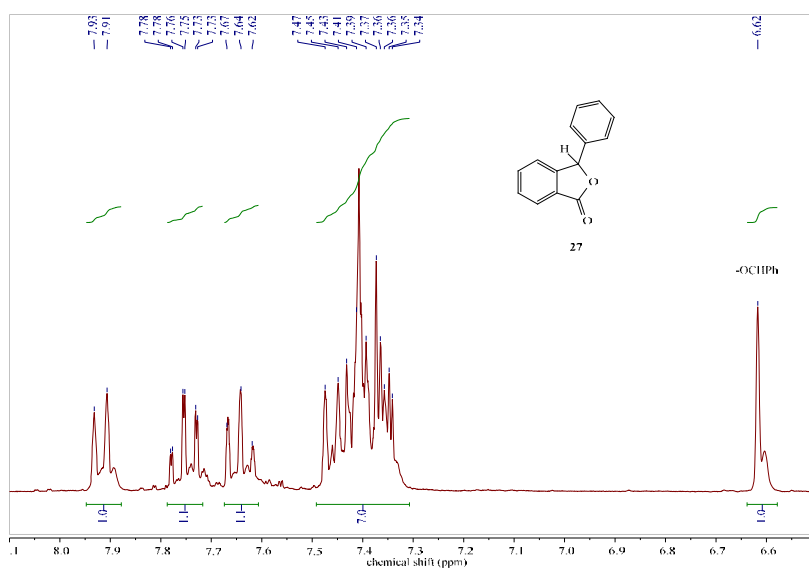
Figure 3.14: ^{1}H-NMR spectrum of **27** (in acetone-d$_6$).
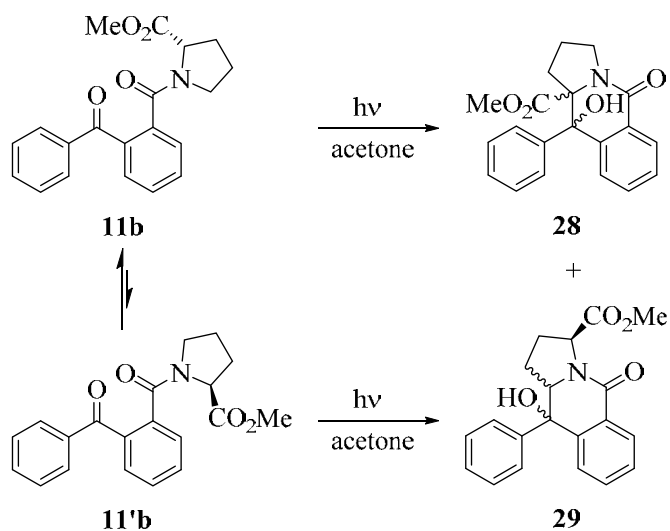
Scheme 3.14: Photocyclization products from the *L*-proline derived benzoylbenzamide **11/11'b**.

Similarly, the methyl thiazolidine-2-carboxylate derived compound **11/11'd** upon irradiation formed the photocyclization products **30** and **31** in a combined yield of 41% (**Scheme 3.15**). Only single diastereoisomers could be obtained for each product. Interestingly, the ratio of the regioisomeric cyclization products **30**:**31** of 3:1 corresponded well to the rotamer ratio **11d:11'd** of 3:1 found for the starting material.
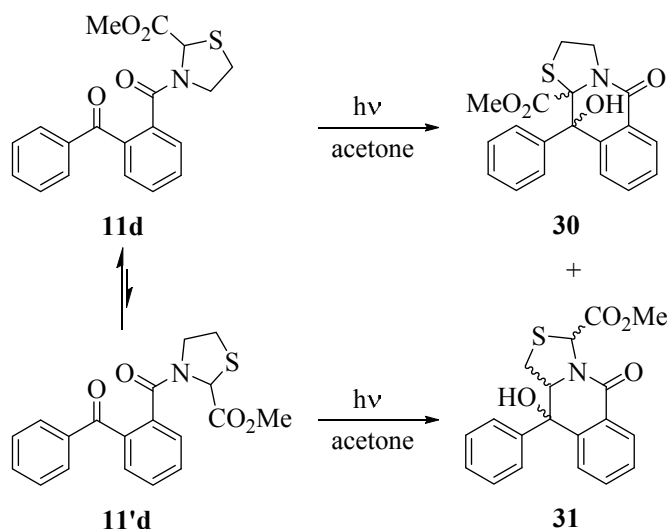
Scheme 3.15: Photocyclization products from the methyl thiazolidine-2-carboxylate derived benzoylbenzamide **11/11'd**.

A representative ^{1}H-NMR spectrum is shown in **Figure 3.15** for one of the fractions obtained. ^{13}C-NMR along with HSQC confirmed the structure as **30** (as a single diastereoisomer).
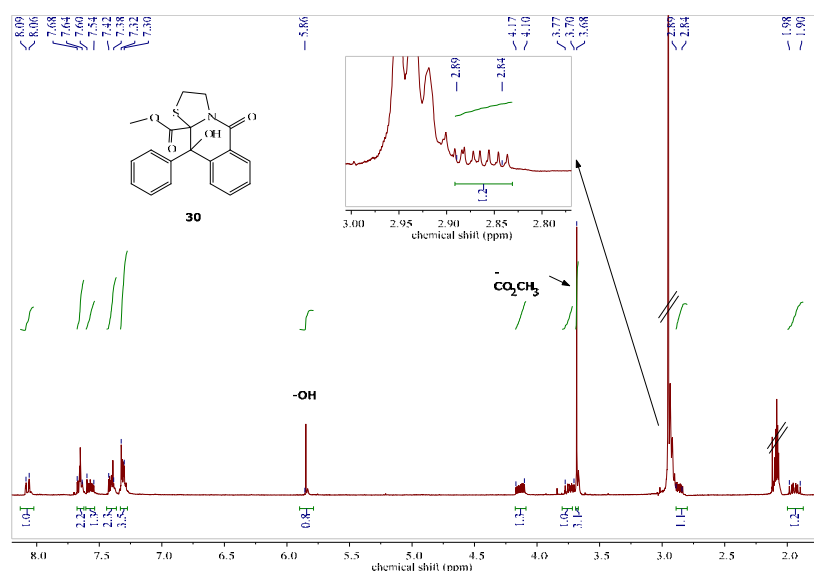
Figure 3.15: ^{1}H-NMR spectrum of photocyclization product **30** (in CDCl$_3$).

Two pairs of complex multiplets belonging to the ethylene bridge (-CH$_2$CH$_2$-) are observed. Of these, the multiplets at 1.94 ppm and 3.73 ppm represent the two non-equivalent -NCH$_2$- protons. Likewise, the second pair of non-equivalent protons of the -SCH$_2$– group appears as multiplets at 2.86 ppm and 4.13 ppm, respectively. The ester group is found as a singlet at 3.68 ppm, whereas the hydroxyl-group gives a broad singlet at 5.86 ppm.

A mixed fraction was furthermore obtained by column chromatography. By subtracting the spectrum of the main component **30** from the ^{1}H-NMR spectrum of this mixture (**Figure 3.16**), the structure of the regioisomeric product **31** was tentatively confirmed. Multiplets at 2.67 ppm, 3.55 ppm and 4.87 ppm represent the three protons in the –NC*HCH$_2$S-bridge. The methine proton at the ester branch (-CHCO$_2$Me) is most likely shown at 5.73 ppm, whereas the -OH group shows a singlet at 5.20 ppm. Likewise, the singlet at 3.80 ppm represents the three hydrogen atoms of the -OCH$_3$ group.
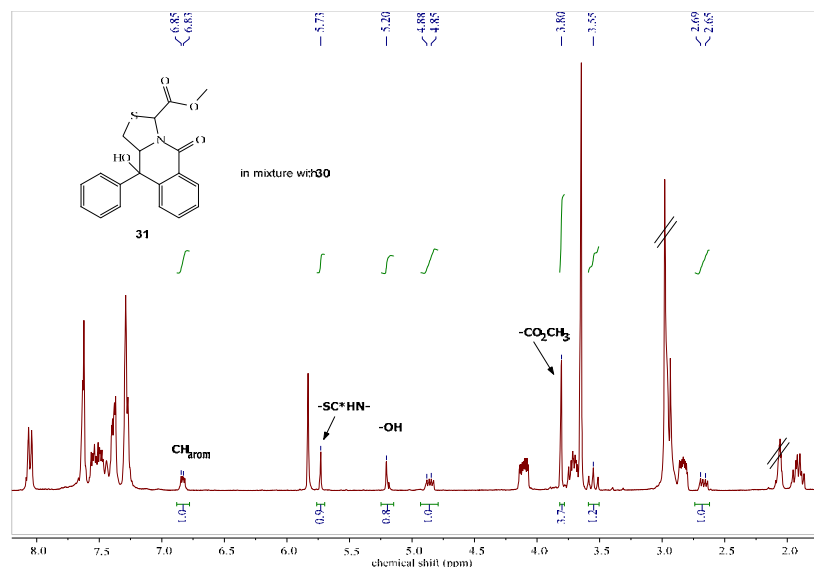
Figure 3.16: ^{1}H-NMR spectrum of a mixture of photocyclization products **30** and **31** (in acetone-d$_6$).

Interestingly, one of the aromatic hydrogen atoms furnishes a narrow multiplet at 6.84 ppm. This upfield shift suggests that the proton is significantly influenced by anisotropy effects of the opposite aromatic ring [86]. Modelling of any of the stereoisomers indeed suggests this effect and an example is shown in **Figure 3.17**.
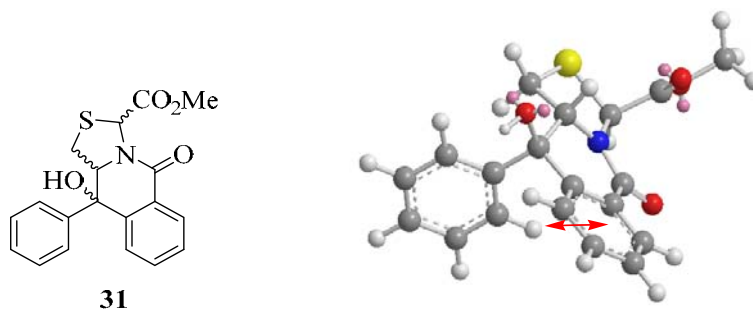
Figure 3.17: Model of a stereoisomer of **31** showing the anisotropy effect (indicated by the red arrow).

Similar shielding effects have been reported for *N*-2-(2-nitro-4, 5-dimethoxyphenyl)-ethylphthalimide, where one methoxy group was closer to the phthalimide group, resulting in a significantly lower chemical shift than the unaffected methoxy group [87].

3.2.6 Photoredox reactions of *N*-phenylglycines and enones under batch and flow conditions [Experiments 40-62]

A mixture of *N*-phenylglycine, furanone and Ru-catalyst in acetonitrile was exposed to cool white light inside a Pyrex Schlenk flask. The reaction furnished the photodecarboxylative addition products **32** and **33** and their structures were confirmed by ^{1}H-NMR spectroscopy (**Scheme 3.16**).
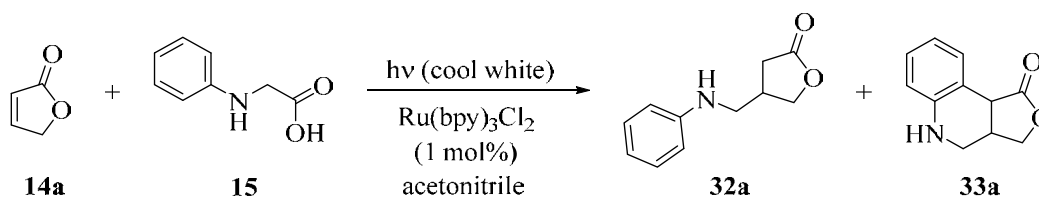
Scheme 3.16: Photoredox reaction of *N*-phenylglycine (**15**) with furanone (**14a**).

The initial crude reaction mixture contained unreacted starting material as well as the photocatalyst. Column chromatography was thus carried out to obtain pure product. The ^{1}H-NMR spectrum of the pure open product **32a** is shown in **Figure 3.18**.

Figure 3.18: ^{1}H-NMRspectrum of the open product **32a** (in CDCl$_3$).
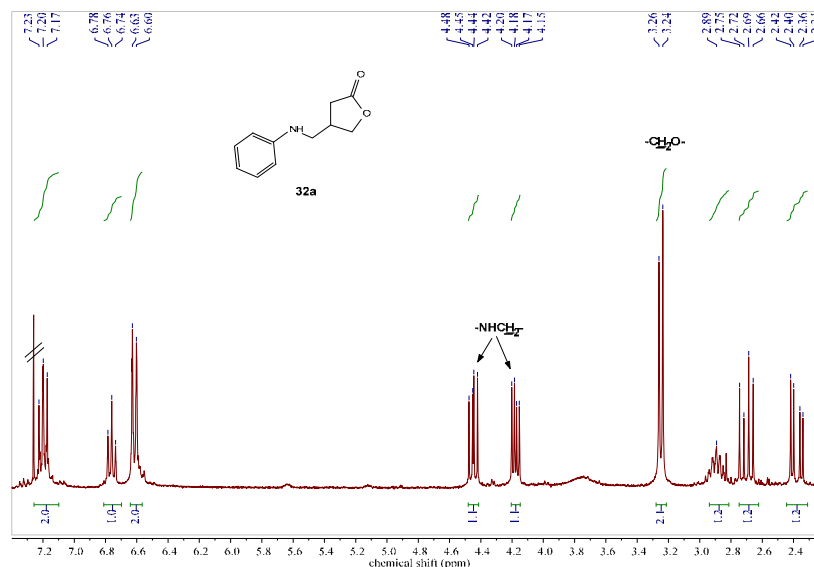
The chiral methine proton (-C$\underline{H}$-) displays a complex multiplet at 2.85 ppm. A pair of doubles of doublets appears at 2.37 ppm and at 2.68 ppm, representing the -C$\underline{H_2}$CO-group. Likewise, an additional pair of doubles of doublets is found at 4.16 ppm and 4.43 ppm for the two non-equivalent protons of -C$\underline{H_2}$O-group. A doublet at 3.23 ppm stood for the methylene bridge (-NC$\underline{H_2}$-). Three signals for aromatic protons appeared between 6.40 to 7.26 ppm. The NH-proton could not be clearly identified.

The ^{1}H-NMR spectrum of the corresponding cyclized product **33a** is shown in **Figure 3.19**. The two bridging -C$\underline{H_2}$- protons appear as two doublets at 3.36 ppm and 3.69 ppm, respectively. A multiplet for the -NC$\underline{H_2}$-bridge is found at 2.99 ppm. Two doublets of doublets at 4.22 ppm and 4.45 ppm represent the -C$\underline{H_2}$O-group. The aromatic protons appear as doubles or doublets of doublets between 6.56 and 7.45 ppm. Again, the NH proton could not be assigned.
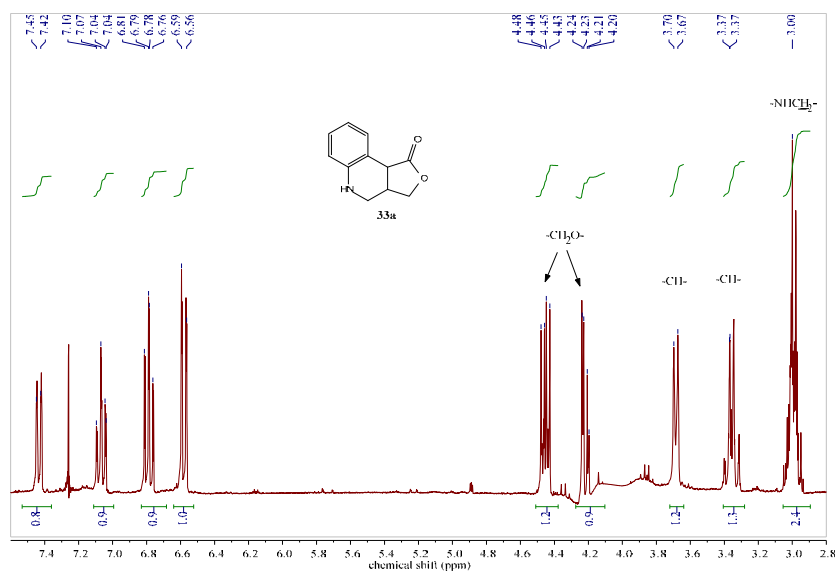
Figure 3.19: ^{1}H-NMR of cyclized product **33a** (in CDCl$_3$).

The reaction was further repeated in four different solvents and up to 24 hours of irradiation. ^{1}H-NMR spectra were recorded after regular intervals to determine conversions and product compositions (**Table 3.9**). No reaction was observed in DMF, whereas the solvent-derived by-products **34** and **35** were found in ethanol and isopropanol (**Scheme 3.17**) [64]. No further progress was observed after 18 hours of irradiation in acetonitrile and the conversion remained at 78%.

Table 3.9: Solvent and irradiation time study.

Entry	Solvent	Time (h)	Conversion (%)[a]
a	Acetonitrile	18	78
b	Ethanol	24	by-product **34**

Entry	Solvent	Time (h)	Conversion (%)[a]
c	Isopropanol	24	by-product **35**
d	DMF	24	n.r.[b]

[a] Based on ^{1}H-NMR analysis. [b] n.r. = no reaction.
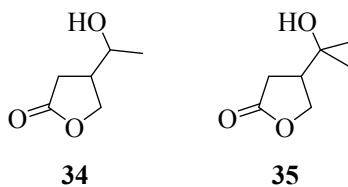
Scheme 3.17: Structures of solvent-derived by-products **34** and **35**.

After the initial solvent optimization, the photocatalyst and its loading were subsequently investigated. After a total irradiation of 18 hours, the conversion rates were determined by ^{1}H-NMR analysis. The results are summarized in **Table 3.10**. Decreasing the amount of ruthenium catalyst to 0.5 mol% led to a decrease in conversion to 35%, while doubling the loading to 2 mol% showed no further increase in the conversion. No reaction was observed in the presence of 4, 4'-dimethoxybenzophenone (DMBP) or methyl orange.

Table 3.10: Catalyst screening and loading study.

Entry	Catalyst	Loading (mol%)	Conversion (%)[a]
a	Ru(bpy)$_3$Cl$_2$	0.5	35
b	Ru(bpy)$_3$Cl$_2$	1	78
c	Ru(bpy)$_3$Cl$_2$	2	78
d	DMBP	1	n.r.[b]
e	methyl orange	1	n.r.[b]

[a] Based on ^{1}H-NMR analysis. [b] n.r. = no reaction.

The photodecarboxylative addition reaction was subsequently attempted with other glycine derivatives and thioether containing acetic acids (**Table 3.11**). No reaction was observed for any of these compounds.

Table 3.11: Carboxylic acid screening study.

Entry	Reactant	Yield (%)
a	*N*-phenylglycine	72 (combined)
b	*N*-acetylglycine	n.r.[a]
c	*N,N*-dimethylglycine	n.r.[a]
d	*N,N*-dimethylphenylglycine	n.r.[a]

Entry	Reactant	Yield (%)
e	(phenylthio)acetic acid	n.r.[a]
f	*p*-amino(phenylthio)acetic acid	n.r.[a]

[a] n.r. = no reaction.

The photocatalytic reactions involving *N*-phenylglycines **15** and **16** were furthermore broadened to other enones (**Scheme 3.18**). The crude products obtained were purified by column chromatography. With the exemption of 5-ethoxyfuranone (**14d**), mixtures of both open chain and cyclized products were obtained in combined yields of 65-76% (**Table 3.12**). The cyclization product **33** was obtained as the main or sole product in all cases.
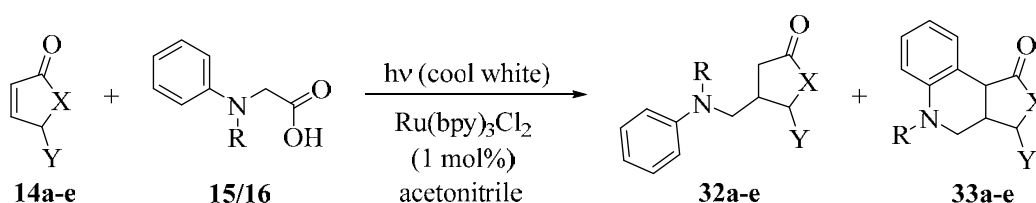
Scheme 3.18: Photoredox reaction of *N*-phenylglycines with enones.

Table 3.12: Photoredox-catalyzed decarboxylations.

Entry	R	14		Time (h)	Yield (%)	
		X	Y		32	33
a	H	O	H	18	21	51
b	H	CH_2	H	18	70[a] (99:1)	
c	H	$(CH_2)_2$	H	18	75[a] (99:1)	
d	H	O	OCH_2CH_3	18	n.d.[b]	65
e	CH_3	O	H	18	21	55

[a] Combined yields. Ratios given in brackets. [b] n.d. = not detected.

Selected examples of photoredox decarboxylations (**Scheme 3.19**) were furthermore investigated under continuous flow conditions using the in-house reactor described in **Figure 3.8** and **Table 3.3**.
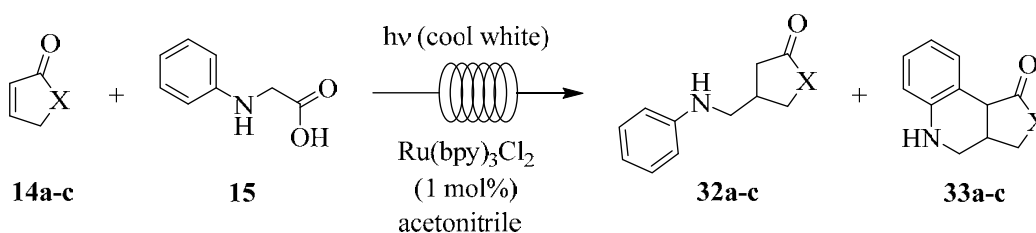
Scheme 3.19: Photoredox catalyzed additions of *N*-phenylglycine to enones in flow.

Transferring the reaction protocol from batch to flow mode caused a significant reduction in reaction times from 18 to 3 hours (**Table 3.13**). Flow operation was also found to be more economical in terms of the light source applied. In particular, the flow reactor utilized a single 8 W fluorescent tube, whereas the larger Rayonet reactor employed 16×8 W tubes instead.

Table 3.13: Photoredox catalysis in flow.

Entry	X	Residence Time (h)	Yield (%) 31	32
a	O	3	23	51
b	CH_2	3	67[a] (99:1)	
c	$(CH_2)_2$	3	69[a] (99:1)	

[a] Combined yields. Ratios given in brackets.

3.2.7   Synthesis of AL12, AL5 and their analogues under batch conditions

3.2.7.1 Photodecarboxylative addition of phenylacetates to *N*-alkylphthalimide under batch conditions [Experiments 63-78]

The previously established procedure for the photodecarboxylative addition of carboxylates to phthalimide was slightly modified for this study [82]. Since hydroxide (HO^-) is formed during the course of the reaction a pH 7 buffer was used instead of water in order to minimize any alternative nucleophilic substitution (S_N) reactions [88]. Mixtures of *N*-bromoalkylphthalimides and phenylacetates in acetone/pH 7 buffer were subsequently irradiated for 3 hours in a Pyrex flask using 300 ± 25 nm light (**Scheme 3.20**). Most products **37a-p** were obtained as colourless crystalline solids in good to excellent yields of 63-91% (**Table 3.14**).
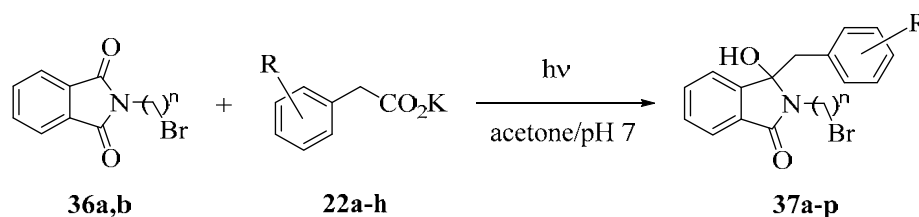
Scheme 3.20: Photodecarboxylative addition of phenylacetates to *N*-bromoalkylphthalimides.

A representative ^{1}H-NMR spectrum for compound **37a** is shown in **Figure 3.20**. Two doublets at 3.13 ppm and 3.51 ppm with a germinal coupling of $^2J = 18$ Hz are observed for the benzylic methylene group (-C$\underline{H}_2$Ph). Three multiplets at 3.66 ppm, 3.76 ppm and 4.13 ppm represent the four ethylene protons (-C$\underline{H}_2$C$\underline{H}_2$Br). The aromatic protons appear between 6.65 and 7.63 ppm. The signal for the -O$\underline{H}$ could not be observed.
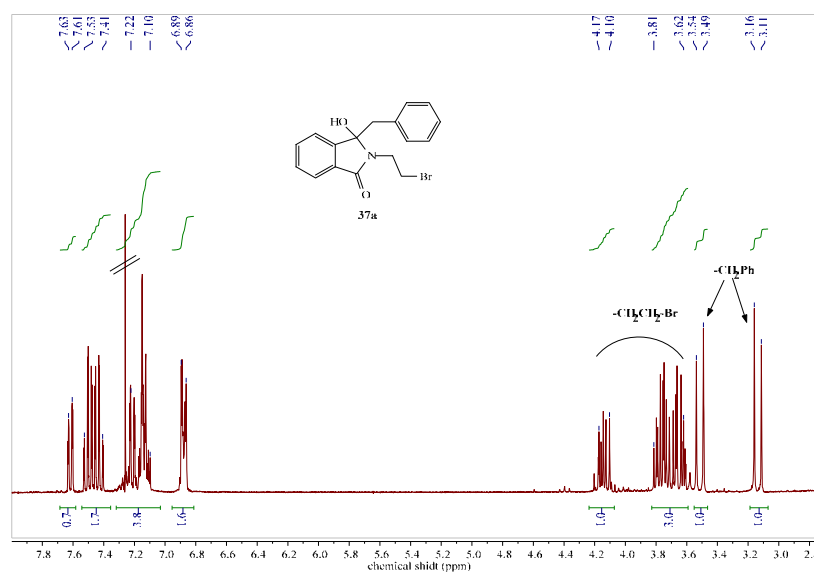
Figure 3.20: ^{1}H-NMR spectrum of photoproduct **37a** (in CDCl$_3$).

Table 3.14: Photodecarboxylative addition of phenylacetates to phthalimides.

Entry	R	n	^{13}C-NMR^a (ppm)	Yield (%)
a	H	2	91.0	87
b	4-F	2	90.0	83
c	4-Cl	2	90.0	79
d	4-Br	2	91.5	63
e	4-CH$_3$O	2	91.9	85
f	4-CH$_3$	2	90.2	88
g	2-CH$_3$	2	91.7	71
h	3-CH$_3$	2	91.2	66
i	H	3	90.1	95
j	4-F	3	93.1	75
k	4-Cl	3	90.0	80
l	4-Br	3	90.5	73
m	4-CH$_3$O	3	89.2	76
n	4-CH$_3$	3	90.3	89
o	3-CH$_3$	3	90.1	73
p	2-CH$_3$	3	91.0	91

^{a} ^{13}C-NMR signal of the C-OH.

The structures of the photoaddition products **37a** and **37b** were unambiguously confirmed by X-ray crystallography (**Figure 3.21**).
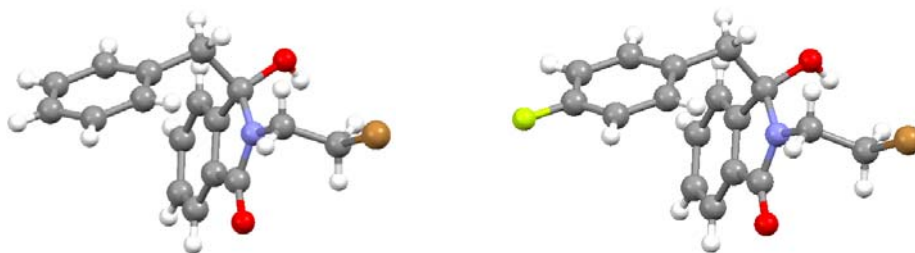
Figure 3.21: Crystal structures of photoaddition products **37a** and **37b**.

3.2.7.2 Dehydration of photoproduct under batch conditions [Experiments 79-94]

Dehydration of the photoproducts **37a-p** obtained in **Chapter 3.2.7.1** was achieved at room temperature in dichloromethane (DCM) and in the presence of catalytic amounts of sulfuric acid. The protocol yielded oily products that crystalized upon standing in excellent yield of 83-95% (**Scheme 3.21** and **Table 3.15**). ^{1}H-NMR analyses revealed that the dehydration products **38a-p** were obtained as *E/Z* mixtures, with the *E*-isomer as the major or sole component.
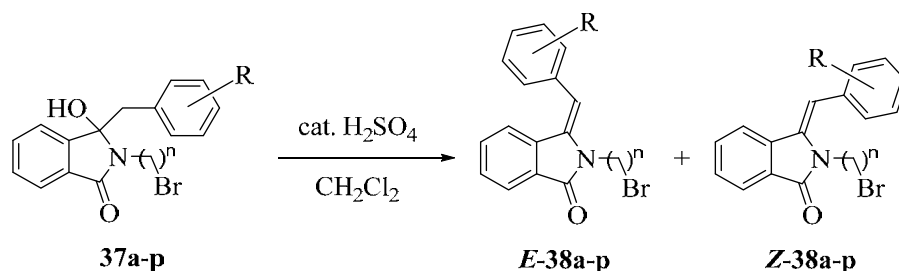
Scheme 3.21: Dehydration of photoproducts.

Table 3.15: Experimental results of the dehydration experiments.

Entry	R	n	^{1}H-NMR[a] (ppm)	*E:Z*[b]	Yield (%)
a	H	2	6.65	91:9	91
b	4-F	2	6.60	100:0	85
c	4-Cl	2	6.53	100:0	88
d	4-Br	2	6.55	99:1	83
e	4-CH$_3$O	2	6.60	100:0	90
f	4-CH$_3$	2	6.59	99:1	94
g	2-CH$_3$	2	6.56	99:1	90
h	3-CH$_3$	2	6.60	100:0	83
i	H	3	6.60	99:1	83
j	4-F	3	6.54	99:1	91
k	4-Cl	3	6.39	99:1	90
l	4-Br	3	6.49	99:1	84
m	4-CH$_3$O	3	6.77	98:2	95

Entry	R	n	^{1}H-NMR^a (ppm)	$E:Z^b$	Yield (%)
n	4-CH$_3$	3	6.58	99:1	92
o	3-CH$_3$	3	6.58	99:1	83
p	2-CH$_3$	3	6.51	99:1	92

^{a} ^{1}H-NMR signal of the olefinic =CH-Ar for the main stereoisomer. ^{b} Determined by ^{1}H-NMR analysis (±3%).

The structure of the dehydration product **E-38a** was furthermore confirmed by X-ray crystallography (**Figure 3.22**). Remarkably, the phenyl-group is positioned almost perpendicular to the isoindolinone ring.
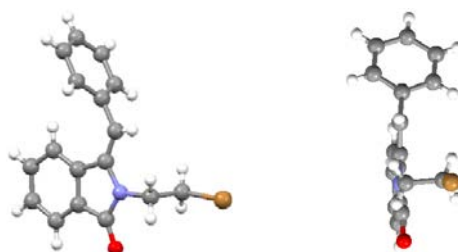
Figure 3.22: Crystal structure of **E-38a**. Side view and front view.

The ^{1}H-NMR of **38a** is exemplarily shown in **Figure 3.23**. Two triplets appeared at 3.45 ppm and 4.12 ppm for the ethylene (-CH$_2$CH$_2$Br) and a singlet at 6.43 ppm for the olefinic proton (=CHPh) of the major *E*-isomer of **38a**.
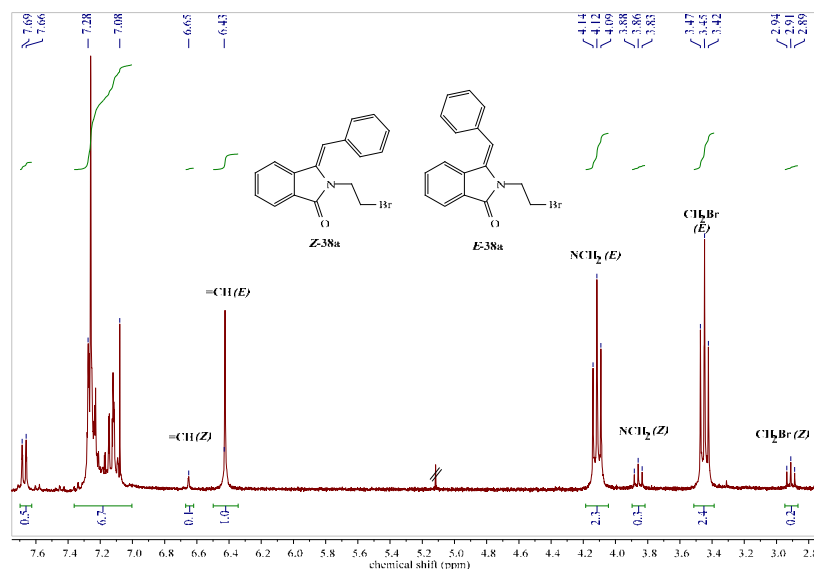
Figure 3.23: ^{1}H-NMR spectrum of dehydration product **39a** (in CDCl$_3$).

The corresponding signals of the minor *Z*-isomer were found as two triplets at 2.91 ppm and 3.86 ppm and a singlet at 6.65 ppm, respectively. The aromatic protons of both isomers appeared between 7.08-7.69 ppm.

3.2.7.3   Amination of dehydrated product under batch conditions [Experiments 95-118]

A modified procedure by Jiang and coworkers was followed for the final amination step [89]. The dehydrated products from **Chapter 3.2.7.2** were heated in the presence of the respective secondary amines and K_2CO_3 in DMF (**Scheme 3.22**). Subsequent workup and isolation furnished the biologically active compounds **AL12**, **AL5** and their analogues as oily or solid products in moderate yields of 49-61% (**Figure 3.16**). Interestingly, the Z-isomer of **39a-x** was formed as the sole product in almost all cases as confirmed by ^{1}H-NMR analyses and by comparison with literature data [90].
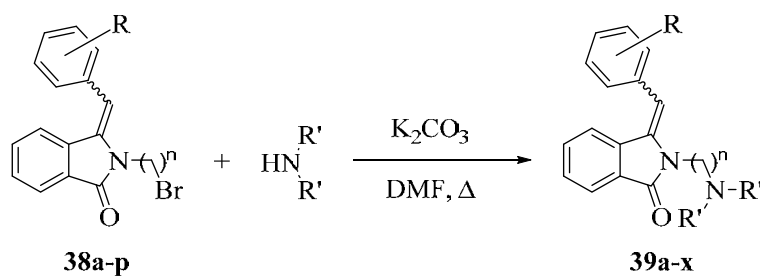
Scheme 3.22: Amination of dehydrated products.

Table 3.16: Amination of dehydrated products under batch conditions.

Entry	R	R'	n	E:Z[a]	Yield (%)
a	H	C_2H_5	2	0:100	55
b	4-F	C_2H_5	2	0:100	55
c	4-Cl	C_2H_5	2	0:100	53
d	4-Br	C_2H_5	2	0:100	51
e	4-CH$_3$O	C_2H_5	2	1:99	50
f	4-CH$_3$	C_2H_5	2	0:100	57
g	2-CH$_3$	C_2H_5	2	0:100	58
h	3-CH$_3$	C_2H_5	2	0:100	51
i	H	C_2H_5	3	1:99	53
j	4-F	C_2H_5	3	0:100	57
k	4-Cl	C_2H_5	3	0:100	60
l	4-Br	C_2H_5	3	0:100	59
m	4-CH$_3$O	C_2H_5	3	0:100	55
n	4-CH$_3$	C_2H_5	3	0:100	58
o	3-CH$_3$	C_2H_5	3	0:100	49
p	2-CH$_3$	C_2H_5	3	0:100	61
q	H	CH_3	2	0:100	58
r	4-F	CH_3	2	0:100	57

Entry	R	R'	n	$E:Z^a$	Yield (%)
s	4-Cl	CH$_3$	2	0:100	55
t	4-CH$_3$O	CH$_3$	2	0:100	49
u	4-CH$_3$	CH$_3$	2	0:100	60
v	H	CH$_3$	3	0:100	58
w	4-F	CH$_3$	3	0:100	55
x	2-CH$_3$	CH$_3$	3	0:100	53

^{a} Determined by ^{1}H-NMR analysis (±3%).

An example of a ^{1}H-NMR spectrum of an aminated product obtained after column chromatographic separation is shown in **Figure 3.24** for the Z-isomer of **39a**. A triplet for the six methyl protons (2 × -C$\underline{H}_3$) and a quartet for the four methylene protons (2 × –NC$\underline{H}_2$–) appeared at 1.08 ppm and at 2.65 ppm. The olefinic =CH–Ph was found at 6.62 ppm. The presence of trace amounts of the corresponding E-isomer of **39a** cannot be excluded due to multiple minor signals in the NMR spectrum.
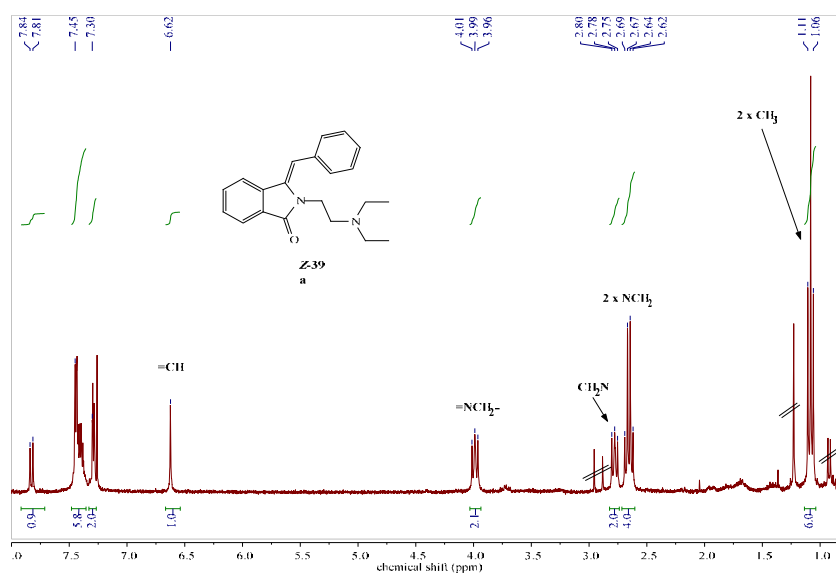
Figure 3.24: ^{1}H-NMR spectrum of **Z-39a** (in CDCl$_3$).

The structure of the amination product **Z-39a** was furthermore established by x-ray crystallography (**Figure 3.25**). The phenyl-group is positioned almost perpendicular to the isoindolinone ring on top of one of the N-ethyl groups of the sidechain.
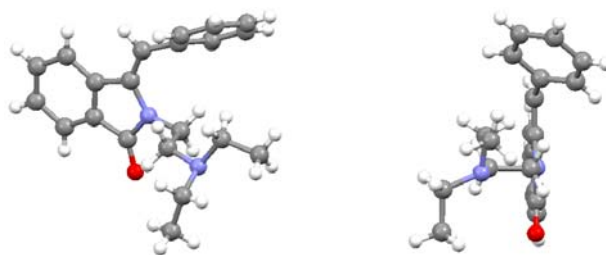
Figure 3.25: Crystal structure of **Z-39a**. Side view and front view.

3.2.8   Synthesis of AL12, AL5 and their analogues in flow [Experiment 119-125]

3.2.8.1   Solvent optimization for multistep continuous flow setup

Under batch conditions, the photodecarboxylation, dehydration and amination steps were performed in three different solvents, *i.e.* acetone/pH7 buffer, dichloromethane and DMF. Since a switch of solvents is difficult under continuous flow conditions, it was necessary to identify a common solvent for all three reaction steps. Therefore, each step for the synthesis of **39a** was repeated separately in batch in acetone, DMF and/or acetonitrile (**Table 3.17**).

Table 3.17: Solvent optimization study for the synthesis of **39a**.

Entry	Step	Solvent	Time (h)	Conversion (%)[a]
a	Photodecarboxylation	acetonitrile[b]	3	80
b		DMF[b]	3	45
c	Dehydration	acetone	5	37[c]
d		acetonitrile	5	83
e		DMF	5	80
f	Amination	acetone	5	46
g		acetonitrile	5	53

[a] Based on ^{1}H-NMR analysis. [b] With pH7 buffer as co-solvent. [c] **40** as a by-product.

The aldol-condensation product of acetone (**40**) was obtained as a by-product when acetone was used in the acid catalyzed dehydration step (**Scheme 3.23**). In contrast, pH7 buffer/DMF gave a low conversion rate of 45% for the photodecarboxylation step. Overall, acetonitrile was found to be the most suitable solvent as it gave acceptable to good conversions for all three reaction steps without the formation of noticeable by-products.

40
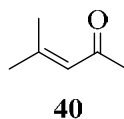
Scheme 3.23: Aldol condensation product of acetone (**40**).

3.2.8.2 Photodecarboxylative addition of phenylacetates to *N*-alkylphthalimides under flow conditions [Experiments 126-140]

Representative examples of photodecarboxylative addition reactions were carried out under flow conditions to compare the efficiency of each technique (**Scheme 3.24**). The results are summarized in **Table 3.18**. The flow reactor proved to be highly efficient with 100% conversion and 80-95% isolated yields with a residence time of 20 minutes in pH7 buffer/acetone. Reactions were again performed in pH7 buffer/acetonitrile as it was previously found to be the most suitable solvent for all three reaction steps. The residence time was extended to 30 min. Good to high conversions and yields of 83-91% were finally obtained.
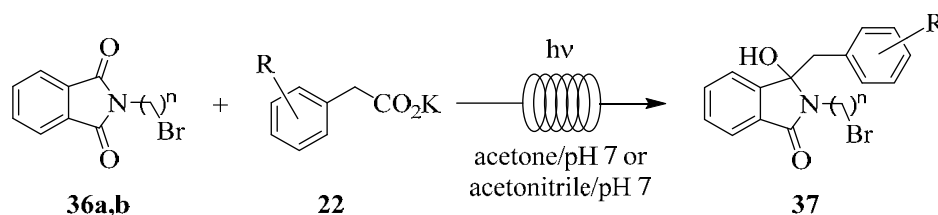
Scheme 3.24: Photodecarboxylative additions of phenylcarboxylates to *N*-bromoalkylated phthalimides in flow.

Table 3.18: Photodecarboxylative addition under flow conditions.

Entry	R	N	Solvent[a]	Residence Time (min)	Yield (%)
a	H	2	acetone	20	87
b	H	2	acetonitrile	30	83
c	4-CH$_3$O	2	acetone	20	85
d	4-CH$_3$O	2	acetonitrile	30	85
e	H	3	acetone	20	95
f	H	3	acetonitrile	30	91
g	4-CH$_3$	3	acetone	20	80
h	4-CH$_3$	3	acetonitrile	30	83
i	4-F	3	acetone	20	89
j	4-F	3	acetonitrile	30	90

[a] With pH7 buffer as co-solvent.

After optimizing the initial photodecarboxylation to complete conversion, the flow step was coupled with the dehydration step for selected examples (**Scheme 3.25**). Again the reaction proceeded in excellent yields of 83-94% with a residence time of 20 minutes in the microflow reactor kept in ultrasonic bath (**Table 3.19**).
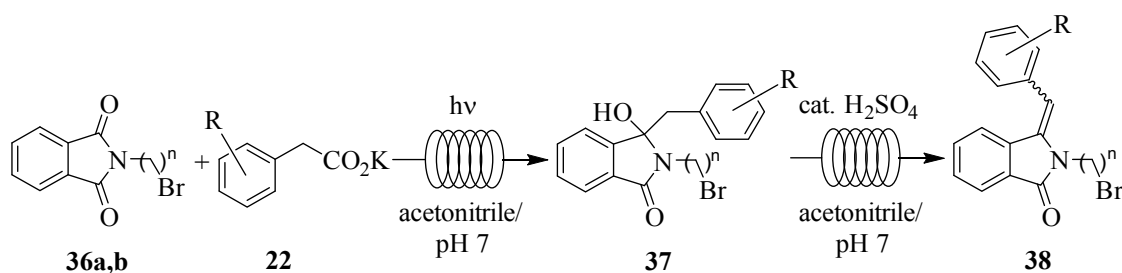
Scheme 3.25: Photodecarboxylation-dehydration in flow.

Table 3.19: Tandem photodecarboxylation and dehydration step underflow conditions.

| Entry | R | n | Residence Time (min) | | Yield (%) |
			Photodecarboxylation	Dehydration	
a	H	2	30	20	91
b	4-CH$_3$O	2	30	20	90
c	H	3	30	20	83
d	4-CH$_3$	3	30	20	86
e	4-F	3	30	20	94

3.2.8.3 In series multistep flow synthesis of AL12, AL5 and their analogues

[Experiments 141-145]

The combined photochemical-thermal-thermal flow setup was designed as shown in **Figure 3.26**. The initial photodecarboxylative addition was performed in the photoreactor module. Subsequent dehydration was achieved in a flow module in an ultrasound bath to prevent clogging. The excess of acid was neutralized using a packed column of anion exchange resin. The final amination was realized in a thermal module in a boiling water heating bath. The actual reactor setup is shown in **Figure 3.11** and described in **Table 3.6**.
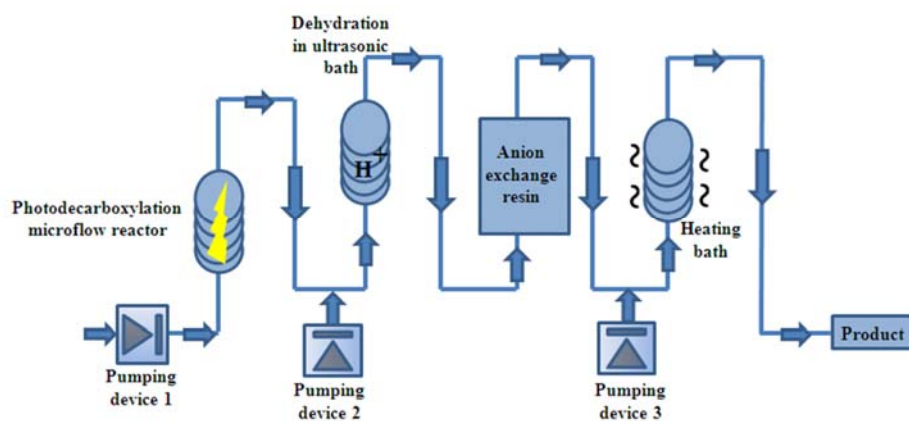
Figure 3.26: Multistep reactor flow chart.

Using the reactor, the continuous flow synthesis of the patented local anesthetics **AL12**, **AL5** and their analogues was successfully achieved (**Scheme 3.26**). The integrated assembly rapidly provided the target compounds in overall yields of 73-77%. Compared to the stepwise batch process, the single-flow protocol gave higher yields in much shorter operation times (**Table 3.20**).
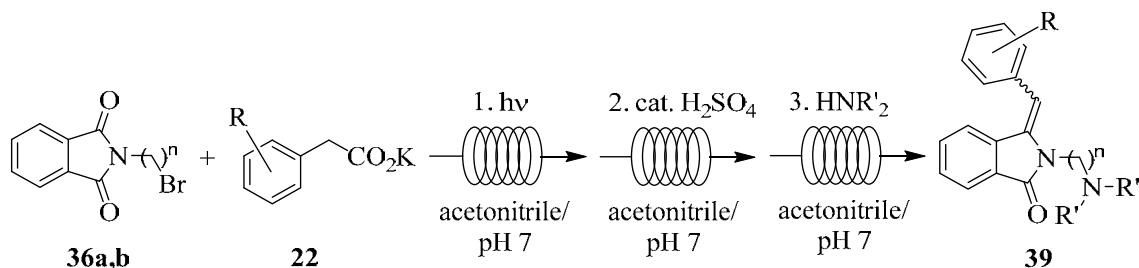
Scheme 3.26: Multistep continuous flow reaction for synthesis of **AL12** and analogues.

Table 3.20: Multistep continuous flow results.

Entry	R	n	R'	Residence Time (min)	Yield (%)
a	H	2	C_2H_5	70	75
b	4-CH_3O	2	C_2H_5	70	73
c	H	3	CH_3	70	75
d	4-CH_3	3	C_2H_5	70	77
e	4-F	3	C_2H_5	70	75

3.2.9 Synthesis of aristolactams [Experiments 146-156]

A three step strategy was likewise devised to access the parent aristolactam skeleton. The first step was the photodecarboxylative addition of *ortho*-iodophenylacetate to *N*-alkylphthalimide. The second step involved the acid-catalyzed dehydration to the corresponding olefinic isomers. The third and final step utilized the photodehydrohalogenation to the final target compound. Overall, the reaction sequence utilizes two photochemical key-steps and one thermal step.

3.2.9.1 Photodecarboxylative addition of *ortho*-iodophenylacetate to phthalimides

A mixture of potassium *ortho*-iodophenylacetate, made *in situ* from the corresponding carboxylic acid and potassium carbonate, and *N*-alkylphthalimide in acetone/pH7 buffer was irradiated for 4 hours in a Pyrex Schlenk flask with UVB light (**Scheme 3.27**). Recrystallization offered pure photoproducts **43** and **45** in yields of 51-67% (**Table 3.21**).
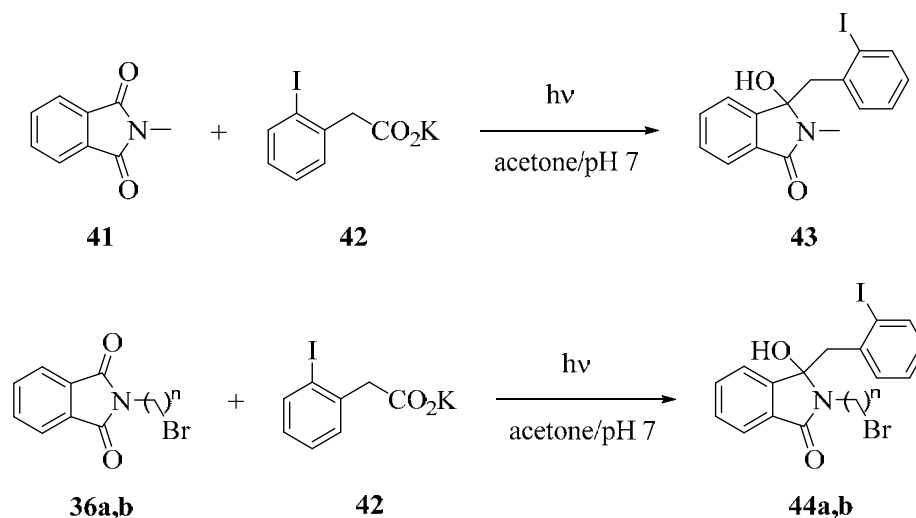
Scheme 3.27: Photodecarboxylative addition of 2-iodophenylacetate to phthalimides.

Table 3.21: Photodecarboxylative additions of *ortho*-iodophenylacetate.

Entry	Phthalimide	^{1}H-NMR^a (ppm)	Yield (%)
a	41	5.42	51 (**43**)
b	36a	5.68	67 (**44a**)
c	36b	5.63	71 (**44b**)

^{a} ^{1}H-NMR signal of the C-O$\underline{H}$.

A representative ^{1}H-NMR spectrum of **44a** is shown in **Figure 3.27**. A characteristic pair of doublets appear at 3.34 ppm and 3.84 ppm with a germinal (^2J) coupling of 18 Hz, representing the benzylic (-C$\underline{H}_2$Ar) bridge.
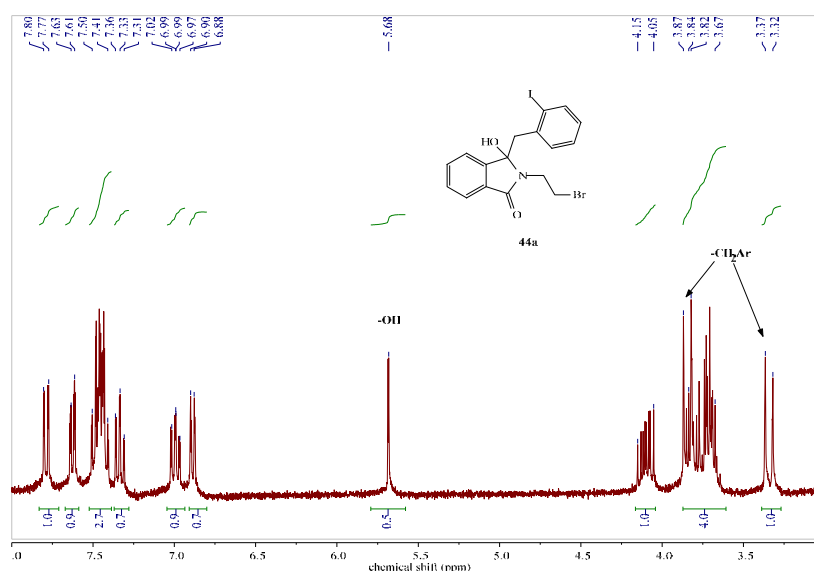
Figure 3.27: ^{1}H-NMR spectrum of **44a** (in acetone-d$_6$).

Two multiplets at 3.75 ppm and 4.10 ppm represent the ethylene protons of the *N*-side chain (-C$\underline{H}_2$C$\underline{H}_2$Br). The newly formed hydroxyl proton (-O$\underline{H}$) gives a singlet at 5.68 ppm, while the aromatic protons appear between 6.88 ppm and 7.80 ppm.

3.2.9.2 Dehydration of photoproducts

Dehydrations were achieved by treating solutions of the photoproducts in dichloromethane with catalytic amounts of sulfuric acid (**Scheme 3.28**). After workup, *E/Z* mixtures of the desired products **45** and **46a**, **b** were obtained in yields of 83-90%. The results are presented in **Table 3.22**.
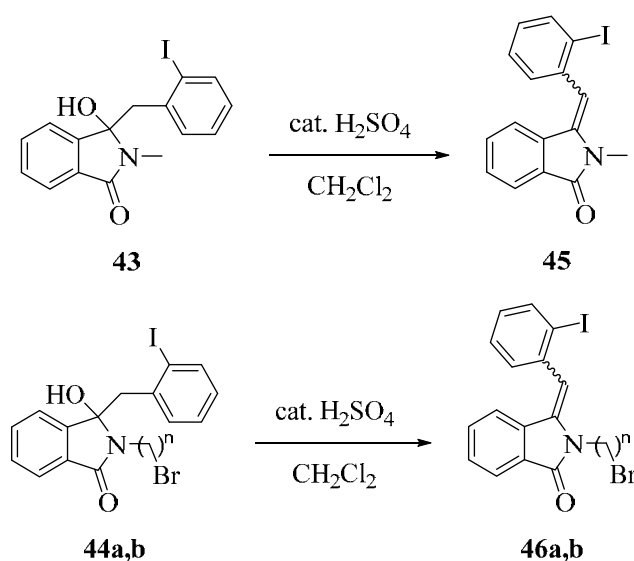
Scheme 3.28: Dehydration of photoproducts.

Table 3.22: Dehydration experiments.

Entry	Photoproduct	^{1}H-NMR^a (ppm)	*E:Z*^{b}	Yield (%)
a	**43**	6.65	89:11	90 (**45**)
b	**44a**	6.36	77:23	90 (**46a**)
c	**44b**	6.48	92:8	83 (**46b**)

^{a} ^{1}H-NMR signal of the olefinic =C$\underline{H}$-Ar for the main stereoisomer. ^{b} Determined by ^{1}H-NMR analysis (±3%).

The ^{1}H-NMR spectrum of **46a** is exemplarily given in **Figure 3.28**. The singlet at 6.36 ppm is characteristic for the olefinic proton (=C$\underline{H}$-) of the product. Two triplets at 3.68 ppm and 4.33 ppm represent the ethylene protons of the *N*-side chain (-C$\underline{H}_2$C$\underline{H}_2$Br). The presence of an *E/Z* mixture is proven by the doubling of signals in the aliphatic and olefinic regions, whereas the signals for the aromatic protons were largely overlapping. The presence of minor impurities could not be excluded.
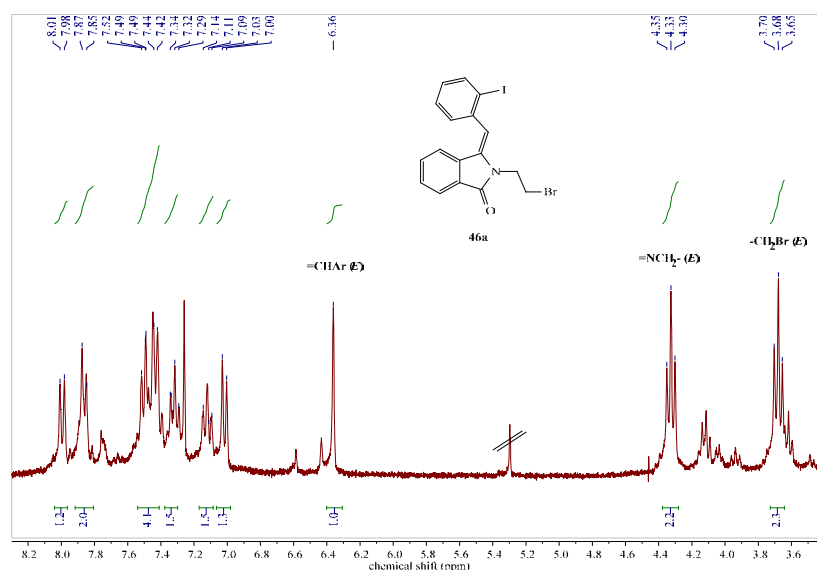
Figure 3.28: ^{1}H-NMR spectrum of the dehydration product **46a** (in CDCl$_3$).

3.2.9.3 Photodehydrohalogenation reactions

Following a modified procedure by Castedo *et al.* [91], the dehydrated products were further irradiated in benzene in a Pyrex flask with UVB light for 15 hours (**Scheme 3.29**).
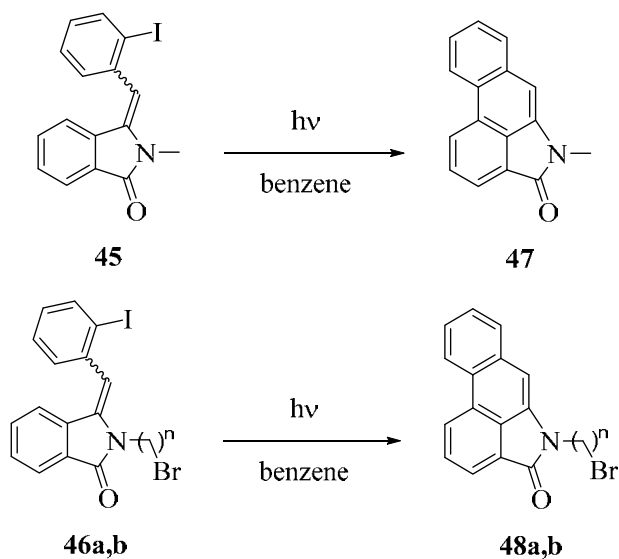
Scheme 3.29: Photodehydrohalogenation of **45** and **46**.

Photodehydohalogenation was observed in all three cases leading to cyclization and formation of the desired aristolactams in yields of 24-57% (**Table 3.23**).

Table 3.23: Dehydrohalogenation experiments.

Entry	Dehydration Product	^{1}H-NMR^a (ppm)	Yield (%)
a	**45**	8.70, 8.82	24 (**47**)
b	**46a**	8.55, 8.64	57 (**48a**)
c	**46b**	8.55, 8.62	55 (**48b**)

^{a} ^{1}H-NMR signals of the downfield H$_{arom}$.

As a typical example, the ^{1}H-NMR spectrum of **48a** is displayed in **Figure 3.29**. Two characteristic doublets in the aromatic region appear at 8.55 ppm and 8.64 ppm and represent the protons next to C-C bond formation position in the product. The isolated =CH-proton is found as a singlet at 7.21 ppm.
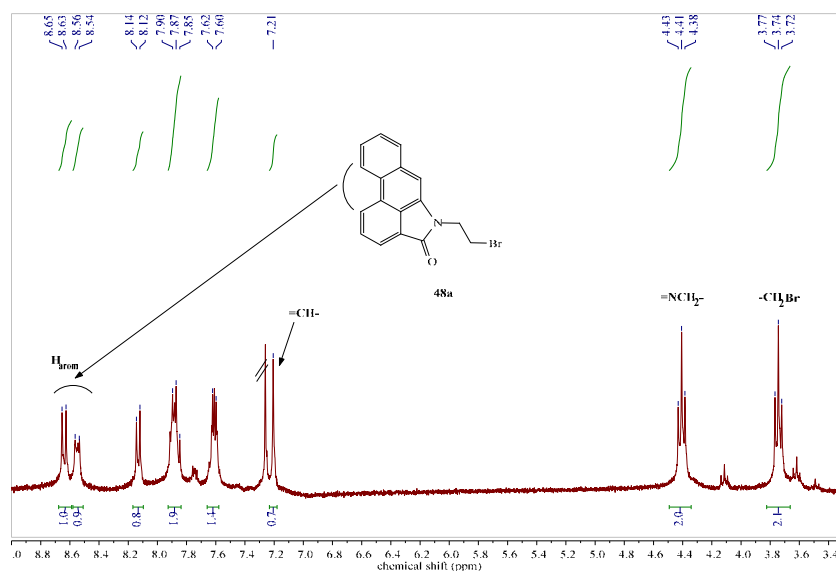
Figure 3.29: ^{1}H-NMR spectrum of **48a** (in CDCl$_3$).

3.2.9.4 Amination of aristolactams

The *N*-bromoalkylphthalimide derived aristolactams **48a**, **b** were subjected to amination using the modified procedure by Jiang and coworkers (**Scheme 3.30**) [89].
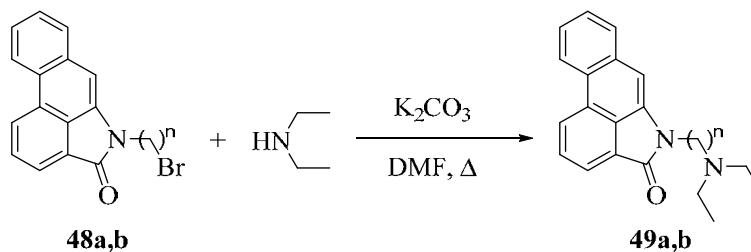
Scheme 3.30: Amination of *N*-alkylbromo-derived aristolactams.

Following this approach and using diethylamine, the corresponding products **49a** and **b** were obtained in yields of 71% and 75% (**Table 3.24**), respectively.

Table 3.24: Amination of aristolactams.

Entry	n	Yield (%)
a	2	71
b	3	75

A representative example of the ^{1}H-NMR spectrum of **49a** is given in **Figure 3.30**. The newly introduced diethylamine group shows a triplet at 1.05 ppm for the terminal methyl groups and a quartet at 2.64 ppm for the methylene protons.
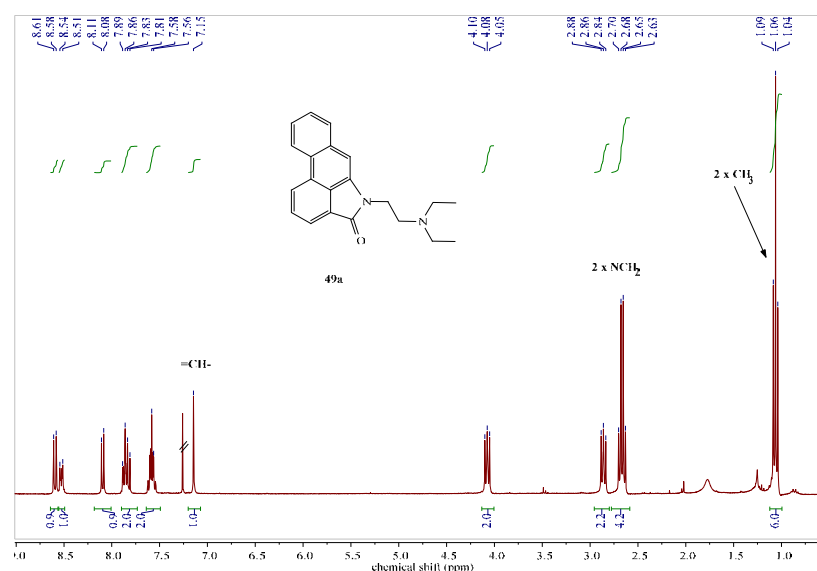
Figure 3.30: ^{1}H-NMR spectrum of **49a** (in CDCl$_3$).

3.2.9.10 Synthesis of AKS186 [Experiment 157]

An additional tandem photochemical-thermal flow protocol was realized using the advanced Vapourtec easy-photochem reactor described in **Figure 3.9** and **Table 3.4**. A solution of *N*-(4-acetoxybenzyl)phthalimide **50** and potassium phenylpropionate in acetone/H$_2$O was pumped into the UV-150 module with an optimized residence time for a conversion of 100%. Neat TFA was injected into the effluent of the photoreactor module before being pumped into the thermal loop. Dehydration and deprotection were achieved in the same thermal step. Following the optimized in series reaction protocol (**Scheme 3.31**), **AKS186** (**53**) was obtained as colourless solid in an overall yield of 80% [71]. NMR analysis revealed that the *E*-isomer is preferentially formed.
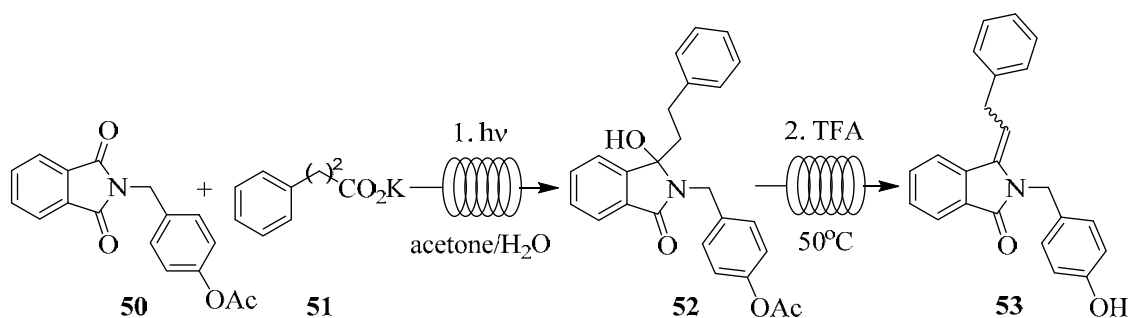
Scheme 3.31: Continuous flow synthesis of **AKS186**.

The ^{1}H-NMR spectrum of the desired **AKS186** product is displayed in **Figure 3.31**. The spectrum shows a doublet at 4.01 ppm for the -C$\underline{H}_2$Ph group, a sharp singlet at 4.97 ppm for the =NC$\underline{H}_2$-methylene group, a broad singlet at 8.29 ppm for the phenolic proton (-O$\underline{H}$) and a triplet at 5.76 ppm for the olefinic proton (=C$\underline{H}$CH$_2$-). The aromatic protons appear broadly between 6.76 ppm and 8.05 ppm. Selected signals of the minor *Z*-isomer can be seen as well.
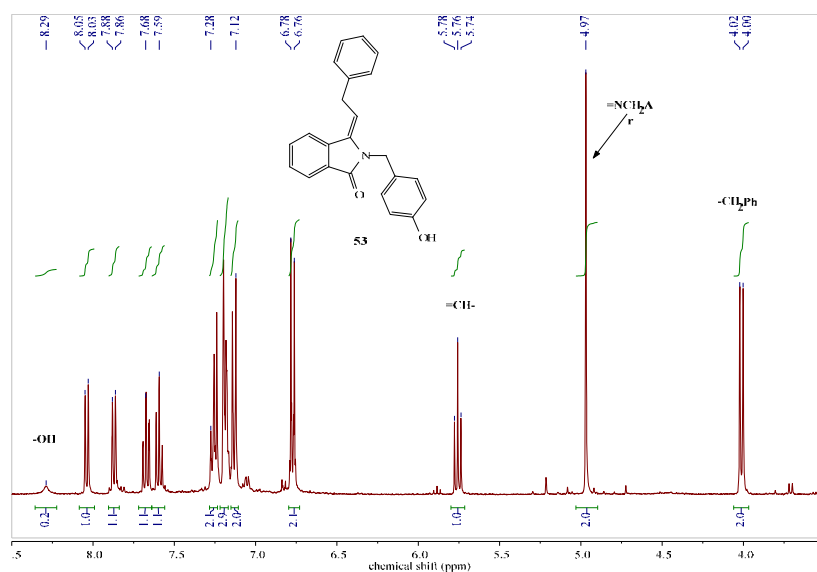
Figure 3.31: ^{1}H-NMR spectrum of **AKS186** (in acetone-d$_6$).

3.2.11 Solar photodecarboxylations [Experiments 158-167]

A series of illumination experiments of various mixtures of phthalimides and phenylacetates (**Scheme 3.32**), using the same concentration as used in batch, were conducted in the parabolic trough concentrating solar reactor described in **Figure 3.10** and **Table 3.5**. Complete conversions (based on ^{1}H-NMR analysis) were observed in all cases except in case of **56** where a 90% conversion was observed instead despite a longer residence time of 53 min (**Table 3.25**). Reference reactions were carried by placing reaction mixtures of *N*-bromoethylphthalimide and

phenylactetate into direct sunlight for 200 min in either a round bottom flask, Schlenk flask or test tube inside a floating reactor. The solar float is shown in **Figure 3.32**. The exposed test tubes are fixed in a frame inside the solar float. Balloons were attached to the top of each test tube to compensate for any pressure buildup due to evaporation or carbon dioxide formation. Water from the surrounding pool entered the holding frame through a mesh on the bottom. No significant product formation was observed by ^{1}H-NMR analysis in any of the three cases.
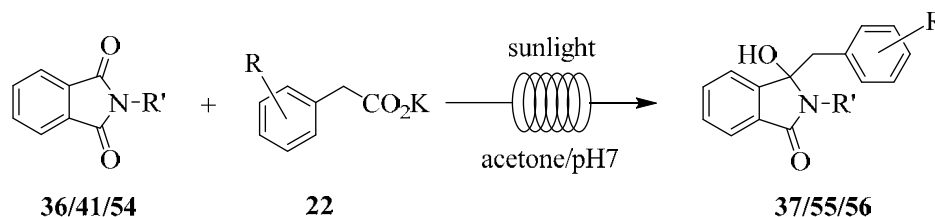
Scheme 3.32: Photodecarboxylative addition under concentrated solar flow conditions.

Table 3.25: Solar photodecarboxylative additions.

Entry	Date	R	R'	Residence Time (min)	Conversion[a] (%)	Yield (%)
a	23/03/2015	H	H (**54**)	40	100	93 (**55**)
b	20/03/2015	H	CH$_3$ (**41**)	53	90	84 (**56**)
c	22/01/2015	H	(CH$_2$)$_2$Br (**36a**)	40	100	74[b] (**37a**)
d	22/01/2015	H	(CH$_2$)$_2$Br (**36a**)	40	100	86[c] (**37a**)
e	11/01/2015	4-CH$_3$O	(CH$_2$)$_2$Br (**36a**)	40	100	83 (**37e**)
f	14/01/2015	4-AcO	(CH$_2$)$_2$Br (**36a**)	40	100	80 (**37q**)
g	10/01/2015	H	(CH$_2$)$_3$Br (**36b**)	40	100	95 (**37i**)
h[e]	22/01/2015	H	(CH$_2$)$_2$Br (**36a**)	200	0	n.r.[d]
i[f]	22/01/2015	H	(CH$_2$)$_2$Br (**36a**)	200	0	n.r.[d]
j[g]	22/01/2015	H	(CH$_2$)$_2$Br (**36a**)	200	0	n.r.[d]

[a] Based on ^{1}H-NMR analysis (±3%). [b] Combine photochemical (**37a**) and thermal product (**57**). [c] Pure photoproduct. [d] n.r.=no reaction. [e] Flask placed in the sun. [f] Schlenk flask placed in the sun. [g] Floating reactor in a paddle pool.

The ^{1}H-NMR spectrum of **56** is given in **Figure 3.33**. A singlet for the -NC$\underline{H}_3$ group appears at 2.96 ppm and the typical pair of doublets for the benzylic group (-C$\underline{H}_2$Ph) shows at 3.12 ppm and 3.48 ppm, respectively. The hydroxyl-group is found as a broad singlet at 3.22 ppm.
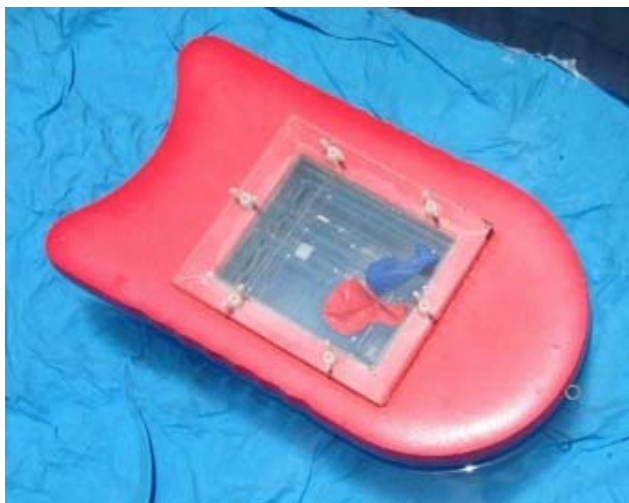
Figure 3.32: Direct illumination using a solar float.
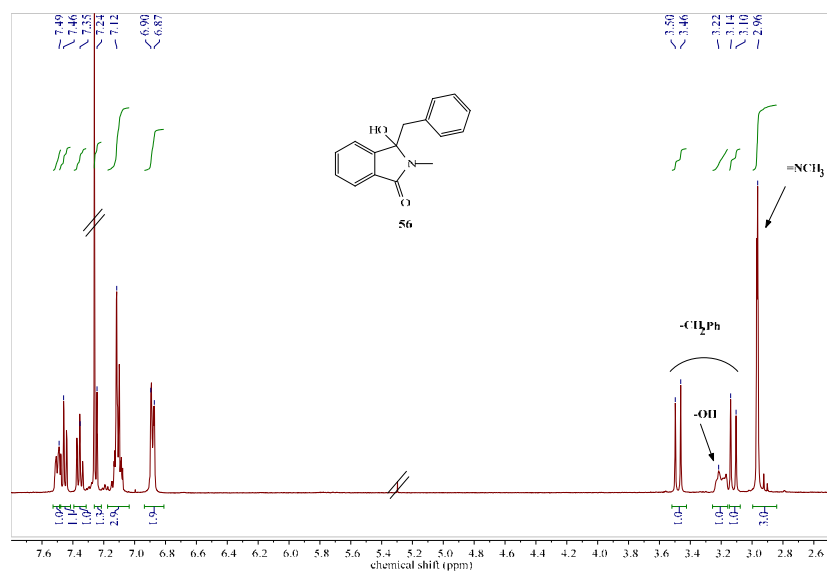
Figure 3.33: ^{1}H-NMR spectrum of **56** (in CDCl$_3$).

In case of the solar photodecarboxylative additions involving *N*-bromoethylphthalimide, the tetracyclic compound **57** was occasionally formed (**Scheme 3.33**). The formation of product **57** could be suppressed when the temperature of the collection flask was kept below 40ºC.

57
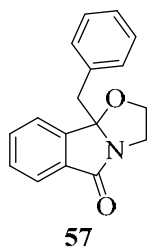
Scheme 3.33: Structure of the tetracyclic by-product **57**.

The structure of the tetracyclic compound **57** was confirmed by ^{1}H-NMR spectroscopy (**Figure 3.34**). The spectrum showed a pair of doublets for the benzylic group (–C$\underline{H}_2$Ph) at 3.30 ppm and 3.44 ppm. The ethylene group of the newly formed ring gave complex multiplets at 3.14, 3.99 and 4.17 ppm, respectively. The aromatic signals were found between 7.16 and 7.69 ppm.
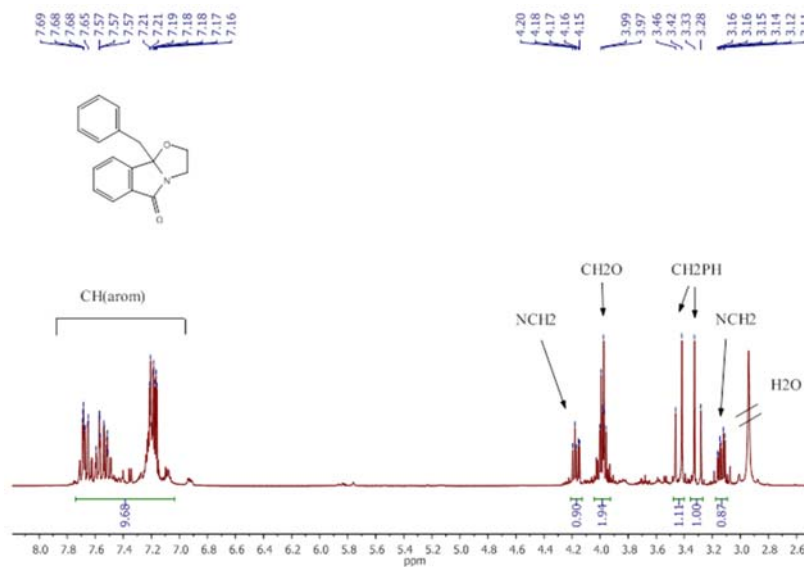
Figure 3.34: ^{1}H-NMR spectrum of **57** (in CDCl$_3$).

Chapter 4:

Discussion

4.   Discussion

4.1   Photoreactions of isatins

4.1.1   Attempted intramolecular photocyclizations of *N*-alkenylisatins

The broad biological activity spectrum of indole-2,3-diones (isatins) has encouraged us to investigate their photochemical behavior [92]. *N*-Alkenylisatins were thus synthesized and subjected to photoirradiation. A reaction similar to the intramolecular [2+2] photocycloaddition reaction of *N*-pentenylphthalimide was anticipated (**Scheme 4.1**) [93].
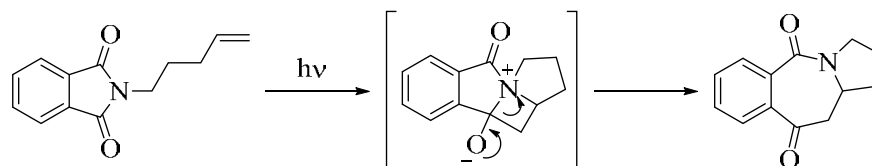
Scheme 4.1: [2+2] Photocyclization of *N*-pentenylphthalimide [93].

The photocyclization of *N*-alkenylisatin may occur on either of the two carbonyl groups. Photoaddition at the adjacent carbonyl (C-2) would yield the desired seven membered ring, whereas reaction at the remote carbonyl (C-3) would form a highly strained Paternò-Büchi product (**Scheme 4.2**).
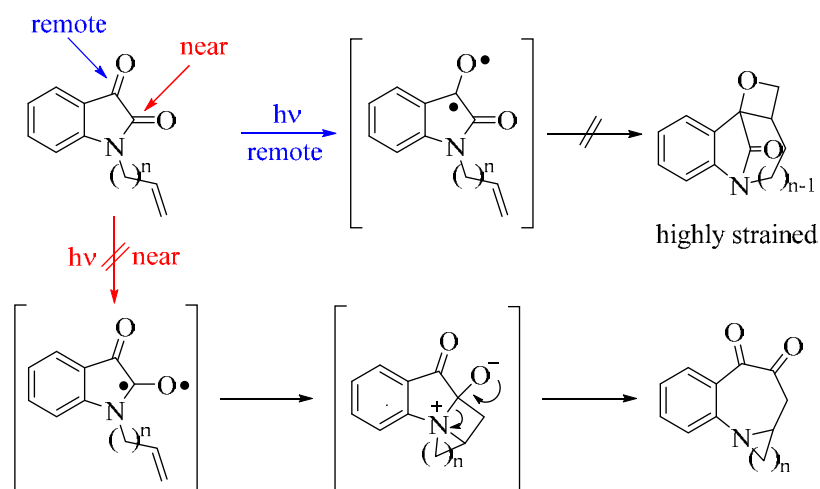
Scheme 4.2: Potential [2+2] photocyclizations of *N*-alkenylisatins.

Although the photocyclization at the near carbonyl can yield a fairly unstrained product, the remote three position of isatin is known to be the photochemically reactive one (**Figure 4.1**). This feature is in line with the favorable n→π* transition of the C=O (ketone) compared to that of the C=O (amide) bond.
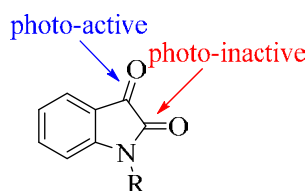
Figure 4.1: Active site of isatin for photocycloaddition.

The reactivity of the three position was, for example, confirmed in the photodimerization reaction of isatin. After excitation, the triplet state of isatin undergoes hydrogen abstraction from the solvent (toluene, *p*-xylene or cumene) forming a pinacol isatide product (**Scheme 4.3**) [94].
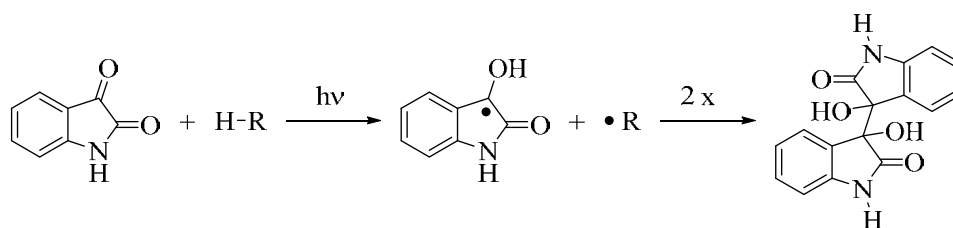
Scheme 4.3: Formation of pinacol isatide.

Photochemical transformations of isatins are rare and only a few examples can be found in the literature. The intermolecular photoaddition of pyrrazolones to isatin formally followed the desired [2+2] photocycloaddition pathway (**Scheme 4.4**). Further investigation of the mechanism, however, revealed that the ring expansion operated via the initial hydrolysis of the amide bond. The intermediary formed isatic acid subsequently reacted with pyrazolone to the final product [95].
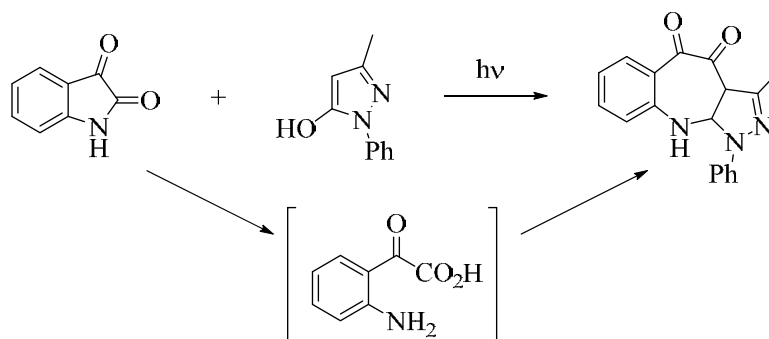
Scheme 4.4: Reaction of isatic acid with the enolic form of prazolone.

N-Acetylisatins display a significantly improved photoreactivity compared to the parent isatins and [2+2], [4+2] and [4+4] photocycloaddition reactions have been described for these

compounds. An example of a successful Paternò-Büchi reaction between *N*-acetylisatin and styrene is shown in **Scheme 4.5** [96].
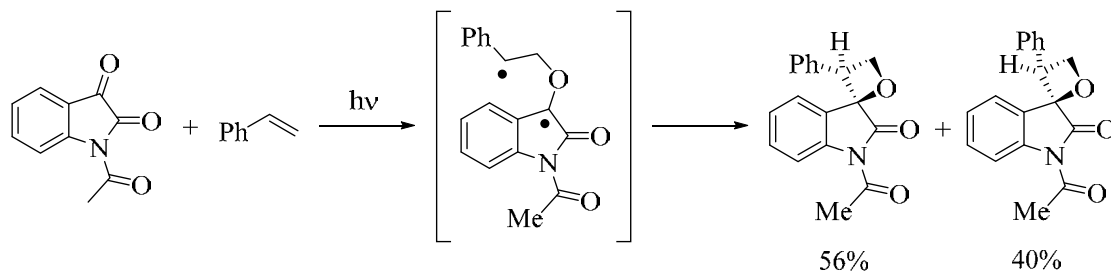
Scheme 4.5: [2+2] photocycloaddition of *N*-acetylisatin and styrene.

The isatin derivatives used in present study proved to be very stable to UV light. Polymerizations were instead observed after prolonged irradiations of 54 hours. This reduced photoactivity may be attributed to their extremely short lived triplet excited state. For the parent isatin, a life time of just 340 ns was determined in benzene [94].

A previous study has also shown that even more energetic light of 220 nm, emitted from a laser source, resulted solely in unselective polymerization [97]. Large quantum yields were nevertheless observed indicating the involvement of high energy excited states. However these states were assumed to undergo effective quenching before undertaking any actual photochemical reaction (**Scheme 4.6**).
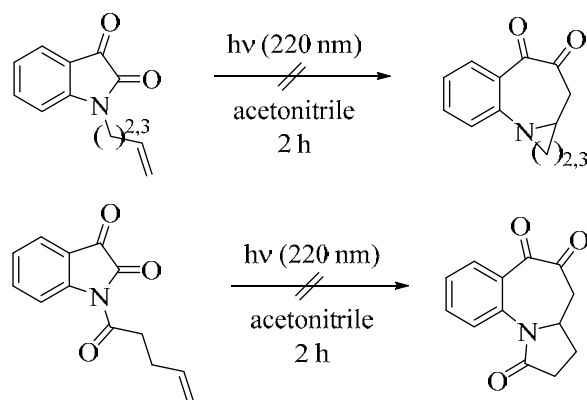
Scheme 4.6: Attempted intermolecular photocyclizations of *N*-substituted isatin.

In contrast to photoadditions, intramolecular photocyclizations furthermore demand a close proximity of the reactive sites for a successful reaction [98]. This approach is typically achieved by conformational changes [99]. For example, studies on the photodecarboxylation (PDC) of phthalimides have shown that intermolecular photoinduced electron transfer (PET) is dependent on the flexibility of the linker chain. Based on its general flexibility, certain macrocyclic rings may be formed after the initial PET-PDC steps [47].

No product was observed during the photoirradiation of *N*-alkenylisatins, even after prolonged irradiation. This lack of photoreactivity may be furthermore explained by the highly unstable and strained nature of the hypothetical Paternò-Büchi products and the missing proximity of chromophore and alkene moiety. The chosen alkenyl-chains are simply too short to overcome these disadvantages. Likewise, the amide C=O bond is not photochemically active and hence, [2+2] photoaddition towards the ring extension product does not operate.

4.1.2   Attempted intermolecular photoreactions of isatins with phenylacetates

In a second approach, intermolecular photodecarboxylative additions of phenylacetates to isatin were studied. This transformation has been used widely for the isosteric phthalimides [82, 88]. The general reaction protocol of the photodecarboxylative addition of carboxylates to phthalimide was thus followed (**Scheme 4.7**).
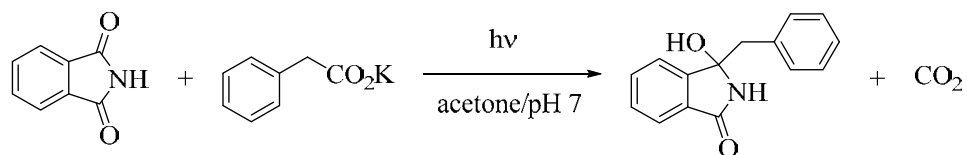
Scheme 4.7: Photodecarboxylative addition of phenylacetate to phthalimide.

N-Methylisatin was irradiated with phenylcarboxylate, expecting decarboxylative addition at the rear carbonyl to yield 3-hydroxy-3-benzyl-*N*-methylisatin (**Scheme 4.8**). Electron transfer from the carboxyl group to the excited state of *N*-methylisatin would yield the corresponding carboxyl radical that rapidly loses carbon dioxide to form a stabilized benzyl radical. Carbon-carbon bond formation and protonation would furnish the desired benzylated product.
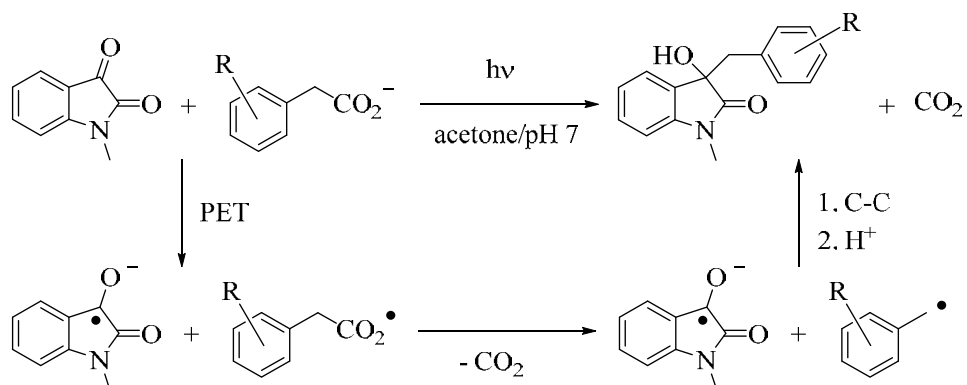
Scheme 4.8: Photodecarboxylative addition of phenylcarboxylate to *N*-methylisatin.

The feasibility of the crucial photoinduced electron transfer was estimated by employing the Rehm-Weller equation (**Equation 4.1**) [6, 7], where E_{ox} (Do) and E_{red} (Acc) represent the

oxidation and reduction potential of the donor or the acceptor, E^*_∞ the electronic excitation energy and E_{coul} the coulombic interaction energy of the intermediates formed.

$$\Delta G = F(E_{ox}\,(Do) - E_{red}\,(Acc)) + E_{coul} - E^*_\infty$$

Equation 4.1: Rehm-Weller equation.

Using the relevant values from the literature (**Table 3.6**), a negative ΔG value of -0.3579 eV was calculated. Hence, electron transfer should be thermodynamically feasible.

Table 4.1: Electrochemical and photophysical data of phenylcarboxylate and isatin.

$E_{ox}\,(\mathbf{PhCO_2^-})^a$	+1.27 V [100]
$E_{red}\,(\mathbf{isatin})^a$	-0.519 V [101]
$\mathbf{E_{coul}}$	negligible in polar solvents
$\mathbf{E^*_\infty}$	2.1379 eV [101]
$\mathbf{\Delta G}$	**-0.3579 eV**

[a] *vs* SCE (standard calomel electrode)

In the actual experiments, an aldol product of isatin and acetone was obtained instead of any photodecarboxylative addition adducts. Meshram *et al.* have recently reported similar aldol condensations of various acetophenones with isatins under microwave irradiation (**Scheme 4.9**) [102]. Likewise, the reaction of isatine and acetone in the presence of an organic base has been described by Braude and Lindwall [84]. It is thus likely that this thermal condensation reaction proceeded faster than the desired photoinitiation.
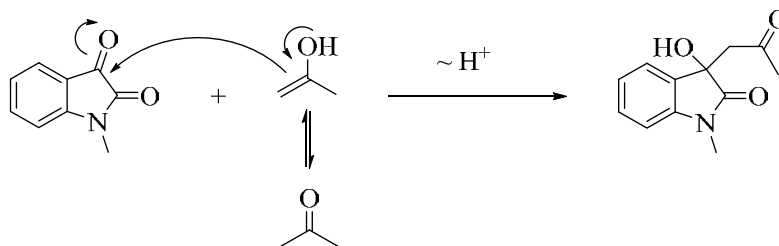
Scheme 4.9: Mechanism of formation of aldol product from acetone and *N*-methylisatin.

A thermal, base-catalyzed decarboxylative addition of α-functionalized carboxylic acids to isatins has been recently described by Ren *et al.* (**Scheme 4.10**) [103]. The procedure opened an easy and rapid access to 3-functionalized 3-hydroxyoxindoles. Various substituted isatins and carboxylic acids could be used as starting materials.
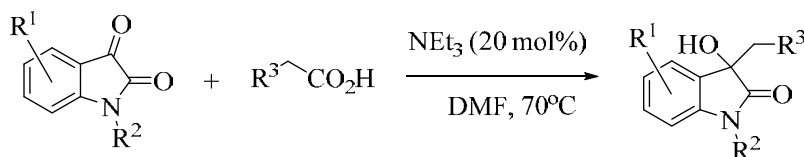
Scheme 4.10: Catalytic thermal decarboxylative addition of α-functionalized carboxylic acids to isatins.

4.2 Attempted photocyclizations of 4-amino-*N*-alkenylphthalimides and a related Schiff's base

For the 4-amino-*N*-alkenylphthalimides and the related Schiff's base, a reaction similar to the well-studied intramolecular [2+2] photocycloadditions of *N*-alkenylphthalimides was expected [104, 105]. Interestingly, the length of the alkenyl chain played an important role in the photocyclization efficiency of these compounds (**Scheme 4.11**).
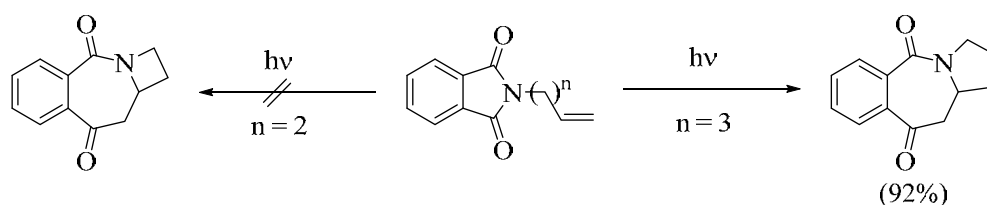
Scheme 4.11: [2+2] Photocyclization of *N*-alkenylphthalimides.

No product was, however, observed for the related 4-amino-*N*-alkenylphthalimides and the Schiff's base. This may be explained based on the different photophysical properties of these highly fluorescing compounds compared to the unsubstituted phthalimide chromophore [8, 106]. For example, the excited states of 4-aminophthalimide are ultrashort lived [107, 108]. In acetonitrile, life times of 14 ns and 21.3 ns have been reported [109, 110]. In protic solvents, fluorescence decreases further due to proton transfer from the solvent or non-radiative internal conversion (IC) [111]. Consequently, ineffective intersystem crossing (ISC) and extremely short life times of the excited states of the 4-amino-*N*-alkenylphthalimides under investigation may prevent any successful photocycloaddition.

Recent investigations on 4-aminophthalimide have shown that its excited state does not support the concerted [2+2] mechanism suggested for phthalimides by Mazzochi [112]. The assumption that the 4-aminophthalimide analogues react accordingly is therefore invalid. The excited state of aminophthalimide was expected to show high electron density between the -C(O)-N bond that would favour the concerted [2+2] mechanism. Instead, the excited state actually shows that electron density resides between the carbonyl and alkene bond (**Figure 4.2**) [113].
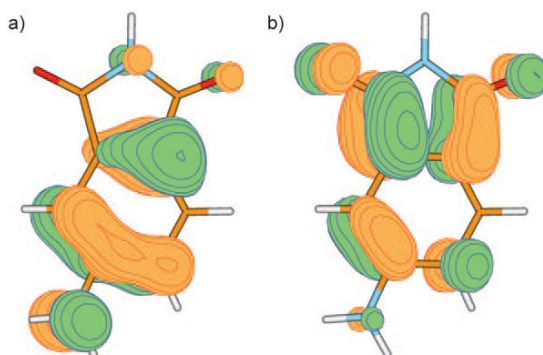
Figure 4.2: Highest-occupied and lowest-unoccupied molecular orbitals (HOMO and LUMO) of 4-aminophthalimide [113].

Accordingly, there is no π-bond character at the C-N, which is a requirement of the desired [2+2] photocyclization. An alternative fragmentation/cyclization mechanism has been suggested by Davies and co-workers (**Scheme 4.12**) [114]. The photostability observed for the 4-amino-*N*-alkenylphthalimides and the related Schiff's base suggests that neither mechanism is operating.
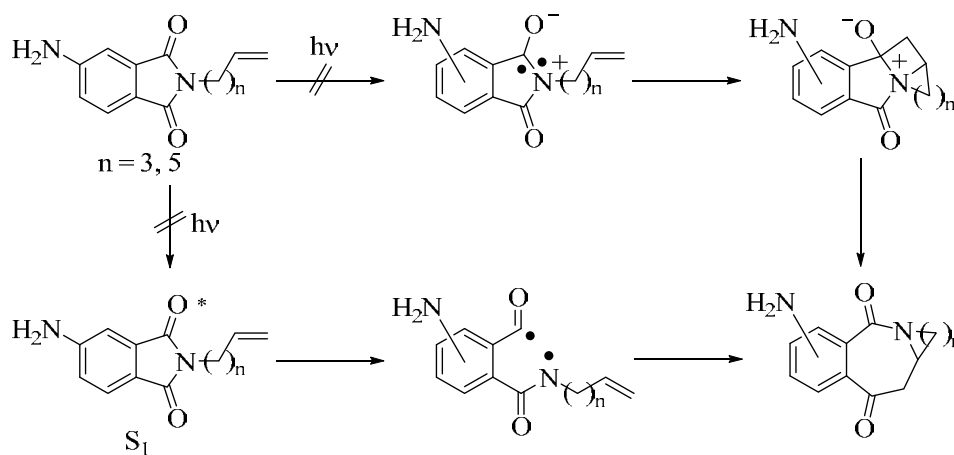
Scheme 4.12: Mechanisms of the photocyclization of 4-amino-*N*-alkenylphthalimides.

4.3 Intramolecular photocyclizations of benzoylbenzamides

4.3.1 Thermal ring-chain tautomerizations

During the synthesis of the starting materials for the desired photochemical investigations, the primary amine-derived benzoylbenzamides were obtained exclusively in their tautomeric cyclic forms. This ring-chain tautomerism is well documented in the literature [80, 115, 116]. The *ortho*-substitution enables close proximity of the amide-nitrogen for nucleophilic addition towards to ketone carbonyl group (**Figure 4.3**).
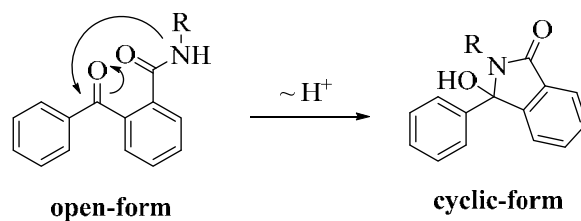
Figure 4.3: Tautomerization in primary amine derived 2-benzoylbenzamide.

Interestingly, the thermal amide-coupling represents an easy access towards to 3-phenylated isoindolinones. These derivatives are not available via the direct photodecarboxylative addition route. In fact, potassium benzoate remained unreactive and *N*-methylphthalimide was recovered in 86% yield after exhaustive irradiation of 48 hours (**Scheme 4.13**) [53]. Therefore the thermal step fills this important gap in phthalimide photodecarboxylations [24].
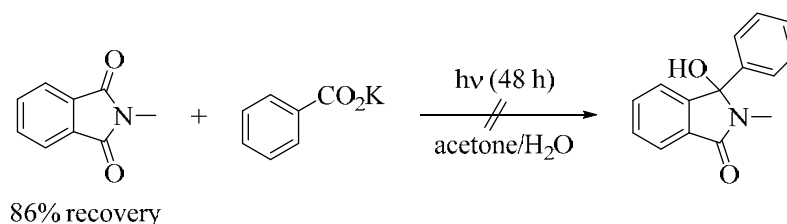
Scheme 4.13: Unsuccessful potodecarboxylative addition of benzoate to *N*-methyl-phthalimide.

Bioactive 3-phenylated isoindolinones with the potential of becoming targeted cancer therapeutics through MDM2-p53 inhibition have been recently reported by Hardcastle and co-workers (**Scheme 4.14**) [117].

$IC_{50} = 15.9\ \mu M$ $\qquad\qquad$ $IC_{50} = 0.17\ \mu M$
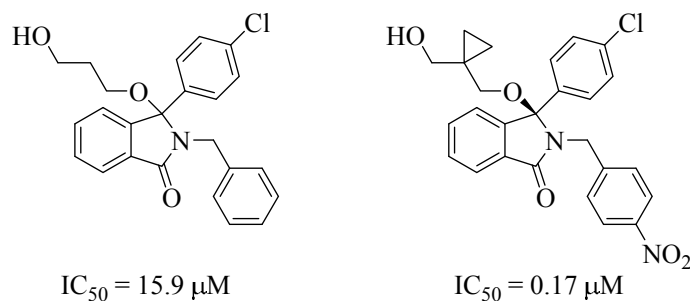
Scheme 4.14: Bioactive 3-phenylated isoindolinones.

4.3.2 Photoirradiations

Upon irradiation, the cyclic 3-hydroxy-3-phenylisoindolin-1-ones remained photostable, suggesting that tautomerization to the open and potentially photoactive form did not operate.

For the phenylglycine methyl ester-derived benzoylbenzamide, Norrish-II photocyclization was anticipated from the open form (**Scheme 4.15**). It was hoped that this photochemical process would eventually convert the cyclic tautomer to the six-membered cyclization product via ε-H abstraction [118, 119].
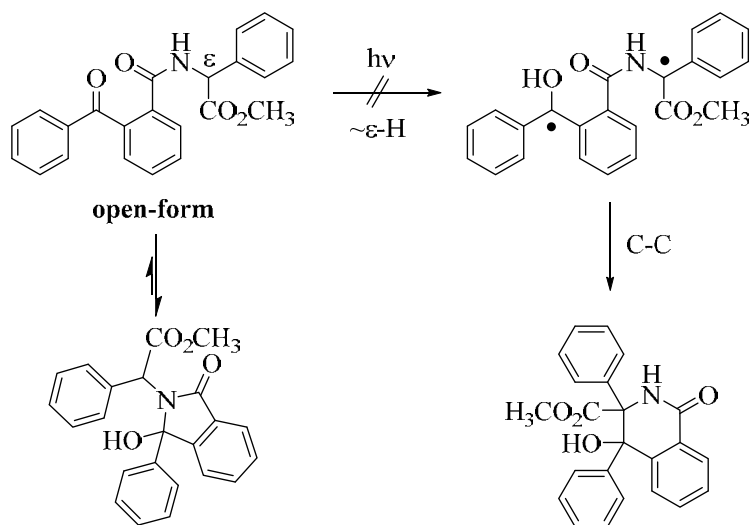
Scheme 4.15: Anticipated Norrish-II photocyclization of the phenylglycine-derived benzoylbenzamide.

It may be speculated if the open chain tautomer, if populated, would be photochemically "deactivated" *via* a geometrically feasible intramolecular hydrogen-bond between the amide and the ketone (**Figure 4.4**).
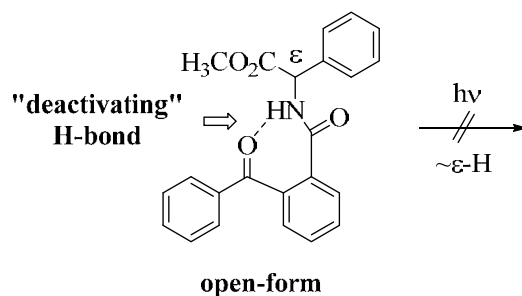
Figure 4.4: Possible "deactivating" intramolecular hydrogen bond in primary amine derived 2-benzoylbenzamides.

Similar deactivating effects of intramolecular hydrogen bonding has previously been reported while studying photodecarboxylations of phthalimides. In particular, phthaloyl glycine and phthaloyl anthranilic acid based dipeptides do not undergo efficient photodecarboxylation by PET (**Figure 4.5**) [47, 48]. Instead, decompositions or simple decarboxylations (-CO2H/-H exchange) are favored.
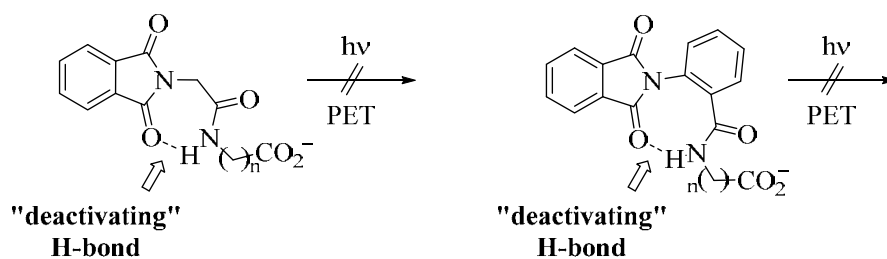
Figure 4.5: Deactivating intramolecular hydrogen bonding in phthalimide derivatives.

A successful Norrish-II photocyclization has been reported for the (*S*)-phenylethylamide derivative of the sterically demanding 2, 4, 6-triisopropylbenzophenone, although cyclization occurred exclusively via geometrically favored γ-H abstraction at the isopropyl-group and not via remote ε-H abstraction at the amide function (**Scheme 4.16**). In the crystalline state, irradiation solely furnished the (*R*, *S*)-cyclobutanol, whereas irradiation in acetonitrile gave a mixture of the (*R*, *S*) and diastereoisomers (*S*, *S*) in 24% and 21% yield, respectively [120, 121]. The isopropyl groups prevent any tautomerization and hence deactivation to the cyclic form.
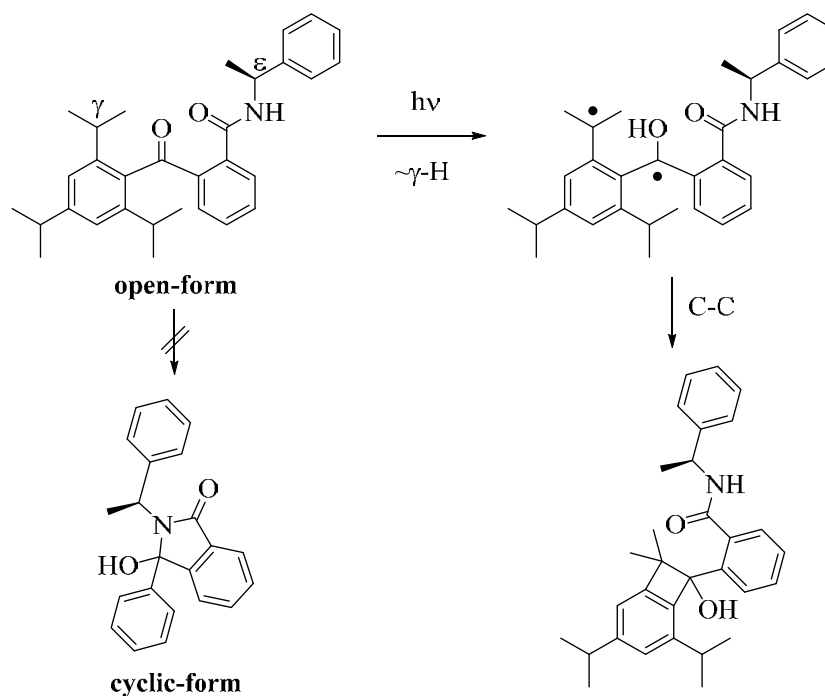
Scheme 4.16: Norrish-II photocyclization of a (*S*)-phenylethylamide-derived 2, 4, 6-triisopropylbenzophenone.

Successful Norrish-II photocyclizations at the amide sidechain have been reported for ketoprofen-derived amides [122, 123]. Due to the meta-substitution, ring-chain tautomerisation is not possible for these compounds. As an example, irradiation of a tetrahydrofuran-containing

benzophenone in acetonitrile for up to 3 hours furnished the corresponding cyclization product as a mixture of diastereosiomers (**Scheme 4.17**) [122]. Although the individual photoproducts were separated by HPLC, isolated yields were not provided.
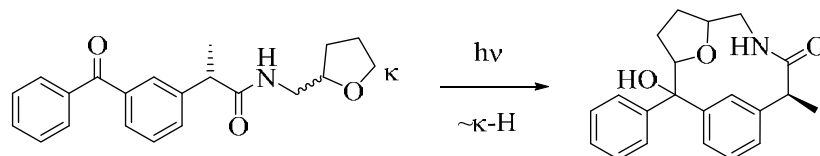
Scheme 4.17: Norrish-II photocyclization of a ketoprofen-derived amide.

In case of the thioether-containing compounds, *i.e.* the *L*-methionine methyl ester and 2-(*tert*-butylthio)ethanamine-derived benzophenones, photocyclizations products from photoinduced electron transfer (PET) from the sulfur atom to the triplet excited benzophenone moiety were preferentially anticipated [124, 125]. For the methionine based compound, regioisomeric products from cyclization at the inner *vs.* outer α-carbon were furthermore expected (**Scheme 4.18**). In contrast, the (*tert*-butylthio)ethanamine-based benzophenone could have only cyclized at the inner α-carbon position. The photostability of both compounds again suggested that the open, photoactive tautomeric form is not sufficiently populated.
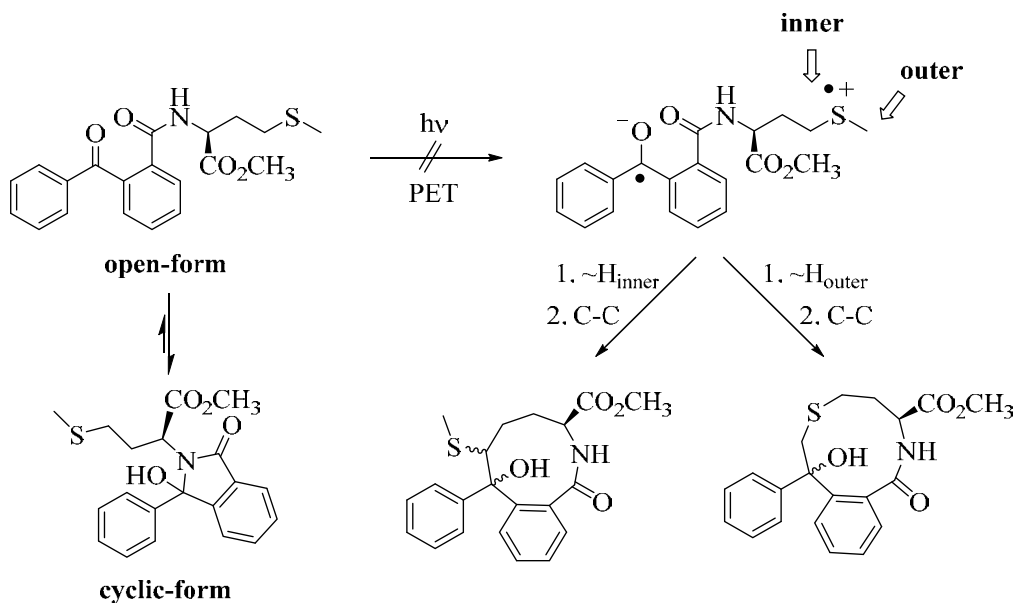
Scheme 4.18: Anticipated PET photocyclizations of the methionine-derived benzoylbenzamide.

Thus far, no successful photocyclizations of a thioether-containing *ortho*-substituted benzoyl-benzamide has been described. However, the successful photocyclization of a rigid *para*-

substituted benzophenone-methionine dyad at the outer methyl-group has been recently proposed by Lewandowska-Andralojc and co-workers (**Scheme 4.19**) [126]. Irradiation in acetonitrile with UVC light furnished the macrocyclic cyclization product as an almost 1:1 diastereoisomeric mixture and in a combined yield of 33%.
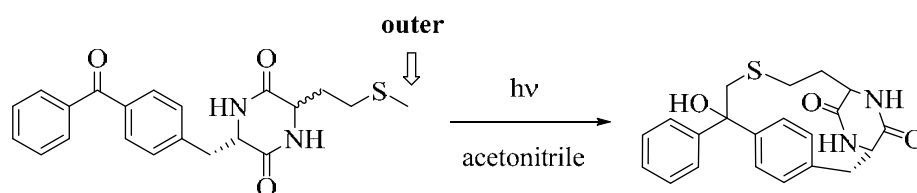
Scheme 4.19: Anticipated PET photocyclizations of the methionine-derived benzoylbenzamide.

In contrast, the secondary amine derived 2-benzoylbenzamides yielded several products upon photoirradiation. The first product, 3-phenylphthalide, is a suspected breakdown product of the initial benzoylbenzamide (**Scheme 4.20**). Its exact formation remains unclear at presence, but evidently involves the release of the amine function, probably as its corresponding imine. This scenario may be explained by a stepwise photoreduction of the benzophenone group, followed by intramolecular nucleophilic cyclization towards the amide carbonyl. The subsequently formed enamine would rearrange to the proposed imine.
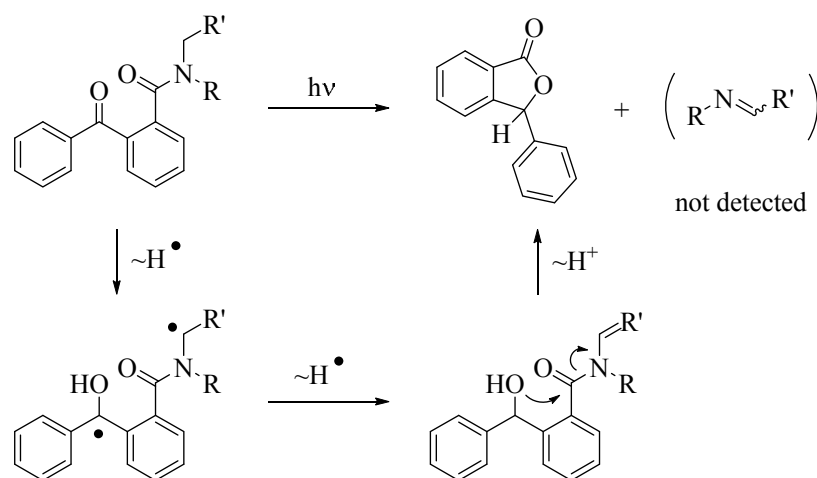
Scheme 4.20: 3-Phenylphthalide from 2-benzoylbenzamide.

Henning and Berlinghoff studied the photoirradiation of two symmetrical 2-benzoyl-benzamides. In aprotic solvents, no reaction was observed. In the hydrogen-donor solvent isopropanol, irradiation furnished photopinacolization type dimers (**Scheme 4.21**) [127]. Yields or reaction conditions were not provided. Notably, the amine-sidechain was removed, although its fate remains unclear.
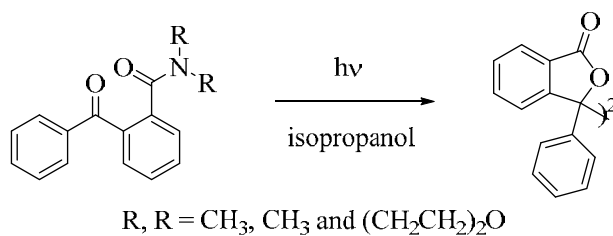
Scheme 4.21: Photopinacolization-type reaction of 2-benzoylbenzamide.

M. Sakamoto *et al.* studied photochemical transformations of a small series of 2-benzoylbenzamides in the solid state [128]. Remarkably, the *N, N*-dimethyl-substituted compound remained photostable after 10 hours, although its morphology changed gradually. In contrast, the powered *N*-phenyl-*N*-methyl-derived benzoylbenzamide furnished the 3-(*N*-methylanilino)-3-phenylphthalide in quantitative yield after 2 hours of irradiation at 15°C (**Scheme 4.22**). The reaction occurred with high enantioselectivity and an enantiomeric excess (*e.e.*) of 80% was obtained. Low temperature irradiation of crystalline material increased the *e.e.* to 97%, but the conversion dropped significantly. A radical pathway rather than a PET-process was suggested for the reaction.
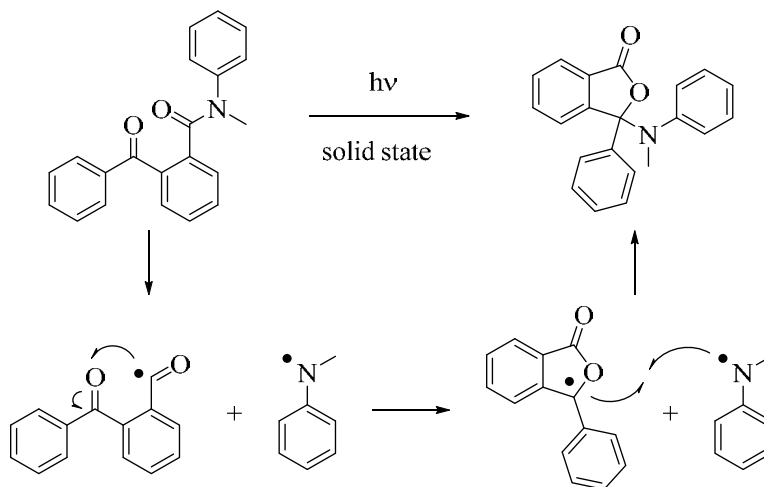
Scheme 4.22: Photorearrangement of *N*-phenyl-*N*-methyl-2-benzoylbenzamide.

The related 2-benzoylbenzoate esters were investigated by Jones and co-workers as photolabile protecting groups for alcohols [129]. When irradiated in cyclohexylamine, the corresponding alcohols were isolated in excellent yields. 3-Phenylphthalide was formed as the breakdown product of the 2-benzoylbenzoate moiety (**Scheme 4.23**). The proposed mechanism involved stepwise photoreduction of the benzophenone-moiety followed by intramolecular cyclization and release of the alcohol. Overall, cyclohexylamine functioned as a reducing agent and was converted into the corresponding imine.
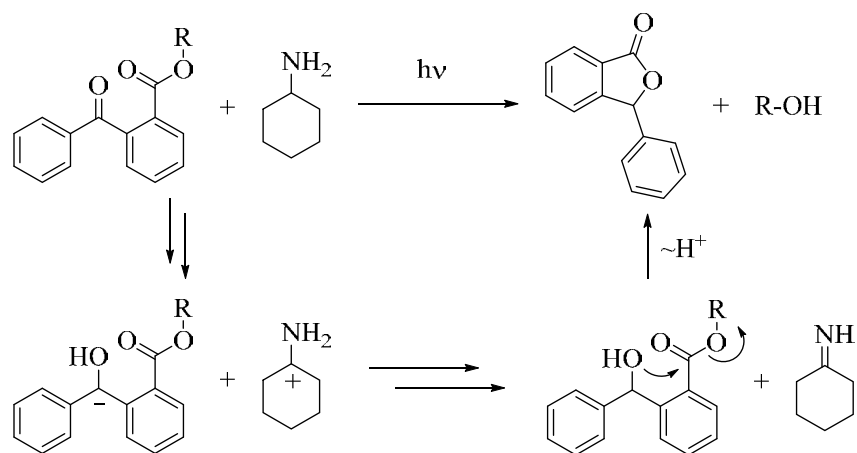
Scheme 4.23: Photorelease of alcohols from 2-benzoylbenzoate esters.

The *L*-proline derived 2-benzoylbenzamide additionally furnished the regioisomeric photoproducts as a single diastereoisomer each following a general Norrish-II mechanism. The different regiosiomers are formed from the corresponding rotamers. ε-Hydrogen abstraction generated the corresponding 1, 6-biradical pairs that subsequently cyclized to the observed products (**Scheme 4.24**).
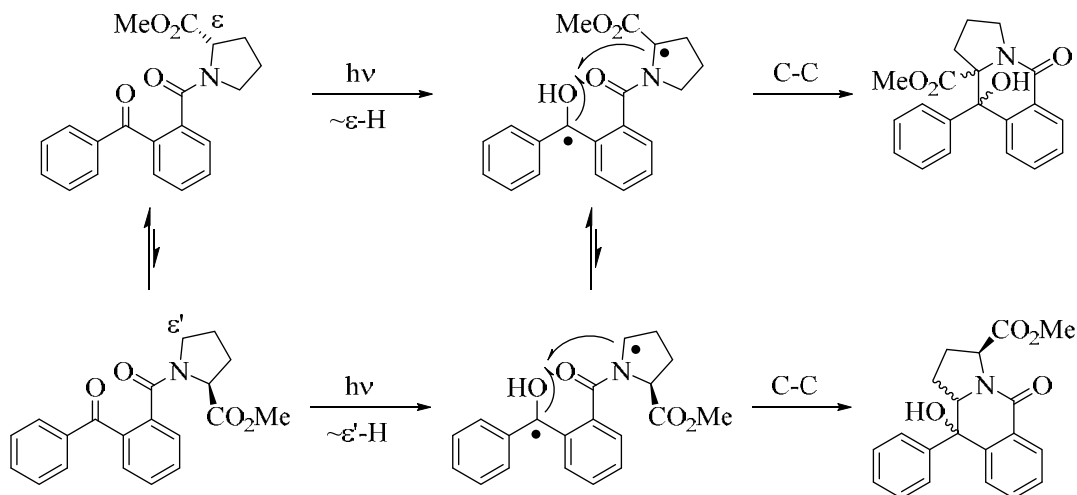
Scheme 4.24: Norrish-II reaction of the *L*-proline methyl ester derived benzoylbenzamide.

A similar product dependence on the corresponding rotamers has been described by Lindemann and co-workers for a sarcosine-based 4-oxo-4-phenylbutanoly amide (**Scheme 4.25**) [130]. In *tert*-butanol, the regioisomeric δ-lactams were formed in a ratio of 28:10. In dichloromethane, solely the main regioisomer was obtained in an improved yield of 63%. The remarkable change in regioselectivity was explained by differences in hydrogen-back transfer for the intermediary 1, 6-biradicals. In *tert*-butanol, hydrogen-bonding prevents rapid hydrogen-back transfer, thus enabling cyclization to both photoproducts.
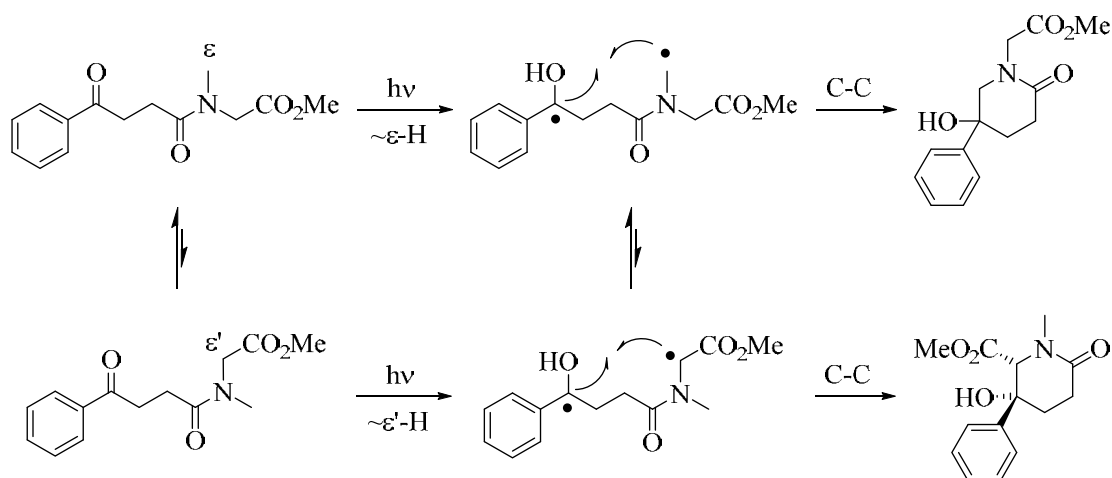
Scheme 4.25: Norrish-II reaction of the sarcosine-based 4-oxo-4-phenylbutanoly amide.

Recently, Liu *et al.* studied decarboxylative photocyclizations of 2-benzoylbenzamides incorporating α-amino acids [131]. Bi- and tri-cyclic benzo-oxazepines were obtained through chemoselective C-O bond formation and with high enantio- and diaststereoselectivity. The later findings suggested that the formation of the two chiral carbon centers was controlled by chiral memory effects. The unique C-O bond formation was confirmed by crystal structure analysis. As an example, the *L*-proline-derived 2-benzoylbenzamide gave the corresponding tricycle in a yield of 48% (**Scheme 4.26**). The commonly observed C-C bond formation product was not found.
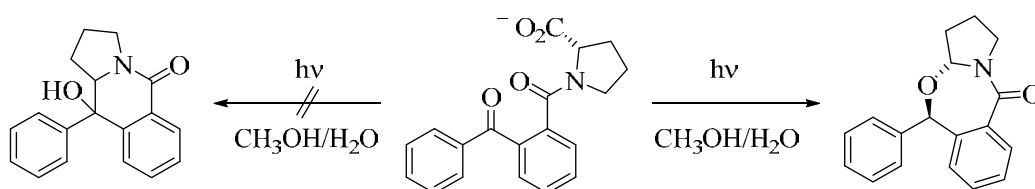
Scheme 4.26: Decarboxylative photocyclization of *L*-proline-derived 2-benzoylbenzamide.

The notable difference in regioselectivity, *i.e.* C-C *vs.* C-O bond formation, of the Norrish-II *vs.* photodecarboxylative cyclization may have been caused by the differences in the mechanistic key-steps of each reaction, which are H-abstraction *vs.* photoinduced electron transfer step (**Figure 4.6**). However, the related phthalimides solely undergo C-C formation upon photodecarboxylation [24].

Norrish-II
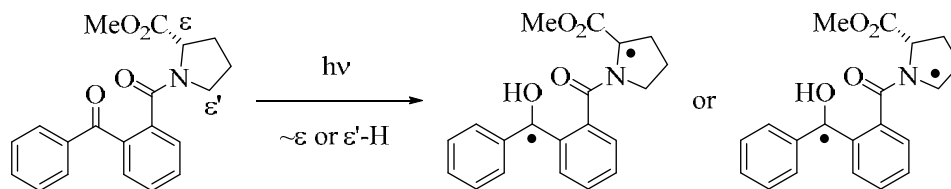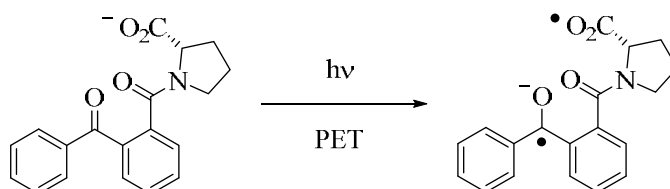
Figure 4.6: H-abstraction *vs.* photoinduced electron transfer step.

In case of the methyl thiazolidine-2-carboxylate-derived benzoylbenzamide, a preferential photoinduced electron transfer mechanism was expected [124, 125]. The products generated, however, confirm that Norrish-II mechanisms compete or even dominate (**Scheme 4.27**). The bridged bicyclic compound originating from cyclization at the -CH$_2$S- methylene carbon was not obtained due to its high strain. The [4.2.1] bicyclic product generated from cyclization at the -SCH-methine can be generated by either mechanisms. The product structures alone thus do not argue for a preferential mechanistic scenario.

Photoinduced Electron Transfer
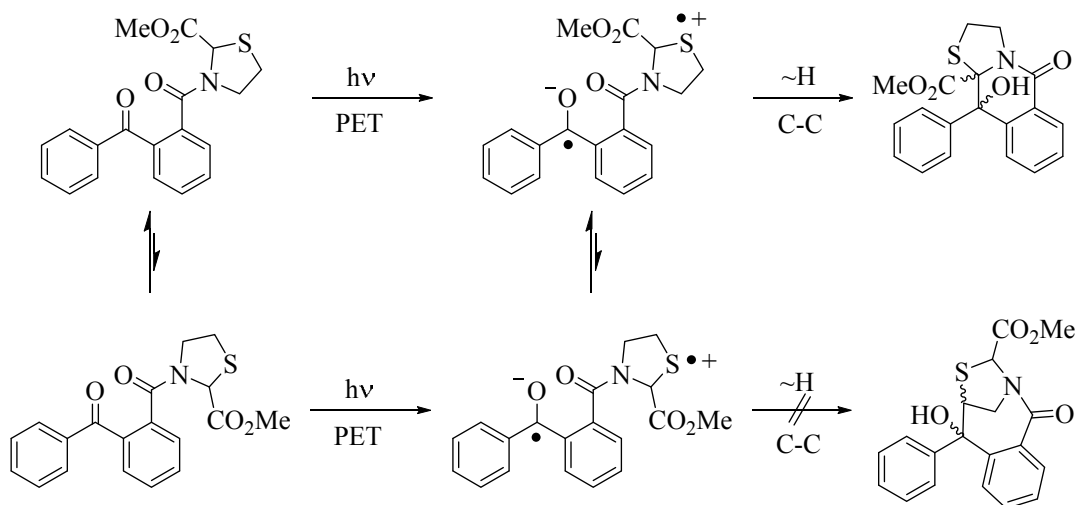
Norrish-II
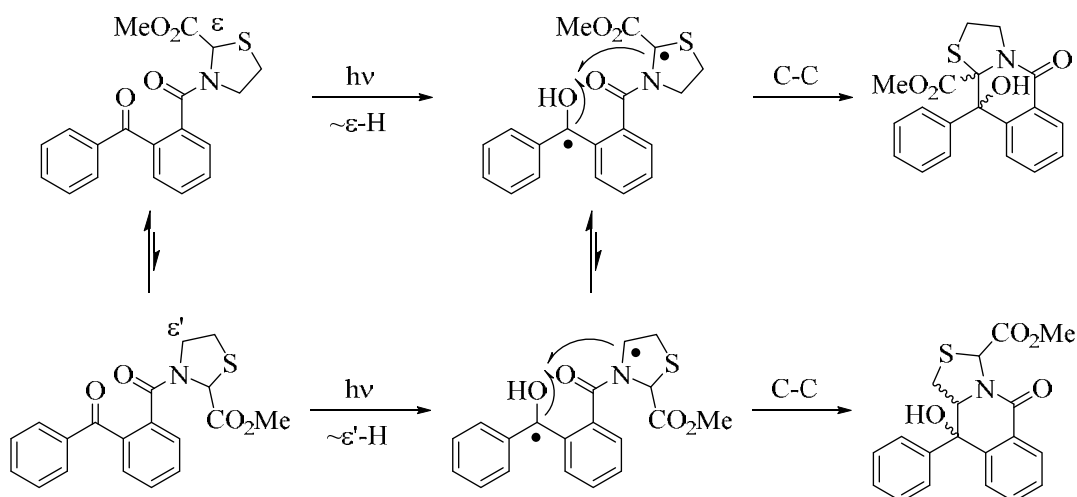
Scheme 4.27: Potential PET and Norrish-II mechanisms for the methyl thiazolidine-2-carboxylate-derived benzoylbenzamide.

For both successful photocyclizations, single diastereoisomers were formed for each of the regioisomeric products. Although the stereochemistry could not be determined, the decarboxylative photocyclizations of 2-benzoylbenzamides shown in **Scheme 4.26** predominantly furnished the *like*-diasteroisomers. Likewise, photodecarboxylations of the related α-amino acid-derived phthalimides showed high diastereoselectivity and solely the *trans*-diastereoisomers were formed (**Scheme 4.28**) [132, 133].
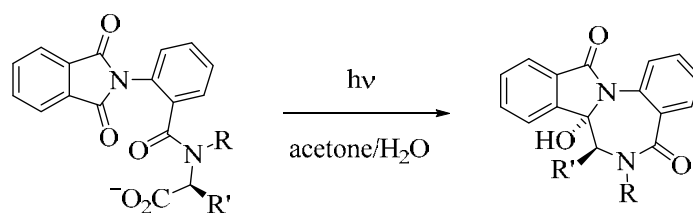
Scheme 4.28: Diastereoselective photodecarboxylations of α-amino acid-derived phthalimides.

For the *L*-proline and methyl thiazolidine-2-carboxylate-derived benzoylbenzamides in this study, the *trans*-diastereoisomer may therefore be formed preferentially as well (**Figure 4.7**). While the configuration at the original chiral center in proline was defined by the starting material, the corresponding methyl thiazolidine-2-carboxylate was used as a racemic mixture.

_L_-Proline case   **Methyl thiazolidine-2-carboxylate case**
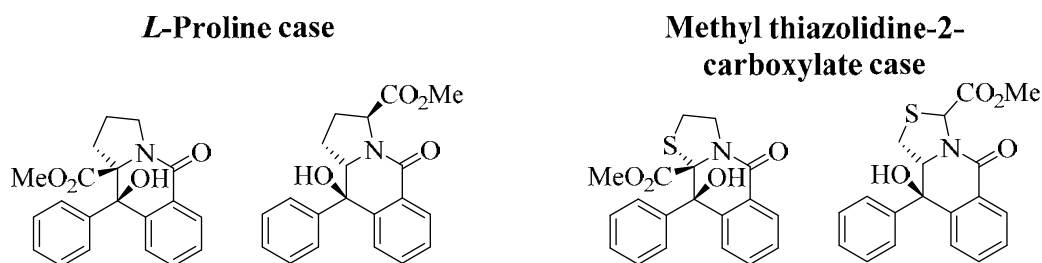
Figure 4.7: Suspected diastereoisomers formed for the _L_-proline and methyl thiazolidine-2-carboxylate-derived benzoylbenzamides.

4.4 Photoredox catalytic additions

4.4.1 Photoredox catalytic additions under batch conditions

Recently, visible light photoredox catalysis has received widespread interest in synthetic organic photochemistry [134]. In particular, it served as a powerful access to α-aminoalkyl radicals, which have found widespread application in organic synthesis [135-137].

In present study, the photoredox decarboxylative addition of phenylglycine with different enones was studied (**Scheme 4.29**).
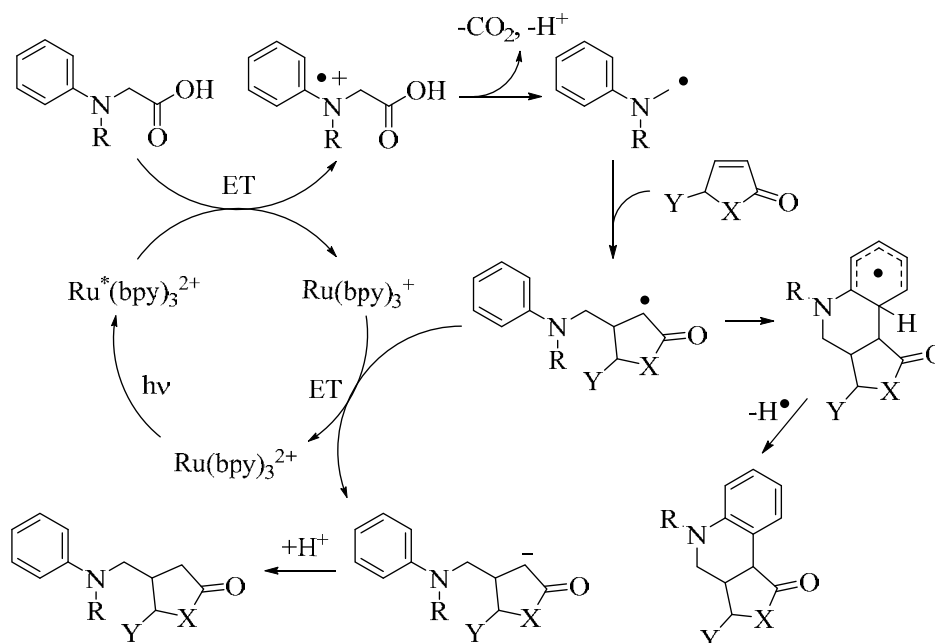
Scheme 4.29: Photoredox decarboxylative addition of phenylglycines to enones.

The reaction is initiated by absorption of visible light by the catalyst. Electron transfer (ET) from the amino-group of phenylglycine to the excited state of the photocatalyst followed by decarboxylation and deprotonation yields the corresponding α-aminoalkyl radical, which subsequently adds to the β-position of the double bond of the enone. Return electron transfer

generates the corresponding anion, which is rapidly protonated to the open addition product. Alternatively, radical attack onto the phenyl ring followed by formal loss of a hydrogen-atom yields the cyclization product. The exact mechanism of the later process remains unclear.

A number of studies have previously obtained open addition products. For example, Miyake *et al.* developed visible light mediated additions of α-aminoalkyl radicals generated from α-silylamines to α, β-unsaturated carbonyl compounds using Ir- and Ru-complexes (**Scheme 4.30**) [138]. The trimethylsilyl-cation functioned as a leaving and directing group [139-143]. The reaction gave silyl enol ethers as initial products that were hydrolyzed to the corresponding ketones in overall yields of 48-87%.
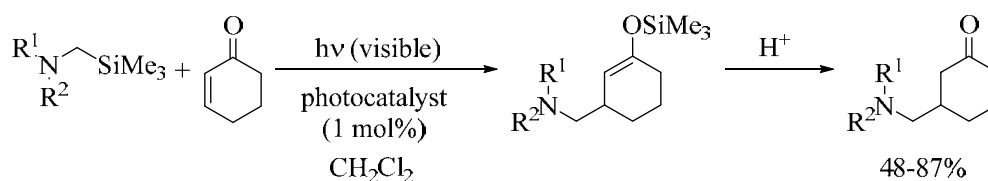
Scheme 4.30: Photocatalytic addition of α-silylamines to cyclohenxanone.

Miyake *et al.* also reported visible light mediated oxidative decarboxylations of arylacetic acids bearing a remote amino group to the respective benzyl radicals and their addition to electron-deficient alkenes using photoredox catalyst (**Scheme 4.31**) [144]. The corresponding open addition products were isolated in yields of 51-93%
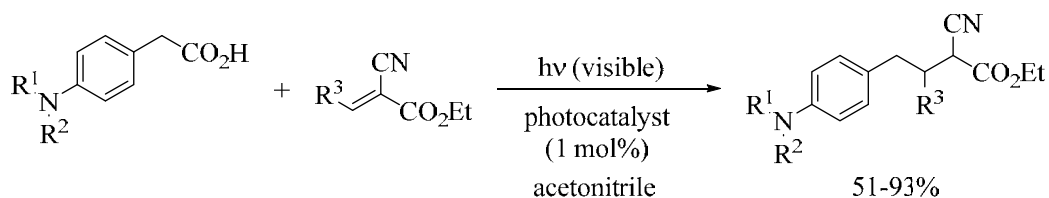
Scheme 4.31: Oxidative decarboxylative addition of arylacetic acids to electron-deficient alkenes.

Likewise, Millet and co-workers have described visible light photoredox decarboxylative additions of amino acid derived α-aminoalkyl radicals to electron deficient olefins (**Scheme 4.32**) [145]. The resultant products were obtained in yields of 42-80%.
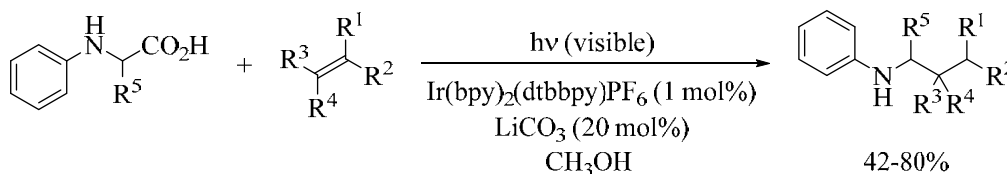
Scheme 4.32: Photoredox decarboxylative additions of *N*-phenyl amino acids to alkenes.

A number of studies reported the formation of cyclic addition products. For example, Bertrand *et al.* studied the addition of *N*, *N*-dimethylaniline to (5*R*)-menthyloxyfuranone. The reaction proceed under UV light in the presence of 4, 4'-bis(*N*, *N*-dimethylamino)benzophenone [Michler's ketone, BDMBP] (**Scheme 4.33**) [146]. While the reaction was somewhat diastereoselective, isolated yields remained low with just 40% in total. Photoreduction and dimerization products of furanone were furthermore isolated. The later were formed as part of the crucial H•-transfer step.
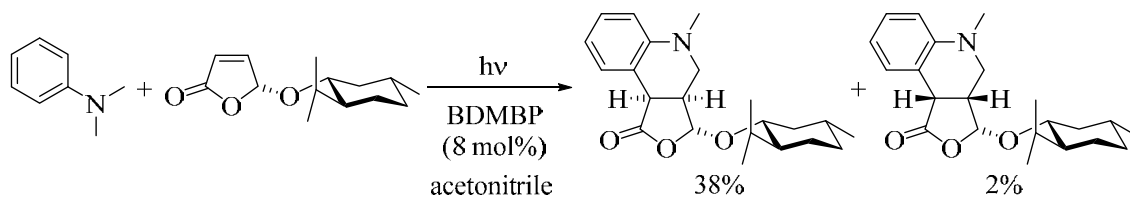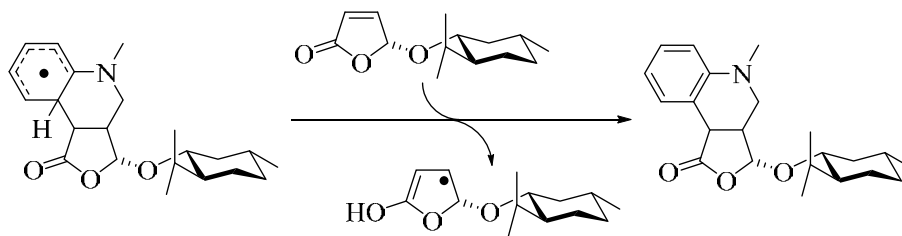
Scheme 4.33: Diastereoselective addition of *N*, *N*-dimethylaniline to (5*R*)-5-menthyloxy-2[*5H*]-furanone and crucial H•-transfer step.

Likewise, Ju and co-workers investigated the addition of *tertiary* anilines to maleimides using visible light redox catalysis. Tetrahydroquinolines were obtained as cyclization products under aerobic conditions in yields of 66-98% (**Scheme 4.34**) [147].
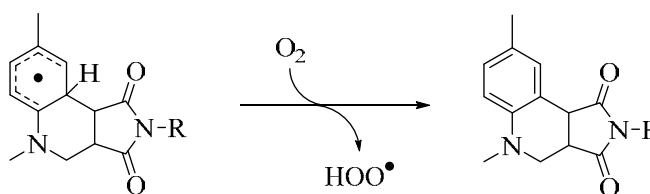
Scheme 4.34: Addition of *N*, *N*-dimethyl-4-methylaniline to maleimides and crucial H•-transfer step.

Oxygen was essential in the terminal H•-transfer step and was subsequently converted into hydrogen peroxide. TiO_2- and Eosin Y-catalyzed versions of this reaction have also been reported [148, 149].

A decarboxylative variant using fluorescein as a photocatalyst has been developed by Chen and co-workers (**Scheme 4.35**) [150]. Various *N*-phenylglycines served as α-aminoalkyl radical precursors. The corresponding cyclization products were isolated in moderate to excellent yields of 51-95%. Although an H•-transfer was proposed in the mechanistic scenario, the H•-acceptor was not revealed.
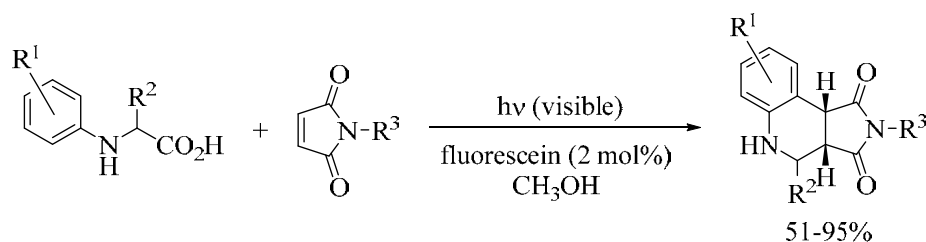
Scheme 4.35: Fluorescein-catalyzed photodecarboxylative addition of *N*-phenylglycines to maleimides.

Alternatively, a thermal route towards the cyclic addition products has been devised by Song and Antonchick. The reaction again involved the addition of α-aminoalkyl radicals to maleimides. Tetrabutylammonium iodide (TBAI) served as a radical initiator and *tert*-butyl hydroperoxide (TBHP) as an oxidant. Polycyclic heterocycles were generated by radical annulation of tertiary arylamine derivatives in moderate to high yields of 40-94% (**Scheme 4.36**) [151]. The reaction is terminated by H•-transfer to either the *tert*-butoxyl or *tert*-butylperoxyl radical.
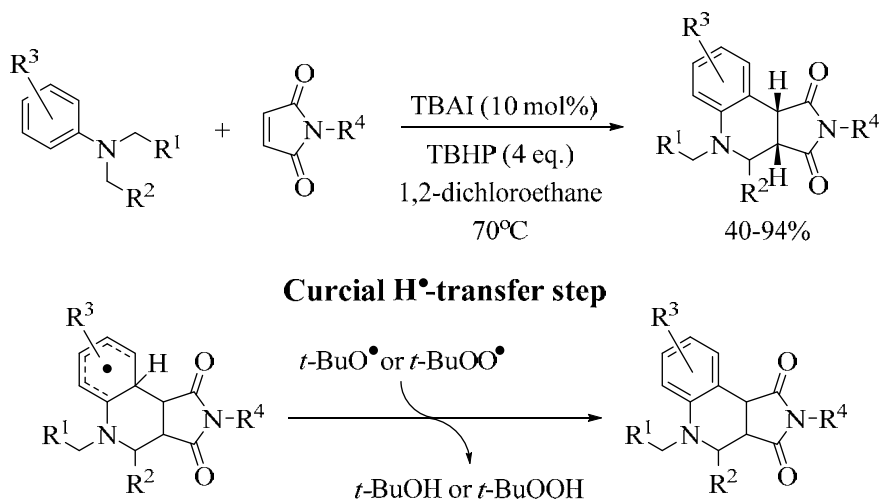
Scheme 4.36: Thermal addition of arylamines to maleimides and crucial H•-transfer step.

An alternative thermal variation utilized inexpensive and easy to handle potassium persulfate ($K_2S_2O_8$) instead [152].

Lenhart and Bach investigated visible light induced additions of *N*-methyl-*N*-((trimethylsilyl)methyl)aniline to α, β-unsaturated carbonyl compounds using an Ir-photocatalyst. Mixtures of open and cyclic addition products were obtained in combined yields of 30-67% (**Scheme 4.37**) [153]. Chemoselectivity varied with the enone substrate. For the six-membered lactones and lactams and for cyclopentenone the open addition products were formed preferentially. In contrast, five-membered α, β-unsaturated lactone and lactam substrates solely furnished the corresponding cyclic adducts. An explanation for this differing selectivity was not provided. Likewise, the H•-acceptor involved in the cyclization was not disclosed.
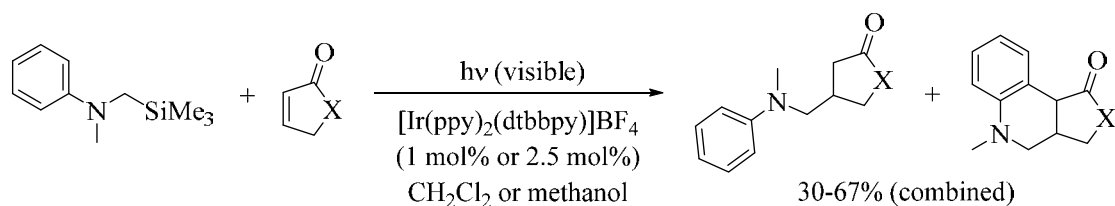
Scheme 4.37: Visible light induced addition of *N*-methyl-*N*-((trimethylsilyl)methyl)aniline to α, β-unsaturated carbonyl compounds.

Several other examples of photoredox catalyzed addition reactions of α-aminomethyl radicals to double bond systems have been described in the literature [154, 155]. Likewise, successful additions using more conventional conditions and UV light have been reported [156, 157]. When acetonitrile was exchanged by either ethanol or isopropanol, the corresponding alcohol addition products were isolated instead. These compounds are known to form under triplet-sensitized conditions in the presence of either acetone or 4, 4'-dimethoxybenzophenone (DMBP) (**Scheme 4.38**) [158, 159].
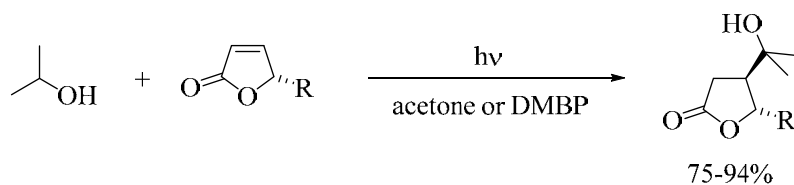
Scheme 4.38: Sensitized isopropanol addition to furanones.

Since alcohol cannot be directly oxidized by photoexcited Ru(bpy)$_3$Cl$_2$, hydrogen abstraction from the alcohol must occur at a later stage of the mechanism. A possible scenario is outline in **Scheme 4.39**. It is assumed that phenylglycine acts as a sacrificial agent that is oxidized and

undergoes deprotonation and decarboxylation. The corresponding α-aminomethyl radical may then abstract a hydrogen from the α-position of the alcohol, yielding *N*-methylaniline as a by-product. The ketyl radical formed subsequently adds to the double bond of furanone. Subsequent return electron transfer and protonation would yield the observed products.
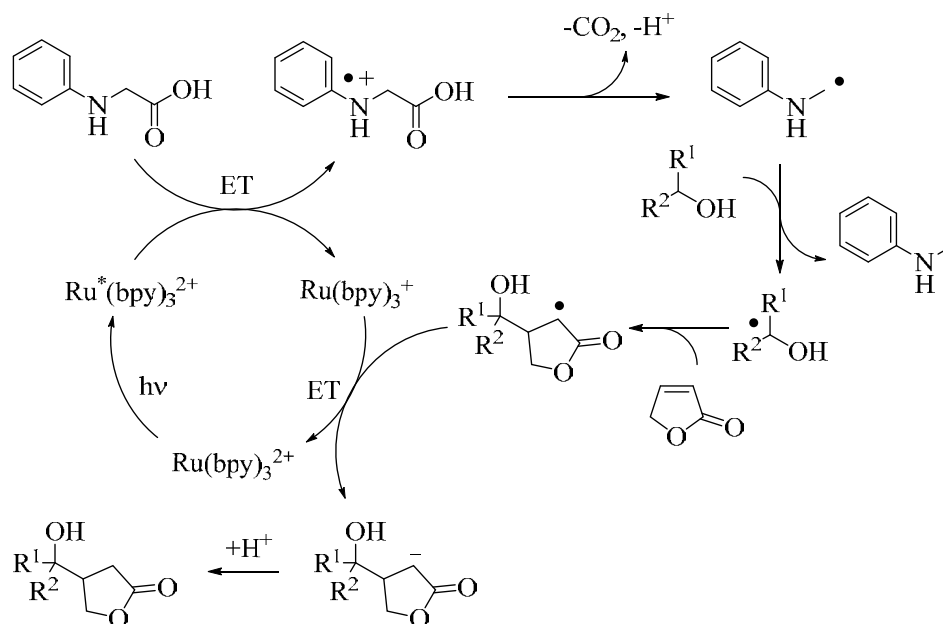
Scheme 4.39: Possible mechanism of photoredox addition of alcohols to furanone.

In contrast, Lenhart and Bach successfully realized photoredox catalyzed additions of *N*-methyl-*N*-((trimethylsilyl) methyl)aniline to furanone in methanol as well as DMF (**Scheme 4.37**) [153]. The authors noted a faster reaction in these polar solvents when compared to dichloromethane, however, all three solvents showed a different chemoselectivity. In methanol, solely the cyclization product was formed, whereas dichloromethane exclusively gave the open addition adduct. In DMF, a roughly 2.5:1 mixture of the cyclized and open product was obtained instead. No explanation was given for these different outcomes. In this study, the photoredox decarboxylative addition did not proceed in DMF at all, while experiments conducted in alcohols solely furnished the corresponding alcohol-addition adducts instead. Possible explanations may come from the different photoredox catalysts, *i.e.* Ru(bpy)$_3$Cl$_2$ *vs.* [Ir(ppy)$_2$(dtbbpy)]BF$_4$, and α-aminomethyl radical sources, *i.e.* phenylglycine *vs.* *N*-methyl-*N*-((trimethylsilyl) methyl)aniline, employed.

DMBP and methyl orange were tested as alternative photosensitizers or photocatalyst but both substrates failed to induce any reaction. DMBP is a triplet sensitizer that undergoes hydrogen transfer rather than electron transfer processes [160]. In contrast, the oxidation power of methyl

orange is not high enough to induce any electron transfer mechanism. In contrast, Eosin Y effectively catalyzed the addition of *tertiary* anilines to maleimides [149]. Likewise, photodecarboxylative additions of *N*-phenylglycines to maleimides have been realized using fluorescein as a photocatalyst [150].

Several other amino acid derivatives with *N*-methyl- or *N*-acyl-groups were furthermore investigated but remained photostable. Likewise, thioether containing acetic acids did not undergo the desired photoredox decarboxylation. This lack in reactivity may be best explained by the different oxidation potentials of anilines, amine, thioethers, amides and carboxylic acids (**Equation 4.2**) [161, 162]. The excited state of Ru*(bpy)$_3^{2+}$ is unable to oxidize these potential donors (**Figure 4.8**). In fact, most photoredox addition reactions utilize *tertiary* anilines and their analogues [135-137]. However, specially designed photocatalysts with higher oxidation power have been used to activate other carboxylic and amino acid derivatives [155, 163].

Anilines < Amines < Thioethers < Carboxylic acids < Amides

Equation 4.2: Reactivity order based on potential electron donor groups.
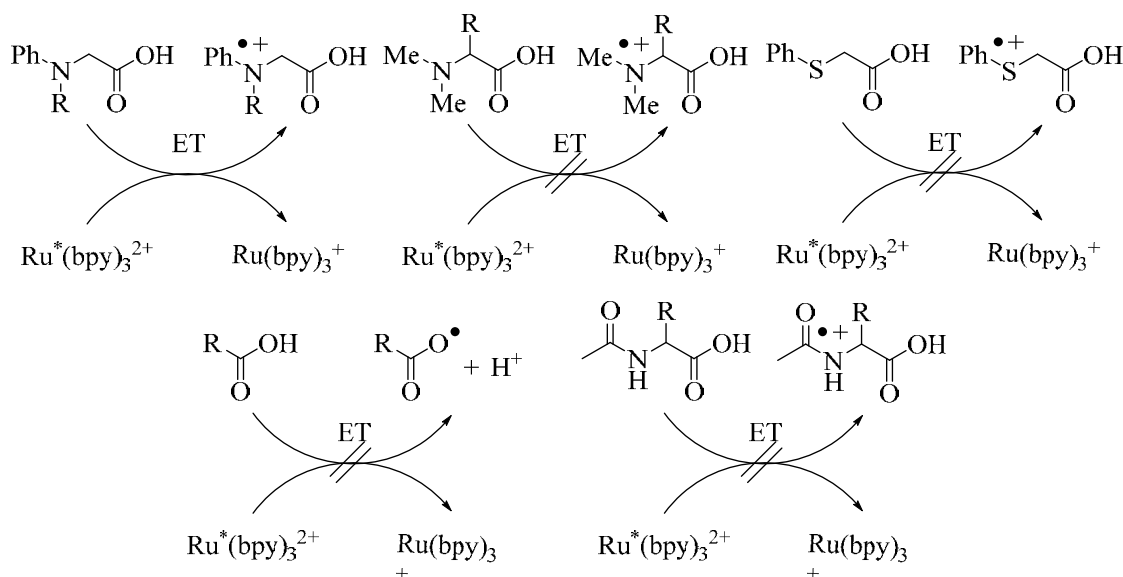
Figure 4.8: Successful and unsuccessful electron transfer steps.

4.4.2   Photoredox catalytic additions under flow conditions

The generally mild reaction conditions have made photoredox catalysis an emerging field in green chemistry [164]. However, the reaction protocols commonly demand long irradiation times on small scales to achieve high conversions. Recently, continuous flow reactors have been utilized to accelerate photochemical reactions. Consequently, photoredox catalytic

reactions have been successfully transferred to continuous flow devices and a reduction in both, reaction time and catalyst loading, was commonly achieved [165, 166].

Thus, the Ru-catalyzed photoredox reactions from this study were further investigated in a microflow setup and compared to their performances in the batch reactor. Following this approach, a reduction in reaction time from 18 hours in batch to a residence time of 3 hours in flow was determined. This finding is best explained by the improved light penetration and irradiated area to volume ratio for the microcapillary reactor (**Table 4.2**). The path length of the Schlenk flask, *i.e.* the space between outer reactor wall and cooling finger, was approx. 4-5 mm. In contrast, the path length, *i.e.* inner diameter, of the capillary reactor was just 0.8 mm or 5-6 ½ times narrower than in the Schlenk flask.

Table 4.2: Comparison of reactor's efficiency.

Reactor parameter	Batch	Flow
Path length (mm)	4-5	0.8
Volume (mL)	60	5[a]
Irradiated area (cm^2)	102[b]	159.3[c]
Irradiated area/volume (cm^2/mL)	1.7	31.86
Lamp power (W)	128 (16 × 8)	8
Lamp power/irradiated area (W/cm^2)	1.25	0.05
Time (h)	18	3 (6[d])
Lamp power × time (W h)	2304	24 (48[e])

[a] Volume of exposed capillary. [b] Assuming a cyclic geometry of the Schlenk flask. [c] Covered cylinder area by capillary. [d] Operation time required to pump all 10 mL through capillary at a flow rate of 1.66 mL/h. [e] Value for whole operation time.

In addition, the flow reactor was found to be more economical in terms of its light utilization, as reflected in its superior lamp power per irradiated area and lamp power over time values. Its *inside-out* irradiation design used a single 8 W fluorescent tube (**Figure 4.9**). In contrast, the larger Rayonet reactor was equipped with 16 × 8 W of fluorescent tubes in an *outside-in* arrangement. Most of the emitted light in the batch reactor is thus lost as it does not hit the reaction vessel, although the reflective wall of the chamber may somewhat limit this light loss. In addition, the distance between fluorescent tube and reaction mixture is much shorter in the capillary tower, thus minimizing the decrease in light intensity reaching the reaction mixture. The diameter of its Pyrex glass cylinder was 6.5 cm, whereas the inner diameter of the Rayonet chamber was 25 cm. The importance of the distance between light source and reactor has been demonstrated by Sugimoto and co-workers for the Barton reaction (nitrite photolysis) of a steroidal substrate [167].
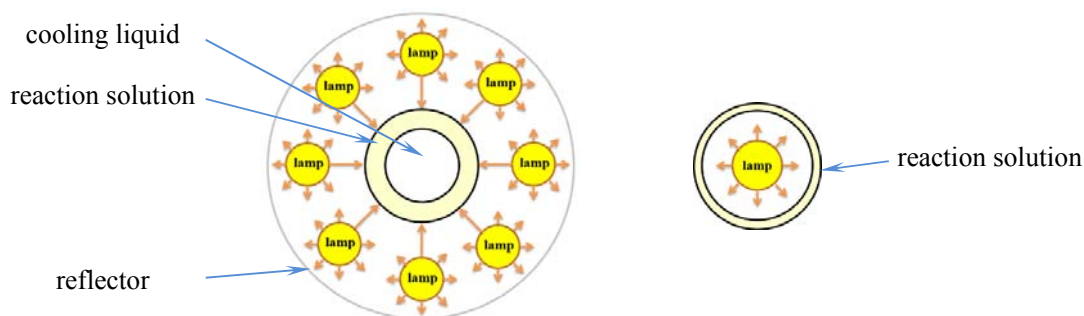
Figure 4.9: Schematics of *outside-in* and *inside-out* irradiation (not to scale).

In contrast, the Rayonet setup showed a better match of light source and Schlenck flask dimensions (**Figure 4.10**).
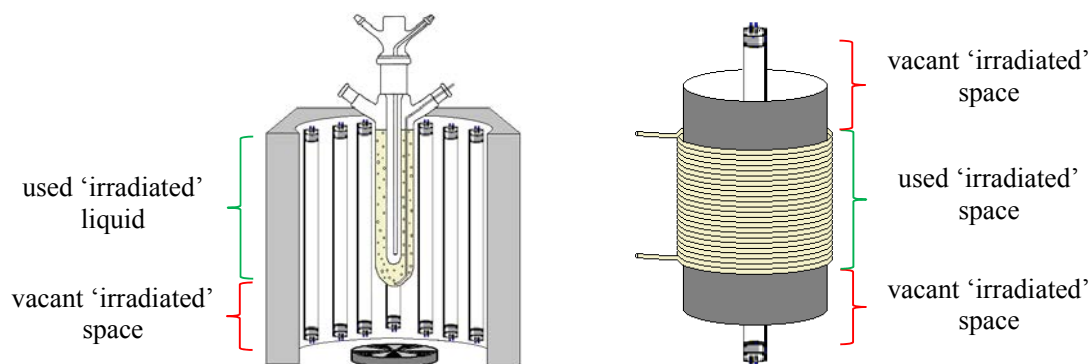
Figure 4.10: Coverage of arc lengths in Rayonet chamber reactor and in the in-house capillary reactor (not to scale).

The usable filling height of the Schenk flask from the bottom of the flask to the side-arms was approx. 15-18 cm. It thus does cover most of the arc length of the fluorescent tube of 23 cm. For the simple *in-house* capillary tower, only approx. ⅓ of the arc length of the fluorescent tube was covered by the capillary instead.

4.5   Synthesis of AL12, AL5 and their analogues

4.5.1   Introduction to AL12 and AL5

One of the primary objectives of the present study was to investigate new pathways towards bioactive compounds. The previously described local anaesthetics **AL12** and **AL5** were thus chosen as model targets (**Figure 4.11**). The compounds have shown better local anaesthetic activities than the traditional medicines procaine, lidocaine (xylocaine) or tetracaine [168].
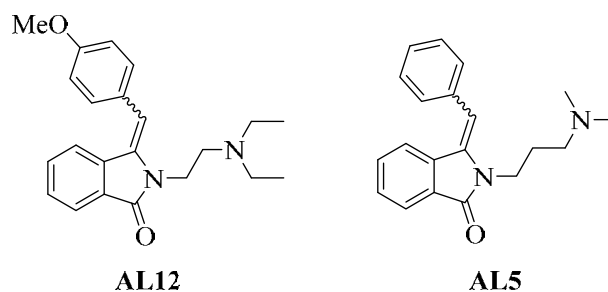
Figure 4.11: Structures of **AL12** and **AL5**.

The original patented synthesis route to **AL12** is shown in **Scheme 4.40** and involves a series of thermal steps. Condensation of phthalic anhydride with 4-hydoxyphenylacetic acid furnished the corresponding hydroxybenzylidene phthalid. Subsequent treatment with diethylamino-ethylamine, followed by acetic anhydride and HCl-saturated ethanol gave the 4-acetoxy-benzylidene-derivative **AL12B** as a hydrochloride salt. Neutralization of the salt and hydrolysis of the acetate with potassium hydroxide, followed by alkylation with methyl iodide furnished the desired **AL12** in an overall yield of 36% over all 4 steps.
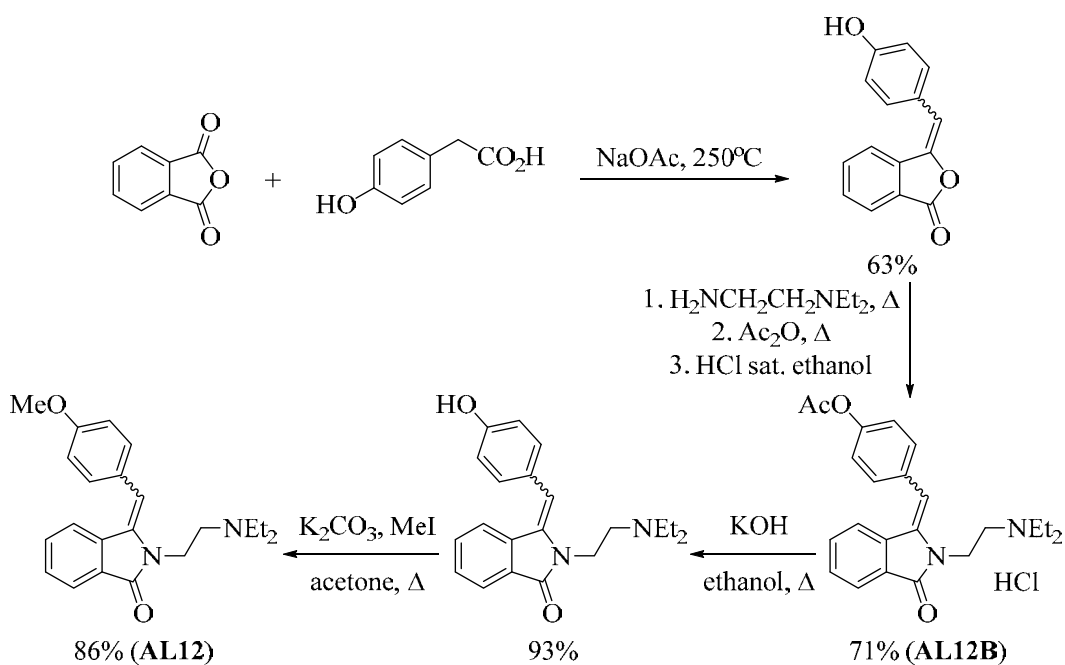
Scheme 4.40: Patented synthesis route for the synthesis of **AL12** and **AL12B**.

4.5.2 Photodecarboxylative additions of phenylacetates to *N*-bromoalkylphthalimides

4.5.2.1 Photodecarboxylative additions under batch conditions

Photodecarboxylation (PDC), *i.e.* elimination of carbon dioxide upon irradiation with light, has been intensively studied in organic photochemistry [31]. The photodecarboxylation involving

phthalimide derivatives in particular has emerged as an efficient pathway to macrocycles and Grignard-type addition products [24].

The retrosynthetic analysis towards **AL12** and its analogues, utilizing the photodecarboxylative benzylation protocol [82, 88], is depicted in **Figure 4.12**. The simple 3-step procedure incorporates two functional group interchange (FGI) steps and one disconnection. In the forward direction, the first step comprises the photodecarboxylative addition of phenylactetate to *N*-bromoalkylphthalimides, yielding hydroxyl phthalimidine derivatives as key intermediates. Subsequent dehydration in the second step, followed by amination in the third step furnishes the desired target compounds. The amino-group is introduced in the last step since it would otherwise interfere with the desired photoreaction. In fact, amines are very potent electron donors and are easily oxidized by the phthalimide chromophore [169].
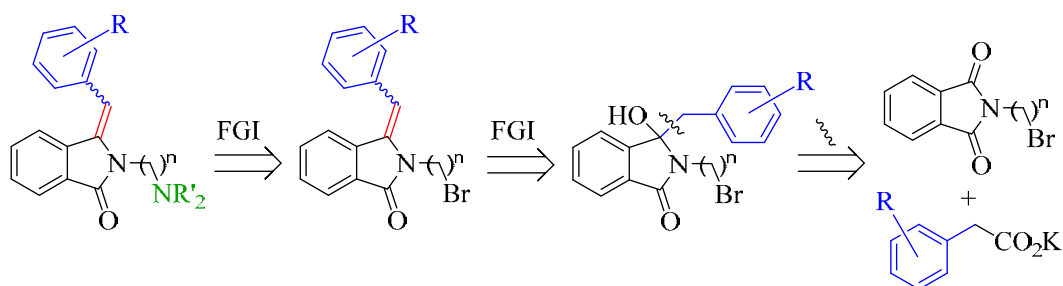
Figure 4.12: Retrosynthetic analysis of **AL12** and its derivatives.

Irradiations of mixtures of *N*-bromoalkylphthalimides and phenylacetates in acetone/pH 7 buffer produced the desired benzylated hydroxyl phthalimidines in good to excellent yields of 63-91%. Acetone was chosen as an effective co-solvent and triplet-sensitizer. The mechanistic scenario is depicted in **Scheme 4.41**. The photoreaction is initiated by the absorption of light by acetone and subsequent population of its triplet excited state *via* intersystem crossing (ISC). Collision energy transfer (EnT) from the excited acetone (T_1 = 309 kJ/mol [170]) to the phthalimide chromophore (T_1 of Pht=N-Me = 297 kJ/mol [8]) generates the corresponding triplet excited phthalimide. Subsequent electron transfer (ET) from the carboxylate function to the triplet excited phthalimide generates an unstable carboxy radical and the phthalimide radical anion. The carboxyl radical rapidly undergoes decarboxylation to the corresponding resonance-stabilized benzyl radical. Protonation of the phthalimide radical anion and C-C bond formation subsequently yields the benzylated hydroxyl phthalimidines. Potassium hydroxide is formed as a by-product. To minimize any nucleophilic displacements of the bromide-group, the reaction is thus carried out in a pH 7 buffer. In acetonitrile, the photodecarboxylation operates *via* direct excitation of the phthalimide chromophore and ISC to its triplet state.

Triplet sensitization

PET-Decarboxylative Addition
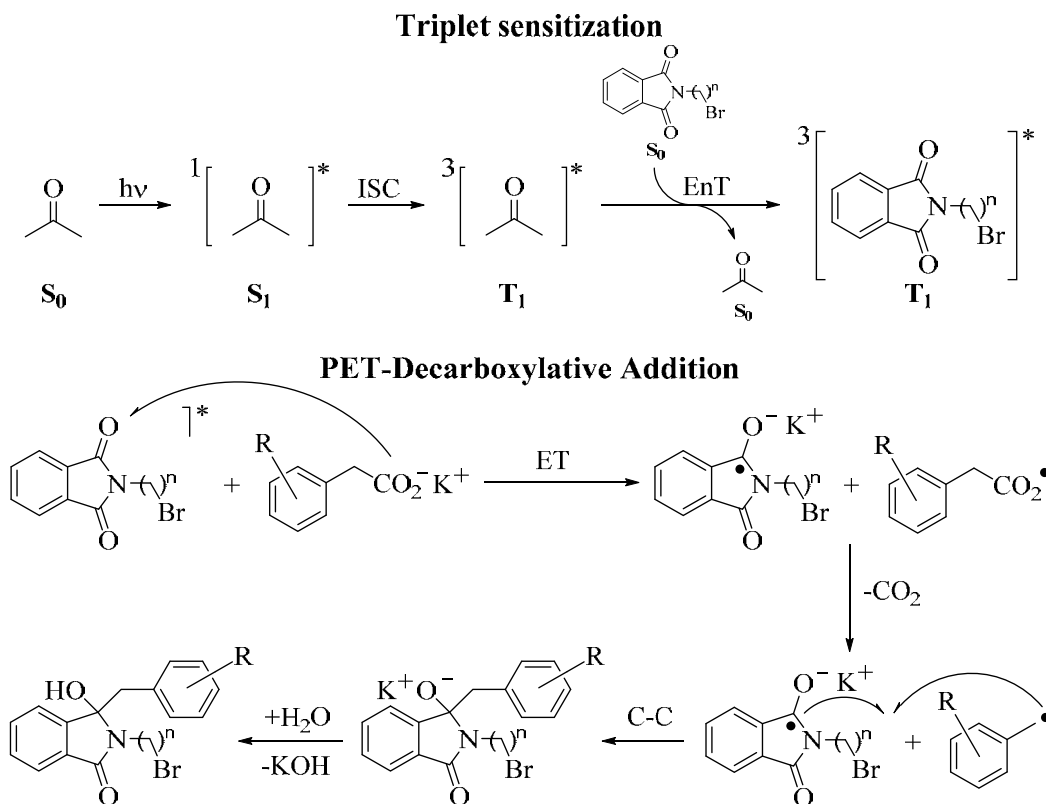
Scheme 4.41: Photodecarboxylative addition of phenylacetates to *N*-bromoalkylphthalimides.

The feasibility of the crucial photoinduced electron transfer step was again estimated utilizing the Rehm-Weller equation (**Equation 4.1**) [6, 7]. Using the relevant values from the literature (**Table 4.3**), a favorable negative ΔG value of -0.46 eV was determined.

Table 4.3: Electrochemical and photophysical data of phenylacetate and phthalimide.

E_{ox} (**PhCH$_2$CO$_2^-$**)[a]	+1.27 V [100]
E_{red} (**Pht=N-Me**)	-1.37 V [11]
E_{coul}	negligible in polar solvents
E^*_∞	3.1 eV [170]
ΔG	**-0.46 eV**

[a] *vs* SCE (standard calomel electrode)

Simple decarboxylations of the phenylacetates, *i.e.* -CO_2^-/-H exchange reactions, are commonly observed side-reactions [53]. These are caused by an alternative back electron transfer (BET) from the phthalimide radical anion to the benzyl radical (**Scheme 4.42**) [171, 172]. Protonation of the resulting carbanion subsequently yields the corresponding toluenes, which are typically not isolated and instead removed during evaporation or column chromatography. To minimize the impact of this reactions, an excess amounts of the phenylacetate is provided.
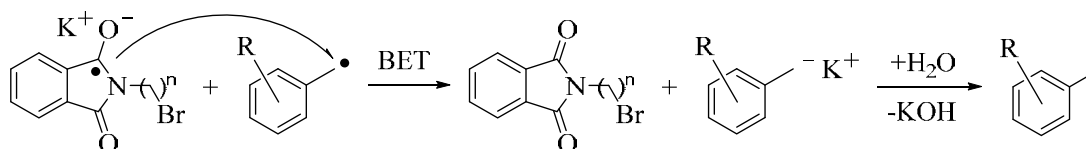
Scheme 4.42: Mechanism of the simple photodecarboxylation of phenylacetates.

Due to the presence of a nucleophilic hydroxyl-group or its corresponding alcoholate, nucleophilc substitution and cyclization was thought to compete with the desired benzylation reaction, especially for reactions involving *N*-bromoethylphthalimide. This nucleophilic cyclization to the oxazolidine-derivative may occur during different stages of the mechanism (**Scheme 4.43**). The phthalimide radical anion may undergo nucleophilic cyclization prior to C-C bond formation. Alternatively, the alcoholate obtained after C-C bond formation may cyclize to the oxazolidine. Similarly, the final benzylated hydroxyl phthalimidine may undergo cyclization instead. To suppress these undesired reactions, the photodecarboxylation was performed in pH 7 buffer media. It was later discovered that cyclizations occurred thermally at elevated temperatures from the benzylated hydroxyl phthalimidines themselves (see **Chapter 4.8**). Temperature control during the reaction, workup and isolation was thus important to suppress the undesired reaction.
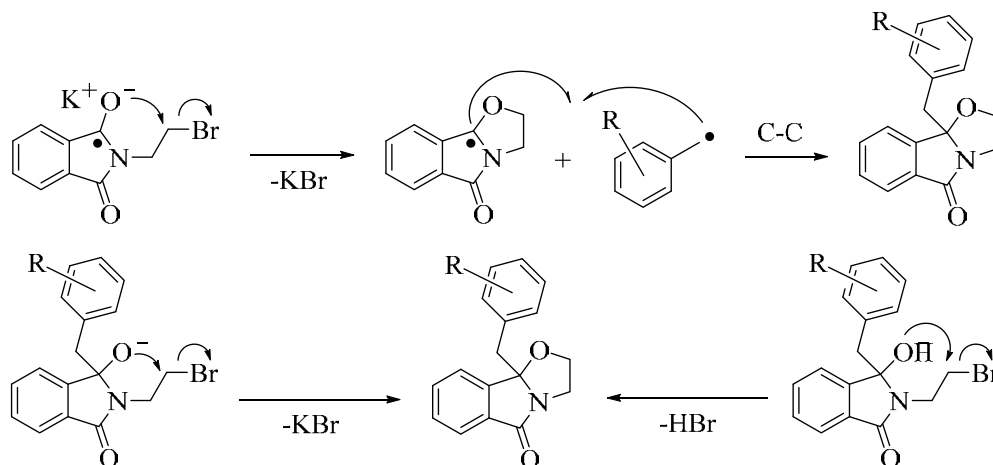
Scheme 4.43: Possible nucleophilic cyclizations.

Cyclization reactions have indeed been reported from various reaction intermediates. For example, the photoreaction of phthaloyl-*L*-methionine in acetone furnished a tetracyclic lactone as the major product in 72% yield [173]. Its formation was rationalized by an initial PET from the sulfur atom, followed by subsequent lactonization *via* nucleophilic attack at the carboxyl group and deprotonation in α-position the sulfur radical cation. Alternatively, C-C bond formation may precede lactonization.
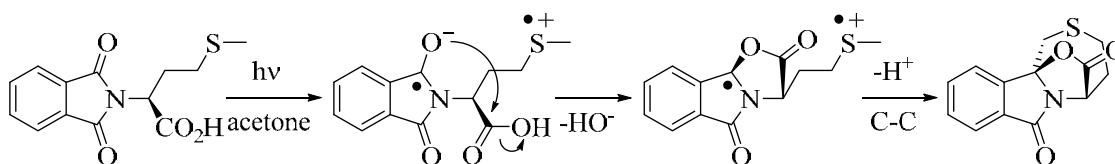
Scheme 4.44: Lactonization during the photoreaction of phthaloyl-*L*-methionine (as suggested by Griesbeck *et al.* [173]).

The reaction of *N*-bromethylphthalimide with Grignard reagents (PhMgBr and BnMgCl) in non-protic solvents solely gave the corresponding oxazolidine. After nucleophilic addition of the Grignard reagent, the alcoholate displaces the bromide in the *N*-sidechain to form the six-membered ring (**Scheme 4.45**) [174].
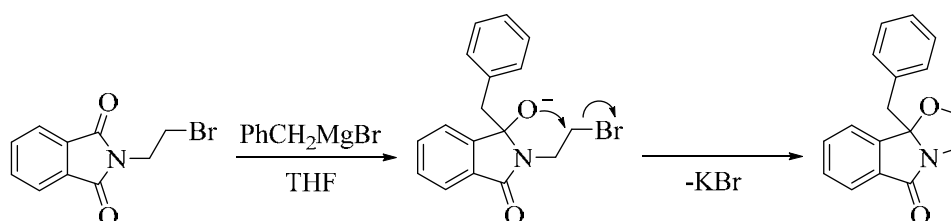
Scheme 4.45: Oxazoloisoindolone formation during Grignard addition.

Grignard-additions can thus not be used for the synthesis of benzylated hydroxyl phthalimidines from *N*-bromethylphthalimide. Organolithium compounds reacted similarly [175].

Wharton and co-workers obtained oxazoloisoindolone by reducing *N*-bromethylphthalimide with NaBH$_4$ and subsequent treatment with a base (**Scheme 4.46**) [176]. Cyclization is again induced by nucleophilic attack of the corresponding alcoholate onto the bromoalkane in the *N*-sidechain.
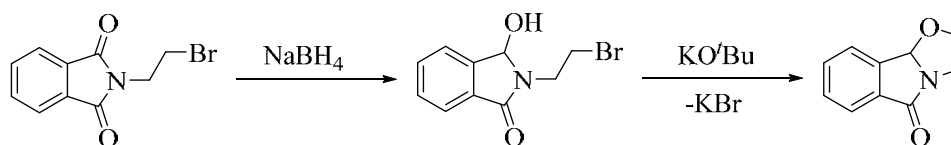
Scheme 4.46: Base-catalyzed oxazoloisoindolone formation.

4.5.2.2 Photodecarboxylative additions under flow conditions

While the photodecarboxylative addition under batch conditions took 3 hours, it required just 20 minutes in the flow reactor to achieve complete conversion. As with the photoredox reactions described in **Chapter 4.4.2**, the microflow photoreactor showed better performances in terms of reaction time and utilization of available light (**Table 4.4**). This was again achieved by to the improved light penetration within the microcapillary in combination with the superior

inside-out reactor design (**Figure 4.9**). The larger Schlenk had a usable filling height of 30-35 cm, which significantly exceeded the arc length of the fluorescent tube of 23 cm.

Table 4.4: Comparison of reactor's efficiency using acetone as a co-solvent.

Reactor parameter	Batch	Flow
Path length (mm)	4-5	0.8
Volume (mL)	120	5^a
Irradiated area (cm^2)	330^b	159.3^c
Irradiated area/volume (cm^2/mL)	2.75	31.86
Lamp power (W)	128 (16 × 8)	8
Lamp power/irradiated area (W/cm^2)	0.39	0.05
Time (h)	3	⅓ ($⅔^d$)
Lamp power × time (W h)	384	2.7 (5.33^e)

[a] Volume of exposed capillary. [b] Assuming a cyclic geometry of the Schlenk flask. [c] Covered cylinder area by capillary. [d] Operation time required to pump all 10 mL through capillary at a flow rate of 15 mL/h. [e] Value for whole operation time.

Even though acetone was the best solvent for the photodecarboxylative addition step, the acidic conditions of the dehydration step led to the formation of its corresponding aldol condensation product, which required additional separation. Thus, acetonitrile was chosen as the solvent of choice for all the three reaction steps. Selected examples of photodecarboxylations were repeated in acetonitrile under microflow conditions and showed a somewhat longer residence time of 30 minutes to reach complete conversions. This difference in reaction time may be explained by the varying efficiencies of triplet-sensitization (acetone) *vs.* direct excitation (acetonitrile) pathways.

4.5.3   Dehydration to 3-arylmethyleneisoindolin-1-ones

Dehydrations of the photoproduct using catalytic amounts of sulfuric acid readily furnished the corresponding olefins in good to excellent yields of 83-95%. Mixture of *E*- and *Z*-stereoisomers were obtained. In most cases, the *E*-isomer was found as the preferred product indicating that it is thermodynamically more stable. The olefinic and *N*-alkylene protons of both isomers are clearly distinguishable by ^{1}H-NMR spectroscopy and can be used to assign the stereochemistry of the dehydration products as proposed by Ang and Halton (**Figure 4.13**) [177]. In particular, the olefinic proton of the *Z*-isomer experiences deshielding as it is in plane to the aromatic ring of the isoindolinone ring [178]. As a result, the olefinic =CH signal is shifted downfield to higher chemical shifts. The =CH group of the *E*-isomer is not effected by the aromatic ring. In

contrast, the *N*-alkylene protons of the *Z*-isomer are shifted upfield because of the shielding effect of the benzylidene group.
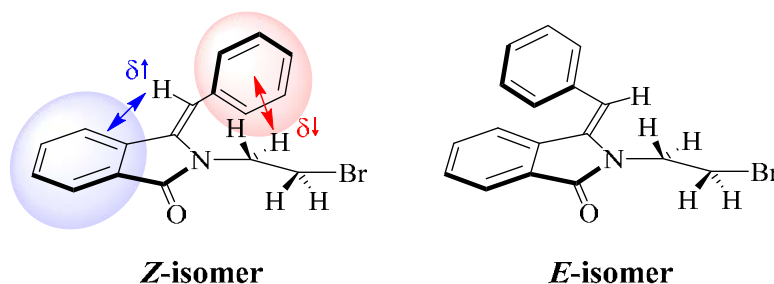
Figure 4.13: Anisotropic effects in a model benzylideneisoindolin-1-one.

Recently Kise *et al.* have conducted density functional studies (DFT) of both stereoisomers of *N*-unsubstituted and *N*-methyl substituted benzylideneisoindolin-1-ones [179]. For the *N*-methylated derivatives, the *E*-isomer was found to be thermodynamically more stable than the corresponding *Z*-isomer. This finding confirms the observations in this study. In contrast, DFT calculations on the *N*-unsubstituted derivatives favoured the *Z*-isomer. For each of the benzylideneisoindolin-1-ones, the thermodynamically more stable isomer could be enriched by refluxing in toluene in the presence of catalytic amounts of pyridinium *p*-toluenesulfonate.

Under flow conditions, the dehydration protocol was carried out in an ultrasound batch. The 3-arylmethyleneisoindolin-1-ones are much less polar than the corresponding benzylated hydroxyl phthalimidines and may thus precipitate inside the capillary, causing clogging, pressure build-up and eventually rupture of the capillary [180]. Ultrasound minimizes precipitation and prevents coagulation of any particles formed at the capillary walls. This was also demonstrated by Horie and co-workers for [2+2] cycloadditions under flow conditions in a capillary system [181].

The dehydration reactions took 20 minutes until completion under flow conditions in acetonitrile, compared to 3 hours in dichloromethane in the batch protocol. The acceleration is caused by the superior heat transfer inside the small diameter of the microcapillary (**Figure 4.14**) [182]. In contrast, conventional heating requires gradual heating up from the outside to the inside of the reaction mixture inside the flask.
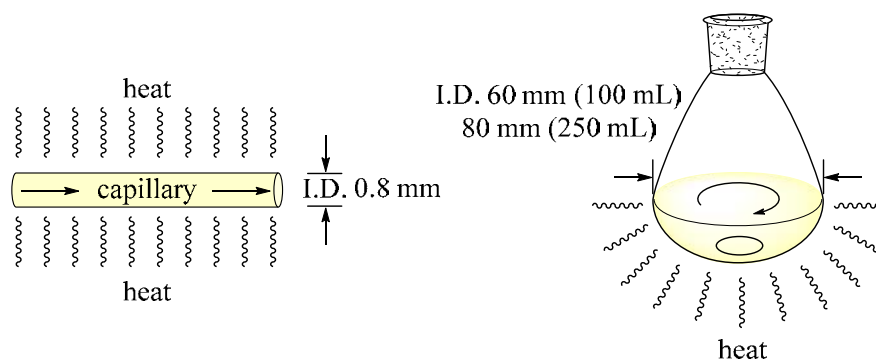
Figure 4.14: Heating in microcapillary and in a round bottom flask.

4.5.4 Amination reactions of 3-arylmethyleneisoindolin-1-ones

Treatment of the unsaturated isoindolinones with secondary amines in the presence of K_2CO_3 and KI gave the desired aminated target compounds in yields of 49-61%. Remarkably, the stereoselectivity of the products shifted entirely towards the Z-isomer. It is assumed that column chromatography on silica gel may have been responsible for this thermal isomerization (**Scheme 4.47**). Protonation of the double bond generates an acylaminium cation intermediate [183]. Subsequent rotation about the C-C bond and deprotonation furnishes the opposite stereoisomer. This scenario would assume that the Z-isomer is more thermodynamically stable than the E-isomer. This change in stability may have been caused by a stabilizing ionic-π interaction between the terminal protonated amino group and the aryl-ring for the Z-isomer during isomerization, as indicated with a red arrow in **Scheme 4.47** [184].
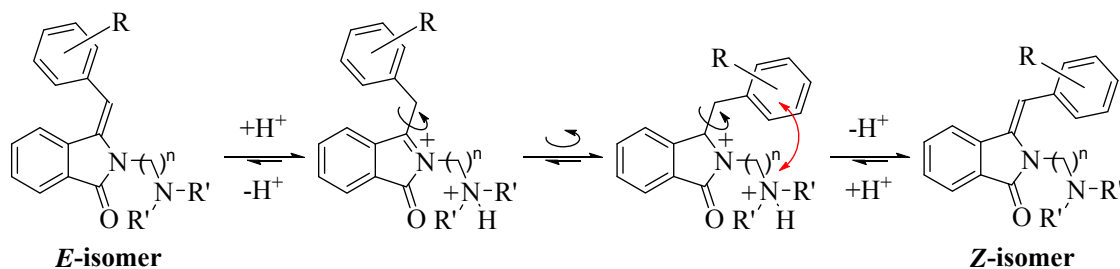
Scheme 4.47: Suggested mechanism for the E/Z-isomerization during amination.

A similar thermal isomerization in the presence of catalytic amounts of pyridinium *p*-toluene-sulfonate (PPTS) has been reported by Kise *et al.* (**Scheme 4.48**) [179]. Following this method, mixtures of the stereoisomeric benzylideneisoindolin-1-ones could be shifted largely or fully towards the thermodynamically more stable stereoisomer.
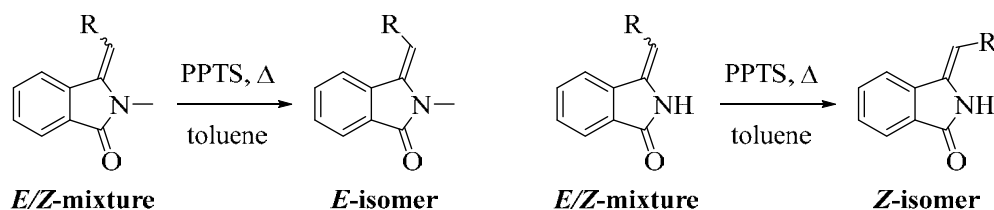
Scheme 4.48: PPTS-catalyzed isomerization of benzylideneisoindolin-1-ones.

4.5.5 One-flow multistep synthesis of local anaesthetic AL12, AL5 and analogues

An interesting feature of flow chemistry is the possible combination of individual reaction steps in series, *i.e.* continuous flow multi-step organic synthesis [185-187]. Thus far, only a few examples of homogeneous multi-step reactions involving a photochemical key-step have been reported [188, 189].

The realization of the one-flow multistep synthesis required some modifications of the individual batch protocols. As a common solvent for all three reaction steps, acetonitrile was selected. A crucial design parameter was the switch from acidic conditions in the dehydration step to basic conditions in the amination step. Initially, excess amounts of amine were injected into the effluent stream of the dehydration in order to neutralize the acid from the dehydration. Following this approach, incomplete aminations were achieved. The need for excess amounts of amine in combination with incomplete conversions made this approach unsatisfactory.

In order to solve the pH-change, a column containing an ion exchange resin was introduced after the second reaction step. The resin material functioned as an acid scavenger [190, 191]. For a better exchange, the reaction mixture was introduce against gravity from the bottom of the cartridge. Strongly basic Dowex anion exchange resin showed the best performance. The resin contained the hydroxyl salts of bound trimethylbenzylammonium cations. The sulfate ions of sulfuric acid are bound through anion exchange. The hydroxyl ions released consequently neutralize the acid protons in the mobile phase (**Figure 4.15**).
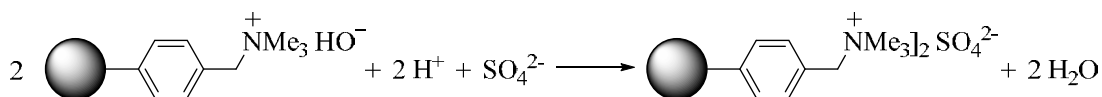
Figure 4.15: Cation exchange and neutralization.

The one-flow setup proved to be an efficient platform for this multicomponent reaction by introducing each reagent at a specific time. Compared to the conventional batch processes, the one-flow system exhibited superior performances and increased yields. This is mainly due to

the reduction of isolation and purification steps. Conventional batch operation requires these operations after each individual reaction step.

4.6 Synthesis of aristolactams

4.6.1 Introduction to aristolactams

Aristolactams are naturally occurring compounds carrying a phenanthrene core. They show a variety of biological activities, including antibacterial, immunostimulanting and cytotoxic properties against various cancer cell lines (**Figure 4.16**) [192, 193]. This made them attractive target compounds for the present study.
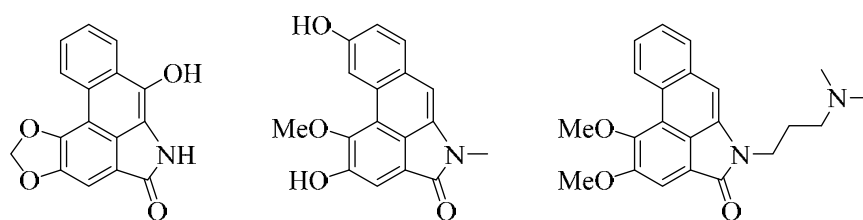
Figure 4.16: Selected examples of bioactive aristolactams.

The retrosynthetic analysis towards the aristolactam skeleton is outlined in **Figure 4.17**. The 3-step procedure utilizes two photochemical steps and one thermal transformation. Two of these steps have also been implemented in the synthesis of **AL12** and **AL5**. In the forward direction, photodecarboxylative addition of 2-iodophenyl acetate to phthalimides initially furnishes benzylated hydroxyl phthalimidine derivatives [82, 88]. Acid-catalyzed dehydration in the second step subsequently generates the stereoisomeric 3-arylmethyleneisoindolin-1-ones. The third step utilizes the photodehydrohalogenation to close the phenanthrene ring [194].
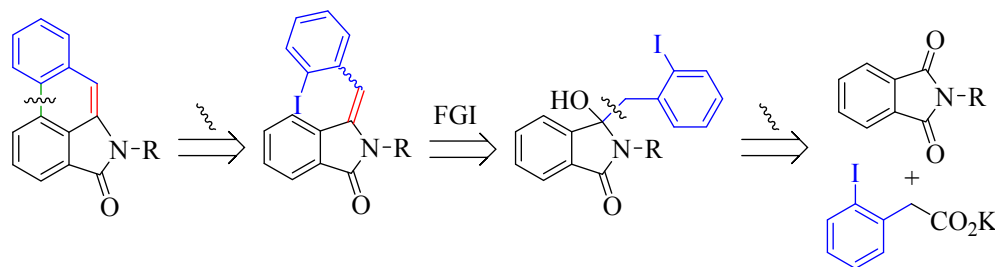
Figure 4.17: Retrosynthetic analysis of aristolactam derivatives.

The photodehydrohalogenation represents a sustainable alternative to the tributyltin hydride-catalyzed dehydrohalogenation described by Couture *et al.* (**Scheme 4.49**) [195]. Although the thermal pathways allowed for a wide range of substituents at the aristolactam skeleton, it

utilized tributyltin hydride and benzene. Tributyltin hydride is toxic, relatively unstable and its residues are difficult to remove from the desired product [196].The photochemical method solely uses light and metal-free conditions instead.
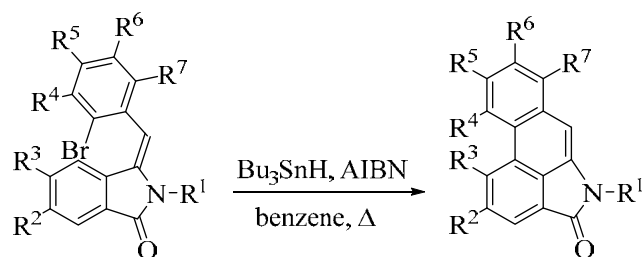
Scheme 4.49: Tributyltin hydride-catalyzed dehydrohalogenation.

Oxidative electrocyclization has been previously ruled-out as an alternative access to the aristolactam ring [197]. Instead, 3-benzylideneisoindolin-1-one solely underwent *E/Z*-isomerization when irradiated with UVB- or UVC-light (**Scheme 4.50**) [88].
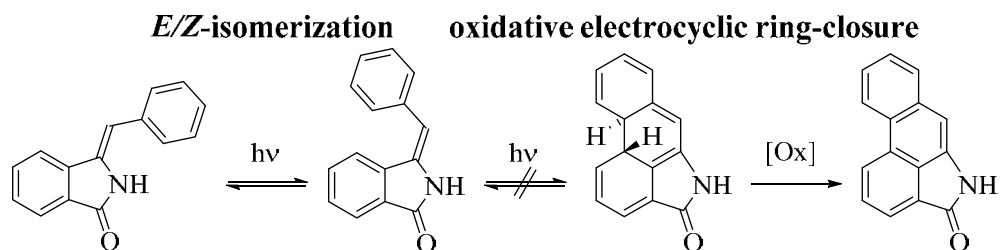
Scheme 4.50: Unsuccessful oxidative electrocyclization of 3-benzylideneisoindolin-1-one.

The general geometry of the 3-benzylideneisoindolin-1-one prevents close contact of the aromatic rings. In particular, the five-membered dihydropyrrole ring positions the benzylidene-group away from the aromatic ring within the isoindolinone moiety. The aromatic rings of the required *E*-isomer are furthermore *out-of-plane*, thus preventing C-C bond formation.

4.6.2   Photodehydrohalogenation to aristolactams

The photodecarboxylative addition and dehydration steps have been discussed in **Chapter 4 (section 4.5.2 & 4.5.3)**. The first two steps in the aristolactam synthesis follow the same mechanistic scenarios. When *N*-bromoalkylphthalimides were used, a fourth step of amination was successfully added to the reaction sequence.

The photodehydrohalogenations conducted in this study furnished the corresponding aristo-lactams in moderate to acceptable yields of 24-57%. The reactions are initiated by homolytic bond cleavage of the C-I bond (**Scheme 4.51**). The bond dissociation energy for the aryl-iodide

(C6H5-I) bond is approx. 280 KJ/mol [198]. The utilized UVB fluorescent tubes peak at 300 nm, corresponding to 399 KJ/mol in energy, far exceeding the required amount for C-I bond cleavage. The resulting phenyl-radical adds to the isoindolinone ring, generating a resonance-stabilized intermediate. Subsequent oxidation followed by deprotonation furnishes the final aristolactam.
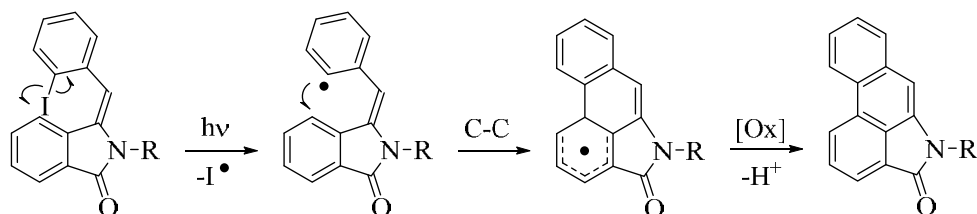
Scheme 4.51: Mechanism of the photodehydroiodogenation.

The efficiency of the dehydrohalogenation was rather low and several by-products, incl. unreactive starting materials, were detected in the crude reaction mixture. This may be explained by the strained nature of the aristolactam structure due to the embedded dihydro-pyrrole, in combination with the spatial separation of the aromatic rings in the initial 3-arylmethyleneisoindolin-1-one. The crucial C-C bond formation step is thus rather disfavored. In addition, solely the *E*-isomer can cyclize, whereas the *Z*-isomer may undergo simple dehalogenation (-I/-H-exchange) instead (**Scheme 4.52**). These dehalogenations are commonly observed in dehydrohalogenation reactions [197] and may also operate for the *E*-isomer.
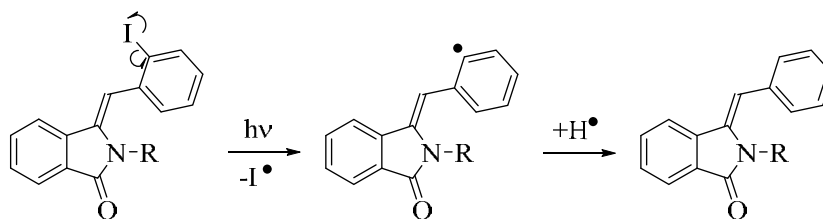
Scheme 4.52: Mechanism of the simple dehalogenation.

Although the yields of the desired aristolactams were generally low, they are higher than the one described by Castedo and co-workers for the synthesis of **cepharanone B** of 25% [91].
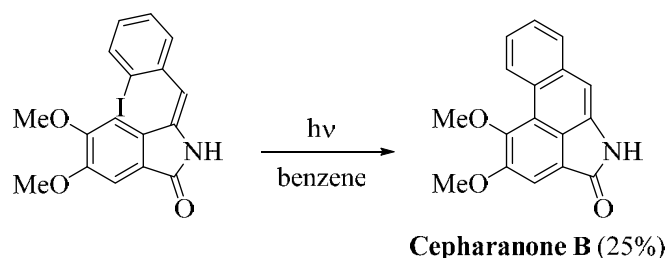
Cepharanone B (25%)

Scheme 4.53: Synthesis of **cepharanone B**.

The bond dissociation energy for alkyl-bromides is significantly higher (for CH_3CH_2-Br: 303 KJ/mol [198]) than that of the aryl-iodide bond. Although the light energy exceeded this amount, no products arising from debromination of the *N*-side chain were observed. This may be explained by the missing absorption of the alkylhalide chromophore in the emission range of the chosen UVB fluorescent tubes (300 ± 25 nm) [199].

4.7 AKS186 synthesis in flow

4.7.1 Introduction to AKS186

AKS186 is a synthetic 3-alkylmethyleneisoindolin-1-one that has been shown to inhibit vaso-constriction induced by thromboxane A_2 analogue (U-46619) (**Figure 4.18**) [192, 200]. This cardiovascular activity makes it an interesting target compound.
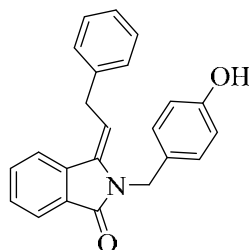
Figure 4.18: Structure of **AKS186**.

The retrosynthetic analysis towards **AKS186** is outlined in **Figure 4.17**. The 2-step procedure utilizes the photodecarboxylative addition of phenylpropanoate to the readily available *N*-(4-acetoxybenzyl)phthalimide, followed by acid-catalyzed dehydration and deprotection. The latter two processes can be performed together.
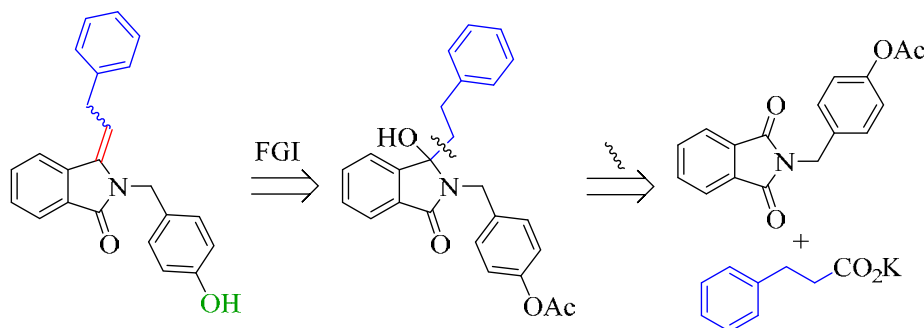
Figure 4.19: Retrosynthetic analysis of **AKS186**.

The reaction sequence has been recently realized under batch conditions by Hatoum *et al.* (**Scheme 4.54**) [58]. Irradiation for 2 hours in a Rayonet chamber reactor furnished the addition product in a yield of 44%. The conversion of the photodecarboxylative key-step was low with

just 52%. Subsequent refluxing in a mixture of acetone/water/conc. hydrochloric acid for 5 h gave **AKS186** in 87% yield as a 10:1 *E/Z*-isomeric mixture.
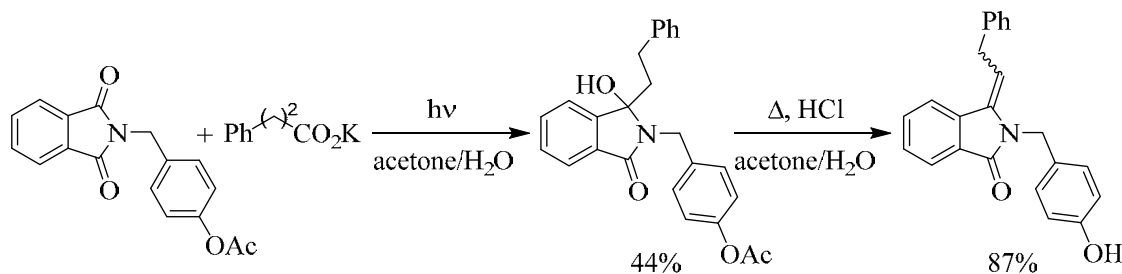
Scheme 4.54: Synthesis of **AKS186** under batch conditions.

4.7.2   AKS186 synthesis in flow

The easy-Photochem reactor enabled the easy combination of photochemical and thermal reaction steps. It was thus considered well suited for the 2-step synthesis of **AKS186** [71]. Some modifications of the individual batch protocols were necessary prior to application to the advance flow module. The reaction was performed in a mixture of acetone/water, which limited the reaction temperature of the thermal step. Reflux inside the capillary coil was considered potentially hazardous due to pressure buildup and possible bursting of the capillary or connections. The thermal loop was thus set to 50°C, safely below the boiling point of acetone of 56°C. To counter the lower reaction temperature, neat trifluoroacetic acid (TFA) was used as acid catalyst, and was injected into the effluent stream of the photo-reactor loop. The easy-Photochem reactor was equipped with a dimmable medium pressure mercury lamp. It was operated at 82 W to avoid any additional cooling. In contrast to the fluorescent tubes, which emit broadly at 300 ± 25 nm, the mercury lamp shows a polychromatic emission spectrum. The wavelength region below 275 nm was considered destructive and was thus cut out using a solid filter insert with a transmittance ranging from 250-390 nm. The unfiltered and filtered emission spectra are compared in **Figure 4.20**.

Another important parameter to consider is the capillary material and its transparency. The reactor coil was fabricated from chemically and photochemically inert and UV transparent fluorinated ethylene propylene (FEP) with a wall thickness of 0.15 mm and an internal diameter (ID) of 1.30 mm. The cutoff wavelength of FEP varies with the wall thickness [201]. For the capillary used in the easy-Photochem module, a transmission of 50% was measured at approx. 250 nm and this dropped to approx. 15% at 200 nm (**Figure 4.21**).
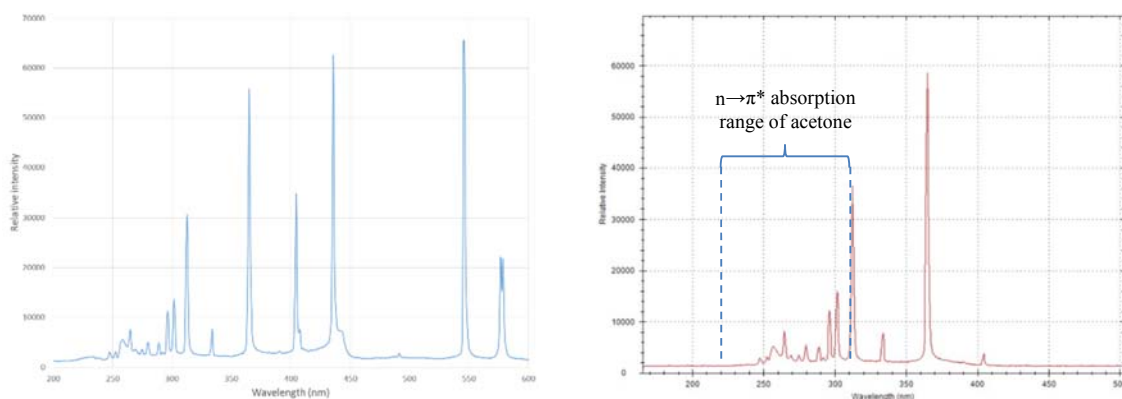
Figure 4.20: Emission spectra of the medium pressure mercury lamp without (left) and with solid filter insert (right). Figures provided by Vapourtec Ltd.
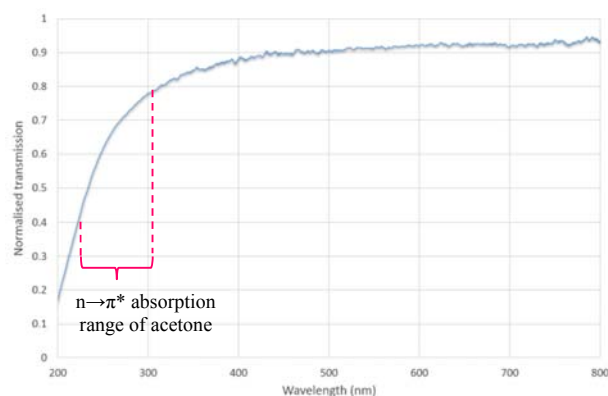
Figure 4.21: Transmission spectrum of the FEP capillary. Figure provided by Vapourtec Ltd.

The important n→π* absorption of the triplet sensitizer acetone in water is found between 220-310 nm, with a maximum at 264 nm [68]. When compared to the remaining emission peaks of the filtered medium pressure mercury lamp (see insert in **Figure 4.20**) [202], the moderate intense emission lines at approx. 297 and 302 nm match well with the absorption of acetone, while the much more intense emission at 313 nm is not available for the desired photoexcitation. In contrast, the FEP capillary shows moderate to good transmission of 30-80% between 220-310 nm (see insert in **Figure 4.21**). Transmission is also high with approx. 77% at 297 and 302 nm, the important emission wavelengths of the lamp.

Following the combined flow approach, **AKS186** was obtained in an isolated yield of 80% over both reaction steps. The mechanistic scenarios of the photodecarboxylative addition and dehydration steps have been described in detail in **Chapter 4 (section 4.5.2 & 4.5.3)**. Residence times were 100 min for the photochemical step and 50 min for the thermal step, respectively. In contrast, the reported stepwise batch procedure furnished an overall yield of 38%, which was largely caused by the low conversion of only 44% for the photochemical step despite an irradiation time of 2 hours (**Table 4.5**) [58, 71]. The tandem easy-Photochem system allows for

a combined in-flow synthesis. Losses due to multiple workup and purification of intermediates are thus avoided. Likewise, the flow photoreactor design and the improved light penetration through the capillary make the easy-Photochem superior over the conventional batch system (see **Chapter 4.4.2** and **Chapter 4.5.2.2** for similar discussions).

Table 4.5: Comparison of reactor's efficiency.

Reactor parameter	Batch	Flow
Irradiation time (h)	2	$1\frac{2}{3}$
Hydrolysis time (h)	5^a	$\frac{5}{6}$
Overall yield (%)	38	80

[a] Reflux time (overnight stirring at room temperature excluded).

4.8 Solar photodecarboxylative additions of phenylacetates to *N*-alkyl-phthalimides

Sunlight represents a sustainable energy and light source for photochemical reactions [203]. The solar spectrum covers a range of 300-700 nm of usable wavelengths, which limits the choice of photochemical transformations. In addition, sunlight at Earth's surface only consists of 3-5% UV radiation (<400 nm), in contrast to 42-43% of visible (400-700 nm) and 52-55% of infrared radiation [204]. Naturally, solar photochemistry also depends on the climatic conditions and is limited to daylight hours.

The acetone-sensitized photodecarboxylative addition of arylacetates to phthalimides was investigated under flow conditions as a borderline example for solar synthesis. Since acetone absorbs light below 310 nm [68], concentrated sunlight was used instead to accelerate the reaction [205].

An example of an acetone-sensitized solar reaction in an advanced concentrating trough reactor has been described by Esser and co-workers (**Scheme 4.55**) [206].
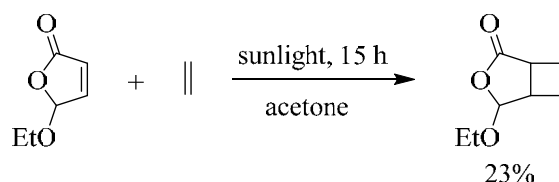
Scheme 4.55: Acetone-sensitized solar [2+2]-cycloaddition in concentrated sunlight.

The SOLARIS module (SOLAR photochemical synthesIS of fine chemicals) utilized a single 8 m² collector, which concentrated sunlight by a factor of 20 onto an absorber tube. Circulation

and solar exposure of an acetone solution of 5-ethoxyfuranone, purged with ethene, for 15 hours over two days produced a moderate conversion of 23% to the corresponding cyclobutane.

4.8.1 Concentrated light solar parabolic trough flow reactor

The simple in-house parabolic trough concentrating solar flow reactor produced the desired benzylated hydroxyl phthalimidines in good to excellent yields of 80-95% using short residence times of 40-53 min. The mechanism of the photodecarboxylative addition has been described in **Chapter 4 (section 4.5.2)**. The utilized FEP capillary showed good transmissions of >78% above 300 nm (**Figure 4.21**), thus allowing effective absorption of sunlight by acetone.

The polished aluminum mirror gave a measured concentration factor of 3 suns. This was significantly lower than the theoretical concentration factor of 13, possible due to its simplified design that caused optical losses. Aluminum nevertheless shows a good reflectivity of >60% above 300 nm [207], which makes it again suitable for acetone sensitization. The general design of the solar flow reactor enables complete illumination of the capillary with the front exposed to direct and the back to concentrated sunlight (**Figure 4.22**). The simple solar trough device can thus utilize both radiation types effectively. However, the comparably small surface area of the capillary at the front of the reactor tube (facing the sun) limits the operation of the reactor under non-ideal sunlight conditions.
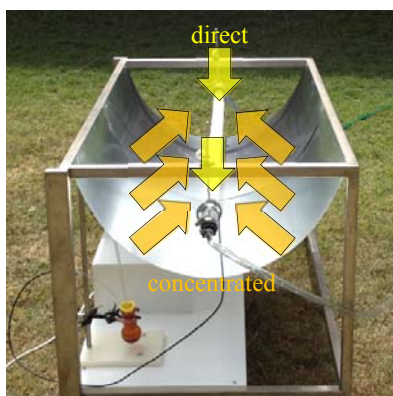
Figure 4.22: Sunlight usage of the solar flow reactor.

The solar radiation data for the respective experimental days were recorded at a nearly photovoltaic station on the JCU campus in Townsville. The radiation data is depicted in **Figure 4.23**. Illuminations were launched at noon, when solar irradiation was most intense, and were typically run until 3-4 pm. As noticeable from the shape of the individual radiation curves, most experiments were conducted under mainly sunny conditions. Clouds caused reductions in the radiation data, as especially noticeable for the 22nd of March 2015.
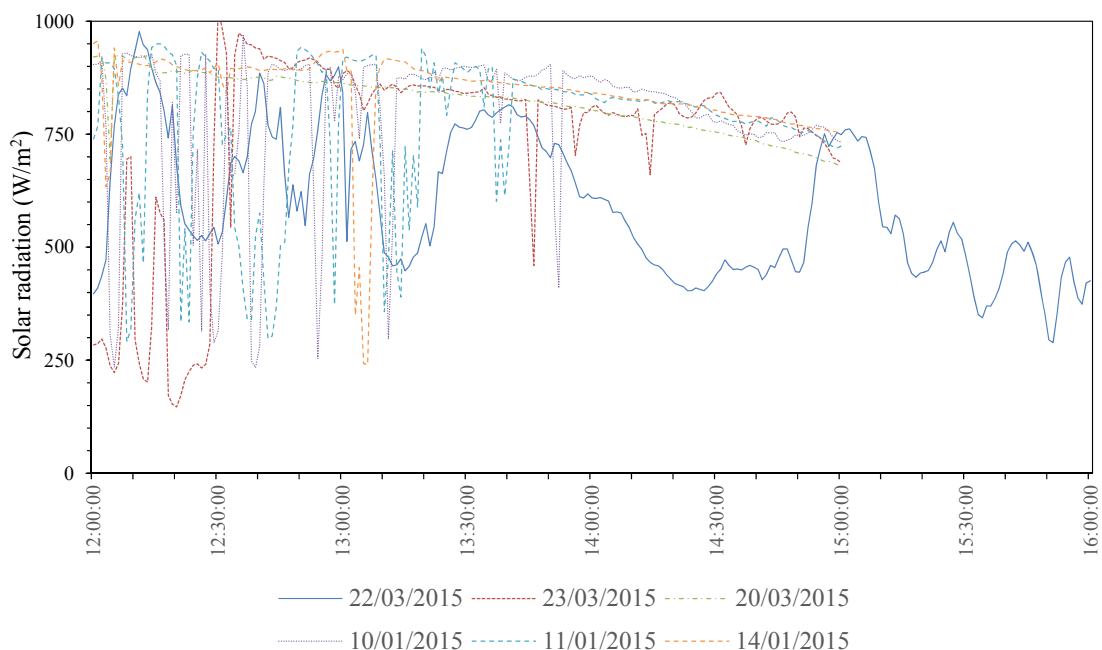
Figure 4.23: Solar radiation data for the experimental days.

Since the temperature of the collection flask rose to 40°C during the outdoor exposure, the *N*-bromoethylphthalimide-derived photoproduct partially formed the corresponding oxazolidine through intramolecular cyclisation (**Scheme 4.56**). This undesired side reaction could be surpassed by storing the collection flask in an ice bath.
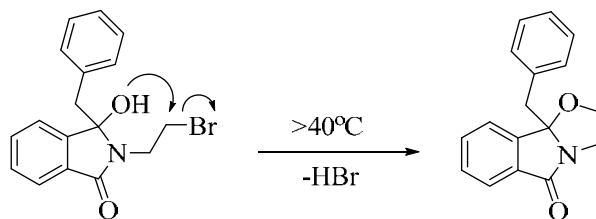
Scheme 4.56: Thermal intramolecular cyclization of *N*-bromoethylphthalimide derived photoproduct.

The performances of the UV-driven batch, UV-driven flow and solar-driven flow processes for a series of photodecarboxylative addition reactions involving *N*-bromoalkylphthalimides (**Scheme 4.57**) are compared in **Table 4.6**. Yields were comparable in all cases and ranged from 83-95%. The flow reactions utilizing artificial UV-light showed the fastest reactions. Although the solar flow process required a doubling in reaction time to achieve complete conversions, the inner diameter of the reaction capillary was also double as wide (1.6 mm *vs.* 0.8 mm). In addition, the usable UV-range of sunlight was low, whereas the UVB-fluorescent tube matched

well with the absorption spectrum of acetone, although in the latter case it had to pass through the Pyrex base of the capillary tower first.
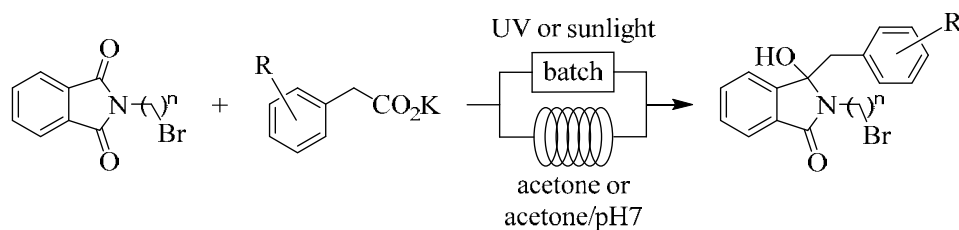
Scheme 4.57: Photodecarboxylative additions used for process comparison.

Table 4.6: Comparison of batch, UV-driven flow and solar-driven flow processes.

| n | R | UV-driven | | | | Solar | |
| | | Batch | | Flow | | Flow | |
		Time (min)	Yield (%)	Time (min)	Yield (%)	Time (min)	Yield (%)
2	H	180	87	20	87	40	86
2	4-MeO	180	85	20	85	40	83
3	H	180	95	20	95	40	95

4.8.2   Solar exposures in direct sunlight

Placing the reaction mixture into direct sunlight did not initiate any measurable conversions, even after prolonged exposure of 200 min. The may be explained by the poor transmission of Pyrex glass in the important UV-range of acetone at <310 nm [207]. Dependent on the thickness of the glass, Pyrex shows a transmission of just about 10-20% at 300%. In addition, the reactions relied solely on direct radiation due to the lack of a solar concentrator. The surface areas of the reaction vessels, *i.e.* round bottom flask, Schlenk flask or test tube, were too small to harvest direct sunlight only.

Chapter 5:

Takeda Work

5. Takeda Work – α-Bromination of acetophenone in batch and flow

5.1 Introduction

This thesis stream was investigated for Takeda Pharmaceutical Co. Ltd in Japan. In general, the α-bromination, also known as Wohl-Ziegler reaction, is a key step in organic chemistry as it allows for further transformations to more complex target compounds [208-210]. The α-bromination of carbonyl compounds is a special type of Wohl-Ziegler reaction and the α-bromoalkanones obtained are important building-blocks in the manufacturing of a variety of biologically active compounds, pharmaceuticals, pesticides and surfactants [211]. In addition, α-bromoacetophenone derivatives play an active role in inhibition of protein tyrosine phosphatase such as SHP-1 and PTP1B [212].

Bromine has been traditionally used for α-bromination of carbonyl compounds with protic and Lewis acids [213], cupric bromide [214], dioxane dibromide [215], tetrabutylammonium tribromide [216] and others. However, bromine is irritating, toxic, corrosive, difficult to handle and environmentally hazardous. In addition, it is highly reactive and can lead to exothermic and non-selective reactions [217]. Alternatively, tetrabutylammonium tribromide [216], pyridium [218], 1, 4-dioxane bromooxonium bromide [219], tribromoacetophenone [220] and copper bromide [214] have previously being used as brominating agents. These reagents have their own limitations such as high costs, low reactivity, long reaction time and others.

The *N*-bromosuccinimide (NBS) catalyzed α-bromination of carbonyl compounds has been reported as a greener and easy to handle alternative [221]. The reaction precedes either through radical or ionic pathways. NBS is sometimes coupled with initiators or catalysts such as azobisisobutyronitrile (AIBN) [222], dibenzoyl peroxide (BPO) [223] or silica-supported sodium hydrogen sulfate and ammonium acetate [221, 224], trimethylsilyl trifluoromethane-sulfonate [225] and *p*-toluenesulfonic acid (PTSA) [226]. The direct α-bromination of acetophenone with NBS without any activating reagent represents the most convenient access to 2-bromoacetophenone (**Scheme 1.1**). The reaction is commonly performed using thermal methods. While photochemical activation is rather uncommon, this alternative is interesting for heat sensitive acetophenone-derivatives and has thus been chosen by Takeda Pharmaceutical Co. Ltd as the preferred method.
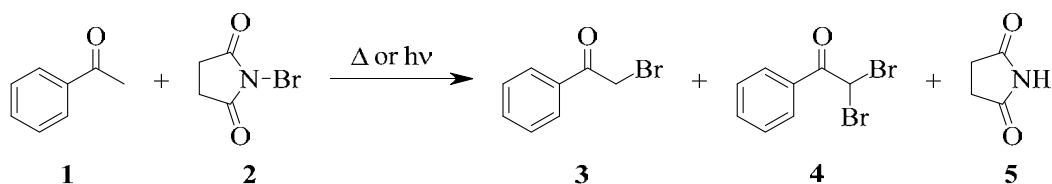
Scheme 5.1: α-Bromination of acetophenone.

5.2   Overview of photochemical methods

Only a few photochemical α-brominations of carbonyl compounds (including acetophenone and its derivatives) using NBS have been described so far [227-232]. Selective procedures are briefly described below and key-details are summarized in **Table 5.1**.

- In 2007, Arbuj and co-workers reported the photochemical α-bromination of acetophenone and its derivatives under UV-vis irradiation. Solvent screening had suggested diethylether to be the most efficient solvent. Irradiations at 30°C for ≥10 min furnished conversions of 15-98% to the desired α-brominated products. The effects of NBS addition in 2-6 portions and the selectivity for mono- vs di-substituted products were also studied [227].

- In 2009, Jereb *et al.* investigated Wohl-Ziegler reactions under solvent free reaction conditions utilizing a 40 W tungsten lamp and 2, 2, 6, 6-tetramethylpiperidin-1-yloxy (TEMPO) as a radical scavenger to suppress side chain brominations [228].

- The flow photochemical bromination of 4-methylpyrimidine derivative using NBS and acetonitrile with a medium pressure mercury lamp (150 W) was studied by Sterk and co-workers in 2012. The desired product was obtained in 5 min with 86% yield [229].

- In the same year Chowdhury *et al.* reported the bromination of acetophenone at room temperature using NBS, diethylether and a Phillips HPL-N lamp (250 W). The product was isolated in 85% yield [230].

- Later in 2014, Cantillo and co-workers investigated the transformation of various toluene and acetophenone derivatives using NBS in acetonitrile, irradiations with a compact florescent light (25 W) for 13-25 min and continuous-flow. Benzylic bromination proceeded excellently for toluene derivatives. The acetophenone derivative 4-methyl acetophenone (**6**) yielded monobromination solely at the benzylic position and furnished **7** in 77% yield with no trace of alternative bromination at the α-carbonyl position (**Scheme 5.2**) [231].
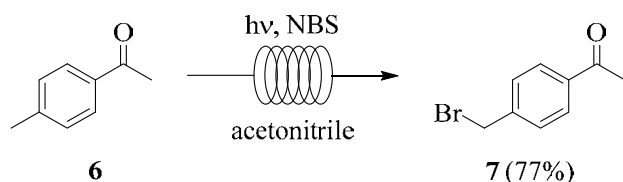
Scheme 5.2: Continuous-flow α-bromination of 4-methyl acetophenone (**6**) to 4-(bromo-methyl)acetophenone (**7**).

- Solar α-brominations have been described by Deshpande *et al.* in 2015. Benzylic brominations were achieved in good to high yields of 56-90% in ≥20 min in acetonitrile under concentrated sunlight. However, solar exposure of acetophenone in acetonitrile for 30 min showed no reaction. Once again, 4-methylacetophene selectively furnished 4-bromomethyl acetophenone in 85% yield [232].

Table 5.1: Photochemical bromination of acetophenone and its derivatives reported in the literature.

Ref.	Starting material(s)	Solvent	Light source	Time	Conv. (%)
[227]	Acetophenone	Et$_2$O	UV-vis	4 min	71
[228]	Acetophenone and various derivatives	solvent free	Tungsten lamp (40 W)	16 h	73
[229]	5-Methylpyrimidine analogues	CH$_3$CN	Medium-pressure Hg lamp (150 W)	5 min[a]	86[b]
[230]	Acetophenone	Et$_2$O	Phillips HPL-N lamp, λ=200-600 nm (250W)	n.s.[c]	85[b]
[231]	Toluene derivatives and 4-methyl acetophenone, phenylacetone	CH$_3$CN	CFL white light (25 W)	13-50 min 13 min 13 min	70-94[b] n.r.[d] (77 & 79)[e]
[232]	Acetophenone, 4-methylacetophenone	CH$_3$CN	Concentrated sunlight	30 min 9 min	n.r.[d] n.r.[d] (85)[e]

[a] Residence time. [b] Isolated yield. [c] n.s. = not specified. [d] n.r. = no reaction. [e] yield of other products.

5.3   Results and Discussion

Out of the reported literature procedures, the methods described by Arbuj *et al.* [227] and Cantillo *et al.* [231] were found most interesting and relevant to this investigation. Photobrominations were initially conducted under batch conditions using a Rayonet chamber reactor before transferring them to continuous-flow operations.

5.3.1   Batch Operation

The Rayonet chamber reactor was equipped with UVA (350 ± 25 nm) fluorescent tubes (16×8 W). Irradiations were performed in Pyrex (transmitting >300 nm) Schlenk flasks with an internal volume of approx. 60 mL and an inserted cold finger. At the end of the irradiation, conversion rates were determined by ^{1}H-NMR spectroscopy using baseline separated signals. The integration value of the CH_3-group of acetophenone at ~2.5 ppm was compared with that of the CH_2Br-group of 2-bromoacetophenone at ~4.4 ppm.

Initially, Arbuj's procedure was investigated under batch conditions and the results are shown in **Table 5.2**. The reaction protocol required diethylether as a solvent, which created a slurry due to the low solubility of NBS in this solvent. Various modifications were tried:

(a)   static reaction without stirring (entries 1-3),

(b)   reaction under stirring (entry 4) and

(c)   the addition of NBS in portions without stirring (entry 5).

Using method (a) irradiation times were furthermore varied and included 7, 12 and 25 min (entries 1-3). Since slurries are not desirable for flow operations due to danger of clogging and thus rupture of tubing, selected transformations were furthermore performed in acetonitrile instead (entries 6 and 7).

Out of all the reactions performed, only those conducted in diethylether showed conversions to the desired **2** of 25-55%. An exemplary ^{1}H-NMR spectrum of entry 3 is shown in **Figure 4.1**.
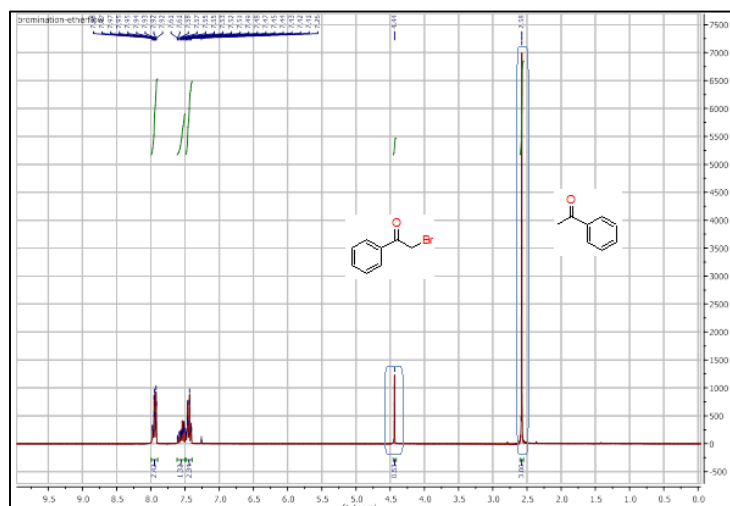
Figure 5.1: ^{1}H-NMR spectrum (in CDCl$_3$) of reaction mixture after irradiation (entry 3).

Dibromination was observed only when NBS was added in portions and a 60:36:4 mixture of unreacted starting material, monobrominated (**3**) and dibrominated product (**4**) was obtained

after 20 min. of irradiation. For compound **4**, the $CHBr_2$-group showed a characteristic singlet at ~6.6 ppm in the ^{1}H-NMR spectrum. In acetonitrile, no reaction was observed even after 2 hours of irradiation.

Table 5.2: Bromination of acetophenone in diethylether using Arbuj's procedure [227].

Entry	Method	Solvent	Time (min)	Conv. (%)[a]
1	**a:** no stirring	Et_2O	7	25
2	**a:** no stirring	Et_2O	12	37
3	**a:** no stirring	Et_2O	25	42
4	**b:** with stirring	Et_2O	20	55
5	**c:** NBS addition in portions, no stirring	Et_2O	20	40[b]
6	**a:** no stirring	CH_3CN	30	n.r.[c]
7	**a:** no stirring	CH_3CN	120	n.r.[c]

[a] Conversion is based on ^{1}H-NMR (±3%). [b] Dibromination was also observed (4). [c] n.r. = no reaction.

5.3.2 Flow Operation

Although irradiations in acetonitrile under batch conditions did not yield any product, acetonitrile was still considered preferable. Successful NBS brominations of toluene derivatives have already been realized by Cantillo *et al.* in continuous-flow mode [231]. Since flow-chemistry is commonly referred to as an "enabling technology", a series of brominations were thus investigated. Three flow reactors were constructed, differing in volume and the UVA light source. **Reactors A** and **C** had a FEP capillary wrapped tightly around a glass column with a UVB fluorescent tube in its center. A cooling fan was positioned underneath the glass column. Reactor model B was based on the Cantillo design and had the capillary wrapped around a beaker (OD: 5.2 cm). A UVA compact fluorescent bulb was placed inside the beaker and the reaction setup was wrapped in aluminum foil and placed inside a cooling bath. For all reactors, the reaction mixture was pumped from the bottom to the top using The FMI Lab rotary pump (model: RP-SY) except in 3rd reactor where Ismatec piston pump (REGLO-CPF digital) was used. For the reactor **models A** & **B** flow rates were controlled manually with a slider. Prior to the experiments, a correlation of flow rate *vs.* slider position was conducted. The reaction mixture was collected in an amber flask containing aqueous sodium thiosulfate ($Na_2S_2O_3$). Following this procedure, any residual bromine inside the final reaction mixture was quenched. The key parameters of both reactors are summarized in **Table 5.3**.

Table 5.3: Flow reactors.

Model	Capillary dimensions (ID: mm, L: m)	Pump	Volume (mL)[a]	Light Source
A	0.8, 100	FMI Lab rotary pump	50	UV-A (20 W)[b]
B	1.58, 10	FMI Lab rotary pump	20	CFB (15 W)[c]
C	1.58, 28	Ismatec piston pump	56	UV-A (24.5 W)[b]

[a] Exposed capillary volume. [b] Fluorescent tube. [c] Compact fluorescent bulb.

Following a modified procedure by Cantillo *et al.* [231], the bromination was initially conducted in acetonitrile using flow reactor **model A** (**Figure 4.16**) and using a residence time of 17 minutes. Under these conditions, no reaction was observed. The procedure was subsequently repeated using residence times of 17 (duplicate), 25 and 50 minutes (**Table 5.4**). No conversions were again observed by ^{1}H-NMR analysis. The results under flow conditions are thus in line with those from the batch reactions (**Table 5.2**).
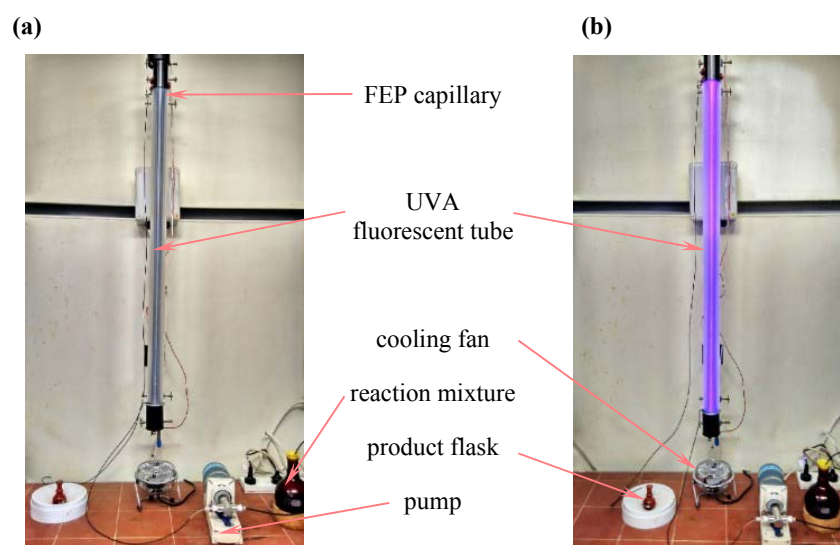
Figure 5.2: Vertical flow reactor **model A** used for bromination. (a) Light off and (b) light turned on.

Table 5.4: Bromination of acetophenone in acetonitrile in flow reactor **model A**.

Entry	Residence time (min)	Conversion (%)[a]
1	17	n.r.[b]
2	17 (duplicate)	n.r.[b]
3	25	n.r.[b]
4	50	n.r.[b]

[a] Conversion checked by ^{1}H-NMR. [b] n.r. = no reaction.

The limited solubility of NBS in diethylether makes it an undesirable solvent for microflow operation (ID <1 mm). However, since no reaction was observed in acetonitrile, flow reactor **models B** and **C** with a larger inner capillary diameter of 1.6 mm were constructed (**Table 5.3**). This wider tubing was expected to minimize the danger of clogging. These meso-scale reactors were subsequently trialed for photobrominations in diethylether. The reagent solution was kept inside an ultrasonic bath to maintain a homogeneous suspension of the starting materials.

A single experiment was conducted in reactor **model B** (**Figure 4.16**). Its compact design only allowed for a capillary length of 10 meters, which corresponds to an internal volume of just 20 ml. The in-house rotary pump limited the residence time to 4 min. Slower flow rates caused clogging inside the capillary and could thus not be used. When Arbuj's procedure [227] was transferred to this setup a reasonable conversion of 21% was determined by ^{1}H-NMR analysis.
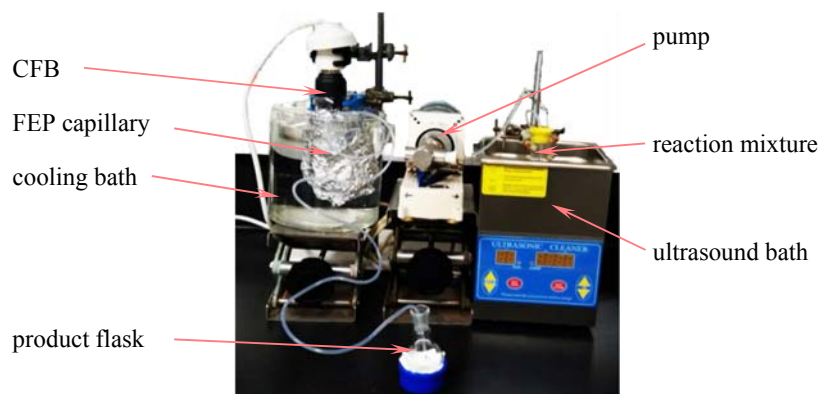
Figure 5.3: Flow reactor **model B** used for bromination.

The improvised design of reactor **model B** limited the residence time due to the short length of the capillary (10 m). A larger reactor **model C** was thus constructed using the same wider FEP capillary of 28 m length and an internal volume of 56 mL (**Figure 5.4**). The slurry of starting material in ether at the minimum possible rate was pumped through the reactor and a 47% conversion was achieved after ~10 min exposure. The available regio-pump is designed to transport homogeneous solutions and is therefore not efficient for transporting suspensions or slurries. Consequently, stable flow rates were difficult to maintain. Any further decrease in residence time by slowing down the slurry flow resulted in sedimentation and finally blockage of the FEP tubing.

The reactor was also used for a solvent study and the photobromination was repeated in three different solvents: acetone, THF and a 1:1 mixture of ether/H_2O. In all three solvent systems a

transparent and clear solution was obtained, which was considered beneficial for flow operation. The results from the solvent study are summarized in **Table 5.5**. No reaction was observed in acetone (entry 2), whereas the reactions in THF and the ether/H$_2$O mixture gave complex mixtures including unreacted starting material (entries 3 and 4), as confirmed by ^{1}H-NMR analysis. Incompatibility of THF with NBS is suggested as a reason for the poor selectivity and this limitation has been reported by Shimizu and co-workers [233].
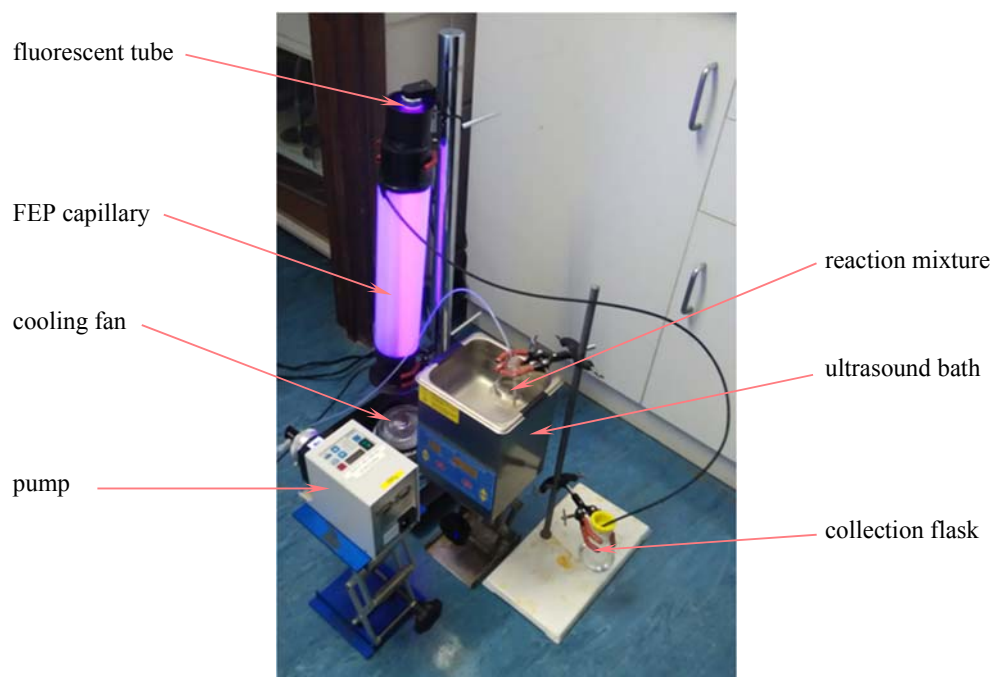
Figure 5.4: Flow reactor **model C** used for α-bromination.

Table 5.5: Bromination of acetophenone in flow reactor **model C**.

Entry	Solvent	Reaction mixture	Residence time (min)	Conversion (%)^a
1	Et$_2$O	Slurry/suspension	10	47
2	acetone	Clear solution	20	n.r.^{b}
3	THF	Clear solution	20	complex mixture^c
4	Et$_2$O/H$_2$O (1:1)	Clear solution	20	complex mixture^c

^{a} Conversion based on ^{1}H-NMR (±3%). ^{b} n.r. = no reaction (by ^{1}H-NMR). ^{c} Including unreacted starting material as confirmed by ^{1}H-NMR.

Although acetonitrile has been described as compatible with NBS [233] and although many efficient benzylic brominations have been reported in this solvent [227, 230], no reaction was observed in case of acetophenone itself. The only reported successful bromination of acetophenone has been achieved in batch and in diethyether as a solvent [229]. Arbuj *et al.* have conducted a solvent study with cyclohexanone (**8**) [227]. While acetonitrile did enable α-

bromination to product **9**, the reaction required prolonged reaction times and gave a lower conversion rate (**Scheme 5.3**). The lack of reactivity of acetophenone in acetonitrile is thus most likely caused by electronic effects. This is also supported by the highly regioselective benzylic bromination of 4-methylacetophenone (**6**) shown in **Scheme 5.2**.

solvent:	time (min):	conversion (%):
Et$_2$O	0.5	86
MeCN	17	78
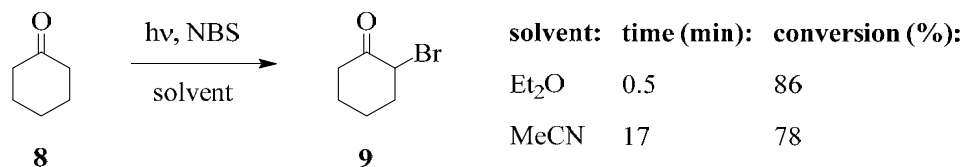
Scheme 5.3: α-Bromination of cyclohexanone.

In 2003 J. C. Lee *et al.* reported the thermal monobromination of acetophenone with NBS in the presence of *p*-toluenesulphonic acid (PTSA) in acetonitrile (**Scheme 5.4**) [221b]. This procedure was thus adopted and investigated under batch conditions, both in light and dark (**Table 5.6**). Reactions were conducted in a Rayonet chamber reactor equipped with 16 × 8 W cool white fluorescent tubes. Experiments were performed in Pyrex (transmitting >300 nm) Schlenk flasks with an internal volume of approx. 60 mL and an inserted cold finger. For the dark experiment, the reaction mixture was left inside the chamber with the fluorescent tubes turned off. At the end of each experiment, conversion rates were determined by ^{1}H-NMR spectroscopy.
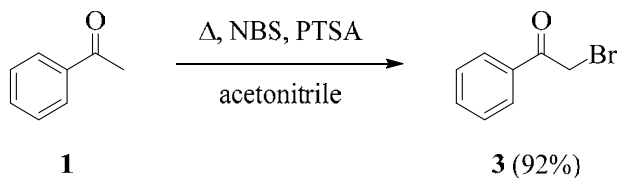
Scheme 5.4: α-Bromination of acetophenone in the presence of PTSA as reported in [221b].

When irradiated by light for 30 min, a conversion of 80% to the desired monobromination product **3** was observed (entry 1). Remarkably, the reaction conducted in the dark also showed a moderate conversion of 43%, indicating that the reaction occurs spontaneously at room temperature without any need of light or heat.

Table 5.6: Bromination of acetophenone in acetonitrile.

Entry	Reagent	Light source	Time (min)	Conversion (%)[a]
1	PTSA + NBS	Cool white (16 × 8 W)	30	80
4	PTSA + NBS	none (dark)	30	43

[a] Conversion based on ^{1}H-NMR (±3%).

The suggested ionic mechanism (**Scheme 5.5**) involves protonation of carbonyl oxygen of NBS which facilitated the formation of a bromonium ion [234]. Guan and co-workers suggested an additional involvement of the enol of acetophenone [235].
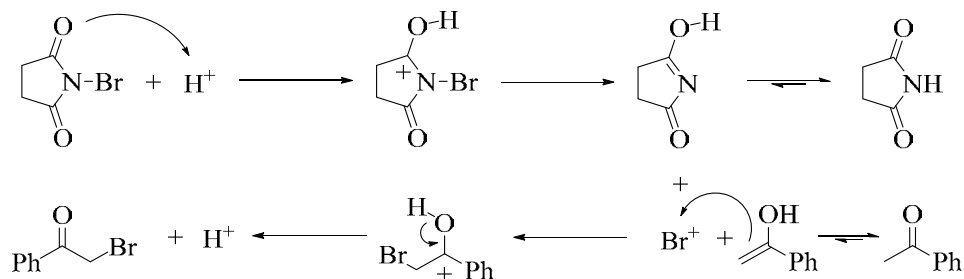
Scheme 5.5: Ionic mechanism of the α-bromination of acetophenone in the presence of PTSA.

The higher conversion upon irradiation suggests that the radical bromination (**Scheme 5.6**) operates in parallel with the ionic mechanism.
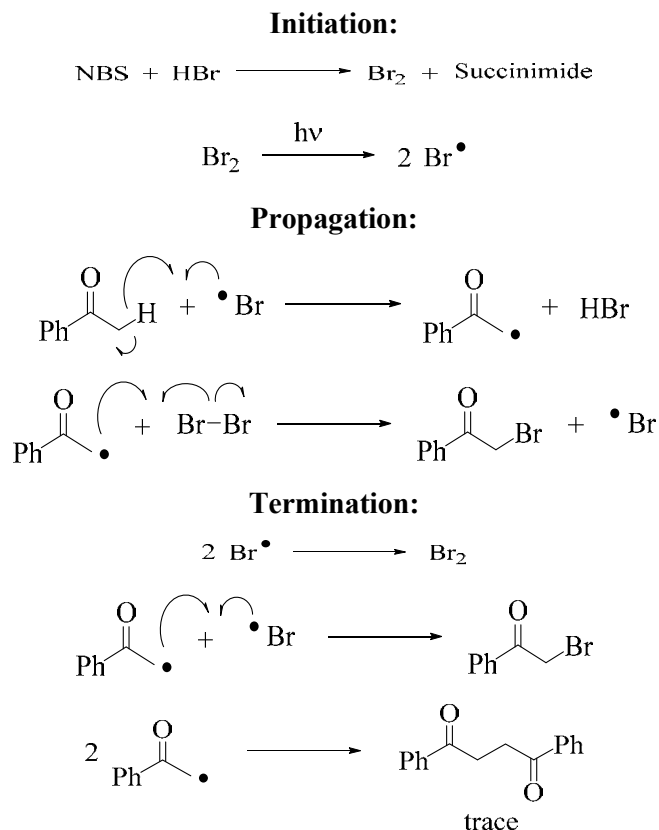
Scheme 5.6: Radical mechanism of the α-bromination of acetophenone.

At this stage, further investigations into the photobromination of acetophenone were stopped as Takeda Pharmaceuticals Co. Ltd was satisfied with the results achieved.

5.4 Summary and Conclusion

Thus far, no successful α-photobromination of acetophenone has been reported under continuous-flow conditions. Likewise, solar illumination under batch conditions in acetonitrile has been reported to yield no reaction in case of acetophenone [232].

A thermal α-bromination of acetophenone with molecular bromine in the presence of hydrogen bromide under flow conditions has been achieved by Becker and co-workers [236]. Under optimized conditions, an excellent selectivity (>98%) and yield (99%) was obtained on a gram-scale (**Scheme 5.7**).
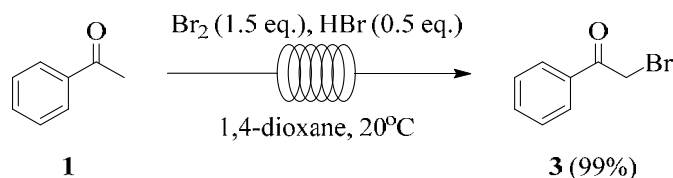
Scheme 5.7: Thermal α-bromination of acetophenone under flow conditions.

Through this study, the photobromination of acetophenone has been successfully achieved, although further optimization is desirable. The experiments with the best performances are summarized in **Table 5.7** for comparison. The results show that α-photobromination of acetophenone is possible in batch as well as in flow operation. The bromination in acetonitrile remained problematic, however, PTSA catalysis was found to be beneficial. Under the later conditions, the highest conversion of 80% was achieved (entry 3). In the absence of PTSA, the bromination was only successful in diethylether as a solvent. Under these conditions, reactions occurred satisfactory under batch and flow conditions (entries 1 and 2). The results somewhat confirm the advantage of continuous flow operation over the batch process. Compared to the batch reaction in a larger chamber reactor, flow operation achieved a comparable conversion of 47% despite a shorter residence time of 10 min and despite a lower light power of 24.5 W. The continuous flow mode is thus likely to be more efficient and less expensive when considering the overall productivity of the process.

Table 5.7: α-Bromination of acetophenone.

Entry	Solvent	Mode	Light source	Time (min)	Conversion (%)[a]
1	Et$_2$O	Batch	UV-A (16 × 8 W)	20	55
2	Et$_2$O	Flow	UV-A (24.5 W)	10	47
3	MeCN[b]	Batch	Cool white (16 × 8 W)	30	80

[a] Conversion is based on ^{1}H-NMR (±3%). [b] In the presence of PTSA.

The slurry-conditions of the photobromination remain challenging. For future studies, the application of a peristaltic pump in combination with even wider tubing is thus recommended. Further reactions may be additionally explored using alternative bromination agents, *e.g.* molecular Br_2, to overcome the issue with solubility of NBS. Combinations of NBS and Br_2 or addition of HBr, AIBN, DBU or TEMPO in acetonitrile may also be considered.

Chapter 6:

NAIST Work

6. NAIST Work – Continuous-flow photochemistry in super-critical carbon dioxide

6.1 Introduction

This thesis stream was investigated in the research group of Prof. Kiyomi Kakiuchi and under the supervision of Assistant-Professor Yasuhiro Nishiyama at the Nara Institute of Science and Technology (NAIST) in Japan as part of the Researcher Mobility Grant Scheme. Organic photochemical reactions are typically performed in inert and transparent solvents, *e.g.* benzene, acetonitrile, carbon tetrachloride, *n*-hexane or methanol. Many of these solvents are hazardous and should thus be replaced by more sustainable alternatives. Another approach utilizes solvent-free reaction conditions or supercritical solvents. The use of supercritical carbon dioxide ($scCO_2$) in this regard is economical, cheap and benign to the environment [237]. $scCO_2$ is considered green as it minimizes organic solvent wastes and allows for task-specific solubilization of chemicals by simply varying temperature and pressure conditions [238]. Similarly, its own viscosity and density is dependent on pressure and temperature. The properties of $scCO_2$ vary considerably upon minor changes at near critical conditions. Previous reports by the Kakuichi/Nishiyama group have revealed that $scCO_2$ can also favor stereoselectivity in photochemical reactions [239]. Using $scCO_2$ in continuous-flow photoreactors is, however, challenging.

6.2 Oxidative Photocyclization of Stilbenes – The Mallory Reaction

For years, the oxidative photocyclization of stilbenes has seen widespread applications in the synthesis of conjugated π-systems. This neglect was mainly caused by the relatively low yields, high dilution conditions and multitude of possible by-products [240, 241]. In 1964, Mallory discovered that iodine can catalyze this reaction and this modification allowed for higher concentrated solutions, gave better yields and showed fewer side products. Mallory reviewed his findings in 1984 but as development on the reaction continued, a number of additional reviews focusing on various aspects of the reaction have become available today [242-249].

As *trans*-stilbenes (*trans*-**1**) can readily isomerize photochemically to its corresponding *cis*-form (*trans*-**2**), both isomers furnish the same oxidative cyclization product **2** or **2'** upon irradiation. Although only the *cis*-form of **1** is capable of further photocyclization, photoiso-merization has made it possible to use a mixture of *cis*- and *trans*-reactants. The unstable

dihydrophenanthrene (**PH₂** or **PH₂'**) formed via electrocyclic ring-closure can be trapped through oxidation or elimination (**Scheme 6.1**) [197, 242, 244, 250, 251].
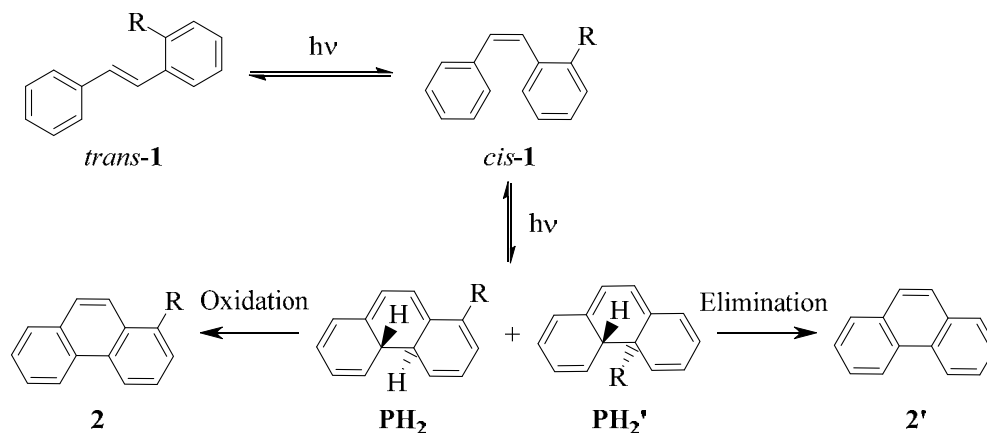
Scheme 6.1: Reaction pathways of the Mallory reaction.

Traces of iodine and oxygen significantly accelerate the oxidative trapping by providing radicals for photochemical chain reactions. Hydrogen iodide is converted back to iodine by molecular oxygen (**Scheme 6.2**) [242, 244]. At higher iodine concentrations, however, elimination, [2+2] cycloaddition, side products from the increasing amounts of HI and formation of saturated stilbenes become competitive reactions.

Initiation:

Propagation:
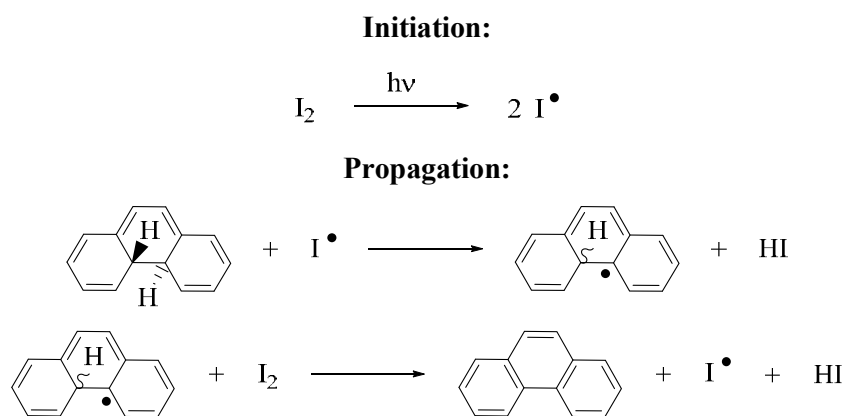
Scheme 6.2: Role of I₂ in the Mallory reaction.

A thorough investigation of the reaction conditions by Katz established optimized conditions for the reaction [252]. The use of methyloxiranes as scavengers proved to be compatible with a verity of functionalities. Later, potassium carbonate has also been reported as an effective HI-scavenger [253-255]. Although the oxidative photocyclisation is sensitive to steric effects of substituents, its regioselectivity is very high. In this regard, Laarhoven has evaluated the reactivity parameters such as valence numbers [256] and localization energies and has been able to determine rules for the cyclization [245, 249].

6.3   Results and Discussion

6.3.1   Introduction

Recently, versatile applications of the Mallory reaction have been developed. For example, Lefebvre and Okamoto *et al.* realized Mallory reactions in scalable and highly efficient continuous flow reactors. Thus, multigram quantities of phenanthrenes and helicenes have been realized with residence times as low as 8 minutes in microcapillary flow photoreactors [257, 258]. In this study, Okamoto's data was used in order to explore the efficiency of the same Mallory reaction in photoflow reactors and using $scCO_2$ as a solvent.

Initially, the setup used by Okamoto and co-workers was reproduced in order to confirm the general reproducibility of the reported results. Likewise, a limited number of experiments was carried out in cyclohexane under batch conditions using various reactors equipped with different light sources. The reaction was subsequently repeated under the same conditions in $scCO_2$ using batch and flow reactors.

The photocyclization of *trans*-stilbene (*trans*-**1**) to phenanthrene (**2**) was investigated under batch and under microflow reaction conditions using both cyclohexane and $scCO_2$ as solvents (**Scheme 6.3**). As a standard reaction, a mixture of 5 mM of *trans*-**1** and 0.1 equiv. I_2 was employed.
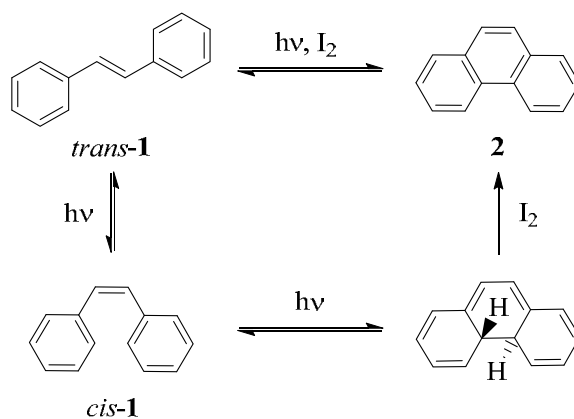
Scheme 6.3: Photocyclization of *trans*-stilbene to phenanthrene.

6.3.2   Reactions in a Conventional Batch Reactor

6.3.2.1   Using a UV Lamp

Initially, Okamoto's procedure was investigated under batch conditions. The reaction protocol required cyclohexane as a solvent. A USHIO Optical Modulex (SX-U1501XQ-500W) was used as light source. The temperature was monitored using a commercially available cryostat (USP-

203 series) for spectrophotometer. Using this setup, 3 mL of the standard reaction mixture inside a quartz cuvette (ID: 1 cm) were exposed to irradiation (**Figure 6.1**). The results from the batch reactions are summarized in **Table 5.1**.

Figure 6.1: Setup for the batch reaction in cyclohexane and cuvette used as a 'batch' reactor.

The oxidative photocyclization reaction of **1** did not operate under N_2 (entry 1) as O_2 is required in the reaction. The reaction was therefore repeated under air. Poor yields of **2** were obtained even after 3 hours of irradiation in air at room temperature (entries 2 & 3). The reaction was therefore repeated at 35ºC, which improved the yields of **2** to 84% and 86% (entries 4 & 5), respectively. A further increase of temperature to 45ºC resulted in 99% yield of **2** after 3 hours (entry 6). Decreasing the reaction time from 3 to 1 hour halved the yield to 50% (entry 7). Irradiation was therefore conducted for 2 hours and a 97% yield was obtained. Further optimization under batch conditions was attempted by doubling the concentration of the reaction but this resulted in a decrease in yield to 50% (entry 8). Thus, the best conditions under batch conditions for the standard concentration comprise of 2 hours irradiation at 45ºC in presence of air (entry 9).

Table 6.1: Batch reaction optimization in cyclohexane using a 500 W Hg lamp.

Entry	Temperature (ºC)	Time (h)	Yield (%)
1	35[a]	1.5	n.r.[b]
2	room temperature[c]	3	ca. 22
3	room temperature[c]	3	19
4	35[c]	3	84
5	35[c]	3	86
6	45[c]	3	99
7	45[c]	1	50

Entry	Temperature (ºC)	Time (h)	Yield (%)
8	45[c,d]	2	50
9	45[c]	2	97

[a] under N_2. [b] n.r. = no reaction. [c] under air. [d] Double concentration.

The absorption spectra of *trans*- and *cis*-stilbene in cyclohexane are shown in **Figure 6.2** [259]. Both compounds absorb light up to wavelengths of 340-345 nm with maxima at approx. 290 nm and 275 nm, respectively.
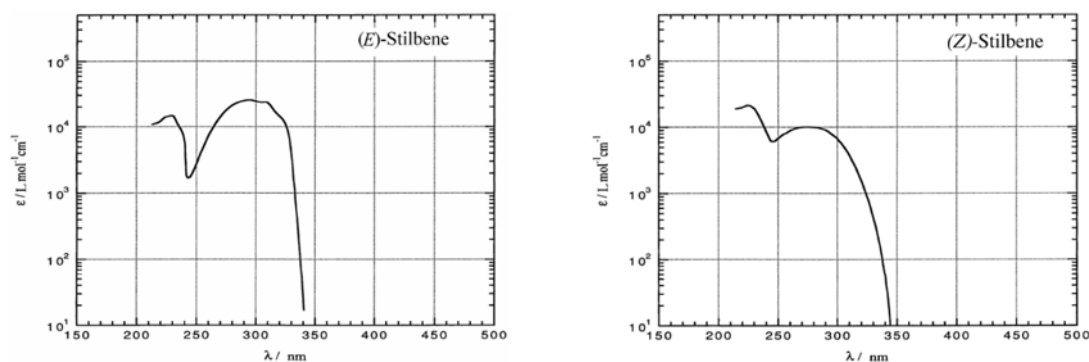
Figure 6.2: UV-spectra of *trans/E*- and *cis/Z*-stilbene in cyclohexane (taken from [259]).

When compared to the emission spectrum of the peaks of Ushio's super high-pressure UV lamp (see insert in **Figure 6.3**) [202], the moderate intense emission lines at approx. 297, 302, 313 and 334 nm match well with the absorptions of stilbenes. Excitation is thus guaranteed. Raising the temperature may favor the necessary rotation about the Ph-CH required for electrocyclic ring closure. Higher temperature may furthermore benefit the terminal oxidation step.
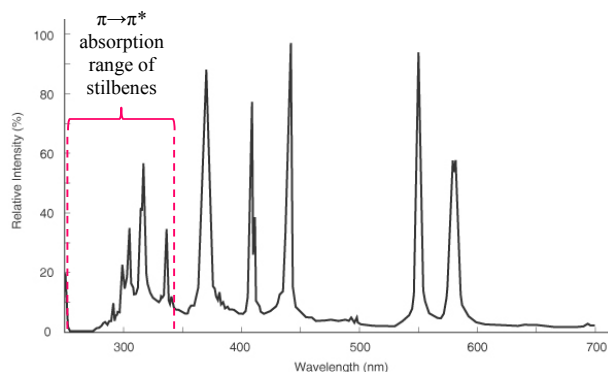
Figure 6.3: Emission spectrum of super high-pressure UV lamp [202].

The ^{1}H-NMR spectrum of an incomplete reaction mixture displays typical peaks for *cis*-stilbene, *trans*-stilbene and phenanthrene (**Figure 6.4**). Two singlets at 6.60 ppm and 7.12 ppm

represent the olefinic hydrogens of *cis-* and *trans-***1**, respectively. A characteristic doublet around 8.70 ppm stands for phenantherene (**2**).
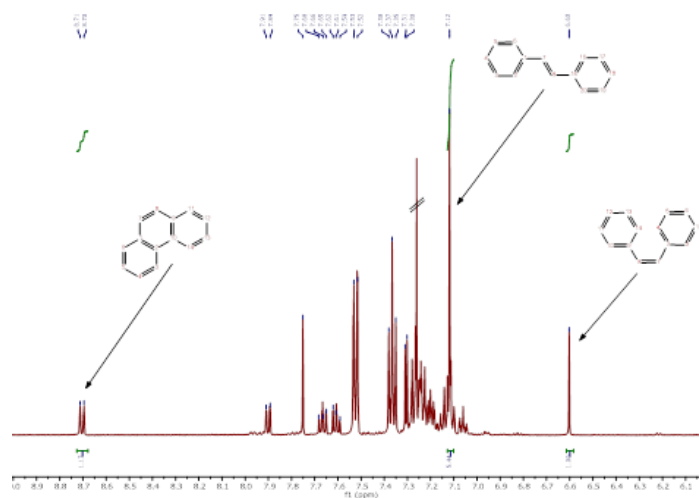
Figure 6.4: ^{1}H-NMR spectrum of reaction mixture in CDCl$_3$ (entry 7, **Table 5.1**).

In comparison, the ^{1}H-NMR spectrum of a complete transformation is shown in **Figure 6.5**. The 'inner' aromatic hydrogens a shifted downfield, whereas all other aromatic hydrogens appear between 7.5-8.0 ppm.
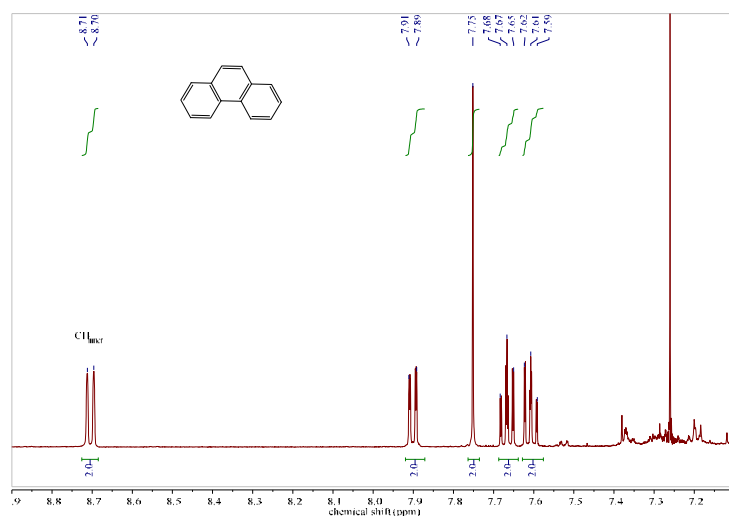
Figure 6.5: ^{1}H-NMR spectrum of pure product in CDCl$_3$ (entry 8, **Table 5.1**).

6.3.2.2 Using a LED Array

The same reaction setup and cryostat were used with an array of six LEDs (total of 1.5 W; λ_{max} = 365 nm). Three hours of irradiation with LED light at 35ºC or 45ºC under batch conditions did not yield any product (**Table 6.2**).

Table 6.2: Reaction under batch conditions in cyclohexane using a LED array.

Entry	Temperature (ºC)	Time (h)	Conversion (%)
10	35	3	n.r.[a]
11	45	2	n.r.[a]

[a] n.r. = no reaction, as determined by GC-analysis.

The chosen LEDs show an emission range of approx. 340-400 nm with a maxima at 365 nm [159, 260]. In contrast, stilbenes **1** absorb below 345 nm (**Figure 6.2**). The LED array is thus unable to initiate the desired photochemical transformation. Temperature alone had no effect on the reaction.

6.3.3 Reactions under Continuous Flow Conditions

6.3.3.1 Using a UV Lamp

The flow reactor setup used is simplified in **Figure 6.6**. A UV transparent fluorinated ethylene propylene (FEP) with an internal diameter (ID) of 0.8 mm, outer dimeter of 1.58 mm and internal volume of 5 mL was tightly wrapped around an immersion well reactor cooler (Duran glass). 10 mL of the reaction mixture were irradiated with a 500 W high pressure mercury lamp both at room temperature using a cooling setup and at 45°C using a thermal setup (**Figure 6.7**).
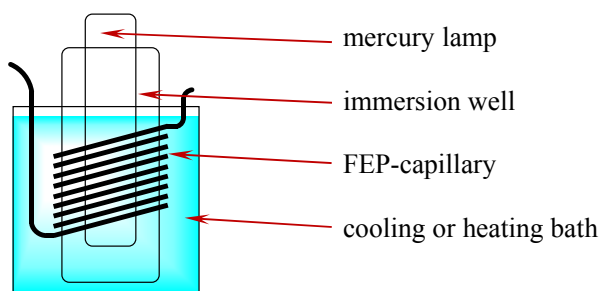
Figure 6.6: Microcapillary flow reactor setup.

The results are summarized in **Table 6.3**. When compared to the two hours irradiation in batch, a full conversion was observed in the flow reactor after a residence time of 8 minutes.

(a) Using cooling bath   (b) Using thermal regulator
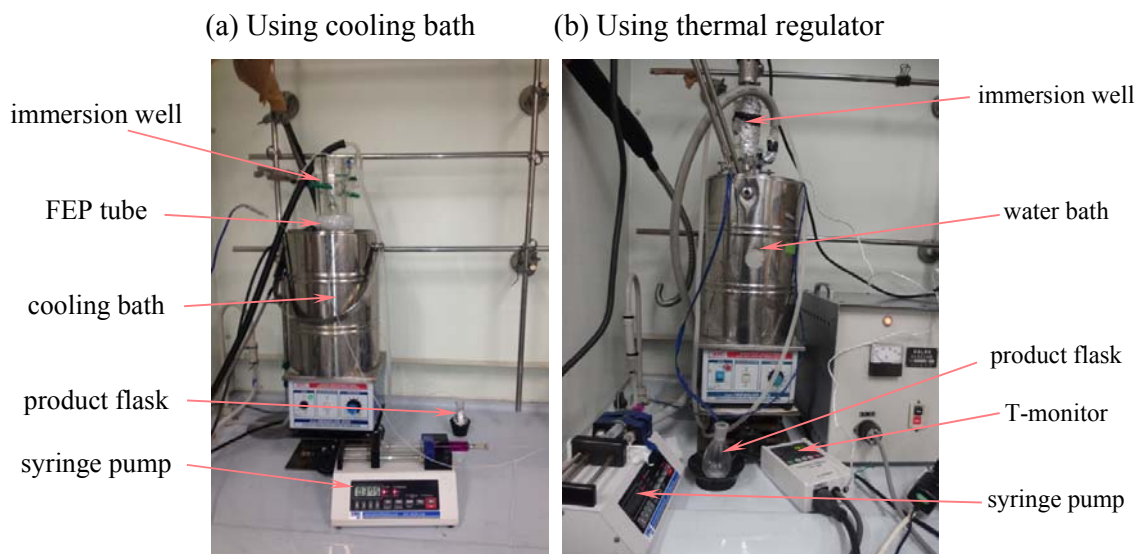
Figure 6.7: Microcapillary flow reactor for cyclohexane.

Table 6.3: Reaction under flow conditions in cyclohexane using a 500 W UV lamp.

Entry	Temperature (ºC)	Time (h)	Conversion (%)[a]	Yield (%)
12	room temperature	8	43	36
13	35	16	100	99
14	45	8	100	87

[a] Determined by GC-analysis.

6.3.3.2   Using a LED Array

Since the micro-flow reactor worked efficiently for the 500 W UV lamp, it was considered worthy to repeat similar reactions under flow conditions using an LED array. Following this approach, experiments were performed using an YMC keychem-Lumino2 microflow reactor with an integrated LED setup consisting of 6 LED lamps (total of 1.5 W; λ_{max} = 365 nm; **Figure 6.8**).

Figure 6.8: YMC keychem-Lumino2 microflow reactor.

Its reaction plate had a width of 1 mm, a depth of 0.2 mm, a length of 5.6 cm and an internal volume of 112 μL. The reaction temperature was controlled by a heating block unit and was fixed to 35°C. No conversion was detected over the feasible range of residence times of 11 to 112 minutes (**Table 6.4**). This lack of reactivity was again caused by the missing overlap of the emission of the UVA-LEDs with the absorption spectra of the stilbenes (**Figure 6.2**).

Table 6.4: Reaction under flow conditions in cyclohexane using an LED array.

Entry	Temperature (°C)	Residence time (min)	Conversion (%)
15	35	11	n.r.[a]
16	35	22	n.r.[a]
17	35	112	n.r.[a]

[a] n.r. = no reaction, as determined by GC-analysis.

6.3.4   Photoreactions in scCO$_2$

6.3.4.1   Under batch conditions in scCO$_2$

Subsequently, reactions were carried out in scCO$_2$ using various temperature and pressure conditions in order to achieve high yields **Figure 6.9**. The USHIO Optical Modulex (SX-U1501XQ-500W) was again used as a light source. The temperature was controlled using a cryostat (USP-203 series) for spectrophotometer.

Figure 6.9: Batch reactor for irradiations in scCO$_2$.

At first, the photoreaction was tried in scCO$_2$ with no air/O$_2$ supply at 35°C. No conversion to phenanthrene (**2**) was observed after 1.5 h of irradiation even at different pressures of approx. 9.5-13.2 MPa (**Table 6.5**).

Table 6.5: Reactions in batch in scCO$_2$ using 500 W UV lamp in the absence of air/O$_2$.

Entry	Pressure (MPa)	Time (h)	Conversion (%)
18	~9.5	1½	n.r.[a]
19	~10.5	1½	n.r.[a]
20	~13.2	1½	n.r.[a]

[a] n.r. = no reaction, as determined by GC-analysis.

The reaction was therefore repeated at 35°C in the presence of air/O$_2$ by running it without pre-degassing of the setup with scCO$_2$ (**Table 6.6**). After the same duration of 1.5 h and using approximately the same pressure conditions as before, trace amounts of product **2** were observed (entries 21-23). The reaction time was subsequently doubled to 3 hours and various pressure conditions were investigated as scCO$_2$ behaves differently at different pressures. Low yields of up to 10% were observed (entries 24-37). Subsequently, the temperature was raised to 45°C and for one case the concentration was reduced to half as well (entries 38 and 39). Low conversion rates of 5% and 9% were established after 3 hours of irradiation.

Table 6.6: Reactions in batch in scCO$_2$ using 500 W UV lamp in the presence of air/O$_2$.

Entry	Pressure (MPa)	Time (h)	Conversion (%)[a]	Yield (%)
21	9.5	1½	trace	n.d.[b]
22	10.5	1½	trace	n.d.[b]
23	13	1½	trace	n.d.[b]
24	7.6	3	2	1.5
25	7.8	3	3	2
26	7.8	3	3	2
27	8.0	3	3	2
28	8.0	3	3	2
29	7.8-8.2	3	3	2
30	7.8-8.2	3	3	2
31	8.5	3	trace	n.d.[b]
32	9.0	3	3	3
33	9.0	3	3	3
34	9.2	3	15	10
35	9.5	3	16	10
36	10.0	3	2	2
37	11.0	3	3	2.5
38[b]	10.0	3	5	4
39[b, c]	10.0	3	9	7

[a] Determined by GC-analysis. [b] Reaction conducted at 45°C. [c] Concentrations halved.

6.3.4.2 Reactions in a dual solvent system (scCO₂ & cyclohexane)

To compare the efficiency of $scCO_2$ and cyclohexane in a batch reactor, the reaction was tried in a dual solvent system by varying the amount of cyclohexane from 1 to 8 mL (**Table 6.7**). After 3 hours of irradiation, complete conversion was observed with 8 mL of cyclohexane at 45ºC (entry 43), where 8 mL is the working volume of the reactor that is directly facing the light source.

Table 6.7: Solvent study in batch in $scCO_2$ using a 500 W Hg lamp in the presence of air/O₂.

Entry	Solvent	Temperature (°C)	Conversion (%)[a]	Yield (%)
40	1 mL cyclohexane + $scCO_2$	35	4	3
41[b]	cyclohexane	35	16	10
42	8 mL cyclohexane[c]	35	70	50
43	8 mL cyclohexane[c]	45	100	65

[a] Determined by GC-analysis. [b] In batch reactor setup for $scCO_2$. [c] Working area only.

6.3.5 Reactions in the scCO₂ Microflow setup

A lab-built setup was used as a flow reactor for photoreactions in $scCO_2$. A 15 cm long Pyrex glass tube with an inner diameter of 0.6 mm served as a microreactor channel. Three glass tubes were connected in series to give a total irradiated length of 9.7 cm (**Figure 6.10**). The whole setup (except CO₂ cylinder and a pump) was kept in an incubator oven for better temperature control (**Figure 6.11**) [239] The flow rate was maintained through the CO₂ pump and a back pressure regulator (BPR).

(a) Microreactor   (b) Microreactor with Hg lamp in front
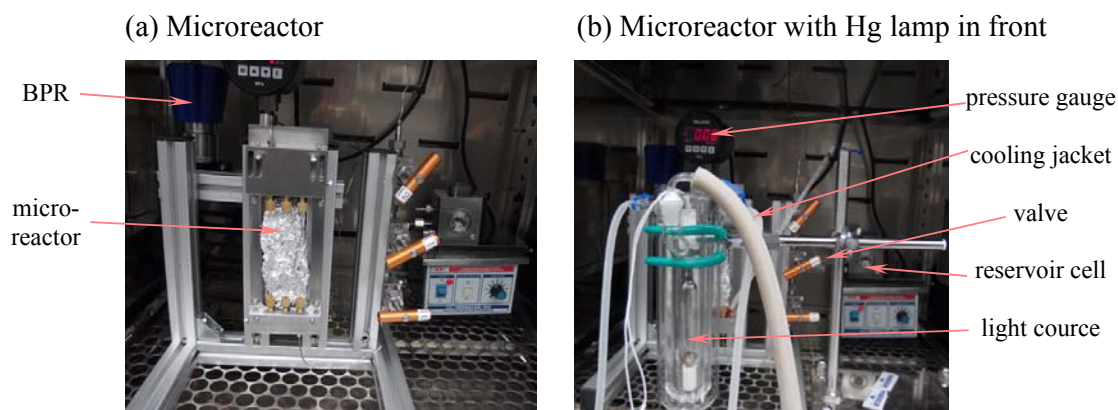
Figure 6.10: Microflow reactor for $scCO_2$ using a 500 W Hg lamp.
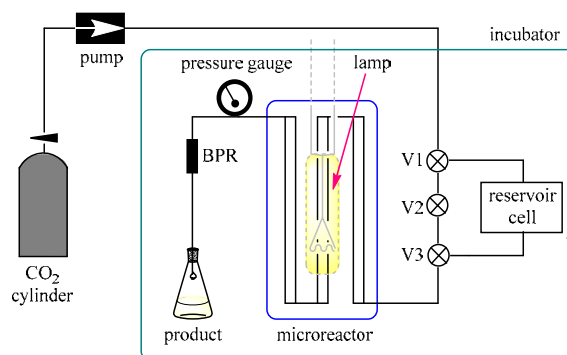
Figure 6.11: Schematic of the scCO₂ microflow reactor.

The reaction mixture was injected into a reservoir cell and pressurized to the set point (step 1). As a second step the reaction unit was filled with CO_2 to the required pressure (step 2). CO_2 was then flown through the reservoir cell, and the reaction mixture was carried into the microreactor for irradiation (step 3) (**Figure 6.12**).

Step 1: pressurizing into reservoir cell

$$\boxed{\text{pump}} \rightarrow \boxed{\text{valve 1}} \rightarrow \boxed{\text{reservoir cell}} \rightarrow \boxed{\text{valve 3}}$$

Step 2: pressurizing into reservoir cell

$$\boxed{\text{pump}} \rightarrow \boxed{\text{valve 1}} \rightarrow \boxed{\text{valve 2}} \rightarrow \boxed{\text{valve 3}} \rightarrow \boxed{\mu\text{-reactor}} \rightarrow \boxed{\text{pressure gauche}} \rightarrow \boxed{\text{BPR}}$$
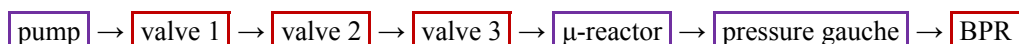
Step 3: flow of CO_2 for reaction progress (V = valve)

$$\boxed{\text{pump}} \rightarrow \boxed{\text{V1}} \rightarrow \boxed{\text{reservoir cell}} \rightarrow \boxed{\text{V3}} \rightarrow \boxed{\mu\text{-reactor}} \rightarrow \boxed{\text{pressure gauche}} \rightarrow \boxed{\text{BPR}} \rightarrow \boxed{\text{product}}$$
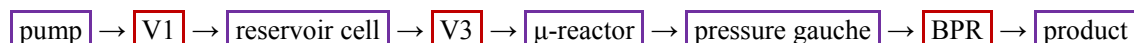
Figure 6.12: Flow chart of the photochemical flow reactor using scCO₂.

Operating the 500 W Hg lamp inside the setup resulted in a 10ºC increase in temperature in the microcapillary. Thus, the flow assembly along with scCO₂ was kept in an oven at 35ºC. When the lamp was turned on, the microcapillaries reached the desired temperature of 45ºC. The pressure was kept at 10 MPa as it was previously established as optimal for 45ºC temperature reactions under batch conditions. Subsequently, the flow reactor yielded improved conversions of up to 50% (entries 45 and 46) compared to the batch reactor (**Table 6.8**). When the concentration of the reagents was halved, a conversion of 70% and an isolated yield of **2** of 50% were obtained (entry 47).

Table 6.8: Reaction in microflow in scCO$_2$ using a 500 W Hg lamp in presence of air/O$_2$ at 45ºC and 10 MPa.

Entry	Residence time (min)	Conversion (%)[a]	Yield (%)
44	8	trace	n.d.[b]
45	16	28	12
46	32	50	23
47[c]	32	70	50

[a] Determined by GC-analysis. [b] n.d. = not determined. [c] Concentrations halved.

6.4   Summary and Conclusion

Okamoto's procedure was found reproducible in terms of residence time and yields under flow conditions (**Table 6.3**). The available LEDs were not suitable to initiate the desired reaction under batch (cyclohexane) or flow conditions (**Table 6.2** and **Table 6.4**). There was no reaction in the absence of air and the availability of air/O$_2$ is thus crucial for the progress of the reaction (**Table 5.1**, entry 1 and **Table 6.5**). An optimization of pressure in scCO$_2$ was done over the range of 7.5-13.2 MPa with special emphasis on the critical solvent phase at 8.0 MPa (**Table 6.6**). While the literature suggested 8.0 MPa being ideal for scCO$_2$ and at 35ºC, the experiments from this study established 9.5 MPa to be optimum for high yields.

Although the path length of both reactors is identical, reactions in scCO$_2$ were not found to be as efficient as those in cyclohexane (**Table 6.7**, entry 42). A gradual increase in conversions was observed in the flow scCO$_2$ reactor with increase in residence time from 8 to 16 and subsequently 32 minutes. In the microflow scCO$_2$ reactor, decreasing the concentration to half significantly improved the yield (**Table 6.8**, entry 47).

Compared to cyclohexane, scCO$_2$ seems not to be the most suitable solvent for this particular reaction (**Table 6.8**, entries 43 and 44). This may be attributed to the high purity (99.9999%) of the CO$_2$ in use, which limits the availability of O$_2$ for the reaction to proceed. The results proved that the microflow scCO$_2$ setup is a lot more efficient than the batch scCO$_2$ reactor (**Table 6.6** and **Table 6.8**). Irradiation of a solution at half concentration of reactants at 45ºC and under 10 MPa pressure in the microflow scCO$_2$ reactor and using a residence time of an hour (flow rate: 0.002 mL/min) should be investigated.

Chapter 7:

Summary and

Outlook

7. Summary and Outlook

7.1 Summary

Although photochemistry is often neglected as a synthesis method, new photochemical transformations may broaden its synthetic potential and acceptance in the synthetic chemistry community. Thus a series of potentially new photochemical reactions was explored.

Despite being isoelectronic to the highly photoactive phthalimides, isatin derivatives remained unreactive and did not yield any inter- or intramolecular photoaddition products. The photo–chemical studies involving benzoylbenzamide resulted in the discovery of new photochemical transformations based one Norrish type-II or photoinduced electron transfer processes. Visible light mediated photoredox decarboxylation reactions of *N*-phenylglycines with enones were successfully carried out using ruthenium tris(bipyridyl) chloride. The developed procedure worked well under batch as well as flow conditions and yielded both, open and ring addition products.

The previously established photodecarboxylative addition of carboxylates to *N*-alkylphthal–imides was used as a key step in the synthesis of biologically active compounds such as **AL12**, **AL5** and their analogues. The initially formed photoproducts were easily converted by acid catalyzed dehydration followed by amination. A library of compounds was synthesized following this procedure and was submitted for antimicrobial screening to the microbiology laboratory at JCU. The photodecarboxylative addition also served as a key step in the aristo–lactam synthesis. The synthesis route combined photodecarboxylative addition, dehydration and photodehydrohalogenation, with the option of further thermal amination. This 3-4 step methodology was successfully applied to the syntheses of unsubstituted 'parent' aristolactams. The multistep synthesis of bioactive **AL12**, **AL5** and selected analogues could be successfully realized under in-series microflow conditions. Compared to the stepwise batch protocols, the in-series operation prevented time- and resource-demanding isolation steps and gave the final product in high purity and improved yield.

Likewise, the cardiovascular active **AKS186** has been synthesized using an advanced, commercially available Vapourtec UV-150 reactor. The reactor consisted of integrated photo-thermal microflow loops. The desired **AKS186** product was obtained in high purity and in a yield of 80% yield, whereas the time demanding batch process only furnished an overall yield of 39%.

Selected examples of photodecarboxylative additions of phenyl acetates to phthalimide derivatives were furthermore realized in a concentrated solar trough flow reactor. The reactor

was designed to focus sunlight onto the reaction capillary. The simple design achieved a three–fold concentration of sunlight. The desired benzylated hydroxyl phthalimidines were isolated in good to excellent yields of 80-95% using short residence times of 40-53 min. Comparison reactions in non-concentrated sunlight showed no conversion for the same duration of exposure.

The monobromination of acetophenone was investigated by request of Takeda pharmaceuticals. The poor solubility of *N*-bromosuccinimide was found to be challenging for flow operations. The best reaction conditions gave 55% conversion with a residence time of 20 minutes in diethyether as a solvent.

The Mallory reaction was investigated in supercritical carbon dioxide during a research stay at NAIST in Japan. This study indicated that supercritical carbon dioxide is not a preferred solvent for oxidative reactions. Nevertheless, the investigated reaction displayed higher yields under microflow scCO$_2$ conditions compared to the batch process.

The results obtained from all flow investigations confirmed the superiority of continuous flow operations over conventional batch procedures.

7.2   Outlook

A deeper investigation into the photochemical behavior of benzoylbenzamides is still required. More interesting products can hopefully be obtained through systematic synthesis and photo–irradiation of these interesting starting materials under a variety of conditions. Likewise, the corresponding *meta*- or *para*-substituted benzoylbenzamide could be of interest to investigate the spatial separation caused by these substitution patterns on the efficiency of any photo–chemical transformation.

The photodecarboxylative addition of phenyl acetates to *N*-bromoalkylphthalimides has successfully provided an entrance to a library of compounds including photoproduct, *E/Z* mixtures of the dehydrated products and finally **AL12**, **AL5** and their analogues for biological testing. A metal free alternative route towards the patented **AL12** and **AL5** has thus been established. To increase the drug-likeliness of the products obtained, additional substitution at the phthalimide core, in particular methoxy-groups, should thus be investigated. This should include an investigation into the photophysical properties of these compounds.

The parent skeleton of the structurally similar tricyclic aristolactams has also become assessable through a photodecarboxylation-dehydration-photodehydrohalogentation cascade. For bio–logical activity, substituents, in particular methoxy- and hydroxyl-groups, are desirable. These substituted analogues could be obtained by simply using substituted phthalimides and 2-iodo–phenylacetates, by varying the *N*-alkyl chain or by further amination using additional

symmetrical and unsymmetrical amines. An *in-series* flow protocol for the synthesis of aristo–lactams should likewise be developed.

The inconvenient design of conventional photoreactors has limited the industrial implementation of photochemistry in early Research & Development (R&D) processes. Replacing conventional reactors with superior performing and easy to install flow photoreactors can broaden its industrial implementation. These devices are especially interesting in early lead finding processes, where only small quantities of materials are required. The presented project demonstrated the efficiency of microflow reactors through comparative studies of photo–decarboxylative additions. Continuous flow setups can easily provide the required quantities of target molecules on demand and on site. Scaling up can be likewise achieved by numbering up or by the development of larger meso-scale flow reactors. Due to their flexible design, micro–flow setups can also be used for the development of combinatorial photochemistry as a future R&D tool. Libraries can be achieved by injecting different reaction mixtures into a carrier solvent stream. The reaction products can be collected based on the residence times. In a miniaturized form, individual reactions may be performed in an array of single droplets inside the flow capillary.

Flow processes can be furthermore combined into single flow operations. Integrated photo-thermal setups and tandem photochemical-thermal continuous flow reactions have been successfully achieved in this study. This concept should thus be advanced to more complex multi-step reactions. The integration of several photochemical key-steps as utilized for the synthesis of aristolactams is hereby desirable.

Solar flow photoreactions in concentrated sunlight have furthermore been successfully demonstrated in this study. Using a simple in-house reactor, sunlight was concentrated onto a capillary in the focal line of the concentrator. Concentration of sunlight is particularly interesting for reactions that occur in the weak UV-range of the solar spectrum. The reactor should thus be utilized for other photochemical transformations. Likewise, photoredox catalytic or photooxygenation reactions use visible light. These transformations are thus optimal for solar flow studies. A more sophisticated solar reactor could incorporate automatic tracking and recording of sunlight.

The monobromination of acetophenone was achieved satisfactorily. Its further optimization was limited by the pump used to transport the reaction slurry. A peristaltic pump should be more suitable to transport slurries. Likewise, wider meso-scale tubing should be selected when constructing a next generation reactor.

The oxidative photocyclization of stilbene was realized under microflow conditions in super critical CO_2. The presence of oxygen was found crucial in order to achieve high yields and conversions. The application of lower grade CO_2 with higher oxygen content may offer a simple solution to this requirement. Alternatively, oxygen may be supplied in a slug flow as successfully demonstrated for photooxygenations.

Chapter 8:

Experimental Part

8. Experimental part

8.1 General methods

8.1.1 Solvents and reagents

All solvents and reagents were commercially available (Sigma-Aldrich or Alfa Aesar) and were used without purification.

8.1.2 Photochemical equipment

Photoreactors: Batch experiments were carried out in a Rayonet RPR-200 photochemical chamber reactor (Southern New England Ultraviolet Company, USA) equipped with 16×8 W fluorescent tubes. In-house setups were used for both in-door as well as outdoor flow reactions.

Glassware: All reactions were performed in Pyrex glassware unless otherwise specified.

8.1.3 Analytical methods

Melting point: Melting points were measured using a Tathastu melting point apparatus and are uncorrected.

IR: Infrared spectra were recorded on a Perkin Elmer Spectrum One FT-IR Spectrometer as solids or thin films, and were recorded in the range 600 cm^{-1}-4000 cm^{-1}. IR peaks are listed in wavenumbers ($\tilde{\nu}$; in cm^{-1}).

NMR: NMR facilities were used at JCU in Townsville and at the biomolecular analysis laboratory at AIMS. At JCU, NMR spectra were recorded on an Oxford 300 (^{1}H: 300 MHz and ^{13}C: 75 MHz) with a ^{UNITY}INOVA system console using the Varian Software VnmrJ program and Bruker 400 Ascend^{TM} (^{1}H: 400 MHz and ^{13}C: 100 MHz). At AIMS, NMR spectra were recorded on a Bruker Avance 300 Ultrashield^{TM} (^{1}H: 300 MHz and ^{13}C: 75 MHz) using the MestReNova v5.3.2-4936 software. Data was acquired using TopSpin 2.1 and 3.0, respectively. Residual solvent peaks served as an internal standard and samples were prepared in CDCl$_3$ (δ = 7.26/77.3 ppm) and acetone-d$_6$ (δ = 2.09/30.6 ppm). Solvent peaks and impurities were compared with literature values [261].

FTMS: High resolution mass spectroscopic data were determined on a Bruker BioApex 47 FT mass spectrometer with an electospray (ESI) Analytica of Branford source at the biomolecular analysis laboratory at AIMS. Ions were

detected in positive mode and/or negative mode within a mass range of m/z 50-2000. Direct infusion of sample (0.2 mg mL^{-1}) was carried out using a Cole Palmer 74900 syringe pump at a flow rate of 100 µl h^{-1}. N$_2$ (sourced from a Domnick Hunter UHPLCMS18 Nitrogen Generator, flow of 3 L/min and maintained at 200ºC) was used as the drying gas to assist in desolvation of the droplets produced by ESI from an on axis grounded needle directed to a metal capped nickel coated glass capillary, approximately 1 cm away. All experimental event sequences were controlled and data reduction performed using Bruker Daltonics XMASS ver. 7.0.3.0 software. Detection was in the direct mode from time domain data sets of 512 k (16 scans per experiment). Each spectrum was subjected to zerofill, Gaussian multiplication, and fast Fourier transform and displayed in magnitude mode. The instrument was calibrated using a methanolic solution of NaTFA (0.1 mg/mL MeOH), 200-2000 *m/z.*

8.1.4 Chromatographic methods

Separations: Column chromatography was carried out in Pyrex glass columns using Scharlan silica gel 60 (particle size 0.06-0.2 nm) 70-230 mesh ASTM. Mixtures of ethyl acetate and cyclohexane or ethyl acetate and *n*-hexane were used as mobile phase.

TLC: Thin layer chromatography was performed in glass jars on Macherey-Nagel polygram sil G/UV$_{254}$. Mixtures of ethyl acetate and cyclohexane or ethyl acetate and *n*-hexane were used as mobile phase.

GC: Gas chromatography samples were analysed on an Agilent 7890A gas chromatograph using the Agilent software, and 7683B auto-injector. The column used during the investigations was a Phenomenex Zebron ZB-5 low polarity (5% phenyl, 95% dimethylsiloxane) column (0.25 mm ID × 0.25 µm film thickness).

8.2 Synthesis of starting materials

8.2.1 Synthesis of 4-amino-*N*-pentenylphthalimide and *N*-alkenylisatin [Experiments 1-5]

General procedure 1 (GP1): 1 mmol of isatin was dissolved in 10 mL of DMF, stirred for 10 minutes before adding 10 mmol of K$_2$CO$_3$. After 1 hour of stirring, 1 mmol of the respective

alkenylbromide was added and the reaction mixture was heated overnight to 80°C. Cooling to room temperature, addition of water (50 mL), extraction using Et_2O (6 × 30 mL), washing with water (3 × 25 mL), drying over $MgSO_4$, evaporation and drying in vacuo furnished the final product.

8.2.1.1 Experiment 1: Synthesis of 2-allyl-5-aminoisoindoline-1,3-dione (3a)
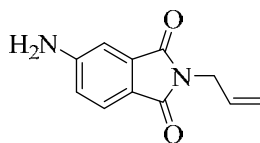
General procedure 1 was followed using 0.162 g of 5-aminophthalimide, 1.382 g of K_2CO_3 0.121 g of allylbromide and 10 mL of DMF. The reaction gave 0.17 g (85%) of the product as a bright yellow oil.

IR: (film)

$\widetilde{\nu}$ (cm^{-1}) = 3421, 1690, 1620, 1450, 920 and 702.

¹H-NMR: (300 MHz, $CDCl_3$)

δ (ppm): 3.63 (t, J = 9 Hz, 2 H, NCH_2), 4.99 (m, 2 H, $CH=CH_2$), 5.80 (m, 1 H, CH), 5.94 (broad s, 2 H, NH_2), 6.96 (dd, J = 3, 9 Hz, 1 H, CH_{arom}), 7.08 (d, J = 3 Hz, 1 H, CH_{arom}), 7.53 (d, J = 9 Hz, 1 H, CH_{arom}).

8.2.1.2 Experiment 2: Synthesis of 5-amino-2-(pent-4-enyl)isoindoline-1,3-dione (3b)
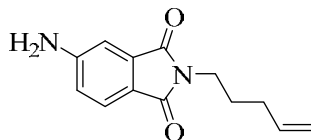
General procedure 1 was followed using 0.162 g of 5-aminophthalimide, 1.382 g of K_2CO_3, 0.149 g of 5-bromo-1-pentene and 10 mL of DMF. After workup, 0.19 g (87%) of the product were obtained as a deep yellow oil.

IR: (film)

$\widetilde{\nu}$ (cm^{-1}) = 3450, 1720, 1600, 1470, 901 and 789.

¹H-NMR: (300 MHz, $CDCl_3$)

δ (ppm): 1.63 (m, 2 H, CH_2), 2.12 (m, 2 H, CH_2), 3.56 (t, J = 9 Hz, 2 H, NCH_2), 4.96 (m, 2 H, $CH=CH_2$), 5.80 (m, 1 H, CH), 5.89 (broad s, 2 H, NH_2), 6.92 (dd, J = 3, 9 Hz, 1 H, CH_{arom}), 7.03 (d, J = 3 Hz, 1 H, CH_{arom}), 7.59 (d, J = 9 Hz, 1 H, CH_{arom}).

8.2.1.3   Experiment 3: Synthesis of 5-amino-2-(hept-6-enyl)isoindoline-1,3-dione (3c)
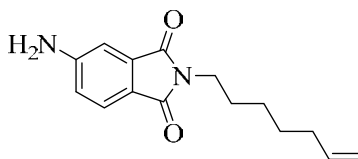
General procedure 1 was followed using 0.147 g of 5-aminophthalimide, 1.382 g of K_2CO_3, 0.177g of 7-bromo-1-heptene and 10 mL of DMF. The reaction gave 0.219 g (85%) of the product as a brownish yellow oil.

IR: (film)

$\widetilde{v}$ (cm^{-1}) = 3429, 1700, 1621, 1450, 920 and 750.

^{1}H-NMR: (300 MHz, CDCl$_3$)

δ (ppm): 1.36 (m, 2 H, CH$_2$), 1.57 (m, 2 H, CH$_2$), 1.92 (m, 2 H, CH$_2$), 2.01 (m, 2 H, CH$_2$), 3.51 (t, J = 9 Hz, 2 H, NCH$_2$), 4.95 (m, 2 H, CH=CH$_2$), 5.08 (broad s, 2 H, NH$_2$), 5.73 (m, 1 H, CH=CH$_2$), 6.79 (m, J = 3 Hz, 1 H, CH$_{arom}$), 6.93 (dd, J = 3, 9 Hz, 1 H, CH$_{arom}$), 7.04 (d, J = 3 Hz, 1 H, CH$_{arom}$), 7.45 (d, J = 9 Hz, 1 H, CH$_{arom}$).

8.2.1.4   Experiment 4: Synthesis of 1-(pent-4-enyl)indole-2,3-dione (5a)
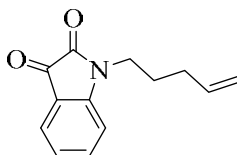
General procedure 1 was followed using 0.147 g of isatin, 1.382 g of K_2CO_3, 0.149 g of 5-bromo-1-pentene and 10 mL of DMF. After reaction, 0.174 g (81%) of the product were obtained as a brownish viscous oil.

IR: (film)

$\widetilde{v}$ (cm^{-1}) = 1728, 1599, 1470, 922 and 762.

^{1}H-NMR: (300 MHz, CDCl$_3$)

δ (ppm): 1.84 (m, 2 H, CH$_2$), 2.20 (m, 2 H, CH$_2$), 3.76 (t, J = 9 Hz, 2 H, NCH$_2$), 5.08 (m, 2 H, CH=CH$_2$), 5.85 (m, 1 H, CH=CH$_2$), 6.93 (d, J = 9 Hz, 1 H, CH$_{arom}$), 7.15 (dd, J = 3, 9 Hz, 1 H, CH$_{arom}$), 7.63 (m, 2 H, CH$_{arom}$).

8.2.1.5 Experiment 5: Synthesis of 1-(hept-6-enyl)indole-2,3-dione (5b)
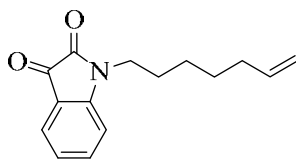
General procedure 1 was followed using 0.147 g of isatin, 1.382 g of K_2CO_3, 0.177 g of 7-bromo-1-heptene and 10 mL of DMF. The reaction gave 0.20 g (83%) of the product as a reddish brown viscous oil.

IR: (film)

$\widetilde{\nu}$ (cm^{-1}) = 1738, 1611, 1471, 1215 and 666.

^{1}H-NMR: (300 MHz, CDCl$_3$)

δ (ppm): 1.43 (m, 2 H, CH$_2$), 1.60 (m, 2 H, CH$_2$), 1.81 (m, 2 H, CH$_2$), 2.20 (m, 1 H, CH$_2$), 3.77 (t, J = 9 Hz, 2 H, NCH$_2$), 5.09 (m, 3 H, CH=CH$_2$), 5.85 (m, 1 H, CH=CH$_2$), 7.07 (d, J = 9 Hz, 1 H, CH$_{arom}$), 7.15 (dd, J = 3, 9 Hz, 1 H, CH$_{arom}$), 7.60 (m, 2 H, CH$_{arom}$).

8.2.2 Synthesis of 5-{[(*E*)-(5-bromo-2-hydroxy-3-methoxyphenyl)methylidene]amino} -1*H*-isoindole-1,3(2*H*)-dione [Experiment 6]
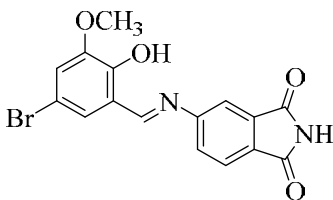
0.231 g of 5-bromo-2-hydroxy-3-methoxybenzaldehyde were dissolved in 10 mL of ethanol. Stirring was continued for 10 minutes and 3 drops of acetic acid were added. After dissolving 0.162 g of 3-aminophthalimide in 10 mL of ethanol, this solution was added to the stirred mixture of aldehyde. Reaction progress was monitored through TLC. Refluxing was continued for 2 hours. Yellow precipitates appeared after cooling the reaction mixture to room temperature. The product was filtered and washed with hot ethanol (~10 mL) in three portions. Drying between filter paper gave 0.266 g (71%) of the product as a deep yellow solid.

^{1}H-NMR: (300 MHz, CDCl$_3$)

δ (ppm): 3.87 (s, 3 H, OCH$_3$), 6.92 (m, 1 H, CH$_{arom}$), 7.29 (m, 1 H, CH$_{arom}$), 7.40 (m, 1 H, CH$_{arom}$), 7.82 (m, 2 H, CH$_{arom}$), 9.10 (s, 1 H, CH=N), not observed (1 H, NH).

8.2.3 **Synthesis of 5-{[(E)-(5-bromo-2-hydroxy-3-methoxyphenyl)methylidene]amino}-(N-pentenyl)-isoindole-1,3(2H)-dione [Experiment 7]**
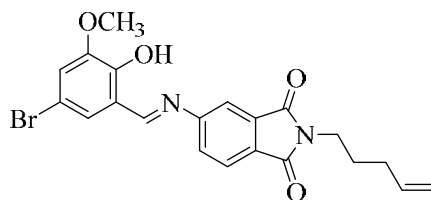
0.147 g of 5-{[(E)-(5-bromo-2-hydroxy-3-methoxyphenyl)methylidene]amino}-1H-isoindole-1,3(2H)-dione were disolved in 10 mL of DMF. After 10 minutes of stirring, 1.382 g of K_2CO_3 were added. Stirring was continued for 1 hour after which 0.149 g of 5-bromo-1-pentene were added and the reaction mixture was heated overnight. The mixture was cooled to room temperature and diluted with water (50 mL). The solution was extracted with Et_2O (6 × 30 mL). The combined organic layer was extracted with water (3 × 25 mL) and dried over $MgSO_4$. Removal of the solvent by rotary evaporator after gravity filtration gave 0.367 g (83%) of the product as a reddish yellow oil.

^{1}H-NMR: (300 MHz, $CDCl_3$)

δ (ppm): 1.43 (m, 2 H, CH_2), 1.66 (m, 2 H, CH_2), 3.65 (t, J = 9 Hz, 2 H, NCH_2), 3.84 (s, 3 H, OCH_3), 4.99 (m, 3 H, $CH=CH_2$), 5.80 (m, 1 H, $CH=CH_2$), 6.13 (m, 1 H, CH_{arom}), 7.22 (m, 1 H, CH_{arom}), 7.53 (m, 1 H, CH_{arom}), 7.78 (m, 2 H, CH_{arom}), 9.10 (s, 1 H, CH=N).

8.2.4 **Synthesis of benzoylbenzamides [Experiments 8-17]**

General procedure 2 (GP2): A mixture of benzoyl benzoic acid and an excess of thionylchloride was refluxed for an hour in ethylacetate. 5% aqueous NaOH and an equimolar amount of the respective amine were simultaneously added dropwise with continuous stirring and ice cooling for 5 hours. Water (50 mL) was added and the reaction mixture was extracted with ethyl acetate (3 × 30 mL), washed with $NaHCO_3$ (3 × 25 mL), diluted HCl solution (3 × 25 mL) and saturated NaCl solution (3 × 25 mL) and dried over $MgSO_4$. Evapoartion and drying in vacuo furnished the final product.

General procedure 3 (GP3): To 30 mL of DCM were added benzoylbenzoic acid (3 mmol), trimethylamine (5 mmol) and 1-ethyl-3-(3-dimethylaminopropyl)carbodiimide hydrochloride (EDC, 4 mmol). Finally, 3 mmol of the corresponding amine were added and the reaction mixture was refluxed for a week. Water (50 mL) was added and the reaction mixture was extracted with DCM (3 × 30 mL), washed with $NaHCO_3$ (3 × 25 mL), diluted HCl solution (3 × 25 mL) and saturated NaCl solution (3 × 25 mL) and dried over $MgSO_4$. Evapoartion and drying in vacuo furnished the final product.

8.2.4.1 Attempted synthesis of methyl phenyl({[2-(phenylcarbonyl)phenyl]carbonyl} amino)acetate (12a) [Experiments 8 and 9]
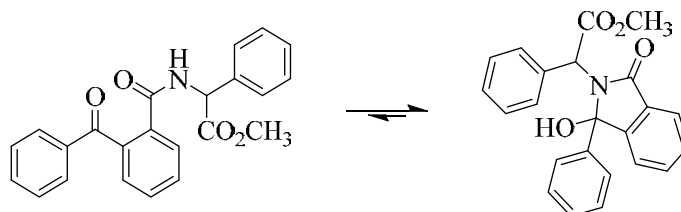
General procedure 2 was followed using 1.135 g of benzoylbenzoic acid, 0.725 mL of thionylchloride, 10 mL of 5% aqueous NaOH, 1.0083 g of phenylglycine methyl ester hydrochloride and 10 mL of ethylacetate. After workup, 1.327 g (71%) of the product were obtained as a colourless amorphous solid.

General procedure 3 was followed using 0.6789 g of benzoylbenzoic acid, 0.5 mL of trimethylamine, 0.6 g of 1-ethyl-3-(3-dimethylaminopropyl)carbodiimide, 0.6049 g of phenylglycine methyl ester hydrochloride and 30 mL of dichloromethane. 0.86 g (77%) of the product were obtained as an amorphous colourless solid.

^{1}H-NMR: (300 MHz, CDCl$_3$)

The complex product mixture did not allow for the assignments of signals.

8.2.4.2 Synthesis of methyl 1-{[2-(phenylcarbonyl)phenyl]carbonyl}pyrrolidine-2-carboxylate (11b, 11'b) [Experiments 10 and 11]
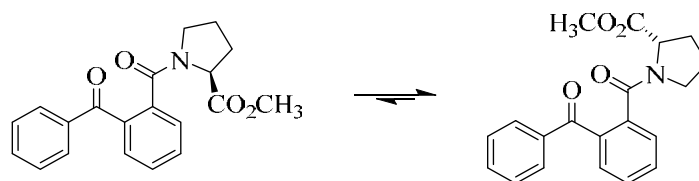
General procedure 2 was followed using 1.135 g of benzoylbenzoic acid, 0.725 mL of thionylchloride, 10 mL of 5% aqueous NaOH, 0.8281 g of *L*-proline methyl ester hydrochloride and 10 mL of ethylacetate. 1.12 g (66%) of the product were obtained as an amorphous colourless powder.

General procedure 3 was followed using 0.6789 g of benzoylbenzoic acid, 0.5 mL of trimethylamine, 0.6 g of 1-ethyl-3-(3-dimethylaminopropyl)carbodiimide, 0.4968 g of *L*-proline methyl ester hydrochloride and 30 mL of dichloromethane. 0.748 g (74%) of the product were obtained as a colourless powder.

^{1}H-NMR: (mixture of rotamers, 300 MHz, CDCl$_3$)

δ (ppm): 1.90 (m, 2 H, CH$_2$), 2.27 (m, 2 H, CH$_2$), 3.43 (m, 2 H, NCH$_2$), 3.50 (s, 3 H, OCH$_3$), 3.52 (m, 2 H, NCH$_2$), 3.78 (s, 3 H, OCH$_3$), 4.27 (m, 1 H, C**H**CO$_2$CH$_3$), 4.58 (m, 1 H, C**H**CO$_2$CH$_3$), 7.26-7.47 (m, 5 H, CH$_{arom}$), 7.62 (m, 2 H, CH$_{arom}$), 8.13 (m, 2 H, CH$_{arom}$).

8.2.4.3 Attempted synthesis of methyl 4-(methylsulfanyl)-2-({[2-(phenylcarbonyl) phenyl]carbonyl}amino)butanoate (12c) [Experiments 12 and 13]
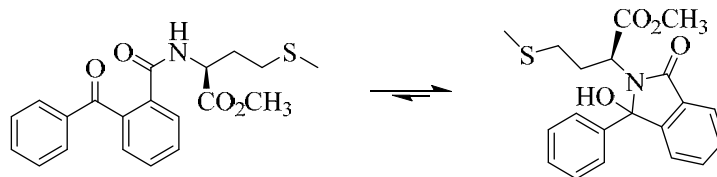
General procedure 2 was followed using 1.135 g of benzoylbenzoic acid, 0.725 mL of thionylchloride, 10 mL of 5% aqueous NaOH, 0.9985 g of *L*-methionine methyl ester hydrochloride and 10 mL of ethylacetate. 1.28 g (69%) of the product were obtained as a colourless solid.

General procedure 3 was followed using 0.6789 g of benzoylbenzoic acid, 0.5 mL of trimethylamine, 0.6 g of 1-ethyl-3-(3-dimethylaminopropyl)carbodiimide, 0.5991 g of *L*-methionine methyl ester hydrochloride and 30 mL of dichloromethane. 0.86 g (77%) of the product were obtained as a colourless powder.

¹H-NMR: (mixture of diastereoisomers, 300 MHz, acetone-d$_6$)

Main diastereoisomer:

δ (ppm): 1.76 (s, 3 H, SCH$_3$), 2.00-2.70 (m, 4 H, 2 × CH$_2$), 3.60 (s, 3 H, CO$_2$CH$_3$), 4.21 (m, 1 H, C**H**CO$_2$CH$_3$), 5.78 (s, 1 H, COH), 7.23-7.74 (m, 9 H, CH$_{arom}$).

Minor diastereoisomer:

δ (ppm): 2.04 (s, 3 H, SCH$_3$), 2.00-2.70 (m, 4 H, 2 × CH$_2$), 3.48 (s, 3 H, CO$_2$CH$_3$), 4.21 (m, 1 H, C**H**CO$_2$CH$_3$), 6.09 (s, 1 H, COH), 7.23-7.74 (m, 9 H, CH$_{arom}$).

8.2.4.4 Synthesis of methyl 2-{[2-(phenylcarbonyl)phenyl]carbonyl}isothiazolidine-3-carboxylate (11d, 11'd) [Experiments 14 and 15]
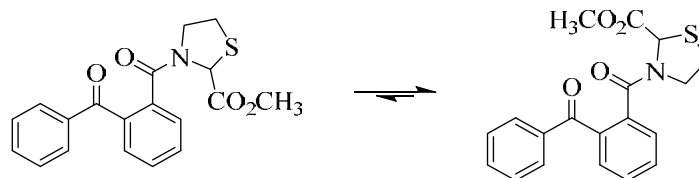
General procedure 2 was followed using 1.135 g of benzoylbenzoic acid, 0.725 mL of thionylchloride, 10 mL of 5% aqueous NaOH, 0.9183g of methyl thiazolidine-2-carboxylate

hydrochloride and 10 mL of ethylacetate. 1.12 g (63%) of product were obtained as an amorphous colourless solid.

General procedure 3 was followed using 0.6789 g of benzoylbenzoic acid, 0.5 mL of trimethylamine, 0.6 g of 1-ethyl-3-(3-dimethylaminopropyl)carbodiimide, 0.5509 g of methyl thiazolidine-2-carboxylate hydrochloride and 30 mL of dichloromethane. 0.778 g (73%) of product were obtained as a colourless powder.

^{1}H-NMR: (mixture of rotamers, 300 MHz, CDCl$_3$)

Main rotamer:

δ (ppm): 3.00-3.40 (m, 2 H, SCH$_2$), 3.77 (s, 3 H, OCH$_3$), 3.83 (broad t, 2 H, NCH$_2$), 5.62 (s, 1 H, C**H**CO$_2$CH$_3$), 7.40-7.70 (m, 7 H, CH$_{arom}$), 7.81 (m, 2 H, CH$_{arom}$).

Minor rotamer:

δ (ppm): 3.00-3.40 (m, 2 H, SCH$_2$), (m, 2 H, CH$_2$), 4.43 (m, 2 H, NCH$_2$), 3.69 (s, 3 H, OCH$_3$), (m, 2 H, NCH$_2$), 5.20 (s, 1 H, C**H**CO$_2$CH$_3$), 7.30 (m, 1 H, CH$_{arom}$), 7.40-7.70 (m, 6 H, CH$_{arom}$), 7.81 (m, 2 H, CH$_{arom}$).

8.2.4.5 Attempted synthesis of N-({[2-(phenylcarbonyl)phenyl]carbonyl}-2-(*tert*-butyl-thio)ethanamine (12e) [Experiments 16 and 17]
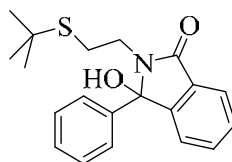
General procedure 2 was followed using 1.135 g of benzoylbenzoic acid, 0.725 mL of thionylchloride, 10 mL of 5% aqueous NaOH, 0.666 g of 2-(*tert*-butylthio)ethanamine and 10 mL of ethylacetate. 1.11 g (65%) of product were obtained as a yellowish solid.

General procedure 3 was followed using 0.6789 g of benzoylbenzoic acid, 0.5 mL of trimethylamine, 0.6 g of 1-ethyl-3-(3-dimethylaminopropyl)carbodiimide, 0.399 g of 2-(*tert*-butylthio)ethanamine and 30 mL of dichloromethane. 0.754 g (74%) of product was obtained as a yellowish solid.

^{1}H-NMR: (300 MHz, CDCl$_3$)

δ (ppm): 1.27 (s, 9 H, 3 × CH$_3$), 2.36 (m, 1 H, CH$_2$), 2.74 (m, 1 H, CH$_2$), 3.10 (m, 1 H, CH$_2$), 3.61 (m, 1 H, CH$_2$), 5.32 (s, 1 H, COH), 7.32-7.57 (m, 8 H, CH$_{arom}$), 7.70 (m, 1 H, CH$_{arom}$).

8.2.5 Synthesis of furanone (14a) [Experiment 18]
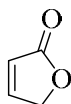
A 2-necked round bottom flask was charged with furfural (27.8 mL, 0.335 mol), anhydrous sodium sulfate (11.03 g, 0.078 mol), *N*, *N*-dimethylethanolamine (8.47 mL, 0.084 mmol), formic acid (25.37 mL, 0.67 mol) and dichloromethane (100 mL). Aqueous 50% hydrogen peroxide (10 mL, 0.213 mol) was added to a vigorously stirring brown solution over the course of 5 minutes. The reaction mixture was heated up to a gentle reflux after which further hydrogen peroxide (32.3 mL, 0.89 mol) was slowly added over the course of 1.5 hours. After stirring for 16 hours the reaction was complete according to TLC analysis. The aqueous phase was extracted with 2 × 50 mL of DCM. The combined organic phases was washed with saturated aqueous sodium bisulfate and dried with sodium sulphate. The reaction mixture was subsequently evaporated and dried. 7.87 g (40%) of product were obtained as a slightly yellowish liquid.

¹H-NMR: (300 MHz, CDCl₃)

δ (ppm): 4.83 (t, 2 H, OCH₂), 6.05 (m, 1 H, =CH), 7.56 (m, 1 H, =CH).

8.2.6 Synthesis of *N*-methylphenylglycine (16) [Experiment 19]
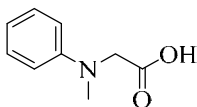
0.151 g of phenylglycine (1 mmol) were added to 10 mL of DMF. After 10 minutes of stirring 1.382 g (10 mmol) of K₂CO₃ were added. Stirring was continued for 1 hour after which 0.062 mL of methyliodide were added. The reaction mixture was subsequently heated to 80°C overnight. After reaction, mixture was cooled to room temperature and diluted with water (50 mL). The solution was extracted with Et₂O (6 × 30 mL). The combined organic layer was washed with water (3 × 25 mL) and dried over MgSO₄. Gravity filtration and removal of the solvent by rotary evaporator gave 0.128 g (78%) of the product as a colourless solid.

Melting Point: 270°C.

¹H-NMR: (400 MHz, CDCl₃)

δ (ppm): 3.07 (s, 3 H, NCH₃), 4.08 (s, 2 H, NCH₂CO), 6.76 (d, J = 9 Hz, 2 H, CH$_{arom}$), 6.81 (dd, J = 3, 9 Hz, 1 H, CH$_{arom}$), 7.23 (dd, J = 3, 9 Hz, 2 H, CH$_{arom}$).

8.3 Photochemical transformations

8.3.1 Attempted photocyclizations of 4-amino-*N*-alkenylphthalimides and *N*-alkenyl-isatins [Experiments 20-29]

General procedure 4 (GP4): A 0.5 mM solution of alkenyl compound in acetone was irradiated for up to 54 hours under UVB or UVA radiation. The reaction mixture was constantly purged with nitrogen gas. The progress of the reaction was monitored by TLC. The crude product mixture was evaporated to dryness and analyzed by NMR spectroscopy.

8.3.1.1 Attempted intramolecular photocyclization of 5-amino-2-(pent-4-enyl)iso-indoline-1,3-dione (17a, 17'a) [Experiments 20 and 21]

General procedure 4 was followed using 0.115 g of 5-amino-2-(pent-4-enyl)isoindoline-1,3-dione in 60 mL of acetone and irradiation with UVB light for 54 hours. 0.051 g (44%) of starting material were recovered as a dark brown oil.

General procedure 4 was followed using 0.115 g of 5-amino-2-(pent-4-enyl)isoindoline-1,3-dione in 60 mL of acetone and irradiation with UVA light for 28 hours.

^{1}H-NMR: (300 MHz, CDCl$_3$)

No conversion to detectable photoproducts was observed in either case.

8.3.1.2 Attempted intramolecular photocyclization of 5-amino-2-(hept-6-enyl)iso-indoline-1,3-dione (17b, 17'b) [Experiments 22 and 23]

General procedure 4 was followed using 0.13 g of 5-amino-2-(hept-6-enyl)isoindoline-1,3-dione in 60 mL of acetone and irradiation with UVB light for 54 hours. 0.066 g (51%) of starting material were recovered as a deep brown oil.

General procedure 4 was followed using 0.13 g of 5-amino-2-(hept-6-enyl)isoindoline-1,3-dione in 60 mL acetone and irradiation with UVA light for 28 hours.

^{1}H-NMR: (300 MHz, CDCl$_3$)

No conversion to detectable photoproducts was observed in either case.

8.3.1.3 Attempted intramolecular photocyclization of 1-(pent-4-enyl)indole-2,3-dione (18a, 19a) [Experiments 24 and 25]

General procedure 4 was followed using 0.108 g of 1-(pent-4-enyl)indole-2,3-dione in 60 mL of acetone and irradiation with UVB light for 54 hours. 0.068 g (63%) of starting material were recovered as a dark brown oil.

General procedure 4 was followed using 0.108 g of 1-(pent-4-enyl)indole-2,3-dione in 60 mL of acetone and irradiation with UVA light for 28 hours.

¹H-NMR: (300 MHz, CDCl₃)

No conversion to detectable photoproducts was observed in either case.

8.3.1.4 Attempted intramolecular photocyclization of 1-(hept-6-enyl)indole-2,3-dione (18b, 19b) [Experiments 26 and 27]

General procedure 4 was followed using 0.122 g of 1-(hept-6-enyl)indole-2,3-dione in 60 mL of acetone and irradiation with UVB light for 54 hours. 0.07 g (57%) of starting material were recovered as a dark brown oil.

General procedure 4 was followed using 0.122 g of 1-(hept-6-enyl)indole-2,3-dione in 60 mL of acetone and irradiation with with UVA light for 28 hours.

¹H-NMR: (300 MHz, CDCl₃)

No conversion to detectable photoproducts was observed in either case.

8.3.1.5 Attempted intramolecular photocyclization of 5-{[(E)-(5-bromo-2-hydroxy-3-methoxyphenyl)methylidene]amino}-2-(pent-4-enyl)-1H-isoindole-1,3(2H)-dione (20) [Experiments 28 and 29]

General procedure 4 was followed using 0.22 g of 5-{[(E)-(5-bromo-2-hydroxy-3-methoxyphenyl)methylidene]amino}-2-(pent-4-enyl)-1H-isoindole-1,3(2H)-dione base in 60 mL of acetone and irradiation with UVB light for 54 hours. 0.11 g (51%) of starting material were recovered as a dark brown oil.

General procedure 4 was followed using 0.22 g of 5-{[(E)-(5-bromo-2-hydroxy-3-methoxyphenyl)methylidene]amino}-2-(pent-4-enyl)-1H-isoindole-1,3(2H)-dione in 60 mL acetone and irradiation with with UVA light for 28 hours.

¹H-NMR: (300 MHz, CDCl₃)

No conversion to detectable photoproducts was observed in either case.

8.3.2 Attempted intermolecular photodecarboxylative additions of phenylacetates to *N*-methylisatin [Experiments 30-34]

General procedure 5 (GP5): 1 mmol of isatin was dissolved in 10 mL of acetone. 4 mmol of phenylacetic acid and 2 mmol of K₂CO₃ were dissolved in 10 mL of pH 7 buffer upon gentle heating. Both the solutions were added to a Pyrex Schlenk flask and the volume was topped up to 60 mL using acetone:pH 7 buffer (50:50). The reaction mixture was irradiated for 3 hours

with UVB light while purging with a gentle stream of nitrogen. The progress of the reaction was monitored by TLC. Most of the acetone was removed by evaporation an dthe remaining reaction mixture was extracted with DCM (3 × 25 mL), washed with diluted $NaHCO_3$ (3 × 20 mL) and brine (2 × 20 mL), dried over $MgSO_4$. Evaporation and drying furnished the crude product which was analyzed by NMR spectroscopy.

8.3.2.1 Attempted synthesis of 3-benzyl-3-hydroxy-1-methylindolin-2-one (23a) and isolation of 1, 3-dihydro-3-hydroxy-1-methyl-3-(2-oxopropyl)-2*H*-indol-2-one (24) [Experiment 30]
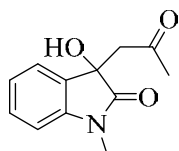
General procedure 5 was followed using 0.161 g of *N*-methylisatin, 0.544 g of phenylacetic acid, 0.207 g of potassium carbonate and 60 mL of acetone/pH 7 buffer. A fine product precipitated during irradiation. Workup furnished 0.153 g (70%) of 1, 3-dihydro-3-hydroxy-1-methyl-3-(2-oxopropyl)-2*H*-indol-2-one as a colourless solid.

1, 3-Dihydro-3-hydroxy-1-methyl-3-(2-oxopropyl)-2*H*-indol-2-one (24):

Melting point: 146-148°C.

IR: (film)

$\widetilde{\nu}$ (cm^{-1}) = 3577, 3240, 1700, 1615, 1477, 1336, 1185, 826 and 729.

^{1}H-NMR: (300 MHz, CDCl$_3$)

δ (ppm): 2.95 (d, J = 18 Hz, 1 H, CH$_2$), 3.20 (d, J = 18 Hz, 1 H, CH$_2$), 4.40 (s, 1 H, COH), 2.18 (s, 3 H, COCH$_3$), 3.30 (s, 3 H, NCH$_3$), 6.84 (d, 1 H, CH$_{arom}$), 7.05 (dd, 1 H, CH$_{arom}$), 7.35 (m, 2 H, CH$_{arom}$).

8.3.2.2 Attempted synthesis of 3-hydroxy-3-(4-methylbenzyl)-1-methylindolin-2-one (23b) and isolation of 1, 3-dihydro-3-hydroxy-1-methyl-3-(2-oxopropyl)-2*H*-indol-2-one (24) [Experiment 31]

General procedure 5 was followed using 0.161 g of *N*-methylisatin, 0.6 g of 4-methylphenyl-acetic acid, 0.207 g of potassium carbonate and 60 mL of acetone/pH 7 buffer. After workup, 0.164 g (75%) of 1, 3-dihydro-3-hydroxy-1-methyl-3-(2-oxopropyl)-2*H*-indol-2-one were obtained as a colourless solid.

1, 3-Dihydro-3-hydroxy-1-methyl-3-(2-oxopropyl)-2*H*-indol-2-one (24):

^{1}H-NMR: (300 MHz, CDCl$_3$)

Identical to Experiment 30.

8.3.2.3 Attempted synthesis of 3-hydroxy-3-(2-methylbenzyl)-1-methylindolin-2-one (23c) and isolation of 1, 3-dihydro-3-hydroxy-1-methyl-3-(2-oxopropyl)-2*H*-indol-2-one (24) [Experiment 32]

General procedure 5 was followed using 0.161 g of *N*-methylisatin, 0.6 g of 2-methylphenyl-acetic acid, 0.207 g of potassium carbonate and 60 mL of acetone/pH 7 buffer. After workup, 0.153 g (70%) of 1, 3-dihydro-3-hydroxy-1-methyl-3-(2-oxopropyl)-2*H*-indol-2-one were obtained as a colourless solid.

1, 3-Dihydro-3-hydroxy-1-methyl-3-(2-oxopropyl)-2*H*-indol-2-one (24):

^{1}H-NMR: (300 MHz, CDCl$_3$)

Identical to Experiment 30.

8.3.2.4 Attempted synthesis of 3-(4-fluorobenzyl)-3-hydroxy-1-methylindolin-2-one (23d) and isolation of 1, 3-dihydro-3-hydroxy-1-methyl-3-(2-oxopropyl)-2*H*-indol-2-one (24) [Experiment 33]

General procedure 5 was followed using 0.161 g of *N*-methylisatin, 0.616 g of 4-fluoro-phenylacetic acid, 0.207 g of potassium carbonate and 60 mL of acetone/pH 7 buffer. Workup furnished 0.155 g (71%) of 1, 3-dihydro-3-hydroxy-1-methyl-3-(2-oxopropyl)-2*H*-indol-2-one as a colourless solid.

1, 3-Dihydro-3-hydroxy-1-methyl-3-(2-oxopropyl)-2*H*-indol-2-one (24):

^{1}H-NMR: (300 MHz, CDCl$_3$)

Identical to Experiment 30.

8.3.2.5 Attempted synthesis of 3-(4-bromobenzyl)-3-hydroxy-1-methylindolin-2-one (23e) and isolation of 1, 3-dihydro-3-hydroxy-1-methyl-3-(2-oxopropyl)-2*H*-indol-2-one (24) [Experiment 34]

General procedure 5 was followed using 0.161 g of *N*-methylisatin, 0.86 g of 4-bromo-phenylacetic acid, 0.207 g of potassium carbonate and 60 mL of acetone/pH 7 buffer. After workup, 0.14 g (64%) of 1, 3-dihydro-3-hydroxy-1-methyl-3-(2-oxopropyl)-2*H*-indol-2-one were obtained as a colourless solid.

1, 3-Dihydro-3-hydroxy-1-methyl-3-(2-oxopropyl)-2*H*-indol-2-one (24):

^{1}H-NMR: (300 MHz, CDCl$_3$)

Identical to Experiment 30.

8.3.3 Photocyclizations of benzoylbenzamides [Experiments 35-39]

General procedure 6 (GP6): 1 mmol of the respective amide was dissolved in 60 mL of acetone and irradiated with UVB light while purging with a gentle stream of nitrogen. The progress of the reaction was monitored by TLC. The crude product mixture was evaporated to dryness and purified by column chromatography. Each fraction was analyzed by NMR spectroscopy.

8.3.3.1 Attempted photoreaction of methyl phenyl({[2-(phenylcarbonyl)phenyl] carbonyl}amino)acetate and isolation of 3-phenylphthalide (27) [Experiment 35]
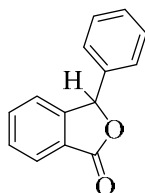
General procedure 6 was followed using 0.373 g of phenylglycine derived benzoylbenzamide and 60 mL of acetone and 4 hours of irradiation. Column chromatography was carried out using 60% EtOAc in cyclohexane but complete separation of the complex reaction mixture was not achieved. The only pure fraction obtained contained 0.05 g (24%) of 3-phenylphthalide as colourless crystals.

3-Phenylphthalide (27):

TLC: (SiO$_2$, ethyl acetate/cyclohexane 6:4)

R$_f$ = 0.32.

Melting point: 117°C.

^{1}H-NMR: (300 MHz, CDCl$_3$)

δ (ppm): 6.62 (s, 1 H, CHPh), 7.34-7.47 (m, 6 H, CH$_{arom}$), 7.64 (ddd, 1 H, CH$_{arom}$), 7.92 (d, 1 H, CH$_{arom}$).

8.3.3.2 Photoreaction of methyl 1-{[2-(phenylcarbonyl)phenyl]carbonyl}pyrrolidine-2-carboxylate (28, 29) [Experiment 36]
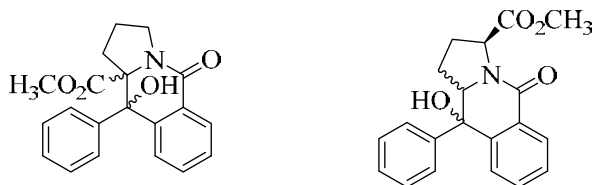
General procedure 6 was followed using 0.321 g of *L*-proline derived benzoylbenzamide and 60 mL of acetone and 4 hours of irradiation. Column chromatography gave 0.128 g (38%) of a mixture of two rotamers as a colourless solid.

TLC: (SiO$_2$, ethyl acetate/cyclohexane 3:1)

R$_f$ = 0.28.

^{1}H-NMR: (mixture of regioisomers, 300 MHz, CDCl$_3$)

δ (ppm): 1.90 (m, 4 H, CH$_2$), 3.22 (m, 1 H, CH$_2$), 3.63 (m, 1 H, NCH$_2$), 3.81 (s, 3 H, OCH$_3$), 3.89 (s, 3 H, OCH$_3$), 4.27 (m, 1 H, C**H**OCH$_3$), 7.23 (m, 2 H, CH$_{arom}$), 7.47 (m, 4 H, CH$_{arom}$), 7.68 (dd, J = 3, 9 Hz, 1 H, CH$_{arom}$), 7.93 (m, 2 H, CH$_{arom}$).

8.3.3.3 Attempted photoreaction of methyl 4-(methylsulfanyl)-2-({[2-(phenylcarbonyl)phenyl]carbonyl}amino)butanoate and isolation of 3-phenylphthalide (27) [Experiment 37]

General procedure 6 was followed using 0.371 g of *L*-methionine derived benzoylbenzamide and 60 mL of acetone and 4 hours of irradiation. Column chromatography was carried out using 60% EtOAc in cyclohexane but complete separation of the complex mixture was not achieved. Only 0.044 g (21%) of 3-phenylphthalide were obtained as colourless crystals.

3-Phenylphthalide (27):

^{1}H-NMR: (300 MHz, CDCl$_3$)

Identical to Experiment 35.

8.3.3.4 Photoreaction of methyl 2-{[2-(phenylcarbonyl)phenyl] carbonyl}isothiazolidine-3-carboxylate (30, 31) [Experiment 38]
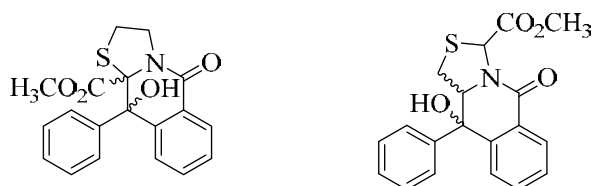
General procedure 6 was followed using 0.355 g of methyl thiazolidine-2-carboxylate derived benzoylbenzamide and 60 mL of acetone and 4 hours of irradiation. Column chromatography gave 0.145 g of a mixture of **30 & 31** in a combine yield of (41%).

Main regioisomer (30):

TLC: (SiO$_2$, ethyl acetate/cyclohexane 3:1)

R$_f$ = 0.30.

^{1}H-NMR: (300 MHz, CDCl$_3$)

δ (ppm): 1.94 (m, 1 H, NCH$_2$), 2.86 (m, 1 H, SCH$_2$), 3.73 (m, 1 H, NCH$_2$), 4.13 (m, 1 H, SCH$_2$), 3.68 (s, 3 H, OCH$_3$), 5.86 (s, 1 H, COH), 7.31 (m, 3 H, CH$_{arom}$), 7.40 (m, 2 H, CH$_{arom}$), 7.57 (m, 1 H, CH$_{arom}$), 7.66 (m, 2 H, CH$_{arom}$), 8.08 (m, 1 H, CH$_{arom}$).

Minor regioisomer (31):

TLC: (SiO$_2$, ethyl acetate/cyclohexane 3:1)

R$_f$ = 0.30.

δ (ppm): 2.67 (m, 1 H, SCH$_2$), 3.55 (m, 1 H, SCH$_2$), 3.80 (s, 3 H, OCH$_3$), 4.87 (m, 1 H, NCH), 5.20 (s, 1 H, COH), 5.73 (s, 1 H, CHCO$_2$Me), 6.84 (m, 1 H, CH$_{arom}$), 7.40-8.20 (covered m, 8 H, CH$_{arom}$).

8.3.3.5 Attempted photoreaction of *N*-({[2-(phenylcarbonyl)phenyl]carbonyl}-2-(*tert*-butylthio)ethanamine and isolation of 3-phenylphthalide (27) [Experiment 37]

General procedure 6 was followed using 0.341 g of 2-(*tert*-butylthio)ethanamine derived benzoylbenzamide and 60 mL of acetone and 4 hours of irradiation. Column chromatography was carried out using 60% EtOAc in cyclohexane but complete separation of the complex mixture was not achieved. 0.04 g (20%) of 3-phenylphthalide were obtained as colourless crystals.

3-Phenylphthalide (27):

^{1}H-NMR: (300 MHz, CDCl$_3$)

Identical to Experiment 35.

8.3.4 Photoredox reactions of *N*-phenylglycines and enones under batch and flow conditions [Experiments 40-62]

8.3.4.1 Optimization study using *N*-phenylglycines and furanone [Experiments 40-54]

General procedure 7 (GP7): A mixture of 2 equivalents of acid, 1 equivalent of furanone and 1 mol% photocatalyst in a solvent was irradiated (16 × 8 W fluorescent tubes, cool white light) in a Schlenk flask under a continuous stream of N$_2$. The progress of the reaction was monitored by TLC. The crude product mixture was evaporated to dryness and purified by column chromatography. Each fraction was analyzed by NMR spectroscopy.

8.3.4.1.1 Synthesis of 4-[(phenylamino)methyl]dihydrofuran-2(3H)-one and 3a,4,5,9b-tetrahydrofuro[3,4-c]quinolin-3(1H)-one (32a, 33a) [Experiment 40]
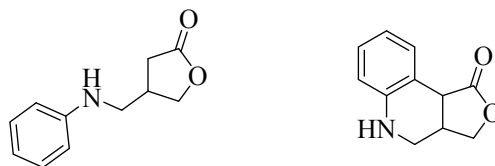
General procedure 7 was followed using 0.302 g *N*-phenylglycine, 0.071 mL furanone, 0.007 g Ru(bpy)$_3$Cl$_2$ and 60 mL of acetonitrile and 24 hours of irradiation. The reaction mixture was concentrated to dryness to leave a reddish brown liquid, which was purified by column chromatography on silica gel using 20% EtOAc in cyclohexane as eluent to give 0.29 g (78%) of **32a** & **33a** as a colourless powder.

4-[(Phenylamino)methyl]dihydrofuran-2(3H)-one (32a):

TLC: (SiO$_2$, ethyl acetate/cyclohexane 2:8)

R$_f$ = 0.28.

^{1}H-NMR: (300 MHz, CDCl$_3$)

δ (ppm): 2.37 (dd, 1 H, CH$_2$CO), 2.68 (dd, 1 H, CH$_2$CO), 2.85 (m, 1 H, CH*), 3.23 (d, 2 H, NCH$_2$), 4.16 (dd, 1 H, CH$_2$O), 4.43 (dd, 1 H, CH$_2$CO), 6.62 (d, 2 H, CH$_{arom}$), 6.76 (dd, 1 H, CH$_{arom}$), 7.20 (dd, 2 H, CH$_{arom}$), not observed (1 H, NH).

^{13}C-NMR: (75 MHz, CDCl$_3$)

δ (ppm): 34.3 (t, 1 C, CH$_2$), 40.1 (d, 1 C, CH), 41.5 (t, 1 C, CH$_2$), 70.0 (t, 1 C, CH$_2$), 115.4 (d, 1 C, CH$_{arom}$), 120.0 (d, 1 C, CH$_{arom}$), 128.2 (d, 2 C, CH$_{arom}$), 131.3 (d, 1 C, CH$_{arom}$), 145.2 (s, 1 C, Cq$_{arom}$), 178.1 (s, 1 C, C=O).

HRMS: (ESI/MeOH)

m/z: calcd for C$_{11}$H$_{13}$NO$_2$Na [M+Na]$^+$: 214.0838, found: 214.0844 ±3 ppm.

3a,4,5,9b-Tetrahydrofuro[3,4-c]quinolin-3(1H)-one (33a):

TLC: (SiO$_2$, ethyl acetate/cyclohexane 2:8)

R$_f$ = 0.28.

^{1}H-NMR: (300 MHz, CDCl$_3$)

δ (ppm): 3.36 (d, 1 H, CH$_2$), 3.69 (d, 1 H, CH$_2$), 2.99 (m, 2 H, NCH$_2$), 4.22 (dd, 1 H, CH$_2$O), 4.45 (dd, 1 H, CH$_2$CO), 6.56 (dd, 2 H, CH$_{arom}$), 7.45 (dd, 2 H, CH$_{arom}$), not observed (1 H, NH).

^{13}C-NMR: (75 MHz, CDCl$_3$)

δ (ppm): 32.1 (t, 1 C, CH$_2$), 35.5 (d, 1 C, CH), 48.0 (t, 1 C, CH$_2$), 71.7 (d, 1 C, CH), 113.4 (d, 2 C, CH$_{arom}$), 119.7 (d, 1 C, Cq$_{arom}$), 129.0 (d, 2 C, CH$_{arom}$), 148.1 (s, 1 C, Cq$_{arom}$), 178.1 (s, 1 C, C=O).

HRMS: (ESI/MeOH)

m/z: calcd for $C_{11}H_{13}NO_2Na$ [M+Na]$^+$: 212.0682, found: 212.0683 ±1 ppm.

8.3.4.1.2 Attempted synthesis of 4-[(phenylamino)methyl]dihydrofuran-2(3H)-one and 3a,4,5,9b-tetrahydrofuro[3,4-c]quinolin-3(1H)-one and isolation of dihydro-4-(1-hydroxyethyl)-2(3H)-furanone (34) [Experiment 41]
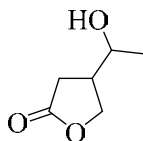
General procedure 7 was followed using 0.302 g *N*-phenylglycine, 0.071 mL furanone, 0.007 g Ru(bpy)₃Cl₂ and 60 mL of ethanol and 24 hours of irradiation. The reaction mixture was concentrated to dryness and a ¹H-NMR of the crude mixture was obtained.

¹H-NMR: (300 MHz, CDCl₃)

The complex spectrum included dihydro-4-(1-hydroxyethyl)-2(3H)-furanone (**34**) [262].

8.3.4.1.3 Attempted synthesis of 4-[(phenylamino)methyl]dihydrofuran-2(3H)-one and 3a,4,5,9b-tetrahydrofuro[3,4-c]quinolin-3(1H)-one and isolation of dihydro-4-(1-hydroxy-1-methylethyl)-2(3H)-furanone (35) [Experiment 42]
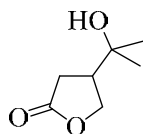
General procedure 7 was followed using 0.302 g *N*-phenylglycine, 0.071 mL furanone, 0.007 g Ru(bpy)₃Cl₂ and 60 mL of isopropanol and 24 hours of irradiation. The reaction mixture was concentrated to dryness and a ¹H-NMR of the crude mixture was obtained.

¹H-NMR: (300 MHz, CDCl₃)

Complex spectrum including dihydro-4-(1-hydroxy-1-methylethyl)-2(3H)-furanone (**35**) [159].

δ (ppm): 1.15 (s, 6 H, 2 × CH₃), 2.51 (m, 3 H, CH and CH₂), 2.62 (s, 1 H, OH), 4.27 (m, 2 H, CH₂O).

8.3.4.1.4 Attempted synthesis of 4-[(phenylamino)methyl]dihydrofuran-2(3H)-one and 3a,4,5,9b-tetrahydrofuro[3,4-c]quinolin-3(1H)-one [Experiment 43]

General procedure 7 was followed using 0.302 g *N*-phenylglycine, 0.071 mL furanone, 0.007 g Ru(bpy)₃Cl₂ and 60 mL of DMF and 24 hours of irradiation. The reaction mixture was concentrated to dryness and a ¹H-NMR of the crude mixture was obtained.

¹H-NMR: (300 MHz, CDCl₃)

No conversion to detectable photoproducts was observed.

8.3.4.1.5 Synthesis of 4-[(phenylamino)methyl]dihydrofuran-2(3H)-one and 3a,4,5,9b-tetrahydrofuro[3,4-c]quinolin-3(1H)-one [Experiment 44]

General procedure 7 was followed using 0.302 g *N*-phenylglycine, 0.071 mL furanone, 0.0037 g Ru(bpy)$_3$Cl$_2$ and 60 mL of acetonitrile and 18 hours of irradiation. The reaction mixture was concentrated to dryness to leave a reddish brown liquid, which was purified by column chromatography on silica gel using 20% EtOAc in cyclohexane as eluent to give 0.133 g (35%) of **32a** & **33a** as a colourless powder.

4-[(Phenylamino)methyl]dihydrofuran-2(3H)-one (32a):

TLC: (SiO$_2$, ethyl acetate/cyclohexane 2:8)

R$_f$ = 0.28.

^{1}H-NMR: (300 MHz, CDCl$_3$)

Identical to Experiment 40.

3a,4,5,9b-Tetrahydrofuro[3,4-c]quinolin-3(1H)-one (33a):

TLC: (SiO$_2$, ethyl acetate/cyclohexane 2:8)

R$_f$ = 0.28.

^{1}H-NMR: (300 MHz, CDCl$_3$)

Identical to Experiment 40.

8.3.4.1.6 Synthesis of 4-[(phenylamino)methyl]dihydrofuran-2(3H)-one and 3a,4,5,9b-tetrahydrofuro[3,4-c]quinolin-3(1H)-one [Experiment 45]

General procedure 7 was followed using 0.302 g *N*-phenylglycine, 0.071 mL furanone, 0.007 g Ru(bpy)$_3$Cl$_2$ and 60 mL of acetonitrile and 18 hours of irradiation. The reaction mixture was concentrated to dryness to leave a reddish brown liquid, which was purified by column chromatography on silica gel using 20% EtOAc in cyclohexane as eluent to give 0.3 g (78%) of **32a** & **33a** as a colourless powder.

4-[(Phenylamino)methyl]dihydrofuran-2(3H)-one (32a):

TLC: (SiO$_2$, ethyl acetate/cyclohexane 2:8)

R$_f$ = 0.28.

^{1}H-NMR: (300 MHz, CDCl$_3$)

Identical to Experiment 40.

3a,4,5,9b-Tetrahydrofuro[3,4-c]quinolin-3(1H)-one (33a):

TLC: (SiO$_2$, ethyl acetate/cyclohexane 2:8)

R$_f$ = 0.28.

^{1}H-NMR: (300 MHz, CDCl$_3$)

Identical to Experiment 40.

8.3.4.1.7 Synthesis of 4-[(phenylamino)methyl]dihydrofuran-2(3H)-one and 3a,4,5,9b-tetrahydrofuro[3,4-c]quinolin-3(1H)-one [Experiment 46]

General procedure 7 was followed using 0.302 g *N*-phenylglycine, 0.071 mL furanone, 0.014 g Ru(bpy)$_3$Cl$_2$ and 60 mL of acetonitrile and 18 hours of irradiation. The reaction mixture was concentrated to dryness to leave a reddish brown liquid, which was purified by column chromatography on silica gel using 20% EtOAc in cyclohexane as eluent to give 0.29 g (78%) of **32a** & **33a** as an amorphous colourless solid.

4-[(Phenylamino)methyl]dihydrofuran-2(3H)-one (32a):

TLC: (SiO$_2$, ethyl acetate/cyclohexane 2:8)

R$_f$ = 0.28.

^{1}H-NMR: (300 MHz, CDCl$_3$)

Identical to Experiment 40.

3a,4,5,9b-Tetrahydrofuro[3,4-c]quinolin-3(1H)-one (33a):

TLC: (SiO$_2$, ethyl acetate/cyclohexane 2:8)

R$_f$ = 0.28.

^{1}H-NMR: (300 MHz, CDCl$_3$)

Identical to Experiment 40.

8.3.4.1.8 Attempted synthesis of 4-[(phenylamino)methyl]dihydrofuran-2(3H)-one and 3a,4,5,9b-tetrahydrofuro[3,4-c]quinolin-3(1H)-one [Experiment 47]

General procedure 7 was followed using 0.302 g *N*-phenylglycine, 0.071 mL furanone, 0.002 g 4,4'-dimethoxybenzophenone (DMBP) and 60 mL of acetonitrile and 18 hours of irradiation. The reaction mixture was concentrated to dryness and a ^{1}H-NMR of the crude mixture was obtained.

^{1}H-NMR: (300 MHz, CDCl$_3$)

No conversion to detectable photoproducts was observed.

8.3.4.1.9 Attempted synthesis of 4-[(phenylamino)methyl]dihydrofuran-2(3H)-one and 3a,4,5,9b-tetrahydrofuro[3,4-c]quinolin-3(1H)-one [Experiment 48]

General procedure 7 was followed using 0.302 g *N*-phenylglycine, 0.071 mL furanone, 0.003 g methyl orange and 60 mL of acetonitrile and 18 hours of irradiation. The reaction mixture was concentrated to dryness and a ^{1}H-NMR of the crude mixture was obtained.

^{1}H-NMR: (300 MHz, CDCl$_3$)

No conversion to detectable photoproducts was observed.

8.3.4.1.10 Synthesis of 4-[(phenylamino)methyl]dihydrofuran-2(3H)-one and 3a,4,5,9b-tetrahydrofuro[3,4-c]quinolin-3(1H)-one [Experiment 49]

General procedure 7 was followed using 0.302 g *N*-phenylglycine, 0.071 mL furanone, 0.007 g Ru(bpy)$_3$Cl$_2$ and 60 mL of acetonitrile and 18 hours of irradiation. The reaction mixture was concentrated to dryness to leave a reddish brown liquid, which was purified by column chromatography on silica gel using 20% EtOAc in cyclohexane as eluent to give 0.28 g (72%) of **32a** & **33a** as an amorphous colourless substance.

4-[(Phenylamino)methyl]dihydrofuran-2(3H)-one (32a):

TLC: (SiO$_2$, ethyl acetate/cyclohexane 2:8)

$R_f = 0.28$.

^{1}H-NMR: (300 MHz, CDCl$_3$)

Identical to Experiment 40.

3a,4,5,9b-Tetrahydrofuro[3,4-c]quinolin-3(1H)-one (33a):

TLC: (SiO$_2$, ethyl acetate/cyclohexane 2:8)

$R_f = 0.28$.

^{1}H-NMR: (300 MHz, CDCl$_3$)

Identical to Experiment 40.

8.3.4.1.11 Attempted synthesis of *N*-[(5-oxotetrahydrofuran-3-yl)methyl]acetamide [Experiment 50]

General procedure 7 was followed using 0.234 g *N*-acetylglycine, 0.071 mL furanone, 0.007 g Ru(bpy)$_3$Cl$_2$ and 60 mL of acetonitrile and 18 hours of irradiation. The reaction mixture was concentrated to dryness and a ^{1}H-NMR of the crude mixture was obtained.

^{1}H-NMR: (300 MHz, CDCl$_3$)

No conversion to detectable photoproducts was observed.

8.3.4.1.12 Attempted synthesis of 4-[(dimethylamino)methyl]dihydrofuran-2(3H)-one [Experiment 51]

General procedure 7 was followed using 0.206 g *N*, *N*-dimethylglycine, 0.071 mL furanone, 0.007 g Ru(bpy)$_3$Cl$_2$ and 60 mL of acetonitrile and 18 hours of irradiation. The reaction mixture was concentrated to dryness and a ^{1}H-NMR of the crude mixture was obtained.

^{1}H-NMR: (300 MHz, CDCl$_3$)

No conversion to detectable photoproducts was observed.

8.3.4.1.13 Attempted synthesis of 4-[(dimethylamino)(phenyl)methyl]dihydrofuran-2(3H)-one [Experiment 52]

General procedure 7 was followed using 0.358 g *N*, *N*-dimethylphenylglycine, 0.071 mL furanone, 0.007 g Ru(bpy)$_3$Cl$_2$ and 60 mL of acetonitrile and 18 hours of irradiation. The reaction mixture was concentrated to dryness and a ^{1}H-NMR of the crude mixture was obtained.

^{1}H-NMR: (300 MHz, CDCl$_3$)

No conversion to detectable photoproducts was observed.

8.3.4.1.14 Attempted synthesis of dihydro-4-((4-phenylsulfanyl)methyl)furan-2(3H)-one [Experiment 53]

General procedure 7 was followed using 0.336 g phenylthioacetic acid, 0.071 mL furanone, 0.007 g Ru(bpy)$_3$Cl$_2$ and 60 mL of acetonitrile and 18 hours of irradiation. The reaction mixture was concentrated to dryness and a ^{1}H-NMR of the crude mixture was obtained.

^{1}H-NMR: (300 MHz, CDCl$_3$)

No conversion to detectable photoproducts was observed.

8.3.4.1.15 Attempted synthesis of 4-{[(4-aminophenyl)sulfanyl]methyl}dihydrofuran-2(3H)-one [Experiment 54]

General procedure 7 was followed using 0.366 g *p*-amino(phenylthio)acetic acid, 0.071 mL furanone, 0.007 g Ru(bpy)$_3$Cl$_2$ and 60 mL of acetonitrile and 18 hours of irradiation. The reaction mixture was concentrated to dryness and a ^{1}H-NMR of the crude mixture was obtained.

^{1}H-NMR: (300 MHz, CDCl$_3$)

No conversion to detectable photoproducts was observed.

8.3.4.2 Photoredox reactions of *N*-phenylglycines and enones under batch conditions [Experiments 55-59]

General procedure 8 (GP8): A mixture of 2 equivalents of phenylglycine derivative, 1 equivalent of the respective enone and 1 mol% of Ru(bpy)$_3$Cl$_2$ in acetonitrile was irradiated (16 × 8 W fluorescent tubes, cool white light) in a Schlenk flask under a continuous stream of N$_2$. The progress of the reaction was monitored by TLC. The crude product mixture was evaporated to dryness and purified by column chromatography. Each fraction was analyzed by NMR spectroscopy.

8.3.4.2.1 Synthesis of 4-[(phenylamino)methyl]dihydrofuran-2(3H)-one and 3a,4,5,9b-tetrahydrofuro[3,4-c]quinolin-3(1H)-one (32a, 33a) [Experiment 55]

General procedure 8 was followed using 0.302 g *N*-phenylglycine, 0.071 mL furanone, 0.007 g Ru(bpy)$_3$Cl$_2$ and 60 mL of acetonitrile and 18 hours of irradiation. The reaction mixture was concentrated to dryness to leave a reddish brown liquid, which was purified by column chromatography on silica gel using 20% EtOAc in cyclohexane as eluent to give 0.08 g (21%) of **32a** and 0.19g (51%) of **33a**.

4-[(Phenylamino)methyl]dihydrofuran-2(3H)-one (32a):

TLC: (SiO$_2$, ethyl acetate/cyclohexane 2:8)

R$_f$ = 0.28.

^{1}H-NMR: (300 MHz, CDCl$_3$)

Identical to Experiment 40.

3a,4,5,9b-Tetrahydrofuro[3,4-c]quinolin-3(1H)-one (33a):

TLC: (SiO$_2$, ethyl acetate/cyclohexane 2:8)

R$_f$ = 0.28.

^{1}H-NMR: (300 MHz, CDCl$_3$)

Identical to Experiment 40.

8.3.4.2.2 Synthesis of 3-[(phenylamino)methyl]cyclopentanone and 1,3,3a,4,5,9b-hexa-hydro-2H-cyclopenta[c]quinolin-2-one (32b, 33b) [Experiment 56]
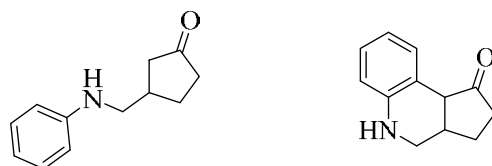
General procedure 8 was followed using 0.302 g *N*-phenylglycine, 0.082 mL pentenone, 0.007 g Ru(bpy)$_3$Cl$_2$ and 60 mL of acetonitrile and 18 hours of irradiation. The reaction mixture was

concentrated to dryness to leave a reddish brown liquid, which was subjected to column chromatography on silica gel using 25% EtOAc in cyclohexane as eluent. A light yellow mixture of **32b** & **33b** was obtained in a combined yield of 0.4 g (70%).

3-[(Phenylamino)methyl]cyclopentanone (32b):

TLC: (SiO$_2$, ethyl acetate/cyclohexane 3:1)

R$_f$ = 0.32.

^{1}H-NMR: (300 MHz, CDCl$_3$)

δ (ppm): 1.64-1.76 (m, 1 H, CH$_2$), 1.99 (dd, J = 9 Hz, 2 H, CH$_2$), 2.14-2.61 (m, 5 H, CH, CH$_2$, NCH$_2$), 3.21 (d, J = 6 Hz, 1 H, NCH$_2$), 6.62 (d, J = 6 Hz, 2 H, CH$_{arom}$), 6.72 (dd, 1 H, CH$_{arom}$), 7.16-7.22 (m, 2 H, CH$_{arom}$), not observed (1 H, NH).

^{13}C-NMR: (75 MHz, CDCl$_3$)

δ (ppm): 27.5 (t, 1 C, CH$_2$), 36.0 (d, 1 C, CH), 38.7 (t, 1 C, CH$_2$), 45.2 (t, 1 C, CH$_2$), 50.0 (t, 1 C, CH$_2$), 115.1 (d, 1 C, CH$_{arom}$), 120.4 (d, 1 C, CH$_{arom}$), 130.0 (d, 2 C, CH$_{arom}$), 143.3 (s, 1 C, Cq$_{arom}$,), 217.8 (s, 1 C, C=O).

HRMS: (ESI/MeOH)

m/z: calcd for C$_{12}$H$_{16}$NO$_2$H [M+H]$^+$: 190.1226, found: 190.1229 ± 1 ppm.

calcd for C$_{12}$H$_{15}$NO$_2$Na [M+Na]$^+$: 212.1046, found: 212.1048 ± 1 ppm.

1,3,3a,4,5,9b-Hexahydro-2H-cyclopenta[c]quinolin-2-one (33b):

^{1}H-NMR: (characteristic peaks only, 300 MHz, CDCl$_3$)

δ (ppm): 2.87 (m, 1 H, CH$_2$), 3.45 (m, 1 H, CH$_2$), 3.65 (m, 3 H, CH$_2$).

HRMS: (ESI/MeOH)

m/z: calcd for C$_{11}$H$_{11}$NO$_2$Na [M+Na]$^+$: 210.2274, found: 210.2273 ± 1 ppm.

8.3.4.2.3 Synthesis of 4-[(phenylamino)methyl]cyclohexanone and 6,6a,7,8,10,10a-hexa-hydrophenanthridin-9(5H)-one (32c, 33c) [Experiment 57]
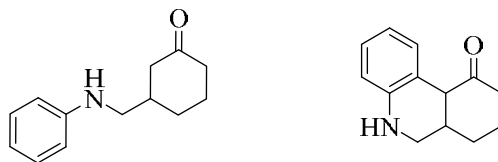
General procedure 8 was followed using 0.302 g *N*-phenylglycine, 0.096 mL hexenone, 0.007 g Ru(bpy)$_3$Cl$_2$ and 60 mL of acetonitrile and 18 hours of irradiation. The reaction mixture was concentrated to dryness to leave a reddish brown liquid, which was subjected to column chromatography on silica gel using 25% EtOAc in cyclohexane as eluent. A light yellow mixture of **32c** & **33c** was obtained in a combined yield of 0.46 g (75%).

4-[(Phenylamino)methyl]cyclohexanone (32c):

TLC: (SiO$_2$, ethyl acetate/cyclohexane 3:1)

R$_f$ = 0.29.

^{1}H-NMR: (300 MHz, CDCl$_3$)

δ (ppm): 1.24 (m, 1 H, CH$_2$), 1.89 (m, 1 H, CH), 2.00 (m, 2 H, CH$_2$), 2.50 (m, 2 H, CH$_2$), 3.12 (m, 1 H, CH$_2$), 3.22 (m, 1 H, CH$_2$), 3.54 (m, 2 H, CH$_2$, NCH$_2$), 3.80 (m, 1 H, NCH$_2$), 6.67 (m, 2 H, CH$_{arom}$), 6.80 (m, 1 H, CH$_{arom}$), 7.19 (m, 2 H, CH$_{arom}$).

^{13}C-NMR: (75 MHz, CDCl$_3$)

δ (ppm): 26.1 (t, 1 C, CH$_2$), 28.9 (d, 1 C, CH), 40.3 (t, 1 C, CH$_2$), 41.5 (t, 1 C, CH$_2$), 51.3 (t, 2 C, CH$_2$),115.7 (d, 1 C, CH$_{arom}$), 124.2 (d, 1 C, CH$_{arom}$), 130.0 (d, 2 C, CH$_{arom}$), 149.8 (s, 1 C, Cq$_{arom}$), 210.0 (s, 1 C, C=O).

HRMS: (ESI/MeOH)

m/z: calcd for C$_{13}$H$_{17}$NONa [M+Na]$^+$: 226.1202, found: 226.1209 ± 3 ppm.

6,6a,7,8,10,10a-Hexahydrophenanthridin-9(5H)-one (33c):

TLC: (SiO$_2$, ethyl acetate/cyclohexane 3:1)

R$_f$ = 0.29.

^{1}H-NMR: (characteristic peaks only, 300 MHz, CDCl$_3$)

δ (ppm): 1.66 (m, 1 H, CH$_2$), 2.21 (m, 2 H, CH$_2$), 2.90 (m, 2 H, CH$_2$), 3.75 (m, 2 H, CH$_2$).

HRMS: (ESI/MeOH)

m/z: calcd for C$_{13}$H$_{15}$NO$_2$Na [M+Na]$^+$: 224.1046, found: 224.1051 ± 2 ppm.

8.3.4.2.4 Synthesis of 3-ethoxy-3a,4,5,9b-tetrahydrofuro[3,4-c]quinolin-1(3H)-one (33d) [Experiment 58]
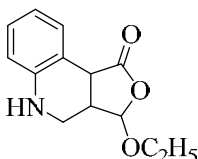
General procedure 8 was followed using 0.302 g *N*-phenylglycine, 0.182 mL 5-ethoxy-furanone, 0.007 g Ru(bpy)$_3$Cl$_2$ and 60 mL of acetonitrile and 18 hours of irradiation. The reaction mixture was concentrated to dryness to leave a reddish brown liquid, which was purified by column chromatography on silica gel using 20% EtOAc in cyclohexane as eluent to give 0.45 g (65%) of **33d** as a light yellow crystaline substance.

TLC: (SiO$_2$, ethyl acetate/cyclohexane 2:8)

R$_f$ = 0.28.

^{1}H-NMR: (300 MHz, CDCl$_3$)

δ (ppm): 1.27 (t, J = 9 Hz, 3 H, CH$_3$), 2.86-3.00 (m, 2 H, CH, NCH), 3.40 (m, 1 H, CH$_2$), 3.64 (m, 1 H, CH$_2$), 3.88 (m, 2 H, NCH, CH), 5.34 (d, J = 3 Hz, 1 H, CH), 6.59 (d, J = 9 Hz, 1 H, CH$_{arom}$), 6.81 (dd, J = 3, 9 Hz, 1 H, CH$_{arom}$), 7.07 (m, 1 H, CH$_{arom}$), 7.45 (d, J = 9 Hz, 1 H, CH$_{arom}$).

^{13}C-NMR: (75 MHz, CDCl$_3$)

δ (ppm): 20.7 (q, 1 C, CH$_3$), 37.2 (d, 2 C, CH), 48.9 (t, 1 C, CH$_2$), 63.6 (t, 1 C, CH$_2$), 100.9 (d, 1 C, CH), 122.2 (d, 1 C, CH$_{arom}$), 127.9 (d, 1 C, CH$_{arom}$), 129.5 (s, 1 C, Cq$_{arom}$), 130.3 (d, 2 C, CH$_{arom}$), 145.5 (s, 1 C, Cq$_{arom}$), 176.1 (s, 1 C, C=O).

HRMS: (ESI/MeOH)

m/z: calcd for C$_{13}$H$_{15}$NO$_3$Na [M+Na]$^+$: 256. 0944, found: 256. 0950 ± 2 ppm.

8.3.4.2.5 Synthesis of 4-{[methyl(phenyl)amino]methyl}dihydrofuran-2(3H)-one and 5-methyl-3a,4,5,9b-tetrahydrofuro[3,2-c]quinolin-2(3H)-one (32e, 33e) [Experiment 59]
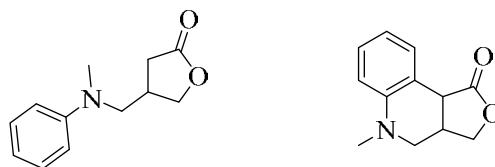
General procedure 8 was followed using 0.330 g *N*-methyl-*N*-phenylglycine, 0.071 mL furanone, 0.007 g Ru(bpy)$_3$Cl$_2$ and 60 mL of acetonitrile and 18 hours of irradiation. The reaction mixture was concentrated to dryness to leave a reddish brown liquid, which was purified by column chromatography on silica gel using 20% EtOAc in cyclohexane as eluent to give 0.26 g (55%) of **32e** and 0.089 g (21%) of **33e** as colourless powders.

4-{[Methyl(phenyl)amino]methyl}dihydrofuran-2(3H)-one (32e):

TLC: (SiO$_2$, ethyl acetate/cyclohexane 1:9)

R$_f$ = 0.34.

^{1}H-NMR: (300 MHz, CDCl$_3$)

δ (ppm): 2.61 (s, 3 H, NCH$_3$), 2.84 (m, 1 H, CH$_2$), 2.99 (m, 1 H, CH$_2$), 3.13 (m, 2 H, NCH$_2$), 3.55 (m, 1 H, CH), 4.00 (m, 1 H, CH$_2$), 4.12 (dd, J = 6, 9 Hz, 1 H, CH$_2$), 6.67 (d, J = 9 Hz, 2 H, CH$_{arom}$), 6.75 (m, 2 H, CH$_{arom}$), 7.16 (m, 1 H, CH$_{arom}$).

^{13}C-NMR: (75 MHz, CDCl$_3$)

δ (ppm): 34.3 (t, 1 C, CH$_2$), 40.1 (d, 1 C, CH), 40.3 (q, 1 C, CH$_3$), 41.5 (t, 1 C, CH$_2$), 70.0 (t, 1 C, CH$_2$), 115.4 (d, 1 C, CH$_{arom}$), 120.0 (d, 1 C, CH$_{arom}$), 128.2 (d, 2 C, CH$_{arom}$), 131.3 (d, 1 C, CH$_{arom}$), 145.2 (s, 1 C, Cq$_{arom}$), 178.0 (s, 1 C, C=O).

5-Methyl-3a,4,5,9b-tetrahydrofuro[3,2-c]quinolin-2(3H)-one (33e):

TLC: (SiO$_2$, ethyl acetate/cyclohexane 1:9)

R$_f$ = 0.34.

^{1}H-NMR: (300 MHz, CDCl$_3$)

δ (ppm): 2.30 (s, 3 H, NCH$_3$), 2.83 (m, 1 H, CH$_2$), 3.00 (m, 1 H, CH$_2$), 3.37 (m, 1 H, CH), 3.74 (m, 1 H, CH), 4.11 (dd, J = 6, 12 Hz, 1 H, NCH$_2$), 4.34 (dd, J = 6, 12 Hz, 1 H, NCH$_2$), 6.65 (d, J = 6 Hz, 2 H, CH$_{arom}$), 6.72 (dd, J = 3, 6 Hz, 1 H, CH$_{arom}$), 7.16 (m, 1 H, CH$_{arom}$).

^{13}C-NMR: (75 MHz, CDCl$_3$)

δ (ppm): 32.1 (t, 1 C, CH$_2$), 35.5 (d, 1 C, CH), 40.3 (q, 1 C, CH$_3$), 48.0 (t, 1 C, CH$_2$), 70.7 (t, 1 C, CH$_2$), 112.1 (d, 2 C, CH$_{arom}$), 119.5 (d, 1 C, Cq$_{arom}$), 129.4 (d, 2 C, CH$_{arom}$), 148.7 (s, 1 C, Cq$_{arom}$), 176.1 (s, 1 C, C=O).

8.3.4.3 Photoredox reactions of *N*-phenylglycines and enones under flow conditions [Experiments 60-62]

General procedure 9 (GP9): 20 mL of a degassed 1:2 mixture of furanone and *N*-phenylglycine in acetonitrile was pumped through the in-house flow photoreactor equipped with a single 8 W fluorescent tube (cool white light). The reaction mixture was collected in an amber flask, was concentrated to dryness and was purified by column chromatography.

8.3.4.3.1 Synthesis of 4-[(phenylamino)methyl]dihydrofuran-2(3H)-one and 3a,4,5,9b-tetrahydrofuro[3,4-c]quinolin-3(1H)-one (32a, 33a) [Experiment 60]

General procedure 9 was followed using 0.1 g *N*-phenylglycine, 0.024 mL furanone, 0.0023 g Ru(bpy)$_3$Cl$_2$ and 10 mL of acetonitrile and a residence time of 3 hours. The reaction mixture was concentrated to dryness to leave a reddish brown liquid, which was purified by column chromatography on silica gel using 20% EtOAc in cyclohexane as eluent to give 0.09 g (74%) of **32a** & **33a** as a colourless amorphous solid.

4-[(Phenylamino)methyl]dihydrofuran-2(3H)-one (32a):

TLC: (SiO$_2$, ethyl acetate/cyclohexane 2:8)

R$_f$ = 0.28.

^{1}H-NMR: (300 MHz, CDCl$_3$)

Identical to Experiment 40.

3a,4,5,9b-Tetrahydrofuro[3,4-c]quinolin-3(1H)-one (33a):

TLC: (SiO$_2$, ethyl acetate/cyclohexane 2:8)

R$_f$ = 0.28.

¹H-NMR: (300 MHz, CDCl₃)

Identical to Experiment 40.

8.3.4.3.2 Synthesis of 3-[(phenylamino)methyl]cyclopentanone and 1,3,3a,4,5,9b-hexa-hydro-2H-cyclopenta[c]quinolin-2-one (32b, 33b) [Experiment 61]

General procedure 9 was followed using 0.1 g *N*-phenylglycine, 0.027 mL cyclopentenone, 0.0023 g Ru(bpy)₃Cl₂ and 10 mL of acetonitrile and a residence time of 3 hours. The reaction mixture was concentrated to dryness to leave a reddish brown liquid, which was subjected to column chromatography on silica gel using 25% EtOAc in cyclohexane as eluent. A yellowish colourless mixture of **32b** & **33b** was obtained in a combined yield of 0.13 g (67%).

3-[(Phenylamino)methyl]cyclopentanone (32b):

TLC: (SiO₂, ethyl acetate/cyclohexane 3:1)

R_f = 0.32.

¹H-NMR: (300 MHz, CDCl₃)

Identical to Experiment 56.

1,3,3a,4,5,9b-Hexahydro-2H-cyclopenta[c]quinolin-2-one (33b):

TLC: (SiO₂, ethyl acetate/cyclohexane 3:1)

R_f = 0.32.

¹H-NMR: (300 MHz, CDCl₃)

Identical to Experiment 56.

8.3.4.3.3 Synthesis of 4-[(phenylamino)methyl]cyclohexanone and 6,6a,7,8,10,10a-hexa-hydrophenanthridin-9(5H)-one (32c, 33c) [Experiment 62]
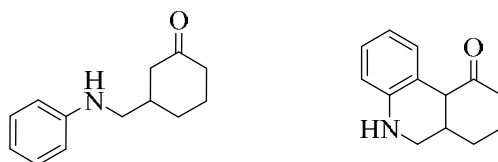
General procedure 9 was followed using 0.1 g *N*-phenylglycine, 0.032 mL cyclohexenone, 0.0023 g Ru(bpy)₃Cl₂ and 10 mL of acetonitrile and a residence time of 3 hours. The reaction mixture was concentrated to dryness to leave a reddish brown liquid, which was subjected to column chromatography on silica gel using 25% EtOAc in cyclohexane as eluent. A yellowish colourless mixture of **32c** & **33c** was obtained in a combined yield of 0.14 g (69%).

4-[(Phenylamino)methyl]cyclohexanone (32c):

TLC: (SiO₂, ethyl acetate/cyclohexane 3:1)

R_f = 0.29.

^{1}H-NMR: (300 MHz, CDCl3)

Identical to Experiment 57.

6,6a,7,8,10,10a-Hexahydrophenanthridin-9(5H)-one (33c):

TLC: (SiO2, ethyl acetate/cyclohexane 3:1)

$R_f = 0.29$.

^{1}H-NMR: (characteristic peaks only, 300 MHz, CDCl3)

Identical to Experiment 57.

8.3.5 Synthesis of AL12, AL5 and their analogues under batch conditions [Experiments 63-118]

8.3.5.1 Photodecarboxylative addition of phenylacetates to *N*-alkylphthalimides under batch conditions [Experiments 63-78]

General procedure 10 (GP10): A mixture of 3 equivalents of phenylacetic acid derivative, 1.5 equivalent K_2CO_3 in 5 mL of acetone and 15 mL of buffer (pH=7) was added to 1 equivalent of *N*-(bromoalkyl)phthalimide in 10 mL of acetone in a Pyrex Schlenk flask, followed by 60 mL of a 1:1 mixture of acetone:buffer (pH = 7). The mixture was irradiated in a Rayonet chamber reactor equipped with UVB light while a continuous slow stream of N_2 is passed through the reaction mixture. The progress of the reaction was monitored by TLC or by passing the leaving gas stream through a saturated $Ba(OH)_2$ solution. When all phthalimide was consumed or when precipitation of $BaCO_2$ had stopped, most of the acetone was removed *via* rotary evaporation at low temperatures (water bath <35°C). The reaction mixture was subsequently extracted with CH_2Cl_2 (3 × 40 mL) and washed with saturated $NaHCO_3$ (2 × 40 mL) and brine (1 × 40 mL). After drying over $MgSO_4$, the reaction mixture was evaporated to dryness on a rotary evaporator at low temperatures (<35°C). When necessary, the crude product was purified by column chromatography.

8.3.5.1.1 Synthesis of 3-benzyl-2-(2-bromoethyl)-3-hydroxy-2,3-dihydro-1H-isoindol-1-one (37a) [Experiment 63]
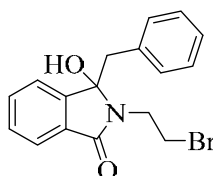
General procedure 10 was followed using 2.04 g of phenylacetic acid, 1.04 g of K_2CO_3, 1.27 g of *N*-bromoethyl phthalimide and 60 mL of acetone/pH 7 buffer (1:1) and 3 hours of

irradiation. A colourless product started to precipitate in the Schlenk flask during irradiation. Workup furnished 1.57 g (87%) of product as a colourless crystalline solid.

Melting point: 148°C.

IR: (film)

$\tilde{\nu}$ (cm^{-1}) = 3310 br, 3123, 1700, 1611, 1320 and 632.

^{1}H-NMR: (300 MHz, CDCl$_3$)

δ (ppm): 3.14 (d, J = 15 Hz, 1 H, CH$_2$Ph), 3.52 (d, J = 15 Hz, 1 H, CH$_2$Ph), 3.61-3.82 (m, 3 H, CH$_2$Br, NCH$_2$), 4.11-4.17 (m, 1 H, NCH$_2$), 6.89 (d, J = 9 Hz, 2 H, CH$_{arom}$), 7.11-7.17 (m, 3 H, CH$_{arom}$), 7.20-7.23 (d, J = 9 Hz, 1 H, CH$_{arom}$), 7.43-7.58 (m, 2 H, CH$_{arom}$), 7.62 (d, J = 9 Hz, 1 H, CH$_{arom}$).

^{13}C-NMR: (75 MHz, CDCl$_3$)

δ (ppm): 29.5 (t, 1 C, CH$_2$Br), 41.4 (t, 1 C, CH$_2$Ph), 43.3 (t, 1 C, NCH$_2$), 91.0 (s, 1 C, COH), 122.9 (d, 1 C, CH$_{arom}$), 123.4 (d, 1 C, CH$_{arom}$), 127.3 (d, 1 C, CH$_{arom}$), 128.2 (d, 2 C, CH$_{arom}$), 129.9 (d, 1 C, CH$_{arom}$), 130.2 (d, 2 C, CH$_{arom}$), 130.9 (d, 1 C, Cq$_{arom}$), 132.3 (d, 1 C, CH$_{arom}$), 134.3 (s, 1 C, Cq$_{arom}$), 146.1(s, 1 C, Cq$_{arom}$), 167.0 (s, 1 C, C=O).

HRMS: (ESI/MeOH)

m/z: calcd for C$_{17}$H$_{16}$O$_2$NBr(M+H)$^+$: 346.0437(M+Na)$^+$ 368.0257, found: 368.0261 ± 1 ppm.

8.3.5.1.2 Synthesis of 2-(2-bromoethyl)-3-(4-fluorobenzyl)-3-hydroxy-2,3-dihydro-1H-isoindol-1-one (37b) [Experiment 64]
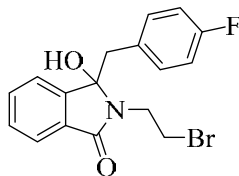
General procedure 10 was followed using 2.31 g of *p*-flurophenylacetic acid, 1.04 g of K$_2$CO$_3$, 1.27 g of *N*-bromoethyl phthalimide and 60 mL of acetone/pH 7 buffer (1:1) and 3 hours of irradiation. A yellowish product started to precipitate during irradiation. Workup gave 1.64 g (83%) of product as a crystalline solid.

Melting point: 157°C.

IR: (film)

$\tilde{\nu}$ (cm^{-1}) = 3352 br, 3110, 1692, 1632, 1167 and 670.

^{1}H-NMR: (300 MHz, CDCl$_3$)

δ (ppm): 3.11 (d, J = 12 Hz, 1 H, CH_2Ar), 3.43 (d, J = 12 Hz, 1 H, CH_2Ar), 3.59-3.74 (m, 3 H, CH_2Br, NCH_2), 4.02-4.12 (m, 1 H, NCH_2), 7.03-7.08 (m, 2 H, CH_{arom}), 7.14-7.25 (m, 4 H, CH_{arom}), 7.50-7.57 (m, 2 H, CH_{arom}).

^{13}C-NMR: (75 MHz, $CDCl_3$)

δ (ppm): 33.1 (t, 1 C, CH_2Br), 39.3 (t, 1 C, NCH_2), 44.2 (t, 1 C, CH_2Ar), 90.0 (s, 1 C, COH), 120.4 (d, 1 C, CH_{arom}), 122.1 (d, 1 C, CH_{arom}), 129.2 (d, 2 C, CH_{arom}), 131.2 (d, 1 C, CH_{arom}), 132.7 (d, 2 C, CH_{arom}), 133.3 (s, 1 C, Cq_{arom}), 132.3 (d, 1 C, CH_{arom}), 134.3 (s, 1 C, Cq_{arom}), 145.0 (s, 1 C, Cq_{arom}), 158.5(s, 1 C, Cq_{arom}), 166.6 (s, 1 C, C=O).

HRMS: (ESI/MeOH)

m/z: calcd for $C_{17}H_{15}O_2NBrF$ (M+H)$^+$: 364.0343, found: 364.0343 ± 0 ppm.

calcd for $C_{17}H_{15}O_2NBrF$ (M+Na)$^+$: 386.0162, found: 386.0165 ± 1 ppm.

8.3.5.1.3 Synthesis of 2-(2-bromoethyl)-3-(4-chlorobenzyl)-3-hydroxy-2,3-dihydro-1H-isoindol-1-one (37c) [Experiment 65]
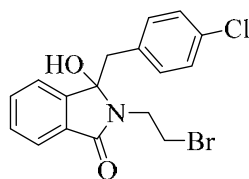
General procedure 10 was followed using 2.56 g of *p*-chlorophenylacetic acid, 1.04 g of K_2CO_3, 1.27 g of *N*-bromoethyl phthalimide and 60 mL of acetone/pH 7 buffer (1:1) and 3 hours of irradiation. After workup, 1.51 g (79%) of product were obtained as a light yellow crystalline solid.

Melting point: 149-153°C.

IR: (film)

$\widetilde{v}$ (cm^{-1}) = 3280 br, 3101, 1644, 1601, 1350 and 666.

^{1}H-NMR: (300 MHz, $CDCl_3$)

δ (ppm): 3.09 (d, J = 15 Hz, 1 H, CH_2Ar), 3.49 (d, J = 15 Hz, 1 H, CH_2Ar), 3.63-3.83 (m, 3 H, CH_2Br, NCH_2), 4.14-4.20 (m, 1 H, NCH_2), 6.83 (d, J = 9 Hz, 1 H, CH_{arom}), 7.10-7.29 (m, 4 H, CH_{arom}), 7.43-7.54 (m, 2 H, CH_{arom}), 7.67 (d, J = 9 Hz, 1 H, CH_{arom}).

^{13}C-NMR: (75 MHz, $CDCl_3$)

δ (ppm): 32.6 (t, 1 C, CH_2Br), 40.0 (t, 1 C, NCH_2), 42.8 (t, 1 C, CH_2Ar), 90.0 (s, 1 C, COH), 119.3 (d, 1 C, CH_{arom}), 121.9 (d, 1 C, CH_{arom}), 122.2 (d, 1 C, CH_{arom}), 122.6 (d, 1 C, CH_{arom}), 123.8 (d, 1 C, CH_{arom}), 128.2 (d, 1 C, CH_{arom}), 130.2 (d, 1 C, CH_{arom}), 132.3 (d, 1 C, CH_{arom}), 134.5 (s, 1 C, Cq_{arom}), 139.4 (s, 1 C, Cq_{arom}), 144.8(s, 1 C, Cq_{arom}), 155.7(s, 1 C, Cq_{arom}), 166.3 (s, 1 C, C=O).

HRMS: (ESI/MeOH)

m/z: calcd for $C_{17}H_{15}NO_2BrCl$ (M+Na)$^+$: 401.9867, found: 401.9868 ± 1 ppm.

8.3.5.1.4 Synthesis of 3-(4-bromobenzyl)-2-(2-bromoethyl)-3-hydroxy-2,3-dihydro-1H-isoindol-1-one (37d) [Experiment 66]
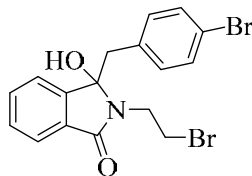
General procedure 10 was followed using 2.23 g of *p*-bromophenylacetic acid, 1.04 g of K_2CO_3, 1.27 g of *N*-bromoethyl phthalimide and 60 mL of acetone/pH 7 buffer (1:1) and 3 hours of irradiation. 1.34 g (63%) of product were obtaind after workup and column chromatography using 40% EtOAc in cyclohexane.

TLC: (SiO$_2$, ethyl acetate/cyclohexane 4:6)

R$_f$ = 0.25.

Melting point: 158-160°C.

IR: (film)

$\widetilde{\nu}$ (cm^{-1}) = 3537 br, 3127, 1665, 1471, 1364 and 654.

TLC: (SiO$_2$, ethyl acetate/cyclohexane 3:7)

R$_f$ = 0.38.

^{1}H-NMR: (300 MHz, CDCl$_3$)

δ (ppm): 3.05 (d, J = 15 Hz, 1 H, CH$_2$Ar), 3.47 (d, J = 15 Hz, 1 H, CH$_2$Ar), 3.61-3.77 (m, 3 H, CH$_2$Br, NCH$_2$), 4.09-4.17 (m, 1 H, NCH$_2$), 6.78 (d, J = 9 Hz, 2 H, CH$_{arom}$), 6.97-7.18 (m, 2 H, CH$_{arom}$), 7.29-7.54 (m, 3 H, CH$_{arom}$), 7.64 (d, J = 9 Hz, 1 H, CH$_{arom}$).

^{13}C-NMR: (75 MHz, acetone-d$_6$)

δ (ppm): 30.4 (t, 1 C, CH$_2$Br), 40.7 (t, 1 C, NCH$_2$), 44.1 (t, 1 C, CH$_2$Ar), 91.5 (s, 1 C, COH), 121.3 (d, 1 C, CH$_{arom}$), 122.6 (d, 1 C, CH$_{arom}$), 125.2 (d, 2 C, CH$_{arom}$), 129.0 (d, 1 C, CH$_{arom}$), 130.1 (d, 1 C, CH$_{arom}$), 132.5 (d, 2 C, CH$_{arom}$), 133.4 (d, 1 C, CH$_{arom}$), 135.3 (d, 1 C, Cq$_{arom}$), 140.1 (s, 1 C, Cq$_{arom}$), 143.4 (s, 1 C, Cq$_{arom}$), 145.7(s, 1 C, Cq$_{arom}$), 166.6 (s, 1 C, C=O).

HRMS: (ESI/MeOH)

m/z: calcd for $C_{17}H_{15}NO_2Br_2$ (M+Na)$^+$: 445.9361, found: 445.9358 ± 1 ppm.

8.3.5.1.5 Synthesis of 2-(2-bromoethyl)-3-hydroxy-3-(4-methoxybenzyl)-2,3-dihydro-1H-isoindol-1-one (37e) [Experiment 67]
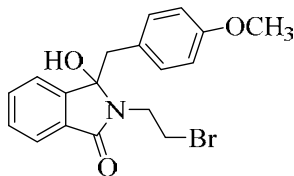
General procedure 10 was followed using 2.49 g of *p*-methoxyphenylacetic acid, 1.04 g of K_2CO_3, 1.27 g of *N*-bromoethyl phthalimide and 60 mL of acetone/pH 7 buffer (1:1) and 3 hours of irradiation. Workup gave 1.97 g of a crude product as a viscous liquid. 1.61 g (85%) of product were obtain after treatment with ethylacetate (10 mL) and cyclohexane (~3 ml, dropwise).

Melting point: 167-168°C.

IR: (film)

$\widetilde{v}$ (cm^{-1}) = 3379 br, 3106, 1685, 1583, 1366, 1268 and 630.

¹H-NMR: (300 MHz, CDCl₃)

δ (ppm): 3.13 (d, J = 15 Hz, 1 H, CH₂Ar), 3.49 (d, J = 15 Hz, 1 H, CH₂Ar), 3. 77 (s, 3 H, OCH₃), 3.72-3.82 (m, 3 H, CH₂Br, NCH₂), 4.15-4.24 (m, 1 H, NCH₂), 6.71 (d, J = 9 Hz, 2 H, CH_arom), 6.84 (d, J = 9 Hz, 2 H, CH_arom), 7.30 (m, 1 H, CH_arom), 7.53 (dd, J = 3, 9 Hz, 2 H, CH_arom), 7.70 (d, J = 9 Hz, 1 H, CH_arom).

¹³C-NMR: (75 MHz, acetone-d₆)

δ (ppm): 29.7 (q, 1 C, OCH₃), 41.7 (t, 1 C, NCH₂), 42.5 (t, 1 C, CH₂Ar), 55.2 (t, 1 C, CH₂Ph), 91.9 (s, 1 C, COH), 113.8 (d, 1 C, CH_arom), 123.1 (d, 1 C, CH_arom), 123.7 (d, 1 C, CH_arom), 127.8 (d, 1 C, CH_arom), 129.8 (d, 1 C, CH_arom), 131.8 (d, 1 C, CH_arom), 132.5 (d, 1 C, Cq_arom), 135.1 (d, 1 C, CH_arom), 147.8 (s, 1 C, Cq_arom), 159.4 (s, 1 C, Cq_arom), 167.0 (s, 1 C, C=O).

HRMS: (ESI/MeOH)

m/z: calcd for $C_{18}H_{18}NO_3Br$ (M+Na)$^+$: 398.0362, found: 398.0369 ± 2 ppm.

8.3.5.1.6 Synthesis of 2-(2-bromoethyl)-3-hydroxy-3-(4-methylbenzyl)-2,3-dihydro-1H-isoindol-1-one (37f) [Experiment 68]
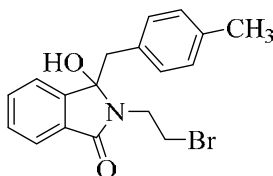
General procedure 10 was followed using 2.25 g of *p*-methylphenylacetic acid, 1.04 g of K_2CO_3, 1.27 g of *N*-bromoethyl phthalimide and 60 mL of acetone/pH 7 buffer (1:1) and 3 hours of irradiation. 1.54 g (88%) of product were obtained after workup as a light yellow crystalline solid.

Melting point: 152°C.

IR: (film)

$\widetilde{v}$ (cm^{-1}) = 3430 br, 3103, 1643, 1628, 1280 and 650.

^{1}H-NMR: (300 MHz, CDCl$_3$)

δ (ppm): 2.24 (s, 3 H, CH$_3$), 3.12 (d, J = 12 Hz, 1 H, CH$_2$Ar), 3.47 (d, J = 12 Hz, 1 H, CH$_2$Ar), 3.62-3.83 (m, 3 H, CH$_2$Br, NCH$_2$), 4.11-4.19 (m, 1 H, NCH$_2$), 6.74 (d, J = 6 Hz, 2 H, CH$_{arom}$), 6.92 (d, J = 6 Hz, 2 H, CH$_{arom}$), 7.28 (m, 1 H, CH$_{arom}$), 7.41-7.54 (m, 2 H, CH$_{arom}$), 7.64 (d, J = 6 Hz, 1 H, CH$_{arom}$).

^{13}C-NMR: (75 MHz, acetone-d$_6$)

δ (ppm): 20.1 (q, 1 C, CH$_3$), 31.3 (t, 1 C, CH$_2$Br), 38.2 (t, 1 C, NCH$_2$), 40.5 (t, 1 C, CH$_2$Ar), 90.2 (s, 1 C, COH), 120.9 (d, 1 C, CH$_{arom}$), 121.0 (d, 1 C, CH$_{arom}$), 123.8 (d, 2 C, CH$_{arom}$), 126.9 (d, 1 C, CH$_{arom}$), 129.1 (d, 1 C, CH$_{arom}$), 130.5 (d, 2 C, CH$_{arom}$), 138.9 (s, 1 C, Cq$_{arom}$), 140.6 (s, 1 C, Cq$_{arom}$), 141.7 (s, 1 C, Cq$_{arom}$), 143.3 (s, 1 C, Cq$_{arom}$), 166.9 (s, 1 C, C=O).

HRMS: (ESI/MeOH)

m/z: calcd for C$_{18}$H$_{18}$NO$_2$Br (M+Na)$^+$: 382.0413, found: 382.0419 ± 2 ppm.

8.3.5.1.7 Synthesis of 2-(2-bromoethyl)-3-hydroxy-3-(2-methylbenzyl)-2,3-dihydro-1H-isoindol-1-one (37g) [Experiment 69]
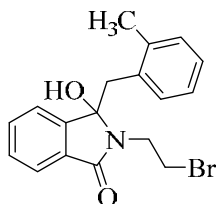
General procedure 10 was followed using 2.25 g of *o*-methylphenylacetic acid, 1.04 g of K_2CO_3, 1.27 g of *N*-bromoethyl phthalimide and 60 mL of acetone/pH 7 buffer (1:1) and 3 hours of irradiation. After workup, 1.33 g (71%) of product were obtained as a colourless crystalline solid.

Melting point: 157°C.

^{1}H-NMR: (300 MHz, CDCl$_3$)

δ (ppm): 1.90 (s, 3 H, CH$_3$), 2.95 (d, J = 16 Hz, 1 H, CH$_2$Ar), 3.53 (d, J = 16 Hz, 1 H, CH$_2$Ar), 3.62-3.88 (m, 3 H, CH$_2$Br, NCH$_2$), 4.09-4.23 (m, 1 H, NCH$_2$), 6.69 (d, J = 9 Hz, 1 H, CH$_{arom}$), 7.07-7.23 (m, 3 H, CH$_{arom}$), 7.33-7.38 (m, 1 H, CH$_{arom}$), 7.43-7.48 (m, 1 H, CH$_{arom}$), 7.73-7.77 (m, 1 H, CH$_{arom}$), 7.82-7.89 (m, 1 H, CH$_{arom}$).

^{13}C-NMR: (75 MHz, acetone-d$_6$)

δ (ppm): 19.7 (q, 1 C, CH$_3$), 30.9 (t, 1 C, CH$_2$Br), 41.2 (t, 1 C, NCH$_2$), 46.3 (t, 1 C, CH$_2$Ar), 91.7 (s, 1 C, COH), 119.1 (d, 1 C, CH$_{arom}$), 121.9 (d, 1 C, CH$_{arom}$), 122.2 (d, 1 C, CH$_{arom}$), 122.8 (d, 1 C, CH$_{arom}$), 128.0 (d, 1 C, CH$_{arom}$), 130.0 (d, 1 C, CH$_{arom}$), 132.2 (d, 1 C, CH$_{arom}$), 134.0 (d, 1 C, CH$_{arom}$), 135.5 (d, 1 C, Cq$_{arom}$), 140.1 (s, 1 C, Cq$_{arom}$), 143.4 (s, 1 C, Cq$_{arom}$), 144.3 (s, 1 C, Cq$_{arom}$), 167.1 (s, 1 C, C=O).

HRMS: (ESI/MeOH)

m/z: calcd for C$_{18}$H$_{18}$NO$_2$Br (M+Na)$^+$: 382.0413, found: 382.0419 ± 1 ppm.

8.3.5.1.8 Synthesis of 2-(2-bromoethyl)-3-hydroxy-3-(3-methylbenzyl)-2,3-dihydro-1H-isoindol-1-one (37g) [Experiment 70]
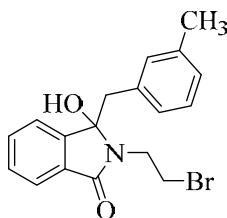
General procedure 10 was followed using 2.25 g of *m*-methylphenylacetic acid, 1.04 g of K$_2$CO$_3$, 1.27 g of *N*-bromoethyl phthalimide and 60 mL of acetone/pH 7 buffer (1:1) and 3 hours of irradiation. After workup, 1.20 g (66%) of product were obtained as a light yellowish crystalline solid.

Melting point: 151-152°C.

^{1}H-NMR: (300 MHz, CDCl$_3$)

δ (ppm): 2.19 (s, 3 H, CH$_3$), 3.09 (d, J = 16 Hz, 1 H, CH$_2$Ar), 3.47 (d, J = 16 Hz, 1 H, CH$_2$Ar), 3.62-3.83 (m, 3 H, CH$_2$Br, NCH$_2$), 4.10-4.17 (m, 1 H, NCH$_2$), 6.65-6.69(m, 2 H, CH$_{arom}$), 7.02-7.04 (m, 2 H, CH$_{arom}$), 7.22-7.25 (m, 1 H, CH$_{arom}$), 7.43-7.57 (m, 2 H, CH$_{arom}$), 7.62-7.65 (m, 1 H, CH$_{arom}$).

^{13}C-NMR: (75 MHz, acetone-d$_6$)

δ (ppm): 20.3 (q, 1 C, CH$_3$), 29.3 (t, 1 C, CH$_2$Br), 38.6 (t, 1 C, NCH$_2$), 42.1 (t, 1 C, CH$_2$Ar), 91.2 (s, 1 C, COH), 121.3 (d, 1 C, CH$_{arom}$), 122.9 (d, 1 C, CH$_{arom}$), 126.9 (d, 1 C, CH$_{arom}$), 127.2 (d, 1 C, CH$_{arom}$), 130.4 (d, 2 C, CH$_{arom}$), 133.1 (d, 1 C, CH$_{arom}$), 134.7

(d, 2 C, CH$_{arom}$), 139.0 (s, 1 C, Cq$_{arom}$), 141.6 (s, 1 C, Cq$_{arom}$), 143.9 (s, 1 C, Cq$_{arom}$), 166.4 (s, 1 C, C=O).

HRMS: (ESI/MeOH)

m/z: calcd for C$_{18}$H$_{18}$NO$_2$Br (M+Na)$^+$: 382.0413, found: 382.0419 ± 1 ppm .

8.3.5.1.9 Synthesis of 3-benzyl-2-(3-bromopropyl)-3-hydroxy-2,3-dihydro-1H-isoindol-1-one (37i) [Experiment 71]
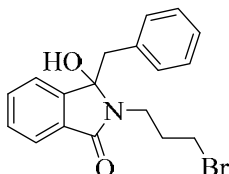
General procedure 10 was followed using 2.04 g of phenylacetic acid, 1.04 g of K$_2$CO$_3$, 1.34 g of *N*-bromopropyl phthalimide and 60 mL of acetone/pH 7 buffer (1:1) and 3 hours of irradiation. The product started to precipitate as a yellowish solid in the Schlenk flask during irradiation. Workup gave 1.71 g (95%) of product as a colourless solid.

Melting point: 160°C.

IR: (film)

$\widetilde{\nu}$ (cm^{-1}) = 3260 br, 3150, 1680, 1650, 1300 and 685.

^{1}H-NMR: (300 MHz, CDCl$_3$)

δ (ppm): 2.26-2.45 (m, 2 H, CH$_2$), 3.13 (d, J = 12 Hz, 1 H, CH$_2$Ph), 3.48-3.58 (m, 4 H, CH$_2$Ph, CH$_2$Br, NCH$_2$), 3.78-3.87 (m, 1 H, NCH$_2$), 6.92 (d, J = 9 Hz, 2 H, CH$_{arom}$), 7.19-7.26 (m, 4 H, CH$_{arom}$), 7.41-7.47 (m, 2 H, CH$_{arom}$), 7.62 (d, J = 9 Hz, 1 H, CH$_{arom}$).

^{13}C-NMR: (75 MHz, CDCl$_3$)

δ (ppm): 32.6 (t, 1 C, CH$_2$), 33.6 (t, 1 C, CH$_2$Br), 39.0 (t, 1 C, NCH$_2$), 43.5 (t, 1 C, CH$_2$Ph), 90.1 (s, 1 C, COH), 123.0 (d, 1 C, CH$_{arom}$), 123.8 (d, 1 C, CH$_{arom}$), 127.4 (d, 1 C, CH$_{arom}$), 128.5 (s, 2 C, CH$_{arom}$), 130.0 (s, 1 C, Cq$_{arom}$), 131.0 (d, 2 C, CH$_{arom}$), 132.3 (d, 1 C, CH$_{arom}$), 132.7 (d, 1 C, CH$_{arom}$), 136.2 (s, 1 C, Cq$_{arom}$), 147.8 (s, 1 C, Cq$_{arom}$), 167.2 (s, 1 C, C=O).

HRMS: (ESI/MeOH)

m/z: calcd for C$_{18}$H$_{18}$NO$_2$Br (M+Na)$^+$: 382.0413, found: 382.0435 ± 6 ppm.

8.3.5.1.10 Synthesis of 2-(3-bromopropyl)-3-(4-fluorobenzyl)-3-hydroxy-2,3-dihydro-1H-isoindol-1-one (37j) [Experiment 72]
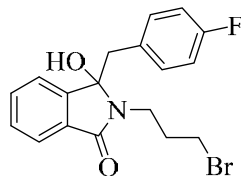
General procedure 10 was followed using 2.31 g of *p*-fluorophenylacetic acid, 1.04 g of K_2CO_3, 1.34 g of *N*-bromopropyl phthalimide and 60 mL of acetone/pH 7 buffer (1:1) and 3 hours of irradiation. The product precipitated as a yellowish solid during irradiation. After workup, 1.49 g (75%) of product were obtained as a yellowish solid.

Melting point: 161°C.

IR: (film)

$\tilde{v}$ (cm^{-1}) = 3382 br, 3110, 1690, 1660, 1146 and 680.

^{1}H-NMR: (300 MHz, CDCl$_3$)

δ (ppm): 2.16-2.44 (m, 2 H, CH$_2$), 3.09 (d, J = 12 Hz, 1 H, CH$_2$Ar), 3.47-3.54 (m, 4 H, CH$_2$Ar, CH$_2$Br, NCH$_2$), 3.76-3.83 (m, 1 H, NCH$_2$), 6.80-6.89 (m, 4 H, CH$_{arom}$), 7.11 (d, J = 9 Hz, 1 H, CH$_{arom}$), 7.42-7.47 (m, 2 H, CH$_{arom}$), 7.61 (d, J = 9 Hz, 1 H, CH$_{arom}$).

^{13}C-NMR: (75 MHz, CDCl$_3$)

δ (ppm): 30.0 (t, 1 C, CH$_2$), 34.8 (t, 1 C, CH$_2$Br), 40.2 (t, 1 C, NCH$_2$), 45.5 (t, 1 C, CH$_2$Ar), 93.1 (s, 1 C, COH), 120.1 (d, 1 C, CH$_{arom}$), 122.7 (d, 1 C, CH$_{arom}$), 124.7 (d, 1 C, CH$_{arom}$), 128.2 (d, 2 C, CH$_{arom}$), 130.7 (s, 1 C, Cq$_{arom}$), 131.3 (d, 2 C, CH$_{arom}$), 132.9 (d, 1 C, CH$_{arom}$), 135.7 (s, 1 C, Cq$_{arom}$), 136.2 (s, 1 C, Cq$_{arom}$), 158.1 (s, 1 C, Cq$_{arom}$), 167.0 (s, 1 C, C=O).

HRMS: (ESI/MeOH)

m/z: calcd for C$_{18}$H$_{17}$O$_2$NFBr (M+Na)$^+$: 400.0319, found: 400.0340 ± 5 ppm.

8.3.5.1.11 Synthesis of Synthesis of 2-(3-bromopropyl)-3-(4-chlorobenzyl)-3-hydroxy-2,3-dihydro-1H-isoindol-1-one (37k) [Experiment 73]
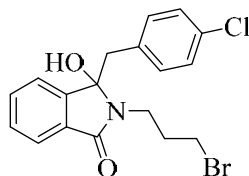
General procedure 10 was followed using 2.56 g of *p*-chlorophenylacetic acid, 1.04 g of K_2CO_3, 1.34 g of *N*-bromopropyl phthalimide and 60 mL of acetone/pH 7 buffer (1:1) and 3 hours of irradiation. After workup, 1.58 g (80%) of product were obtained as a yellowish solid.

Melting point: 158-160°C.

IR: (film)

$\widetilde{\nu}$ (cm^{-1}) = 3380 br, 3091, 1683, 16027, 1338 and 671.

^{1}H-NMR: (300 MHz, CDCl$_3$)

δ (ppm): 2.24-2.43 (m, 2 H, CH$_2$), 3.05 (d, J = 12 Hz, 1 H, CH$_2$Ar), 3.41-3.54 (m, 4 H, CH$_2$Ar, CH$_2$Br, NCH$_2$), 3.73-3.82 (m, 1 H, NCH$_2$), 6.85 (d, J = 6 Hz, 2 H, CH$_{arom}$), 7.09-7.13 (m, 3 H, CH$_{arom}$), 7.40-7.46 (m, 2 H, CH$_{arom}$), 7.58 (d, J = 6 Hz, 1 H, CH$_{arom}$).

^{13}C-NMR: (75 MHz, CDCl$_3$)

δ (ppm): 29.7 (t, 1 C, CH$_2$), 33.2 (t, 1 C, CH$_2$Br), 41.6 (t, 1 C, NCH$_2$), 44.9 (t, 1 C, CH$_2$Ar), 93.1 (s, 1 C, COH), 119.6 (d, 1 C, CH$_{arom}$), 120.1 (d, 1 C, CH$_{arom}$), 122.4 (d, 1 C, CH$_{arom}$), 123.7 (d, 1 C, CH$_{arom}$), 125.3 (d, 1 C, CH$_{arom}$), 129.3 (s, 1 C, Cq$_{arom}$), 130.5 (s, 1 C, CH$_{arom}$), 131.4 (s, 1 C, CH$_{arom}$), 132.0 (s, 1 C, CH$_{arom}$), 134.3 (s, 1 C, Cq$_{arom}$), 135.9 (s, 1 C, Cq$_{arom}$), 140.4 (s, 1 C, Cq$_{arom}$), 167.3 (s, 1 C, C=O).

HRMS: (ESI/MeOH)

m/z: calcd for C$_{18}$H$_{16}$BrClNO$_2$ (M+Na)$^+$: 416.0024, found: 416.0027 ± 1 ppm.

8.3.5.1.12 Synthesis of Synthesis of 2-(3-bromopropyl)-3-(4-bromobenzyl)-3-hydroxy-2,3-dihydro-1H-isoindol-1-one (37l) [Experiment 74]
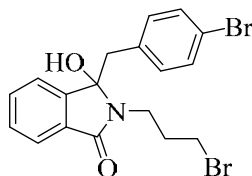
General procedure 10 was followed using 3.23 g of *p*-bromophenylacetic acid, 1.04 g of K$_2$CO$_3$, 1.34 g of *N*-bromopropyl phthalimide and 60 mL of acetone/pH 7 buffer (1:1) and 3 hours of irradiation. Workup furnished a reddish brown liquid, which was purified by column chromatography on silica gel using 20% EtOAc in cyclohexane as eluent to give 1.59 g (73%) of **37l** as a slightly off-white crystalline solid.

Melting point: 159°C.

IR: (film)

$\widetilde{\nu}$ (cm^{-1}) = 3550 br, 3120, 1685, 1401, 1324 and 683.

^{1}H-NMR: (300 MHz, CDCl$_3$)

δ (ppm): 2.27-2.40 (m, 2 H, CH$_2$), 3.05 (d, J = 15 Hz, 1 H, CH$_2$Ar), 3.44-3.53 (m, 4 H, CH$_2$Ar, CH$_2$Br, NCH$_2$), 3.76-3.84 (m, 1 H, NCH$_2$), 6.80 (d, J = 9 Hz, 2 H, CH$_{arom}$), 7.09-7.12 (m, 1 H, CH$_{arom}$), 7.27-7.29 (m, 2 H, CH$_{arom}$), 7.41-7.48 (d, J = 9 Hz, 2 H, CH$_{arom}$), 7.62 (d, J = 9 Hz, 1 H, CH$_{arom}$).

¹³C-NMR: (75 MHz, CDCl₃)

δ (ppm): 30.1 (t, 1 C, CH₂), 34.7 (t, 1 C, CH₂Br), 40.9 (t, 1 C, NCH₂), 45.0 (t, 1 C, CH₂Ar), 90.5 (s, 1 C, COH), 120.5 (d, 2 C, CH$_{arom}$), 122.4 (d, 1 C, CH$_{arom}$), 123.7 (d, 1 C, CH$_{arom}$), 125.3 (d, 1 C, CH$_{arom}$), 129.3 (d, 1 C, CH$_{arom}$), 130.5 (s, 1 C, Cq$_{arom}$), 131.4 (d, 1 C, CH$_{arom}$), 132.0 (d, 1 C, CH$_{arom}$), 134.3 (s, 1 C, Cq$_{arom}$), 135.9 (s, 1 C, Cq$_{arom}$), 140.4 (s, 1 C, Cq$_{arom}$), 166.2 (s, 1 C, C=O).

HRMS: (ESI/MeOH)

m/z: calcd for C₁₈H₁₇NO₂Br₂ (M+Na)⁺: 459.9518, found: 459.9548 ± 7 ppm.

8.3.5.1.13 Synthesis of 2-(3-bromopropyl)-3-hydroxy-3-(4-methoxybenzyl)-2,3-dihydro-1H-isoindol-1-one (37m) [Experiment 75]
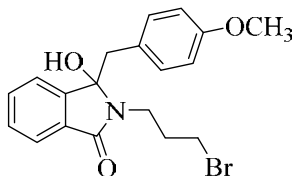
General procedure 10 was followed using 2.49 g of *p*-methoxyphenylacetic acid, 1.04 g of K₂CO₃, 1.34 g of *N*-bromopropyl phthalimide and 60 mL of acetone/pH 7 buffer (1:1) and 3 hours of irradiation. After workup, 1.55 g (76%) of product were obtained as colourless crystals.

Melting point: 167-168°C.

IR: (film)

$\widetilde{v}$ (cm⁻¹) = 3380 br, 3123, 1670, 1597, 1328, 1250 and 647.

¹H-NMR: (300 MHz, CDCl₃)

δ (ppm): 2.37-2.46 (m, 2 H, CH₂), 3.32 (d, J = 15 Hz, 1 H, CH₂Ar), 3.54 (d, J = 15 Hz, 1 H, CH₂Ar), 3.64 (t, J = 6 Hz, 2 H, CH₂Br), 3.71 (s, 3 H, OCH₃), 3.79 (s, 1 H, NCH₂), 3.83-3.92 (m, 1 H, NCH₂), 6.68 (d, J = 9 Hz, 2 H, CH$_{arom}$), 6.84-6.89 (m, 2 H, CH$_{arom}$), 7.17 (d, J = 9 Hz, 1 H, CH$_{arom}$), 7.45-7.50 (m, 3 H, CH$_{arom}$).

¹³C-NMR: (75 MHz, acetone-d₆)

δ (ppm): 31.4 (q, 1 C, OCH₃), 31.9 (t, 1 C, CH₂), 36.8 (t, 1 C, CH₂Br), 38.6 (t, 1 C, NCH₂), 55.6 (t, 1 C, CH₂Ar), 89.2 (s, 1 C, COH), 114.5 (d, 1 C, CH$_{arom}$), 123.5 (d, 1 C, CH$_{arom}$), 124.3 (d, 1 C, CH$_{arom}$), 128.1 (d, 2 C, CH$_{arom}$), 129.6 (s, 1 C, Cq$_{arom}$), 130.1 (d, 2 C, CH$_{arom}$), 132.4 (d, 1 C, CH$_{arom}$), 133.1 (d, 1 C, CH$_{arom}$), 134.9 (s, 1 C, Cq$_{arom}$), 136.0 (s, 1 C, Cq$_{arom}$), 166.5 (s, 1 C, C=O).

HRMS: (ESI/MeOH)

m/z: calcd for C₁₉H₂₀NO₃Br (M+Na)⁺: 412.0519, found: 412.0512 ± 2 ppm.

8.3.5.1.14 Synthesis of 2-(3-bromopropyl)-3-hydroxy-3-(4-methylbenzyl)-2,3-dihydro-1H-isoindol-1-one (37n) [Experiment 76]
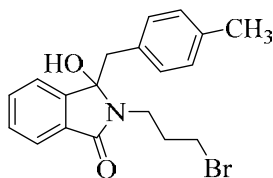
General procedure 10 was followed using 2.25 g of *p*-methylphenylacetic acid, 1.04 g of K$_2$CO$_3$, 1.34 g of *N*-bromopropyl phthalimide and 60 mL of acetone/pH 7 buffer (1:1) and 3 hours of irradiation. After workup, 1.66 g (89%) of product were obtained as a colourless crystals.

Melting point: 156-157°C.

IR: (film)

$\widetilde{v}$ (cm^{-1}) = 3442 br, 3232, 1680, 1600, 1272 and 664.

^{1}H-NMR: (300 MHz, CDCl$_3$)

δ (ppm): 2.25 (s, 3 H, CH$_3$), 2.28-2.43 (m, 3 H, CH$_2$, CH$_2$Ar), 3.11 (d, J = 12 Hz, 1 H, CH$_2$Ar), 3.48-3.57 (m, 4 H, CH$_2$Br, NCH$_2$), 6.78 (d, 2 H, J = 9 Hz, CH$_{arom}$), 6.94 (d, 2 H, J = 9 Hz, CH$_{arom}$), 7.18-7.21 (m, 1 H, CH$_{arom}$), 7.39-7.50 (m, 2 H, CH$_{arom}$), 7.62 (d, J = 9 Hz, 1 H, CH$_{arom}$).

^{13}C-NMR: (75 MHz, CDCl$_3$)

δ (ppm): 20.6 (q, 1 C, CH$_3$),30.2 (t, 1 C, CH$_2$), 34.7 (t, 1 C, CH$_2$Br), 40.1 (t, 1 C, NCH$_2$), 45.0 (t, 1 C, CH$_2$Ar), 90.3 (s, 1 C, COH), 121.3 (d, 2 C, CH$_{arom}$), 122.7 (d, 1 C, CH$_{arom}$), 125.0 (d, 2 C, CH$_{arom}$), 129.0 (s, 1 C, Cq$_{arom}$), 130.8 (s, 1 C, CH$_{arom}$), 131.3 (s, 1 C, CH$_{arom}$), 132.0 (s, 1 C, CH$_{arom}$), 134.3 (s, 1 C, Cq$_{arom}$), 135.9 (s, 1 C, Cq$_{arom}$), 140.4 (s, 1 C, Cq$_{arom}$), 166.5 (s, 1 C, C=O).

HRMS: (ESI/MeOH)

m/z: calcd for C$_{19}$H$_{20}$O$_2$NBr (M+Na)$^+$: 396.0570, found: 396.0568 ± 1 ppm.

8.3.5.1.15 Synthesis of 2-(3-bromopropyl)-3-hydroxy-3-(2-methylbenzyl)-2,3-dihydro-1H-isoindol-1-one (37o) [Experiment 77]
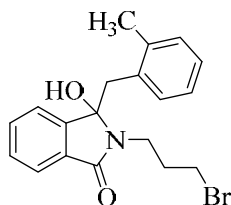
General procedure 10 was followed using 2.25 g of *o*-methylphenylacetic acid, 1.04 g of K$_2$CO$_3$, 1.34 g of *N*-bromopropyl phthalimide and 60 mL of acetone/pH 7 buffer (1:1) and 3 hours of irradiation. After workup, 1.37 g (73%) of product were obtained as a light yellow crystalline solid.

Melting point: 155°C.

IR: (film)

$\widetilde{v}$ (cm^{-1}) = 3396 br, 3145, 1689, 1630, 1207 and 692.

^{1}H-NMR: (300 MHz, CDCl$_3$)

δ (ppm): 2.24 (s, 3 H, CH$_3$), 2.32-2.42 (m, 2 H, CH$_2$Br), 3.11 (d, J = 15 Hz, 1 H, CH$_2$Ar), 3.50-3.57 (m, 2 H, CH$_2$Br, CH$_2$Ar), 3.76-3.86 (m, 1 H, NCH$_2$), 4.10-4.17 (m, 1 H, CH$_2$Br, NCH$_2$), 6.72-6.77 (m, 2 H, CH$_{arom}$), 7.00-7.06 (m, 2 H, CH$_{arom}$), 7.17-7.24 (m, 1 H, CH$_{arom}$), 7.44-7.50 (m, 2 H, CH$_{arom}$), 7.58-7.62 (m, 1 H, CH$_{arom}$).

^{13}C-NMR: (75 MHz, CDCl$_3$)

δ (ppm): 20.1 (q, 1 C, CH$_3$),29.7 (t, 1 C, CH$_2$), 33.2 (t, 1 C, CH$_2$Br), 41.6 (t, 1 C, NCH$_2$), 44.9 (t, 1 C, CH$_2$Ar), 90.1 (s, 1 C, COH), 120.1 (d, 1 C, CH$_{arom}$), 121.9 (d, 1 C, CH$_{arom}$), 123.7 (d, 1 C, CH$_{arom}$), 124.0 (d, 1 C, CH$_{arom}$), 126.0 (d, 1 C, CH$_{arom}$), 129.1 (s, 1 C, Cq$_{arom}$), 130.7 (d, 1 C, CH$_{arom}$), 131.4 (d, 1 C, CH$_{arom}$), 132.3 (d, 1 C, CH$_{arom}$), 135.8 (s, 2 C, Cq$_{arom}$), 140.0 (s, 1 C, Cq$_{arom}$), 167.0 (s, 1 C, C=O).

HRMS: (ESI/MeOH)

m/z: calcd for C$_{19}$H$_{20}$O$_2$NBr (M+Na)$^+$: 396.0570, found: 396.0570 ± 0 ppm.

8.3.5.1.16 Synthesis of 2-(3-bromopropyl)-3-hydroxy-3-(3-methylbenzyl)-2,3-dihydro-1H-isoindol-1-one (37p) [Experiment 78]
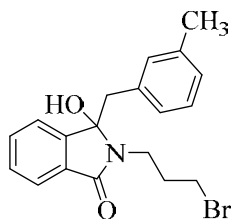
General procedure 10 was followed using 2.25 g of *m*-methylphenylacetic acid, 1.04 g of K$_2$CO$_3$, 1.34 g of *N*-bromopropyl phthalimide and 60 mL of acetone/pH 7 buffer (1:1) and 3 hours of irradiation. Workup furnished a viscous brownish liquid, which was further purified through column chromatography using 50% ethylacetate in cyclohexane as eluent. 1.7 g (91%) of product were obtained as a yellowish powder.

Melting point: 156-158°C.

IR: (film)

$\widetilde{v}$ (cm^{-1}) = 3453 br, 3156, 1684, 1645, 1297 and 662.

^{1}H-NMR: (300 MHz, CDCl$_3$)

δ (ppm): 1.91 (s, 3 H, CH$_3$), 2.32-2.51 (m, 3 H, CH$_2$Ar, CH$_2$Br), 2.91 (d, J = 15 Hz, 1 H, CH$_2$Ar), 3.50-3.62 (m, 4 H, CH$_2$Br, NCH$_2$), 6.61(d, J = 9 Hz, 2 H, CH$_{arom}$), 7.08-7.20 (m, 3 H, CH$_{arom}$), 7.32-7.46 (m, 3 H, CH$_{arom}$), 7.73 (d, J = 9 Hz, 1 H, CH$_{arom}$).

^{13}C-NMR: (75 MHz, CDCl$_3$)

δ (ppm): 20.3 (q, 1 C, CH$_3$),29.7 (t, 1 C, CH$_2$), 33.8 (t, 1 C, CH$_2$Br), 42.0 (t, 1 C, NCH$_2$), 44.9 (t, 1 C, CH$_2$Ar), 91.0 (s, 1 C, COH), 121.1 (d, 1 C, CH$_{arom}$), 122.4 (d, 1 C, CH$_{arom}$), 123.0 (d, 1 C, CH$_{arom}$), 123.7 (d, 1 C, CH$_{arom}$), 128.1 (d, 1 C, CH$_{arom}$), 130.1 (s, 1 C, Cq$_{arom}$), 131.5 (s, 1 C, CH$_{arom}$), 131.9 (s, 1 C, CH$_{arom}$), 132.7 (s, 1 C, CH$_{arom}$), 134.0 (s, 1 C, Cq$_{arom}$), 135.3 (s, 1 C, Cq$_{arom}$), 139.7 (s, 1 C, Cq$_{arom}$), 166.6 (s, 1 C, C=O).

HRMS: (ESI/MeOH)

m/z: calcd for C$_{19}$H$_{20}$O$_2$NBr (M+Na)$^+$: 396.0570, found: 396.0585 ± 4 ppm .

8.3.5.2 Dehydration of photoproduct under batch conditions [Experiments79-94]

General procedure 11 (GP11): 4 mmol of the photoproduct **37a-p** were dissolved in 30 mL of CH$_2$Cl$_2$. Approximately 3 drops of concentrated H$_2$SO$_4$ were added and the solution was stirred at room temperature. After 3-5 hours, 30 mL of water were added and the organic layer was separated, washed with saturated NaHCO$_3$ (2 × 40 mL) and brine (1 × 40 mL) and dried over MgSO$_4$. The filtrate was then evaporated to dryness by rotary evaporation. In most of cases, ^{1}H-NMR showed the presence of both, *E*- and *Z*-isomer, with a large preference for the *E*-isomer.

8.3.5.2.1 Synthesis of 3-benzylidene-2-(2-bromoethyl)-2,3-dihydro-1H-isoindol-1-one (38a) [Experiment 79]
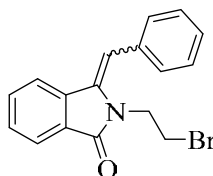
General procedure 11 was followed using 1.38 g of photoproduct **37a**, 3 drops of conc. H$_2$SO$_4$ and 30 mL of CH$_2$Cl$_2$. After workup, 1.19 g (91%) of product were obtained as a yellowish solid.

Melting point: 102°C.

IR: (film)

$\widetilde{\nu}$ (cm^{-1}) = 3140, 1658, 1620, 1580, 1301, 832 and 689.

^{1}H-NMR: (mixture of stereoisomers, 300 MHz, CDCl$_3$)

Main *E*-isomer:

δ (ppm): 3.67 (t, J = 6 Hz, 2 H, CH$_2$Br), 4.34 (t, J = 6 Hz, 2 H, NCH$_2$), 6.65 (s, 1 H, CH$_{olef.}$), 7.30-7.50 (m, 8 H, CH$_{arom}$), 7.90 (d, J = 9 Hz, 1 H, CH$_{arom}$).

Minor *Z*-isomer: characteristic peaks only.

δ (ppm): 3.15 (t, J = 6 Hz, 2 H, CH$_2$Br), 4.14 (t, J = 6 Hz, 2 H, NCH$_2$), 6.85 (s, 1 H, CH$_{olef.}$).

^{13}C-NMR: (mixture of stereoisomers, 75 MHz, CDCl$_3$)

Main *E*-isomer:

δ (ppm): 27.7 (t, 1 C, CH$_2$Br), 41.1 (t, 1 C, NCH$_2$), 110.4 (d, 1 C, CH$_{olef}$), 123.4 (s, 1 C, C$_q$), 123.4 (d, 2 C, CH$_{arom}$), 128.9 (d, 2 C, CH$_{arom}$), 129.3 (d, 1 C, CH$_{arom}$), 129.6 (d, 1 C, CH$_{arom}$), 129.6 (d, 1 C, CH$_{arom}$), 129.9 (d, 1 C, CH$_{arom}$), 132.0 (s, 1 C, CHq$_{arom}$), 134.8 (d, 1 C, C$_{arom}$), 135.7 (d, 1 C, CHq$_{arom}$), 135.8 (s, 1 C, Cq$_{arom}$), 166.6 (s, 1 C, C=O).

Minor *Z*-isomer: quantity too low to assign peaks.

HRMS: (mixture of stereoisomers, ESI/MeOH)

m/z: calcd for C$_{17}$H$_{14}$ONBr (M+Na)$^+$: 350.0151, found: 350.0149 ± 1 ppm.

8.3.5.2.2 Synthesis of 2-(2-bromoethyl)-3-(4-fluorobenzylidene)-2,3-dihydro-1H-isoindol-1-one (38b) [Experiment 80]
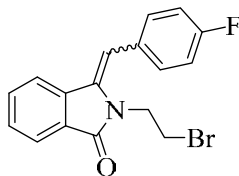
General procedure 11 was followed using 1.46 g of photoproduct **37b**, 3 drops of conc. H$_2$SO$_4$ and 30 mL of CH$_2$Cl$_2$. Workup furnished 1.24 g (85%) of the product as a yellow oil.

IR: (film)

$\widetilde{\nu}$ (cm^{-1}) = 3125, 1692, 1632, 1546, 1167, 830, 670.

^{1}H-NMR: (mixture of stereoisomers, 300 MHz, CDCl$_3$)

Main *E*-isomer:

δ (ppm): 3.53 (t, J = 6 Hz, 2 H, CH$_2$Br), 4.37 (t, J = 6 Hz, 2 H, NCH$_2$), 6.60 (s, 1 H, CH$_{olef}$), 7.11-7.15 (m, 2 H, CH$_{arom}$), 7.45-7.50 (m, 2 H, CH$_{arom}$), 7.90 (m, 4 H, CH$_{arom}$).

Minor *Z*-isomer: quantity too low to assign peaks.

^{13}C-NMR: (mixture of stereoisomers, 75 MHz, CDCl$_3$)

Main *E*-isomer:

δ (ppm): 33.0 (t, 1 C, CH$_2$Br), 40.4 (t, 1 C, NCH$_2$), 107.0 (d, 1 C, CH$_{olef}$), 114.3 (d, 2 C, CH$_{arom}$), 123.5 (d, 1 C, CH$_{arom}$), 123.7 (s, 1 C, Cq$_{arom}$), 127.0 (s, 1 C, Cq$_{arom}$), 128.2 (d, 1 C, CH$_{arom}$), 129.4 (d, 1 C, CH$_{arom}$), 130.9 (d, 2 C, CH$_{arom}$), 131.9 (s, 1 C, Cq$_{arom}$), 134.4 (d, 1 C, CH$_{arom}$), 134.3 (s, 1 C, Cq$_{arom}$), 158.6 (s, 1 C, Cq$_{arom}$), 166.6 (s, 1 C, C=O).

Minor Z-isomer: quantity too low to assign peaks.

HRMS: (mixture of stereoisomers, ESI/MeOH)

m/z: calcd for C$_{17}$H$_{13}$ONBrF (M+Na)$^+$: 368.0057, found: 368.0059 ± 1 ppm.

8.3.5.2.3 Synthesis of 2-(2-bromoethyl)-3-(4-chlorobenzylidene)-2,3-dihydro-1H-isoindol-1-one (38c) [Experiment 81]
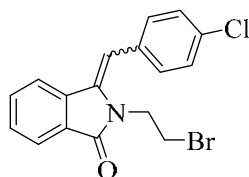
General procedure 11 was followed using 1.52 g of photoproduct **37c**, 3 drops of conc. H$_2$SO$_4$ and 30 mL of CH$_2$Cl$_2$. After workup, 1.28 g (88%) of product were obtained as a crystalline dark yellowish solid.

Melting point: 120°C.

IR: (film)

$\widetilde{v}$ (cm^{-1}) = 3112, 1644, 1601, 1558, 1350, 845 and 666.

^{1}H-NMR: (mixture of stereoisomers, 300 MHz, CDCl$_3$)

Main E-isomer:

δ (ppm): 3.62 (t, J = 9 Hz, 2 H, CH$_2$Br), 4.28 (t, J = 9 Hz, 2 H, NCH$_2$), 6.53 (s, 1 H, CH$_{olef}$), 7.24-7.30 (m, 2 H, CH$_{arom}$), 7.36-7.49 (m, 5 H, CH$_{arom}$), 7.84-7.87 (m, 1 H, CH$_{arom}$).

Minor Z-isomer: quantity too low to assign peaks.

^{13}C-NMR: (mixture of stereoisomers, 75 MHz, CDCl$_3$)

Main E-isomer:

δ (ppm): 32.8 (t, 1 C, CH$_2$Br), 40.0 (t, 1 C, NCH$_2$), 106.9 (d, 1 C, CH$_{olef}$), 117.0 (d, 2 C, CH$_{arom}$), 123.0 (d, 1 C, CH$_{arom}$), 124.9 (s, 1 C, Cq$_{arom}$), 127.0 (s, 1 C, Cq$_{arom}$), 128.7 (d, 1 C, CH$_{arom}$), 129.2 (d, 1 C, CH$_{arom}$), 130.0 (d, 2 C, CH$_{arom}$), 131.5 (s, 1 C, Cq$_{arom}$), 133.8 (d, 1 C, CH$_{arom}$), 134.0 (s, 1 C, Cq$_{arom}$), 155.7 (s, 1 C, Cq$_{arom}$), 166.0 (s, 1 C, C=O).

Minor Z-isomer: quantity too low to assign peaks.

HRMS: (mixture of stereoisomers, ESI/MeOH)

m/z: calcd for C$_{17}$H$_{13}$ONBrCl (M+Na)$^+$: 383.9761, found: 383.9762 ± 1 ppm.

8.3.5.2.4 Synthesis of 3-(4-bromobenzylidene)-2-(2-bromoethyl)-2,3-dihydro-1H-isoindol-1-one (38d) [Experiment 82]
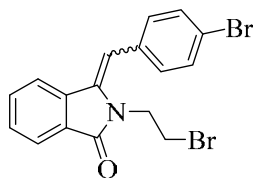
General procedure 11 was followed using 1.70 g of photoproduct **37d**, 3 drops of conc. H_2SO_4 and 30 mL of CH_2Cl_2. Workup furnished 1.35 g (83%) of product as a yellow oil.

IR: (film)

$\widetilde{\nu}$ (cm^{-1}) = 3138, 1665, 1471, 1572, 1364, 841 and 654.

^{1}H-NMR: (mixture of stereoisomers, 300 MHz, CDCl$_3$)

Main *E*-isomer:

δ (ppm): 3.63 (t, J = 9 Hz, 2 H, CH$_2$Br), 4.29 (t, J = 9 Hz, 2 H, NCH$_2$), 6.53 (s, 1 H, CH$_{olef}$), 7.11-7.17 (dd, J = 3, 9 Hz, 2 H, CH$_{arom}$), 7.32-7.48 (m, 5 H, CH$_{arom}$), 7.86 (d, J = 9 Hz, 1 H, CH$_{arom}$).

Minor *Z*-isomer: quantity too low to assign peaks.

^{13}C-NMR: (mixture of stereoisomers, 75 MHz, CDCl$_3$)

Main *E*-isomer:

δ (ppm): 29.9 (t, 1 C, CH$_2$Br), 40.4 (t, 1 C, NCH$_2$), 106.4 (d, 1 C, CH$_{olef}$), 114.7 (d, 1 C, CH$_{arom}$), 115.0 (d, 1 C, CH$_{arom}$), 123.2 (d, 1 C, CH$_{arom}$), 123.3 (s, 1 C, Cq$_{arom}$), 127.8 (s, 1 C, Cq$_{arom}$), 128.9 (d, 1 C, CH$_{arom}$), 129.6 (d, 1 C, CH$_{arom}$), 130.3 (d, 2 C, CH$_{arom}$), 131.7 (s, 1 C, Cq$_{arom}$), 134.7 (d, 1 C, CH$_{arom}$), 135.2 (s, 1 C, Cq$_{arom}$), 145.3 (s, 1 C, Cq$_{arom}$), 167.2 (s, 1 C, C=O).

Minor *Z*-isomer: quantity too low to assign peaks.

HRMS: (mixture of stereoisomers, ESI/MeOH)

m/z: calcd for C$_{17}$H$_{14}$ONBr$_2$ (M+Na)$^+$: 427.9256, found: 427.9255 ± 1 ppm.

8.3.5.2.5 Synthesis of 2-(2-bromoethyl)-3-(4-methoxybenzylidene)-2,3-dihydro-1H-isoindol-1-one (38e) [Experiment 83]
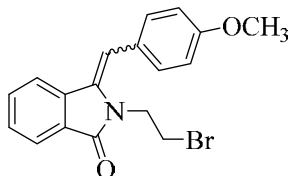
General procedure 11 was followed using 1.50 g of photoproduct **37e**, 3 drops of conc. H_2SO_4 and 30 mL of CH_2Cl_2. After workup, 1.288 g (90%) of product were obtained as a bright yellow oil.

IR: (film)

$\widetilde{v}$ (cm^{-1}) = 3126, 1685, 1583, 1581, 1366, 1268, 826 and 630.

¹H-NMR: (mixture of stereoisomers, 300 MHz, $CDCl_3$)

Main *E*-isomer:

δ (ppm): 3.66 (t, J = 9 Hz, 2 H, CH_2Br), 3.93 (s, 3 H, OCH_3), 4.33 (t, J = 9 Hz, 2 H, NCH_2), 6.60 (s, 1 H, CH_{olef}), 7.02 (d, J = 9 Hz, 2 H, CH_{arom}), 7.40-7.43 (m, 5 H, CH_{arom}), 7.90 (d, J = 9 Hz, 1 H, CH_{arom}).

Minor *Z*-isomer: quantity too low to assign peaks.

¹³C-NMR: (mixture of stereoisomers, 75 MHz, $CDCl_3$)

Main *E*-isomer:

δ (ppm): 27.8 (t, 1 C, CH_2Br), 42.1 (t, 1 C, NCH_2), 55.2 (q, 1 C, OCH_3), 107.0 (d, 1 C, CH_{olef}), 114.3 (d, 2 C, CH_{arom}), 123.5 (d, 1 C, CH_{arom}), 123.7 (s, 1 C, Cq_{arom}), 127.0 (s, 1 C, Cq_{arom}), 128.2 (d, 1 C, CH_{arom}), 129.4 (d, 1 C, CH_{arom}), 130.9 (d, 2 C, CH_{arom}), 131.9 (s, 1 C, Cq_{arom}), 134.4 (d, 1 C, CH_{arom}), 134.3 (s, 1 C, Cq_{arom}), 159.6 (s, 1 C, Cq_{arom}), 166.6 (s, 1 C, C=O).

Minor *Z*-isomer: quantity too low to assign peaks.

HRMS: (mixture of stereoisomers, ESI/MeOH)

m/z: calcd for $C_{18}H_{16}O_2NBr$ $(M+Na)^+$: 380.0257, found: 380.0252 ± 1 ppm.

8.3.5.2.6 Synthesis of 2-(2-bromoethyl)-3-(4-methylbenzylidene)-2,3-dihydro-1H-isoindol-1-one (38f) [Experiment 84]
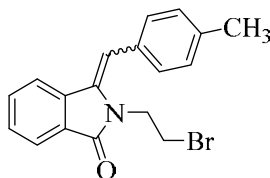
General procedure 11 was followed using 1.44 g of photoproduct **37f**, 3 drops of conc. H_2SO_4 and 30 mL of CH_2Cl_2. After workup, 1.29 g (94%) of product were obtained as a yellow oil.

IR: (film)

$\widetilde{v}$ (cm^{-1}) = 3101, 1643, 1628, 1550, 1278, 837 and 678.

¹H-NMR: (mixture of stereoisomers, 300 MHz, $CDCl_3$)

Main *E*-isomer:

δ (ppm): 2.43 (s, 3 H, CH₃), 3.62 (t, J = 9 Hz, 2 H, CH₂Br), 4.29 (t, J = 9 Hz, 2 H, NCH₂), 6.59 (s, 1 H, CH_olef), 7.33-7.46 (m, 6 H, CH_arom), 7.85 (d, J = 6 Hz, 1 H, CH_arom).

Minor Z-isomer: quantity too low to assign peaks.

¹³C-NMR: (mixture of stereoisomers, 75 MHz, CDCl₃)

Main E-isomer:

δ (ppm): 21.0 (q, 1 C, CH₃), 27.8 (t, 1 C, CH₂Br), 41.1 (t, 1 C, NCH₂), 106.9 (d, 1 C, CH_olef), 115.9 (d, 1 C, CH_arom), 120.2 (d, 1 C, CH_arom), 123.6 (d, 1 C, CH_arom), 123.6 (s, 1 C, Cq_arom), 125.9 (d, 1 C, CH_arom), 126.9 (s, 1 C, Cq_arom), 129.1 (d, 1 C, CH_arom), 129.8 (d, 1 C, CH_arom), 130.2 (d, 1 C, CH_arom), 131.4 (s, 1 C, Cq_arom), 134.7 (d, 1 C, CH_arom), 135.1 (s, 1 C, Cq_arom), 138.4 (s, 1 C, Cq_arom), 167.8 (s, 1 C, C=O).

Minor Z-isomer: quantity too low to assign peaks.

HRMS: (mixture of stereoisomers, ESI/MeOH)

m/z: calcd for $C_{18}H_{16}NOBr$ (M+Na)⁺: 364.0307, found: 364.0307 ± 1 ppm.

8.3.5.2.7 Synthesis of 2-(2-bromoethyl)-3-(2-methylbenzylidene)-2,3-dihydro-1H-isoindol-1-one (38g) [Experiment 85]

General procedure 11 was followed using 1.44 g of photoproduct **37g**, 3 drops of conc. H₂SO₄ and 30 mL of CH₂Cl₂. Workup furnished 1.23 g (90%) of product as a yellow oil.

IR: (film)

$\widetilde{\nu}$ (cm⁻¹) = 3130, 1633, 1600, 1572, 1260, 832 and 681.

¹H-NMR: (mixture of stereoisomers, 300 MHz, CDCl₃)

Main E-isomer:

δ (ppm): 2.31 (s, 3 H, CH₃), 3.66 (t, J = 9 Hz, 2 H, CH₂Br), 4.12 (t, J = 9 Hz, 2 H, NCH₂), 6.56 (s, 1 H, CH_olef), 6.96 (d, J = 6 Hz, 1 H, CH_arom), 7.29-7.44 (m, 5 H, CH_arom), 7.73-7.89 (m, 2 H, CH_arom).

Minor Z-isomer: quantity too low to assign peaks.

¹³C-NMR: (mixture of stereoisomers, 75 MHz, CDCl₃)

Main E-isomer:

δ (ppm): 21.3 (q, 1 C, CH₃), 27.3 (t, 1 C, CH₂Br), 40.0 (t, 1 C, NCH₂), 107.0 (d, 1 C, CH_olef), 117.3 (d, 1 C, CH_arom), 121.7 (d, 1 C, CH_arom), 123.1 (s, 1 C, Cq_arom), 123.8 (d, 1 C,

CH$_{arom}$), 126.9 (s, 1 C, Cq$_{arom}$), 128.9 (d, 1 C, CH$_{arom}$), 129.7 (d, 1 C, CH$_{arom}$), 130.9 (d, 2 C, CH$_{arom}$), 131.5 (s, 1 C, Cq$_{arom}$), 134.3 (d, 1 C, CH$_{arom}$), 135.1 (s, 1 C, Cq$_{arom}$), 138.9 (s, 1 C, Cq$_{arom}$), 167.5 (s, 1 C, C=O).

Minor Z-isomer: quantity too low to assign peaks.

HRMS: (mixture of stereoisomers, ESI/MeOH)

m/z: calcd for C$_{18}$H$_{16}$NOBr (M+Na)$^+$: 364.0307, found: 364.0305 ± 1 ppm.

8.3.5.2.8 Synthesis of 2-(2-bromoethyl)-3-(3-methylbenzylidene)-2,3-dihydro-1H-isoindol-1-one (38h) [Experiment 86]
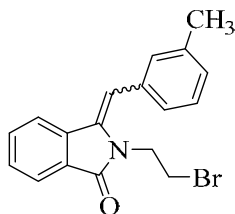
General procedure 11 was followed using 1.44 g of photoproduct **37h**, 3 drops of conc. H$_2$SO$_4$ and 30 mL of CH$_2$Cl$_2$. After workup, 1.14 g (83%) of product were obtained as a yellow oil.

IR: (film)

$\widetilde{\nu}$ (cm^{-1}) = 3129, 1632, 1601, 1565, 1282, 841 and 678.

^{1}H-NMR: (mixture of stereoisomers, 300 MHz, CDCl$_3$)

Main E-isomer:

δ (ppm): 2.40 (s, 3 H, CH$_3$), 3.62 (t, J = 6 Hz, 2 H, CH$_2$Br), 4.12 (t, J = 6 Hz, 2 H, NCH$_2$), 6.60 (s, 1 H, CH$_{olef}$), 7.13-7.23 (m, 2 H, CH$_{arom}$), 7.30-7.36 (m, 2 H, CH$_{arom}$), 7.40-7.46 (m, 1 H, CH$_{arom}$), 7.73-7.77 (m, 1 H, CH$_{arom}$), 7.83-7.89 (m, 2 H, CH$_{arom}$).

Minor Z-isomer: quantity too low to assign peaks.

^{13}C-NMR: (mixture of stereoisomers, 75 MHz, CDCl$_3$)

Main E-isomer:

δ (ppm): 21.0 (q, 1 C, CH$_3$), 27.5 (t, 1 C, CH$_2$Br), 40.3 (t, 1 C, NCH$_2$), 110.4 (d, 1 C, CH$_{olef}$), 114.5 (d, 1 C, CH$_{arom}$), 120.3 (d, 1 C, CH$_{arom}$), 122.6 (d, 1 C, CH$_{arom}$), 123.6 (s, 1 C, Cq), 126.9 (s, 1 C, Cq$_{arom}$), 129.1 (d, 1 C, CH$_{arom}$), 129.8 (d, 1 C, CH$_{arom}$), 130.5 (d, 1 C, CH$_{arom}$), 130.9 (d, 1 C, CH$_{arom}$), 131.2 (s, 1 C, Cq$_{arom}$), 133.9 (d, 1 C, CH$_{arom}$), 135.3 (s, 1 C, Cq$_{arom}$), 138.7 (s, 1 C, Cq$_{arom}$), 167.6 (s, 1 C, C=O).

Minor Z-isomer: quantity too low to assign peaks.

HRMS: (mixture of stereoisomers, ESI/MeOH)

m/z: calcd for C$_{18}$H$_{16}$NOBr (M+Na)$^+$: 364.0307, found: 364.0309 ± 1 ppm.

8.3.5.2.9 Synthesis of 3-benzylidene-2-(3-bromopropyl)-2,3-dihydro-1H-isoindol-1-one (38i) [Experiment 87]
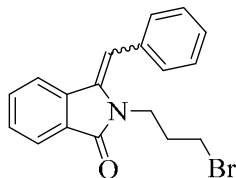
General procedure 11 was followed using 1.44 g of photoproduct **37i**, 3 drops of conc. H_2SO_4 and 30 mL of CH_2Cl_2. After workup, 1.135 g (83%) of product were obtained as a yellow oil.

IR: (film)

$\widetilde{\nu}$ $(cm^{-1}) = 3148, 1633, 1663, 1574, 1327, 841$ and 680.

^{1}H-NMR: (mixture of stereoisomers, 300 MHz, CDCl$_3$)

Main *E*-isomer:

δ (ppm): 2.34 (m, 2 H, CH$_2$), 3.52 (t, J = 9 Hz, 2 H, CH$_2$Br), 4.05 (t, J = 9 Hz, 2 H, NCH$_2$), 6.60 (s, 1 H, CH$_{olef}$), 7.29-7.32 (m, 2 H, CH$_{arom}$), 7.42-7.46 (m, 6 H, CH$_{arom}$), 7.83 (d, J = 9 Hz, 1 H, CH$_{arom}$).

Minor *Z*-isomer: quantity too low to assign peaks.

^{13}C-NMR: (mixture of stereoisomers, 75 MHz, CDCl$_3$)

Main *E*-isomer:

δ (ppm): 30.7 (t, 1 C, CH$_2$), 31.5 (t, 1 C, CH$_2$Br), 38.1 (t, 1 C, NCH$_2$), 110.5 (d, 1 C, CH$_{olef}$), 123.2 (d, 1 C, CH$_{arom}$), 123.3 (d, 1 C, Cq$_{arom}$), 128.0 (d, 1 C, CH$_{arom}$), 128.4 (d, 2 C, CH$_{arom}$), 128.8 (d, 2 C, CH$_{arom}$), 129.6 (d, 1 C, Cq$_{arom}$), 131.7 (d, 1 C, CH$_{arom}$), 135.0 (s, 1 C, Cq$_{arom}$), 136.1 (s, 1 C, Cq$_{arom}$), 136.1 (s, 1 C, Cq$_{arom}$), 166.8 (s, 1 C, C=O).

Minor *Z*-isomer: quantity too low to assign peaks.

HRMS: (mixture of stereoisomers, ESI/MeOH)

m/z: calcd for C$_{18}$H$_{16}$NOBr (M+Na)$^+$: 364.0307, found: 364.0316 ± 3 ppm.

8.3.5.2.10 Synthesis of 2-(3-bromopropyl)-3-(4-fluorobenzylidene)-2,3-dihydro-1H-isoindol-1-one (38j) [Experiment 88]
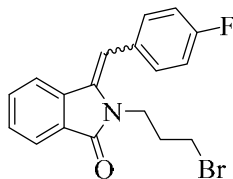
General procedure 11 was followed using 1.51 g of photoproduct **37j**, 3 drops of conc. H_2SO_4 and 30 mL of CH_2Cl_2. After workup, 1.38 g (91%) of product were obtained as a yellow oil.

IR: (film)

$\widetilde{v}$ (cm^{-1}) = 3129, 1654, 1663, 1582, 1151, 825 and 683.

^{1}H-NMR: (mixture of stereoisomers, 300 MHz, CDCl$_3$)

Main *E*-isomer:

δ (ppm): 2.33 (t, J = 6 Hz, 2 H, CH$_2$), 3.51(t, J = 6 Hz, 2 H, CH$_2$Br), 4.04 (t, J = 6 Hz, 2 H, NCH$_2$), 6.54 (s, 1 H, CH$_{olef}$), 7.14 (dd, J = 3, 6 Hz, 2 H, CH$_{arom}$), 7.31-7.47 (m, 5 H, CH$_{arom}$), 7.84 (d, J = 6 Hz, 1 H, CH$_{arom}$).

Minor *Z*-isomer: quantity too low to assign peaks.

^{13}C-NMR: (mixture of stereoisomers, 75 MHz, CDCl$_3$)

Main *E*-isomer:

δ (ppm): 27.8 (t, 1 C, CH$_2$), 30.6 (t, 1 C, CH$_2$Br), 39.3 (t, 1 C, NCH$_2$), 110.9 (d, 1 C, CH$_{olef}$), 114.6 (d, 1 C, CH$_{arom}$), 119.4 (d, 1 C, CH$_{arom}$), 123.1 (d, 1 C, CH$_{arom}$), 126.9 (d, 1 C, Cq$_{arom}$), 129.1 (d, 1 C, CH$_{arom}$), 129.4 (d, 1 C, CH$_{arom}$), 129.8 (d, 1 C, CH$_{arom}$), 130.9 (d, 1 C, CH$_{arom}$), 131.7 (d, 1 C, Cq$_{arom}$), 132.3 (d, 1 C, CH$_{arom}$), 135.1 (s, 1 C, Cq$_{arom}$), 138.4 (s, 1 C, Cq$_{arom}$), 159.5 (s, 1 C, Cq$_{arom}$), 167.8 (s, 1 C, C=O).

Minor *Z*-isomer: quantity too low to assign peaks.

HRMS: (mixture of stereoisomers, ESI/MeOH)

m/z: calcd for C$_{18}$H$_{15}$NOBrF (M+Na)$^+$: 382.0213, found: 382.0215 ± 1 ppm.

8.3.5.2.11 Synthesis of 2-(3-bromopropyl)-3-(4-chlorobenzylidene)-2,3-dihydro-1H-isoindol-1-one (38k) [Experiment 89]

General procedure 11 was followed using 1.58 g of photoproduct **37k**, 3 drops of conc. H$_2$SO$_4$ and 30 mL of CH$_2$Cl$_2$. Workup furnished 1.35 g (90%) of product as a yellow oil.

IR: (film)

$\widetilde{v}$ (cm^{-1}) = 3156, 1680, 1639, 1580, 1346, 828 and 678.

^{1}H-NMR: (mixture of stereoisomers, 300 MHz, CDCl$_3$)

Main *E*-isomer:

δ (ppm): 2.33 (t, J = 9 Hz, 2 H, CH$_2$), 3.51 (t, J = 9 Hz, 2 H, CH$_2$Br), 4.04 (t, J = 9 Hz, 2 H, NCH$_2$), 6.39 (s, 1 H, CH$_{olef}$), 7.34 (t, J = 3, 9 Hz, 3 H, CH$_{arom}$), 7.41 (s, 4 H, CH$_{arom}$), 7.84 (d, J = 9 Hz, 1 H, CH$_{arom}$).

Minor *Z*-isomer: quantity too low to assign peaks.

^{13}C-NMR: (mixture of stereoisomers, 75 MHz, CDCl$_3$)

Main *E*-isomer:

δ (ppm): 28.1 (t, 1 C, CH$_2$), 30.6 (t, 1 C, CH$_2$Br), 41.0 (t, 1 C, NCH$_2$), 110.4 (d, 1 C, CH$_{olef}$), 114.2 (d, 1 C, CH$_{arom}$), 119.4 (d, 1 C, CH$_{arom}$), 123.3 (d, 1 C, CH$_{arom}$), 123.6 (d, 1 C, Cq$_{arom}$), 129.2 (d, 1 C, CH$_{arom}$), 129.3 (d, 1 C, CH$_{arom}$), 130.6 (d, 1 C, CH$_{arom}$), 130.9 (d, 1 C, CH$_{arom}$), 131.5 (d, 1 C, Cq$_{arom}$), 134.3 (d, 1 C, CH$_{arom}$), 135.2 (s, 1 C, Cq$_{arom}$), 138.4 (s, 1 C, Cq$_{arom}$), 159.4 (s, 1 C, Cq$_{arom}$), 166.5 (s, 1 C, C=O).

Minor *Z*-isomer: quantity too low to assign peaks.

HRMS: (mixture of stereoisomers, ESI/MeOH)

m/z: calcd for C$_{18}$H$_{15}$NOBrCl (M+Na)$^+$: 397.9918, found: 397.9924 ± 2 ppm.

8.3.5.2.12 Synthesis of 3-(4-bromobenzylidene)-2-(3-bromopropyl)-2,3-dihydro-1H-isoindol-1-one (38l) [Experiment 90]
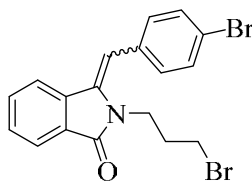
General procedure 11 was followed using 1.76 g of photoproduct **37l**, 3 drops of conc. H$_2$SO$_4$ and 30 mL of CH$_2$Cl$_2$. After workup, 1.41 g (84%) of product were obtained as a yellowish solid.

Melting point: 134-135°C.

IR: (film)

$\widetilde{\nu}$ (cm^{-1}) = 3122, 1676, 1550, 1465, 1338, 832 and 681.

^{1}H-NMR: (mixture of stereoisomers, 300 MHz, CDCl$_3$)

Main *E*-isomer:

δ (ppm): 2.32 (t, J = 6 Hz, CH$_2$), 3.51 (t, J = 6 Hz, 2 H, CH$_2$Br), 4.03 (t, J = 6 Hz, 2 H, NCH$_2$), 6.49 (s, 1 H, CH$_{olef}$), 7.32 (m, 1 H, CH$_{arom}$), 7.35 (s, 2 H, CH$_{arom}$), 7.45 (dd, J = 2, 6 Hz, 2 H, CH$_{arom}$), 7.57 (d, J = 6 Hz, 2 H, CH$_{arom}$), 7.84 (d, J = 6 Hz, 1 H, CH$_{arom}$).

Minor *Z*-isomer: quantity too low to assign peaks.

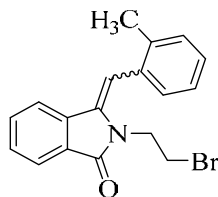**^{13}C-NMR:** (mixture of stereoisomers, 75 MHz, CDCl$_3$)

Main *E*-isomer:

δ (ppm): 30.3 (t, 1 C, CH$_2$), 32.5 (t, 1 C, CH$_2$Br), 39.0 (t, 1 C, NCH$_2$), 109.6 (d, 1 C, CH$_{olef}$), 114.9 (d, 1 C, CH$_{arom}$), 122.1 (d, 1 C, CH$_{arom}$), 125.0 (d, 1 C, Cq$_{arom}$), 128.7 (d, 1 C, CH$_{arom}$), 129.2 (d, 2 C, CH$_{arom}$), 130.9 (d, 2 C, CH$_{arom}$), 131.5 (d, 1 C, Cq$_{arom}$), 132.6 (d, 1 C, CH$_{arom}$), 135.5 (s, 1 C, Cq$_{arom}$), 137.1 (s, 1 C, Cq$_{arom}$), 145.1 (s, 1 C, Cq$_{arom}$), 167.5 (s, 1 C, C=O).

Minor Z-isomer: quantity too low to assign peaks.

HRMS: (mixture of stereoisomers, ESI/MeOH)

m/z: calcd for $C_{18}H_{15}NOBr_2$ (M+Na)$^+$: 441.9413, found: 441.9433 ± 5 ppm.

8.3.5.2.13 Synthesis of 2-(3-bromopropyl)-3-(4-methoxybenzylidene)-2,3-dihydro-1H-isoindol-1-one (38m) [Experiment 91]
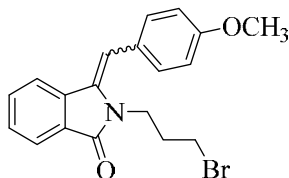
General procedure 11 was followed using 1.56 g of photoproduct **37m**, 3 drops of conc. H_2SO_4 and 30 mL of CH_2Cl_2. After wokup, 1.41 g (95%) of product were obtained as a yellowish solid.

Melting point: 126°C.

IR: (film)

$\widetilde{v}$ (cm^{-1}) = 3145, 1684, 1600, 1567, 1378, 1248, 880 and 649.

^{1}H-NMR: (mixture of stereoisomers, 300 MHz, CDCl$_3$)

Main E-isomer:

δ (ppm): 2.30-2.35 (m, 2 H, CH$_2$), 3.64 (t, J = 6 Hz, 2 H, CH$_2$Br), 3.90 (s, 3 H, OCH$_3$), 4.07 (t, J = 6 Hz, 2 H, NCH$_2$), 6.77 (s, 1 H, CH$_{olef}$), 7.06 (d, J = 9 Hz, 2 H, CH$_{arom}$), 7.44-7.46 (m, 5 H, CH$_{arom}$), 7.79 (d, J = 9 Hz, 1 H, CH$_{arom}$).

Minor Z-isomer: quantity too low to assign peaks.

^{13}C-NMR: (mixture of stereoisomers, 75 MHz, CDCl$_3$)

Main E-isomer:

δ (ppm): 30.7 (t, 1 C, CH$_2$), 31.6 (t, 1 C, CH$_2$Br), 38.0 (t, 1 C, NCH$_2$), 55.3 (q, 1 C, OCH$_3$), 110.4 (d, 1 C, CH$_{olef}$), 114.2 (d, 1 C, CH$_{arom}$), 123.2 (d, 1 C, CH$_{arom}$), 123.5 (d, 1 C, Cq), 127.2 (d, 1 C, CH$_{arom}$), 127.3 (d, 2 C, CH$_{arom}$), 129.2 (d, 2 C, CH$_{arom}$), 129.4 (d, 1 C, Cq$_{arom}$), 130.2 (d, 1 C, CH$_{arom}$), 132.0 (s, 1 C, Cq$_{arom}$), 134.1 (s, 1 C, Cq$_{arom}$), 159.6 (s, 1 C, Cq$_{arom}$), 166.7 (s, 1 C, C=O).

Minor Z-isomer: quantity too low to assign peaks.

HRMS: (mixture of stereoisomers, ESI/MeOH)

m/z: calcd for $C_{19}H_{18}O_2NBr$ (M+Na)$^+$: 394.0413, found: 394.0421 ± 2 ppm.

8.3.5.2.14 Synthesis of 2-(3-bromopropyl)-3-(4-methylbenzylidene)-2,3-dihydro-1H-isoindol-1-one (38n) [Experiment 92]
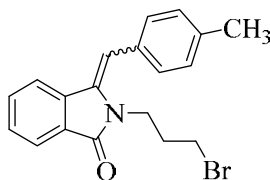
General procedure 11 was followed using 1.50 g of photoproduct **37n**, 3 drops of conc. H_2SO_4 and 30 mL of CH_2Cl_2. After wokup, 1.31 g (92%) of product were obtained as a yellow oil.

IR: (film)

$\tilde{\nu}$ (cm^{-1}) = 3101, 1679, 1602, 1581, 1372, 846 and 669.

^{1}H-NMR: (mixture of stereoisomers, 300 MHz, CDCl$_3$)

Main *E*-isomer:

δ (ppm): 2.31-2.36 (m, 2 H, CH$_2$), 2.43 (s, 3 H, CH$_3$), 3.51 (t, J = 6 Hz, 2 H, CH$_2$Br), 4.04(t, J = 6 Hz, 2 H, NCH$_2$), 6.58 (s, 1 H, CH$_{olef}$), 7.23-7.29 (m, 1 H, CH$_{arom}$), 7.32-7.45 (m, 6 H, CH$_{arom}$), 7.83 (d, J = 6 Hz, 1 H, CH$_{arom}$).

Minor *Z*-isomer: quantity too low to assign peaks.

^{13}C-NMR: (mixture of stereoisomers, 75 MHz, CDCl$_3$)

Main *E*-isomer:

δ (ppm): 21.3 (q, 1 C, CH$_3$), 28.3 (t, 1 C, CH$_2$), 30.6 (t, 1 C, CH$_2$Br),41.3 (t, 1 C, NCH$_2$), 107.1 (d, 1 C, CH$_{olef}$), 114.2 (d, 1 C, CH$_{arom}$), 119.1 (d, 1 C, CH$_{arom}$), 123.0 (d, 1 C, CH$_{arom}$), 123.5 (d, 1 C, Cq$_{arom}$), 127.9 (d, 1 C, CH$_{arom}$), 129.2 (d, 1 C, CH$_{arom}$), 130.9 (d, 1 C, CH$_{arom}$), 131.3 (d, 1 C, CH$_{arom}$), 131.6 (d, 1 C, Cq$_{arom}$), 134.5 (d, 1 C, CH$_{arom}$), 135.7 (s, 1 C, Cq$_{arom}$), 138.0 (s, 1 C, Cq$_{arom}$), 141.4 (s, 1 C, Cq$_{arom}$), 166.5 (s, 1 C, C=O).

Minor *Z*-isomer: quantity too low to assign peaks.

HRMS: (mixture of stereoisomers, ESI/MeOH)

m/z: calcd for C$_{19}$H$_{18}$NOBr (M+Na)$^+$: 378.0464, found: 378.0471 ± 2 ppm.

8.3.5.2.15 Synthesis of 2-(3-bromopropyl)-3-(2-methylbenzylidene)-2,3-dihydro-1H-isoindol-1-one (38o) [Experiment 93]

General procedure 11 was followed using 1.50 g of photoproduct **37o**, 3 drops of conc. H_2SO_4 and 30 mL of CH_2Cl_2. Workup furnished 1.18 g (83%) of product as a yellow oil.

IR: (film)

$\widetilde{v}$ (cm^{-1}) = 3137, 1680, 1635, 1578, 1291, 830 and 691.

^{1}H-NMR: (mixture of stereoisomers, 300 MHz, CDCl$_3$)

Main *E*-isomer:

δ (ppm): 2.31-2.36 (m, 2 H, CH$_2$), 2.40 (s, 3 H, CH$_3$), 3.51 (t, J = 9 Hz, 2 H, CH$_2$Br), 4.05(t, J = 9 Hz, 2 H, NCH$_2$), 6.58 (s, 1 H, CH$_{olef}$), 7.02-7.25 (m, 2 H, CH$_{arom}$), 7.27-7.33 (m, 4 H, CH$_{arom}$), 7.39-7.45 (m, 1 H, CH$_{arom}$),7.84 (d, J = 9 Hz, 1 H, CH$_{arom}$).

Minor *Z*-isomer: quantity too low to assign peaks.

^{13}C-NMR: (mixture of stereoisomers, 75 MHz, CDCl$_3$)

Main *E*-isomer:

δ (ppm): 21.2 (t, 1 C, CH$_2$), 28.1 (t, 1 C, CH$_2$), 30.6 (t, 1 C, CH$_2$Br),40.9 (t, 1 C, NCH$_2$), 109.4 (d, 1 C, CH$_{olef}$), 114.2 (d, 1 C, CH$_{arom}$), 119.4 (d, 1 C, CH$_{arom}$), 122.3 (d, 1 C, CH$_{arom}$), 123.7 (d, 1 C, Cq$_{arom}$), 129.2 (d, 1 C, CH$_{arom}$), 129.7 (d, 1 C, CH$_{arom}$), 130.1 (d, 1 C, CH$_{arom}$), 130.5 (d, 1 C, CH$_{arom}$), 131.2 (d, 1 C, Cq$_{arom}$), 134.0 (d, 1 C, CH$_{arom}$), 135.2 (s, 1 C, Cq$_{arom}$), 138.5 (s, 1 C, Cq$_{arom}$), 141.7 (s, 1 C, Cq$_{arom}$), 166.2 (s, 1 C, C=O).

Minor *Z*-isomer: quantity too low to assign peaks.

HRMS: (mixture of stereoisomers, ESI/MeOH)

m/z: calcd for $C_{19}H_{18}NOBr$ (M+Na)$^+$: 378.0464, found: 378.0473 ± 2 ppm.

8.3.5.2.16 Synthesis of 2-(3-bromopropyl)-3-(3-methylbenzylidene)-2,3-dihydro-1H-isoindol-1-one (38p) [Experiment 94]
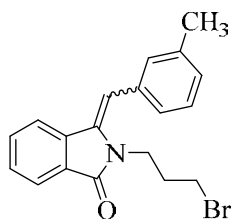
General procedure 11 was followed using 1.50 g of photoproduct **37o**, 3 drops of conc. H_2SO_4 and 30 mL of CH_2Cl_2. After workup, 1.31 g (92%) of product were obtained as a yellow oil.

IR: (film)

$\widetilde{v}$ (cm^{-1}) = 3098, 1682, 1640, 1580, 1250, 832 and 694.

^{1}H-NMR: (mixture of stereoisomers, 300 MHz, CDCl$_3$)

Main *E*-isomer:

δ (ppm): 2.26 (s, 3 H, CH$_3$), 2.30 (t, J = 6 Hz, 2 H, CH$_2$), 3.47 (t, J = 6 Hz, 2 H, CH$_2$Br), 4.02 (t, J = 9 Hz, 2 H, NCH$_2$), 6.51 (s, 1 H, CH$_{olef}$), 6.92 (d, J = 9 Hz, 1 H, CH$_{arom}$), 7.18-7.22 (m, 2 H, CH$_{arom}$), 7.24-7.27 (m, 2 H, CH$_{arom}$), 7.30-7.38 (m, 2 H, CH$_{arom}$), 7.78 (d, J = 9 Hz, 1 H, CH$_{arom}$).

Minor *Z*-isomer: quantity too low to assign peaks.
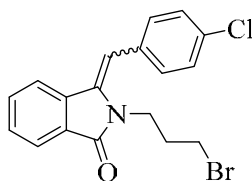
**¹³C-NMR:** (mixture of stereoisomers, 75 MHz, CDCl$_3$)

Main *E*-isomer:

δ (ppm): 20.9 (t, 1 C, CH$_2$), 28.1 (t, 1 C, CH$_2$), 30.9 (t, 1 C, CH$_2$Br), 40.7 (t, 1 C, NCH$_2$), 109.6 (d, 1 C, CH$_{olef}$), 114.5 (d, 1 C, CH$_{arom}$), 119.2 (d, 1 C, CH$_{arom}$), 123.2 (d, 1 C, CH$_{arom}$), 123.4 (d, 1 C, Cq$_{arom}$), 129.2 (d, 1 C, CH$_{arom}$), 129.6 (d, 1 C, CH$_{arom}$), 130.3 (d, 1 C, CH$_{arom}$), 130.9 (d, 1 C, CH$_{arom}$), 131.1 (d, 1 C, Cq$_{arom}$), 134.9 (d, 1 C, CH$_{arom}$), 135.5 (s, 1 C, Cq$_{arom}$), 138.6 (s, 1 C, Cq$_{arom}$), 141.3 (s, 1 C, Cq$_{arom}$), 166.5 (s, 1 C, C=O).

Minor *Z*-isomer: quantity too low to assign peaks.

HRMS: (mixture of stereoisomers, ESI/MeOH)

m/z: calcd for C$_{19}$H$_{18}$NOBr (M+Na)$^+$: 378.0464, found: 378.0490 ± 7 ppm .

8.3.5.3   Amination of dehydrated product under batch conditions [Experiments 95-118]

General procedure 12 (GP12): A mixture of an amine (1.1 eq.), dehydrated product **38a-p** (1 eq.), KI (a tip of a spatula) and K$_2$CO$_3$ (1.5 eq.) in 10 mL DMF was heated to 100ºC for 3 hours. After cooling down to room temperature, an excess of water was added and the solution was acidified using 1 M HCl. The solution was subsequently washed with ethyl acetate (50 mL). The aqueous layer containing the target compound was then basified to pH 10 using ammonia solution and extracted with CH$_2$Cl$_2$ (3 × 50 mL). The combined organic phase was collected, washed with brine (1 × 50 mL) and dried over MgSO$_4$. The dried organic layer was evaporated to dryness by rotary evaporation. In most of cases, ¹H-NMR showed the presence of both, *E*- and *Z*-isomer, with a large preference for the *Z*-isomer.

8.3.5.3.1   Synthesis of 3-benzylidene-2-[2-(diethylamino)ethyl]-2,3-dihydro-1H-isoindol-1-one (39a) [Experiment 95]
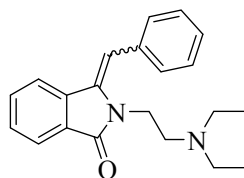
General procedure 12 was followed using 0.34 mL of diethylamine, 0.98 g dehydrated product **38a**, catalytic amounts of KI, 0.62 g K_2CO_3 and 10 mL of DMF. After workup, 0.54 g (55%) of product were obtained as a brownish solid.

Melting point: 43°C.

IR: (film)

$\tilde{v}$ (cm^{-1}) = 3132, 1645, 1612, 1574, 1300, 824 and 691.

^{1}H-NMR: (mixture or stereoisomers, 300 MHz, CDCl$_3$)

Main Z-isomer:

δ (ppm): 1.13 (t, J = 9 Hz, 6 H, 2 × CH$_3$), 2.67-2.74 (m, 4 H, N(CH$_2$)$_2$), 2.83 (t, J = 9 Hz, 2 H, NCH$_2$), 4.04 (t, J = 9 Hz, 2 H, NCH$_2$), 6.68 (s, 1 H, CH$_{olef}$), 7.33-7.49 (m, 8 H, CH$_{arom}$), 7.87 (dd, J = 9, 9 Hz, 1 H, CH$_{arom}$).

Minor E-isomer: quantity too low to assign peaks.

^{13}C-NMR: (mixture of stereoisomers, 75 MHz, CDCl$_3$)

Main E-isomer:

δ (ppm): 12.1 (q, 2 C, CH$_3$), 39.2 (t, 1 C, CH$_2$N), 47.1 (t, 2 C, N(CH$_2$)$_2$), 50.3 (t, 1 C, NCH$_2$), 106.4 (d, 1 C, CH$_{olef}$), 119.3 (d, 1 C, CH$_{arom}$), 123.3 (s, 1 C,Cq), 127.7 (d, 1 C, CH$_{arom}$), 128.4 (d, 2 C, CH$_{arom}$), 128.5 (d, 1 C, CH$_{arom}$), 129.0 (d, 2 C, CH$_{arom}$), 129.8 (s, 1 C, Cq$_{arom}$), 131.9 (d, 1 C, CH$_{arom}$), 134.9 (s, 1 C, Cq$_{arom}$), 135.0 (s, 1 C, Cq$_{arom}$), 138.6 (s, 1 C, Cq$_{arom}$), 169.0 (s, 1 C, C=O).

Minor E-isomer: quantity too low to assign peaks.

HRMS: (mixture of stereoisomers, ESI/MeOH)

m/z: calcd for $C_{21}H_{24}ON_2$ (M+Na)$^+$: 343.1781, found: 343.1792 ± 3 ppm.

8.3.5.3.2 Synthesis of 2-[2-(diethylamino)ethyl]-3-(4-fluorobenzylidene)-2,3-dihydro-1H-isoindol-1-one (39b) [Experiment 96]
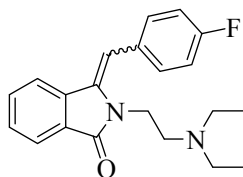
General procedure 12 was followed using 0.34 mL of diethylamine, 1.04 g dehydrated product **38b**, catalytic amounts of KI, 0.62 g K_2CO_3 and 10 mL of DMF. After workup, 0.59 g (55%) of product were obtained as a brownish oil.

IR: (film)

$\tilde{v}$ (cm^{-1}) = 3140, 1680, 1624, 1550, 1154, 819 and 653.

^{1}H-NMR: (mixture or stereoisomers, 300 MHz, CDCl$_3$)

Main Z-isomer:

δ (ppm): 1.03 (t, J = 9 Hz, 6 H, 2 × CH$_3$), 2.60-2.70 (m, 4 H, N(CH$_2$)$_2$), 2.80 (t, J = 9 Hz, 2 H, CH$_2$Br), 4.00 (t, J = 9 Hz, 2 H, NCH$_2$), 6.65 (s, 1 H, CH$_{olef}$), 7.23-7.27 (m, 2 H, CH$_{arom}$), 7.32-7.40 (m, 5 H, CH$_{arom}$), 7.84 (dd, J = 9, 9 Hz, 1 H, CH$_{arom}$).

Minor E-isomer: quantity too low to assign peaks.

^{13}C-NMR: (mixture of stereoisomers, 75 MHz, CDCl$_3$)

Main E-isomer:

δ (ppm): 12.1 (q, 2 C, CH$_3$), 38.9 (t, 1 C, CH$_2$N), 47.2 (t, 2 C, N(CH$_2$)$_2$), 50.5 (t, 1 C, NCH$_2$), 107.1 (d, 1 C, CH$_{olef}$), 119.7 (d, 1 C, CH$_{arom}$), 123.2 (s, 1 C, Cq), 127.3 (d, 1 C, CH$_{arom}$), 128.5 (d, 2 C, CH$_{arom}$), 129.0 (d, 1 C, CH$_{arom}$), 130.7 (d, 2 C, CH$_{arom}$), 131.5 (s, 1 C, Cq$_{arom}$), 134.3 (d, 1 C, CH$_{arom}$), 135.3 (s, 1 C, Cq$_{arom}$), 138.4 (s, 1 C, Cq$_{arom}$), 159.7 (s, 1 C, Cq$_{arom}$), 166.5 (s, 1 C, C=O).

Minor E-isomer: quantity too low to assign peaks.

HRMS: (mixture of stereoisomers, ESI/MeOH)

m/z: calcd for C$_{21}$H$_{23}$N$_2$OF (M+Na)$^+$: 361.1687, found: 361.1678 ± 1 ppm.

8.3.5.3.3 Synthesis of 2-[2-(diethylamino)ethyl]-3-(4-chlorobenzylidene)-2,3-dihydro-1H-isoindol-1-one (39c) [Experiment 97]
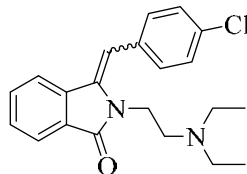
General procedure 12 was followed using 0.34 mL of diethylamine, 1.09 g dehydrated product **38c**, catalytic amounts of KI, 0.62 g K$_2$CO$_3$ and 10 mL of DMF. After workup, 0.56 g (53%) of product were obtained as a brownish oil.

IR: (film)

$\widetilde{v}$ (cm^{-1}) = 3102, 1632, 1600, 1548, 1378, 855 and 671.

^{1}H-NMR: (mixture or stereoisomers, 300 MHz, CDCl$_3$)

Main Z-isomer:

δ (ppm): 1.07 (t, J = 6 Hz, 6 H, 2 × CH$_3$), 2.61-2.68 (m, 4 H, N(CH$_2$)$_2$), 2.76 (t, J = 6 Hz, 2 H, NCH$_2$), 3.97 (t, J = 6 Hz, 2 H, NCH$_2$), 6.53 (s, 1 H, CH$_{olef}$), 7.30-7.45 (m, 7 H, CH$_{arom}$), 7.85 (d, J = 9 Hz, 1 H, CH$_{arom}$).

Minor E-isomer: quantity too low to assign peaks.
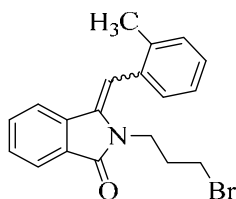
^{13}C-NMR: (mixture of stereoisomers, 75 MHz, CDCl$_3$)

Main E-isomer:

δ (ppm): 12.3 (q, 2 C, CH$_3$), 38.5 (t, 1 C, CH$_2$N), 47.5 (t, 2 C, N(CH$_2$)$_2$), 50.4 (t, 1 C, NCH$_2$), 106.9 (d, 1 C, CH$_{olef}$), 119.3 (d, 1 C, CH$_{arom}$), 123.9 (s, 1 C, Cq), 127.7 (d, 1 C, CH$_{arom}$), 128.0 (d, 2 C, CH$_{arom}$), 129.5 (d, 1 C, CH$_{arom}$), 130.3 (d, 2 C, CH$_{arom}$), 131.8 (s, 1 C, Cq$_{arom}$), 134.8 (d, 1 C, CH$_{arom}$), 135.7 (s, 1 C, Cq$_{arom}$), 138.1 (s, 1 C, Cq$_{arom}$), 150.5 (s, 1 C, Cq$_{arom}$), 166.5 (s, 1 C, C=O).

Minor *E*-isomer: quantity too low to assign peaks.

HRMS: (mixture of stereoisomers, ESI/MeOH)

m/z: calcd for C$_{21}$H$_{23}$N$_2$OCl (M+Na)$^+$: 377.1391, found: 377.1400 ± 2 ppm.

8.3.5.3.4 Synthesis of 2-[2-(diethylamino)ethyl]-3-(4-bromobenzylidene)-2,3-dihydro-1H-isoindol-1-one (39d) [Experiment 98]
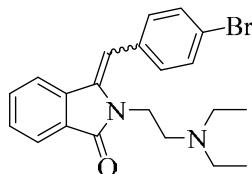
General procedure 12 was followed using 0.34 mL of diethylamine, 1.22 g dehydrated product **38d**, catalytic amounts of KI, 0.62 g K$_2$CO$_3$ and 10 mL of DMF. After workup, 0.61 g (51%) of product were obtained as a brownish oil.

IR: (film)

$\widetilde{\nu}$ (cm^{-1}) = 3140, 1663, 1450, 1568, 1370, 860 and 673.

^{1}H-NMR: (mixture or stereoisomers, 300 MHz, CDCl$_3$)

Main *Z*-isomer:

δ (ppm): 1.11 (t, J = 6 Hz, 6 H, 2 × CH$_3$), 2.65-2.70 (m, 4 H, N(CH$_2$)$_2$), 2.82 (t, J = 9 Hz, 2 H, CH$_2$Br), 4.14 (t, J = 9 Hz, 2 H, NCH$_2$), 6.57 (s, 1 H, CH$_{olef}$), 7.34-7.41 (m, 5 H, CH$_{arom}$), 7.47 (d, J = 9 Hz, 2 H, CH$_{arom}$), 7.88 (dd, J = 9, 9 Hz, 1 H, CH$_{arom}$).

Minor *E*-isomer: quantity too low to assign peaks.

**^{13}C-NMR:** (mixture of stereoisomers, 75 MHz, CDCl$_3$)

Main *E*-isomer:

δ (ppm): 12.2 (q, 2 C, CH$_3$), 38.1 (t, 1 C, CH$_2$N), 47.3 (t, 2 C, N(CH$_2$)$_2$), 50.7 (t, 1 C, NCH$_2$), 106.2 (d, 1 C, CH$_{olef}$), 119.0 (d, 1 C, CH$_{arom}$), 123.4 (s, 1 C, Cq), 126.9 (d, 1 C, CH$_{arom}$), 128.5 (d, 2 C, CH$_{arom}$), 129.3 (d, 1 C, CH$_{arom}$), 130.7 (d, 2 C, CH$_{arom}$), 131.9 (s, 1 C, Cq$_{arom}$), 134.3 (d, 1 C, CH$_{arom}$), 135.6 (s, 1 C, Cq$_{arom}$), 138.9 (s, 1 C, Cq$_{arom}$), 145.1 (s, 1 C, Cq$_{arom}$), 166.5 (s, 1 C, C=O).

**Minor *E*-isomer:** quantity too low to assign peaks.

HRMS: (mixture of stereoisomers, ESI/MeOH)

m/z: calcd for $C_{21}H_{24}BrON_2$ (M+Na)$^+$: 421.0885, found: 421.0882 $\pm$ 1 ppm.

8.3.5.3.5 Synthesis of 2-[2-(diethylamino)ethyl]-3-(4-methoxybenzylidene)-2,3-dihydro-1H-isoindol-1-one (39e) [Experiment 99]
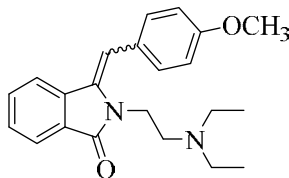
General procedure 12 was followed using 0.34 mL of diethylamine, 1.07 g dehydrated product **38e**, catalytic amounts of KI, 0.62 g K_2CO_3 and 10 mL of DMF. After workup, 0.525 g (50%) of product were obtained as a brownish oil.

IR: (film)

$\widetilde{v}$ (cm^{-1}) = 3130, 1679, 1589, 1371, 1268, 830 and 680.

^{1}H-NMR: (mixture or stereoisomers, 300 MHz, CDCl$_3$)

Main Z-isomer:

δ (ppm): 1.12 (t, J = 9 Hz, 6 H, 2 $\times$ CH$_3$), 2.65-2.72 (m, 4 H, N(CH$_2$)$_2$), 2.81 (t, J = 9 Hz, 2 H, NCH$_2$), 3.92 (s, 3 H, OCH$_3$), 4.02 (t, J = 9 Hz, 2 H, NCH$_2$), 6.61 (s, 1 H, CH$_{olef}$), 7.01 (d, J = 9 Hz, 2 H, CH$_{arom}$), 7.40-7.45 (m, 5 H, CH$_{arom}$), 7.87 (d, J = 9 Hz, 1 H, CH$_{arom}$).

Minor E-isomer: quantity too low to assign peaks.

^{13}C-NMR: (mixture of stereoisomers, 75 MHz, CDCl$_3$)

Main E-isomer:

δ (ppm): 12.0 (q, 2 C, CH$_3$), 38.0 (t, 1 C, CH$_2$N), 47.2 (t, 2 C, N(CH$_2$)$_2$), 50.3 (t, 1 C, NCH$_2$), 55.4 (q, 1 C, OCH$_3$), 106.4 (d, 1 C, CH$_{olef}$), 119.1 (d, 1 C, CH$_{arom}$), 123.1 (s, 1 C,Cq), 127.0 (d, 1 C, CH$_{arom}$), 128.8 (d, 2 C, CH$_{arom}$), 129.1 (d, 1 C, CH$_{arom}$), 130.4 (d, 2 C, CH$_{arom}$), 131.9 (s, 1 C, Cq$_{arom}$), 134.4 (d, 1 C, CH$_{arom}$), 135.8 (s, 1 C, Cq$_{arom}$), 138.7 (s, 1 C, Cq$_{arom}$), 159.3 (s, 1 C, Cq$_{arom}$), 166.5 (s, 1 C, C=O).

Minor E-isomer: quantity too low to assign peaks.

HRMS: (mixture of stereoisomers, ESI/MeOH)

m/z: calcd for $C_{22}H_{26}O_2N_2$ (M+H)$^+$: 351.2067, found: 351.2061 $\pm$ 2 ppm.

calcd for $C_{22}H_{26}O_2N_2$ (M+Na)$^+$: 373.1886, found: 373.1886 $\pm$ 0 ppm.

8.3.5.3.6 Synthesis of 2-[2-(diethylamino)ethyl]-3-(4-methylbenzylidene)-2,3-dihydro-1H-isoindol-1-one (39f) [Experiment 100]
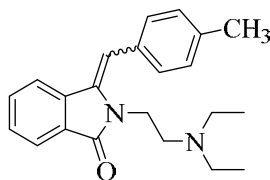
General procedure 12 was followed using 0.34 mL of diethylamine, 1.03 g dehydrated product **38f**, catalytic amounts of KI, 0.62 g K_2CO_3 and 10 mL of DMF. After workup, 0.57 g (57%) of product were obtained as a brownish oil.

IR: (film)

$\tilde{v}$ (cm^{-1}) = 3106, 1634, 1616, 1535, 1257, 820 and 681.

¹H-NMR: (mixture or stereoisomers, 300 MHz, $CDCl_3$)

Main *Z*-isomer:

δ (ppm): 1.12 (t, J = 6 Hz, 6 H, 2 × CH_3), 2.31 (s, 3 H, CH_3), 2.65-2.72 (m, 4 H, $N(CH_2)_2$), 2.81 (t, J = 9 Hz, 2 H, CH_2Br), 4.05 (t, J = 9 Hz, 2 H, NCH_2), 6.59 (s, 1 H, CH_{olef}), 7.14 (d, J = 9 Hz, 2 H, CH_{arom}), 7.35-7.42 (m, 5 H, CH_{arom}), 7.81 (d, J = 9 Hz, 1 H, CH_{arom}).

Minor *E*-isomer: quantity too low to assign peaks.

¹³C-NMR: (mixture of stereoisomers, 75 MHz, $CDCl_3$)

Main *E*-isomer:

δ (ppm): 12.5 (q, 2 C, CH_3), 20.1 (q, 1 C, CH_3), 38.7 (t, 1 C, CH_2N), 45.7 (t, 2 C, $N(CH_2)_2$), 50.2 (t, 1 C, NCH_2), 107.1 (d, 1 C, CH_{olef}), 120.6 (d, 1 C, CH_{arom}), 123.4 (s, 1 C, Cq), 127.7 (d, 1 C, CH_{arom}), 128.0 (d, 2 C, CH_{arom}), 129.9 (d, 1 C, CH_{arom}), 130.7 (d, 2 C, CH_{arom}), 131.0 (s, 1 C, Cq_{arom}), 134.7 (d, 1 C, CH_{arom}), 135.5 (s, 1 C, Cq_{arom}), 138.5 (s, 1 C, Cq_{arom}), 143.7 (s, 1 C, Cq_{arom}), 166.5 (s, 1 C, C=O).

Minor *E*-isomer: quantity too low to assign peaks.

HRMS: (mixture of stereoisomers, ESI/MeOH)

m/z: calcd for $C_{22}H_{26}N_2O$ (M+Na)⁺: 357.1937, found: 357.1934 ± 1 ppm.

8.3.5.3.7 Synthesis of 2-[2-(diethylamino)ethyl]-3-(2-methylbenzylidene)-2,3-dihydro-1H-isoindol-1-one (39g) [Experiment 101]
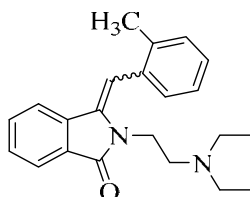
General procedure 12 was followed using 0.34 mL of diethylamine, 1.03 g dehydrated product **38g**, catalytic amounts of KI, 0.62 g K_2CO_3 and 10 mL of DMF. After workup, 0.58 g (58%) of product were obtained as a brownish oil.

IR: (film)

$\widetilde{v}$ (cm^{-1}) = 3231, 1650, 1605, 1563, 1233, 816 and 671.

^{1}H-NMR: (mixture or stereoisomers, 300 MHz, CDCl$_3$)

Main Z-isomer:

δ (ppm): 1.10 (t, J = 6 Hz, 6 H, 2 × CH$_3$), 2.31 (s, 3 H, CH$_3$), 2.65-2.72 (m, 4 H, N(CH$_2$)$_2$), 2.82 (t, J = 9 Hz, 2 H, NCH$_2$),4.00-4.05 (m, 2 H, NCH$_2$), 6.56 (s, 1 H, CH$_{olef}$), 6.98 (d, J = 9 Hz, 2 H, CH$_{arom}$), 7.31-7.42 (m, 5 H, CH$_{arom}$), 7.82 (d, J = 9 Hz, 1 H, CH$_{arom}$).

Minor E-isomer: quantity too low to assign peaks.

^{13}C-NMR: (mixture of stereoisomers, 75 MHz, CDCl$_3$)

Main E-isomer:

δ (ppm): 12.0 (q, 2 C, CH$_3$), 21.3 (q, 1 C, CH$_3$), 38.9 (t, 1 C, CH$_2$N), 47.3 (t, 2 C, N(CH$_2$)$_2$), 50.4 (t, 1 C, NCH$_2$), 106.7 (d, 1 C, CH$_{olef}$), 120.3 (d, 1 C, CH$_{arom}$), 123.7 (s, 1 C, Cq), 127.3 (d, 1 C, CH$_{arom}$), 128.8 (d, 2 C, CH$_{arom}$), 129.3 (d, 1 C, CH$_{arom}$), 130.5 (d, 2 C, CH$_{arom}$), 133.8(s, 1 C, Cq$_{arom}$), 134.0 (d, 1 C, CH$_{arom}$), 135.7 (s, 1 C, Cq$_{arom}$), 138.2 (s, 1 C, Cq$_{arom}$), 140.8 (s, 1 C, Cq$_{arom}$), 166.6 (s, 1 C, C=O).

Minor E-isomer: quantity too low to assign peaks.

HRMS: (mixture of stereoisomers, ESI/MeOH)

m/z: calcd for $C_{22}H_{26}N_2O$ (M+Na)$^+$: 357.1937, found: 357.1934 ± 1 ppm.

8.3.5.3.8 Synthesis of 2-[2-(diethylamino)ethyl]-3-(3-methylbenzylidene)-2,3-dihydro-1H-isoindol-1-one (39h) [Experiment 102]
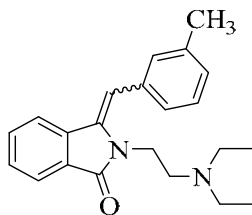
General procedure 12 was followed using 0.34 mL of diethylamine, 1.03 g dehydrated product **38h**, catalytic amounts of KI, 0.62 g K_2CO_3 and 10 mL of DMF. After workup, 0.51 g (51%) of product were obtained as a brownish oil.

IR: (film)

$\widetilde{v}$ (cm^{-1}) = 3130, 1626, 1610, 1580, 1287, 829 and 668.

^{1}H-NMR: (mixture or stereoisomers, 300 MHz, CDCl$_3$)

Main *Z*-isomer:

δ (ppm): 1.09 (t, J = 9 Hz, 6 H, 2 × CH₃), 2.40 (s, 3 H, CH₃), 2.63-2.70 (m, 4 H, N(CH₂)₂), 2.78 (t, J = 9 Hz, 2 H, NCH₂), 3.99 (t, J = 9 Hz, 2 H, NCH₂), 6.60 (s, 1 H, CH$_{olef}$), 7.18-7.25 (m, 2 H, CH$_{arom}$), 7.29-7.33 (m, 3 H, CH$_{arom}$), 7.38-7.43 (m, 2 H, CH$_{arom}$), 7.83 (d, J = 9 Hz, 1 H, CH$_{arom}$).

Minor *E*-isomer: quantity too low to assign peaks.

**¹³C-NMR:** (mixture of stereoisomers, 75 MHz, CDCl₃)

Main *E*-isomer:

δ (ppm): 12.0 (q, 2 C, CH₃), 20.0 (q, 1 C, CH₃), 38.5 (t, 1 C, CH₂N), 47.2 (t, 2 C, N(CH₂)₂), 50.4 (t, 1 C, NCH₂), 106.1 (d, 1 C, CH$_{olef}$), 119.1 (d, 1 C, CH$_{arom}$), 123.1 (s, 1 C, Cq), 127.0 (d, 1 C, CH$_{arom}$), 128.8 (d, 2 C, CH$_{arom}$), 129.0 (d, 1 C, CH$_{arom}$), 130.9 (d, 1 C, CH$_{arom}$), 131.3 (s, 1 C, Cq$_{arom}$), 132.7 (d, 1 C, CH$_{arom}$), 134.0 (d, 1 C, CH$_{arom}$), 135.4 (s, 1 C, Cq$_{arom}$), 138.7 (s, 1 C, Cq$_{arom}$), 143.1 (s, 1 C, Cq$_{arom}$), 166.2 (s, 1 C, C=O).

Minor *E*-isomer: quantity too low to assign peaks.

HRMS: (mixture of stereoisomers, ESI/MeOH)

m/z: calcd for $C_{22}H_{26}N_2O$ (M+Na)⁺: 357.1937, found: 357.1945 ± 2 ppm.

8.3.5.3.9 Synthesis of 3-benzylidene-2-[2-(diethylamino)propyl]-2,3-dihydro-1H-isoindol-1-one (39i) [Experiment 103]
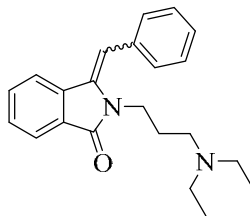
General procedure 12 was followed using 0.34 mL of diethylamine, 1.03 g dehydrated product **38i**, catalytic amounts of KI, 0.62 g K₂CO₃ and 10 mL of DMF. After workup, 0.53 g (53%) of product were obtained as a brownish oil.

IR: (film)

$\widetilde{v}$ (cm⁻¹) = 3133, 1642, 1673, 1564, 1324, 849 and 674.

¹H-NMR: (mixture or stereoisomers, 300 MHz, acetone-d₆)

Main *Z*-isomer:

δ (ppm): 1.03 (t, J = 9 Hz, 6 H, 2 × CH₃), 1.87-1.96 (m, 2 H, CH₂), 2.52-2.59 (m, 6 H, N(CH₂)₂, NCH₂), 3.93 (t, J = 9 Hz, 2 H, NCH₂), 6.58 (s, 1 H, CH$_{olef}$), 7.25-7.32 (m, 8 H, CH$_{arom}$), 7.83 (t, J = 9 Hz, 1 H, CH$_{arom}$).

Minor *E*-isomer: quantity too low to assign peaks.

^{13}C-NMR: (mixture of stereoisomers, 75 MHz, CDCl$_3$)

Main *E*-isomer:

δ (ppm): 11.6 (q, 2 C, CH$_3$), 25.9 (t, 1 C, CH$_2$), 37.8 (t, 1 C, CH$_2$N), 46.9 (t, 2 C, N(CH$_2$)$_2$), 50.4 (t, 1 C, NCH$_2$), 106.8 (d, 1 C, CH$_{olef}$), 119.2 (d, 1 C, CH$_{arom}$), 123.1 (s, 1 C,Cq), 123.3 (d, 1 C, CH$_{arom}$), 126.7 (d, 1 C, CH$_{arom}$), 128.2 (d, 2 C, CH$_{arom}$), 129.0 (d, 1 C, CH$_{arom}$), 130.2 (s, 1 C, Cq$_{arom}$), 129.8 (d, 1 C, CH$_{arom}$), 131.9 (d, 1 C, CH$_{arom}$), 135.2 (d, 1 C, CH$_{arom}$), 136.0 (s, 1 C, Cq$_{arom}$), 138.5 (s, 1 C, Cq$_{arom}$), 168.7 (s, 1 C, C=O).

Minor *E*-isomer: quantity too low to assign peaks.

HRMS: (mixture of stereoisomers, ESI/MeOH)

m/z: calcd for C$_{22}$H$_{26}$N$_2$O (M+H)$^+$: 335.2118, found: 335.2117 ± 1 ppm.

calcd for C$_{22}$H$_{26}$N$_2$O (M+Na)$^+$: 357.1937, found: 357.1943 ± 2 ppm.

8.3.5.3.10 Synthesis of 2-[2-(diethylamino)propyl]-3-(4-fluorobenzylidene)-2,3-dihydro-1H-isoindol-1-one (39j) [Experiment 104]
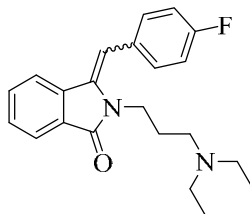
General procedure 12 was followed using 0.34 mL of diethylamine, 1.08 g dehydrated product **38j**, catalytic amounts of KI, 0.62 g K$_2$CO$_3$ and 10 mL of DMF. After workup, 0.636 g (57%) of product were obtained as a brownish solid.

Melting point: 40°C.

IR: (film)

$\widetilde{\nu}$ (cm^{-1}) = 3230, 1671, 1648, 1576, 1148, 836 and 671.

^{1}H-NMR: (mixture or stereoisomers, 300 MHz, acetone-d$_6$)

Main *Z*-isomer:

δ (ppm): 1.02 (t, J = 6 Hz, 6 H, 2 × CH$_3$), 1.90 (t, J = 6 Hz, 2 H, CH$_2$), 2.54 (t, J = 6 Hz, 6 H, N(CH$_2$)$_2$, NCH$_2$), 3.92 (t, J = 9 Hz, 2 H, NCH$_2$), 6.54 (s, 1 H, CH$_{olef}$), 7.12 (t, J = 9 Hz, 2 H, CH$_{arom}$), 7.21 (d, J = 9 Hz, 1 H, CH$_{arom}$), 7.30-7.44 (m, 4 H, CH$_{arom}$), 7.83 (dd, J = 9, 9 Hz, 1 H, CH$_{arom}$).

Minor *E*-isomer: quantity too low to assign peaks.

**^{13}C-NMR:** (mixture of stereoisomers, 75 MHz, CDCl$_3$)

Main *E*-isomer:

δ (ppm): 11.6 (q, 2 C, CH$_3$), 25.7 (t, 1 C, CH$_2$), 38.0 (t, 1 C, CH$_2$N), 46.3 (t, 2 C, N(CH$_2$)$_2$), 50.5 (t, 1 C, NCH$_2$), 106.9 (d, 1 C, CH$_{olef}$), 110.7 (d, 1 C, CH$_{arom}$), 114.5 (s, 1 C, Cq), 119.7 (d, 1 C, CH$_{arom}$), 127.5 (d, 1 C, CH$_{arom}$), 128.3 (d, 2 C, CH$_{arom}$), 130.4 (d, 1 C, CH$_{arom}$), 131.2 (s, 1 C, Cq$_{arom}$), 131.7 (s, 1 C, Cq$_{arom}$), 134.0 (d, 1 C, CH$_{arom}$), 135.8 (d, 1 C, CH$_{arom}$), 138.9 (s, 1 C, Cq$_{arom}$), 158.5 (s, 1 C, Cq$_{arom}$), 167.1 (s, 1 C, C=O).

Minor *E*-isomer: quantity too low to assign peaks.

HRMS: (mixture of stereoisomers, ESI/MeOH)

m/z: calcd for C$_{22}$H$_{25}$N$_2$OF (M+H)$^+$: 353.2024, found: 353.2031 ± 2 ppm.

8.3.5.3.11 Synthesis of 2-[2-(diethylamino)propyl]-3-(4-chlorobenzylidene)-2,3-dihydro-1H-isoindol-1-one (39k) [Experiment 105]
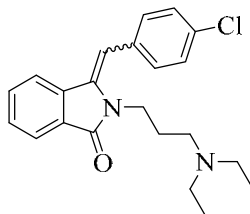
General procedure 12 was followed using 0.34 mL of diethylamine, 1.13 g dehydrated product **38k**, catalytic amounts of KI, 0.62 g K$_2$CO$_3$ and 10 mL of DMF. After workup, 0.66 g (60%) of product were obtained as a brownish oil.

IR: (film)

$\tilde{v}$ (cm^{-1}) = 3141, 1648, 1611, 1576, 1332, 841 and 678.

^{1}H-NMR: (mixture or stereoisomers, 300 MHz, acetone-d$_6$)

Main *Z*-isomer:

δ (ppm): 0.88 (t, J = 9 Hz, 6 H, 2 × CH$_3$), 1.77 (t, J = 9 Hz, 2 H, CH$_2$), 2.38-2.45 (m, 6 H, N(CH$_2$)$_2$, NCH$_2$), 3.78 (t, J = 9 Hz, 2 H, NCH$_2$), 6.39 (s, 1 H, CH$_{olef}$), 7.12-7.19 (m, 3 H, CH$_{arom}$), 7.22-7.25 (m, 2 H, CH$_{arom}$), 7.27-7.32 (m, 2 H, CH$_{arom}$), 7.69 (d, J = 9 Hz, 1 H, CH$_{arom}$).

Minor *E*-isomer: quantity too low to assign peaks.

^{13}C-NMR: (mixture of stereoisomers, 75 MHz, CDCl$_3$)

Main *E*-isomer:

δ (ppm): 11.8 (q, 2 C, CH$_3$), 25.3 (t, 1 C, CH$_2$), 38.1 (t, 1 C, CH$_2$N), 45.8 (t, 2 C, N(CH$_2$)$_2$), 50.1 (t, 1 C, NCH$_2$), 106.1 (d, 1 C, CH$_{olef}$), 110.7 (d, 1 C, CH$_{arom}$), 114.4 (s, 1 C, Cq), 119.1 (d, 1 C, CH$_{arom}$), 127.2 (d, 1 C, CH$_{arom}$), 128.7 (d, 2 C, CH$_{arom}$), 130.4 (d, 1 C, CH$_{arom}$), 130.7 (s, 1 C, Cq$_{arom}$), 131.3 (s, 1 C, Cq$_{arom}$), 134.9 (d, 2 C, CH$_{arom}$), 135.1 (d, 1 C, CH$_{arom}$), 137.2 (s, 1 C, Cq$_{arom}$), 155.7 (s, 1 C, Cq$_{arom}$), 166.6 (s, 1 C, C=O).

Minor *E*-isomer: quantity too low to assign peaks.

HRMS: (mixture of stereoisomers, ESI/MeOH)

m/z: calcd for $C_{22}H_{25}N_2OCl$ (M+H)$^+$: 369.1728, found: 369.1735 ± 2 ppm.

        calcd for $C_{22}H_{25}N_2OCl$ (M+Na)$^+$: 391.1548, found: 391.1569 ± 5 ppm.

8.3.5.3.12 Synthesis of 2-[2-(diethylamino)propyl]-3-(4-bromobenzylidene)-2,3-dihydro-1H-isoindol-1-one (39l) [Experiment 106]
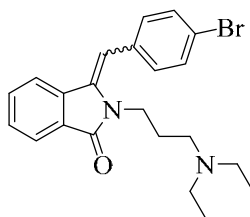
General procedure 12 was followed using 0.34 mL of diethylamine, 1.26 g dehydrated product **38l**, catalytic amounts of KI, 0.62 g K_2CO_3 and 10 mL of DMF. After workup, 0.73 g (59%) of product were obtained as a redish brown oil.

IR: (film)

$\widetilde{v}$ (cm^{-1}) = 3136, 1681, 1538, 1460, 1347, 829 and 688.

^{1}H-NMR: (mixture or stereoisomers, 300 MHz, acetone-d$_6$)

Main *Z*-isomer:

δ (ppm): 1.02 (t, J = 9 Hz, 6 H, 2 × CH$_3$), 1.90 (t, J = 6 Hz, 2 H, CH$_2$), 2.52-2.58 (m, 6 H, N(CH$_2$)$_2$, NCH$_2$), 3.91 (t, J = 6 Hz, 2 H, NCH$_2$), 6.49 (s, 1 H, CH$_{olef}$), 7.29-7.35 (m, 4 H, CH$_{arom}$), 7.43 (t, J = 9 Hz, 1 H, CH$_{arom}$), 7.56 (d, J = 9 Hz, 2 H, CH$_{arom}$), 7.83 (d, J = 9 Hz, 1 H, CH$_{arom}$).

Minor *E*-isomer: quantity too low to assign peaks.

**^{13}C-NMR:** (mixture of stereoisomers, 75 MHz, CDCl$_3$)

Main *E*-isomer:

δ (ppm): 11.9 (q, 2 C, CH$_3$), 25.2 (t, 1 C, CH$_2$), 38.0 (t, 1 C, CH$_2$N), 45.3 (t, 2 C, N(CH$_2$)$_2$), 51.5 (t, 1 C, NCH$_2$), 107.6 (d, 1 C, CH$_{olef}$), 110.4 (d, 1 C, CH$_{arom}$), 114.9 (s, 1 C, Cq), 120.3 (d, 1 C, CH$_{arom}$), 127.3 (d, 1 C, CH$_{arom}$), 128.7 (d, 2 C, CH$_{arom}$), 130.1 (d, 1 C, CH$_{arom}$), 130.5 (s, 1 C, Cq$_{arom}$), 131.8 (s, 1 C, Cq$_{arom}$), 134.3 (d, 2 C, CH$_{arom}$), 135.7 (d, 1 C, CH$_{arom}$), 138.9 (s, 1 C, Cq$_{arom}$), 145.3 (s, 1 C, Cq$_{arom}$), 166.7 (s, 1 C, C=O).

Minor *E*-isomer: quantity too low to assign peaks.

HRMS: (mixture of stereoisomers, ESI/MeOH)

m/z: calcd for $C_{22}H_{25}N_2OBr$ (M+Na)$^+$: 435.1042, found: 435.1035 ± 2 ppm.

8.3.5.3.13 Synthesis of 2-[2-(diethylamino)propyl]-3-(4-methoxybenzylidene)-2,3-dihydro-1H-isoindol-1-one (39m) [Experiment 107]
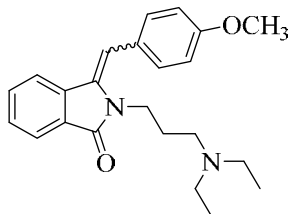
General procedure 12 was followed using 0.34 mL of diethylamine, 1.12 g dehydrated product **38m**, catalytic amounts of KI, 0.62 g K_2CO_3 and 10 mL of DMF. After workup, 0.59 g (55%) of product were obtained as a brownish oil.

IR: (film)

$\widetilde{\nu}$ (cm^{-1}) = 3158, 1662, 1658, 1558, 1362, 1239, 865 and 686.

^{1}H-NMR: (mixture or stereoisomers, 300 MHz, CDCl$_3$)

Main Z-isomer:

δ (ppm): 1.06 (t, J = 9 Hz, 6 H, 2 × CH$_3$), 1.89-1.99 (m, 2 H, CH$_2$), 2.55-2.62 (m, 6 H, N(CH$_2$)$_2$, NCH$_2$), 3.91 (s, 3 H, OCH$_3$), 3.95 (t, J = 9 Hz, 2 H, NCH$_2$), 6.60 (s, 1 H, CH$_{olef}$), 7.00 (d, J = 9 Hz, 2 H, CH$_{arom}$), 7.36-7.41 (m, 5 H, CH$_{arom}$), 7.87 (d, J = 9 Hz, 1 H, CH$_{arom}$).

Minor E-isomer: quantity too low to assign peaks.

^{13}C-NMR: (mixture of stereoisomers, 75 MHz, CDCl$_3$)

Main E-isomer:

δ (ppm): 11.5 (q, 2 C, CH$_3$), 25.1 (t, 1 C, CH$_2$), 37.8 (t, 1 C, CH$_2$N), 46.7 (t, 2 C, N(CH$_2$)$_2$), 50.4 (t, 1 C, NCH$_2$), 55.3 (q, 1 C, OCH$_3$), 106.6 (d, 1 C, CH$_{olef}$), 110.5 (d, 1 C, CH$_{arom}$), 114.1 (s, 1 C,Cq), 119.2 (d, 1 C, CH$_{arom}$), 127.0 (d, 1 C, CH$_{arom}$), 128.2 (d, 2 C, CH$_{arom}$), 130.3 (d, 1 C, CH$_{arom}$), 130.9 (s, 1 C, Cq$_{arom}$), 131.4 (s, 1 C, Cq$_{arom}$), 134.2 (d, 1 C, CH$_{arom}$), 135.6 (d, 1 C, CH$_{arom}$), 138.5 (s, 1 C, Cq$_{arom}$), 159.1 (s, 1 C, Cq$_{arom}$), 167.6 (s, 1 C, C=O).

**Minor E-isomer:** quantity too low to assign peaks.

HRMS: (mixture of stereoisomers, ESI/MeOH)

m/z: calcd for $C_{23}H_{28}N_2O_2$ (M+H)$^+$: 365.2224, found: 365.2230 ± 2 ppm.

calcd for $C_{23}H_{28}N_2O_2$ (M+Na)$^+$: 387.2043, found: 387.2054 ± 3 ppm.

8.3.5.3.14 Synthesis of 2-[2-(diethylamino)propyl]-3-(4-methylbenzylidene)-2,3-dihydro-1H-isoindol-1-one (39n) [Experiment 108]
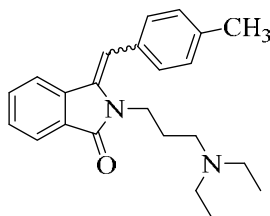
General procedure 12 was followed using 0.34 mL of diethylamine, 1.07 g dehydrated product **38n**, catalytic amounts of KI, 0.62 g K_2CO_3 and 10 mL of DMF. After workup, 0.67 g (58%) of product were obtained as a brownish oil.

IR: (film)

$\widetilde{\nu}$ (cm^{-1}) = 3101, 1682, 1612, 1565, 1361, 850 and 673.

^{1}H-NMR: (mixture or stereoisomers, 300 MHz, CDCl$_3$)

Main Z-isomer:

δ (ppm): 1.02 (t, J = 6 Hz, 6 H, 2 × CH$_3$), 1.91 (t, J = 9 Hz, 2 H, CH$_2$), 2.42 (s, 3 H, CH$_3$), 2.52-2.59 (m, 6 H, N(CH$_2$)$_2$), 3.93 (t, J = 9 Hz, 2 H, NCH$_2$), 6.58 (s, 1 H, CH$_{olef}$), 7.23 (d, J = 9 Hz, 2 H, CH$_{arom}$), 7.29-7.36 (m, 4 H, CH$_{arom}$), 7.40-7.43 (m, 1 H, CH$_{arom}$), 7.82 (d, J = 9 Hz, 1 H, CH$_{arom}$).

Minor E-isomer: quantity too low to assign peaks.

^{13}C-NMR: (mixture of stereoisomers, 75 MHz, CDCl$_3$)

Main E-isomer:

δ (ppm): 11.9 (q, 2 C, CH$_3$), 19.5 (q, 1 C, CH$_3$), 25.7 (t, 1 C, CH$_2$), 38.8 (t, 1 C, CH$_2$N), 43.7 (t, 2 C, N(CH$_2$)$_2$), 51.3 (t, 1 C, NCH$_2$), 106.1 (d, 1 C, CH$_{olef}$), 111.2 (d, 1 C, CH$_{arom}$), 114.0 (s, 1 C, Cq), 120.3 (d, 1 C, CH$_{arom}$), 127.0 (d, 1 C, CH$_{arom}$), 128.4 (d, 2 C, CH$_{arom}$), 130.9 (d, 1 C, CH$_{arom}$), 131.1 (s, 1 C, Cq$_{arom}$), 131.7 (s, 1 C, Cq$_{arom}$), 134.4 (d, 1 C, CH$_{arom}$), 135.0 (d, 1 C, CH$_{arom}$), 138.7 (s, 1 C, Cq$_{arom}$), 140.1 (s, 1 C, Cq$_{arom}$), 166.7 (s, 1 C, C=O).

Minor E-isomer: quantity too low to assign peaks.

HRMS: (mixture of stereoisomers, ESI/MeOH)

m/z: calcd for $C_{23}H_{28}N_2O$ (M+Na)$^+$: 371.2094, found: 371.2103 ± 3 ppm.

8.3.5.3.15 Synthesis of 2-[2-(diethylamino)propyl]-3-(2-methylbenzylidene)-2,3-dihydro-1H-isoindol-1-one (39o) [Experiment 109]
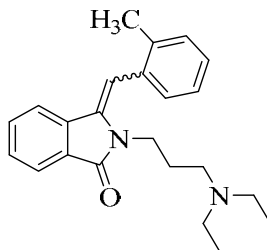
General procedure 12 was followed using 0.34 mL of diethylamine, 1.07 g dehydrated product **38o**, catalytic amounts of KI, 0.62 g K_2CO_3 and 10 mL of DMF. After workup, 0.51 g (49%) of product were obtained as a brownish oil.

IR: (film)

$\widetilde{\nu}$ (cm^{-1}) = 3142, 1681, 1636, 1570, 1284, 854 and 690.

^{1}H-NMR: (mixture or stereoisomers, 300 MHz, CDCl$_3$)

Main Z-isomer:

δ (ppm): 1.01 (t, J = 6 Hz, 6 H, 2 × CH$_3$), 1.93 (t, J = 6 Hz, 4 H, CH$_2$), 2.41 (s, 3 H, CH$_3$), 2.48-2.55 (m, 6 H, N(CH$_2$)$_2$), 4.02 (t, J = 6 Hz, 2 H, NCH$_2$), 6.57 (s, 1 H, CH$_{olef}$), 7.21 (d, J = 9 Hz, 2 H, CH$_{arom}$), 7.28-7.36 (m, 4 H, CH$_{arom}$), 7.38-7.41 (m, 1 H, CH$_{arom}$), 7.86 (d, J = 9 Hz, 1 H, CH$_{arom}$).

Minor E-isomer: quantity too low to assign peaks.

^{13}C-NMR: (mixture of stereoisomers, 75 MHz, CDCl$_3$)

Main E-isomer:

δ (ppm): 12.0 (q, 2 C, CH$_3$), 20.1 (q, 1 C, CH$_3$), 25.2 (t, 1 C, CH$_2$), 37.1 (t, 1 C, CH$_2$N), 46.4 (t, 2 C, N(CH$_2$)$_2$), 50.0 (t, 1 C, NCH$_2$), 105.6 (d, 1 C, CH$_{olef}$), 110.7 (d, 1 C, CH$_{arom}$), 114.5 (s, 1 C, Cq), 119.5 (d, 1 C, CH$_{arom}$), 127.7 (d, 1 C, CH$_{arom}$), 128.0 (d, 2 C, CH$_{arom}$), 130.5 (d, 1 C, CH$_{arom}$), 130.7 (s, 1 C, Cq$_{arom}$), 131.3 (s, 1 C, Cq$_{arom}$), 134.2 (d, 1 C, CH$_{arom}$), 135.6 (d, 1 C, CH$_{arom}$), 138.8 (s, 1 C, Cq$_{arom}$), 140.5 (s, 1 C, Cq$_{arom}$), 167.1 (s, 1 C, C=O).

Minor E-isomer: quantity too low to assign peaks.

HRMS: (mixture of stereoisomers, ESI/MeOH)

m/z: calcd for C$_{23}$H$_{28}$N$_2$O (M+H)$^+$: 349.2274, found: 349.2288 ± 4 ppm.

m/z: calcd for C$_{23}$H$_{28}$N$_2$O (M+Na)$^+$: 371.2094, found: 371.2109 ± 4 ppm.

8.3.5.3.16 Synthesis of 2-[2-(diethylamino)propyl]-3-(3-methylbenzylidene)-2,3-dihydro-1H-isoindol-1-one (39p) [Experiment 110]
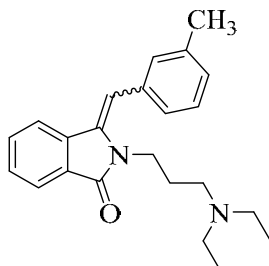
General procedure 12 was followed using 0.34 mL of diethylamine, 1.07 g dehydrated product **38p**, catalytic amounts of KI, 0.62 g K_2CO_3 and 10 mL of DMF. After workup, 0.64 g (61%) of product were obtained as a brownish oil.

IR: (film)

$\widetilde{v}$ (cm^{-1}) = 3106, 1685, 1640, 1587, 1243, 834 and 684.

^{1}H-NMR: (mixture or stereoisomers, 300 MHz, CDCl$_3$)

Main Z-isomer:

δ (ppm): 1.06 (t, J = 9 Hz, 6 H, 2 × CH$_3$), 1.97 (t, J = 9 Hz, 2 H, CH$_2$), 2.34 (s, 3 H, CH$_3$), 2.55-2.64 (m, 6 H, N(CH$_2$)$_3$), 3.99 (t, J = 9 Hz, 2 H, NCH$_2$), 6.51 (s, 1 H, CH$_{olef}$), 6.98 (d, J = 6 Hz, 1 H, CH$_{arom}$), 7.30-7.46 (m, 6 H, CH$_{arom}$), 7.86 (d, J = 6 Hz, 1 H, CH$_{arom}$).

Minor E-isomer: quantity too low to assign peaks.

^{13}C-NMR: (mixture of stereoisomers, 75 MHz, CDCl$_3$)

Main E-isomer:

δ (ppm): 12.3 (q, 2 C, CH$_3$),19.3 (q, 1 C, CH$_3$), 25.1 (t, 1 C, CH$_2$), 37.8 (t, 1 C, CH$_2$N), 46.7 (t, 2 C, N(CH$_2$)$_2$), 50.4 (t, 1 C, NCH$_2$), 106.6 (d, 1 C, CH$_{olef}$), 110.5 (d, 1 C, CH$_{arom}$), 114.1 (s, 1 C, Cq), 119.2 (d, 1 C, CH$_{arom}$), 127.0 (d, 1 C, CH$_{arom}$), 128.2 (d, 2 C, CH$_{arom}$), 130.3 (d, 1 C, CH$_{arom}$), 130.9 (s, 1 C, Cq$_{arom}$), 131.4 (s, 1 C, Cq$_{arom}$), 134.2 (d, 1 C, CH$_{arom}$), 135.6 (d, 1 C, CH$_{arom}$), 138.1 (s, 1 C, Cq$_{arom}$), 140.2 (s, 1 C, Cq$_{arom}$), 166.9 (s, 1 C, C=O).

Minor E-isomer: quantity too low to assign peaks.

HRMS: (mixture of stereoisomers, ESI/MeOH)

m/z: calcd for $C_{23}H_{28}N_2O$ (M+H)$^+$: 349.2274, found: 349.2288 ± 4 ppm.

8.3.5.3.17 Synthesis of 3-benzylidene-2-[2-(dimethylamino)ethyl]-2,3-dihydro-1H-isoindol-1-one (39q) [Experiment 111]
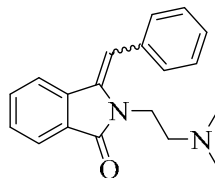
General procedure 12 was followed using 0.40 mL dimethylamine, 0.98 g dehydrated product **38a**, catalytic amounts of KI, 0.62 g K_2CO_3 and 10 mL of DMF. After workup, 0.51 g (58%) of product were obtained as a yellow oil.

IR: (film)

$\tilde{\nu}$ (cm^{-1}) = 3154, 1660, 1634, 1576, 1336, 834 and 678.

^{1}H-NMR: (mixture or stereoisomers, 300 MHz, CDCl$_3$)

Main Z-isomer:

δ (ppm): 2.42 (s, 6 H, N(CH$_3$)$_2$), 2.71 (t, J = 6 Hz, 2 H, NCH$_2$), 4.08 (t, J = 6 Hz, 2 H, NCH$_2$), 6.58 (s, 1 H, CH$_{olef}$), 7.33-7.55 (m, 8 H, CH$_{arom}$), 7.88 (d, J = 9 Hz, 1 H, CH$_{arom}$).

Minor E-isomer: quantity too low to assign peaks.

^{13}C-NMR: (mixture of stereoisomers, 75 MHz, CDCl$_3$)

Main E-isomer:

δ (ppm): 31.1 (t, 1 C, NCH$_2$), 37.8 (t, 2 C, N(CH$_3$)$_2$), 56.9 (t, 1 C, CH$_2$N), 110.3 (d, 1 C, CH$_{olef}$), 123.2 (d, 1 C, CH$_{arom}$), 123.3 (s, 1 C, Cq), 127.9 (d, 1 C, CH$_{arom}$), 128.4 (d, 1 C, CH$_{arom}$), 128.8 (d, 2 C, CH$_{arom}$), 129.7 (d, 2 C, CH$_{arom}$), 132.1 (s, 2 C, Cq$_{arom}$), 135.2 (d, 1 C, CH$_{arom}$), 135.3 (s, 1 C, Cq$_{arom}$), 138.2 (d, 1 C, CH$_{arom}$), 168.3 (s, 1 C, C=O).

Minor E-isomer: quantity too low to assign peaks.

HRMS: (mixture of stereoisomers, ESI/MeOH)

m/z: calcd for $C_{20}H_{22}ON_2$ (M+Na)$^+$: 329.1624, found: 293.1624 ± 0 ppm.

8.3.5.3.18 Synthesis of 2-[2-(dimethylamino)ethyl]-3-(4-fluorobenzylidene)-2,3-dihydro-1H-isoindol-1-one (39r) [Experiment 112]
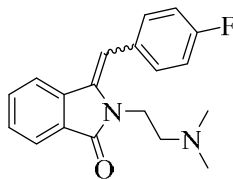
General procedure 12 was followed using 0.40 mL dimethylamine, 1.04 g dehydrated product **38b**, catalytic amounts of KI, 0.62 g K_2CO_3 and 10 mL of DMF. After workup, 0.56 g (57%) of product were obtained as a brownish oil.

IR: (film)

$\widetilde{\nu}$ (cm^{-1}) = 3134, 1687, 1651, 1564, 1154, 828 and 678.

^{1}H-NMR: (mixture or stereoisomers, 300 MHz, CDCl$_3$)

Main Z-isomer:

δ (ppm): 2.39 (s, 6 H, N(CH$_3$)$_2$), 2.57 (t, J = 6 Hz, 2 H, NCH$_2$), 4.17 (t, J = 6 Hz, 2 H, NCH$_2$), 6.55 (s, 1 H, CH$_{olef}$), 7.29-7.36 (m, 2 H, CH$_{arom}$), 7.41-7.50 (m, 5 H, CH$_{arom}$), 7.79 (d, J = 9 Hz, 1 H, CH$_{arom}$).

Minor E-isomer: quantity too low to assign peaks.

^{13}C-NMR: (mixture of stereoisomers, 75 MHz, CDCl$_3$)

Main E-isomer:

δ (ppm): 30.9 (t, 1 C, NCH$_2$), 37.3 (t, 1 C, N(CH$_3$)), 37.7 (t, 1 C, N(CH$_3$)), 56.4 (t, 1 C, CH$_2$N), 109.7 (d, 1 C, CH$_{olef}$), 123.0 (d, 1 C, CH$_{arom}$), 123.1 (s, 1 C, Cq), 127.9 (d, 1 C, CH$_{arom}$), 128.4 (d, 1 C, CH$_{arom}$), 128.8 (d, 1 C, CH$_{arom}$), 129.7 (d, 2 C, CH$_{arom}$), 130.3 (s, 1 C, Cq$_{arom}$), 132.1 (s, 1 C, Cq$_{arom}$), 135.2 (d, 1 C, CH$_{arom}$), 135.3 (s, 2 C, Cq$_{arom}$), 138.2 (d, 1 C, CH$_{arom}$), 168.7 (s, 1 C, C=O).

Minor E-isomer: quantity too low to assign peaks.

HRMS: (mixture of stereoisomers, ESI/MeOH)

m/z: calcd for C$_{19}$H$_{19}$NOF (M+H)$^+$: 311.1554, found: 311.1554 ± 1 ppm.

calcd for C$_{19}$H$_{19}$NOF (M+Na)$^+$: 333.1374, found: 333.1376 ± 1 ppm.

8.3.5.3.19 Synthesis of 2-[2-(dimethylamino)ethyl]-3-(4-chlorobenzylidene)-2,3-dihydro-1H-isoindol-1-one (39s) [Experiment 113]
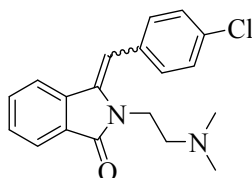
General procedure 12 was followed using 0.40 mL dimethylamine, 1.09 g dehydrated product **38c**, catalytic amounts of KI, 0.62 g K$_2$CO$_3$ and 10 mL of DMF. After workup, 0.54 g (55%) of product were obtained as a yellowish brown oil.

IR: (film)

$\widetilde{\nu}$ (cm^{-1}) = 3102, 1664, 1600, 1548, 1348, 850 and 669.

^{1}H-NMR: (mixture or stereoisomers, 300 MHz, CDCl$_3$)

Main Z-isomer:

δ (ppm): 2.40 (s, 6 H, N(CH$_3$)$_2$), 2.70 (t, J = 6 Hz, 2 H, NCH$_2$), 4.05 (t, J = 6 Hz, 2 H, NCH$_2$), 6.57 (s, 1 H, CH$_{olef}$), 7.21-7.35 (m, 3 H, CH$_{arom}$), 7.21-7.35 (m, 2 H, CH$_{arom}$), 7.21-7.35 (m, 2 H, CH$_{arom}$), 7.88 (d, J = 9 Hz, 1 H, CH$_{arom}$).

Minor E-isomer: quantity too low to assign peaks.

^{13}C-NMR: (mixture of stereoisomers, 75 MHz, CDCl$_3$)

Main E-isomer:

δ (ppm): 31.4 (t, 1 C, NCH$_2$), 37.8 (t, 1 C, N(CH$_3$)), 38.0 (t, 1 C, N(CH$_3$)), 55.7 (t, 1 C, CH$_2$N), 110.5 (d, 1 C, CH$_{olef}$), 121.1 (d, 1 C, CH$_{arom}$), 122.9 (s, 1 C, Cq), 127.4 (d, 1 C, CH$_{arom}$), 128.0 (d, 1 C, CH$_{arom}$), 128.7 (d, 1 C, CH$_{arom}$), 129.0 (d, 2 C, CH$_{arom}$), 129.7 (s, 1 C, Cq$_{arom}$), 132.4 (s, 1 C, Cq$_{arom}$), 135.9 (d, 1 C, CH$_{arom}$), 136.0 (s, 2 C, Cq$_{arom}$), 138.1 (d, 1 C, CH$_{arom}$), 168.6 (s, 1 C, C=O).

Minor E-isomer: quantity too low to assign peaks.

HRMS: (mixture of stereoisomers, ESI/MeOH)

m/z: calcd for C$_{19}$H$_{19}$N$_2$OCl (M+Na)$^+$: 349.1078, found: 349.1079 ± 1 ppm.

8.3.5.3.20 Synthesis of 2-[2-(dimethylamino)ethyl]-3-(4-methoxybenzylidene)-2,3-dihydro-1H-isoindol-1-one (39t) [Experiment 114]
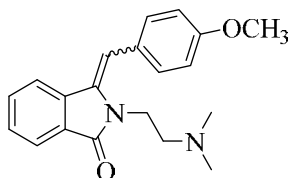
General procedure 12 was followed using 0.40 mL dimethylamine, 1.50 g dehydrated product **38d**, catalytic amounts of KI, 0.62 g K$_2$CO$_3$ and 10 mL of DMF. After workup, 0.47 g (49%) of product were obtained as light brownish crystals.

Melting point: 39-41°C.

IR: (film)

$\widetilde{v}$ (cm^{-1}) = 3120, 1682, 1580, 1368, 1250, 816 and 660.

^{1}H-NMR: (mixture or stereoisomers, 300 MHz, CDCl$_3$)

Main Z-isomer:

δ (ppm): 2.43 (s, 6 H, N(CH$_3$)$_2$), 2.76 (t, J = 6 Hz, 2 H, NCH$_2$), 3.62 (s, 3 H, OCH$_3$), 4.12 (t, J = 6 Hz, 2 H, NCH$_2$), 6.56 (s, 1 H, CH$_{olef}$), 7.47-7.55 (m, 4 H, CH$_{arom}$), 7.57-7.60 (m, 2 H, CH$_{arom}$), 7.79-7.86 (m, 2 H, CH$_{arom}$).

Minor E-isomer: quantity too low to assign peaks.

**^{13}C-NMR:** (mixture of stereoisomers, 75 MHz, CDCl$_3$)

Main E-isomer:

δ (ppm): 31.0 (t, 1 C, NCH$_2$), 37.7 (t, 1 C, N(CH$_3$)), 38.2 (t, 1 C, N(CH$_3$)), 56.0 (t, 1 C, CH$_2$N), 56.5 (q, 1 C, OCH$_3$), 109.3 (d, 1 C, CH$_{olef}$), 122.3 (d, 1 C, CH$_{arom}$), 123.4 (s, 1 C, Cq), 127.3 (d, 1 C, CH$_{arom}$), 127.9 (d, 1 C, CH$_{arom}$), 128.7 (d, 1 C, CH$_{arom}$), 129.0 (d, 2 C, CH$_{arom}$), 130.7 (s, 1 C, Cq$_{arom}$), 132.4 (s, 1 C, Cq$_{arom}$), 133.9 (d, 1 C, CH$_{arom}$), 135.0 (s, 2 C, Cq$_{arom}$), 138.7 (d, 1 C, CH$_{arom}$), 168.8 (s, 1 C, C=O).

Minor *E*-isomer: quantity too low to assign peaks.

HRMS: (mixture of stereoisomers, ESI/MeOH)

m/z: calcd for C$_{20}$H$_{22}$N$_2$O$_2$ (M+H)$^+$: 323.1754, found: 323.1761 ± 2 ppm.

calcd for C$_{20}$H$_{22}$N$_2$O$_2$ (M+Na)$^+$: 345.1573, found: 345.1575 ± 1 ppm.

8.3.5.3.21 Synthesis of 2-[2-(dimethylamino)ethyl]-3-(4-methylbenzylidene)-2,3-dihydro-1H-isoindol-1-one (39u) [Experiment 115]
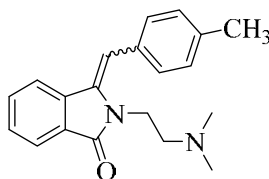
General procedure 12 was followed using 0.40 mL dimethylamine, 1.44 g dehydrated product **38e**, catalytic amounts of KI, 0.62 g K$_2$CO$_3$ and 10 mL of DMF. After workup, 0.55 g (60%) of product were obtained as a brownish oil.

IR: (film)

$\widetilde{v}$ (cm^{-1}) = 3122, 1651, 1622, 1581, 1288, 847 and 678.

^{1}H-NMR: (mixture or stereoisomers, 300 MHz, CDCl$_3$)

Main *Z*-isomer:

δ (ppm): 2.01 (s, 3 H, CH$_3$), 2.41 (s, 6 H, N(CH$_3$)$_2$), 2.68 (t, J = 6 Hz, 2 H, NCH$_2$), 4.00 (t, J = 6 Hz, 2 H, NCH$_2$), 6.53 (s, 1 H, CH$_{olef}$), 7.35-7.43 (m, 3 H, CH$_{arom}$), 7.57-7.60 (m, 3 H, CH$_{arom}$), 7.69-7.75 (m, 2 H, CH$_{arom}$).

Minor *E*-isomer: quantity too low to assign peaks.

**^{13}C-NMR:** (mixture of stereoisomers, 75 MHz, CDCl$_3$)

Main *E*-isomer:

δ (ppm): 20.1 (q, 1 C, CH$_3$), 31.9 (t, 1 C, NCH$_2$), 45.4 (t, 2 C, N(CH$_3$)$_2$), 55.8 (t, 1 C, CH$_2$N), 110.1 (d, 1 C, CH$_{olef}$), 123.0 (d, 1 C, CH$_{arom}$), 123.3 (s, 1 C, Cq), 127.5 (d, 1 C, CH$_{arom}$), 128.7 (d, 1 C, CH$_{arom}$), 129.1 (d, 1 C, CH$_{arom}$), 129.2 (d, 1 C, CH$_{arom}$), 130.0 (s, 2 C, Cq$_{arom}$), 130.7 (d, 1 C, CH$_{arom}$), 131.4 (d, 1 C, CH$_{arom}$), 135.4 (d, 1 C, CH$_{arom}$), 135.5 (s, 1 C, Cq$_{arom}$), 136.7 (s, 1 C, Cq$_{arom}$), 166.5 (s, 1 C, C=O).

Minor *E*-isomer: quantity too low to assign peaks.

HRMS: (mixture of stereoisomers, ESI/MeOH)

m/z: calcd for $C_{20}H_{22}N_2O$ (M+H)$^+$: 307.1805, found: 307.1806 ± 1 ppm.

calcd for $C_{20}H_{22}N_2O$ (M+Na)$^+$: 329.1624, found: 329.1623 ± 1 ppm.

8.3.5.3.22 Synthesis of 3-benzylidene-2-[3-(dimethylamino)propyl]-2,3-dihydro-1H-isoindol-1-one (39v) [Experiment 116]
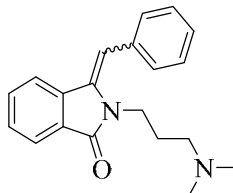
General procedure 12 was followed using 0.40 mL dimethylamine, 1.44 g dehydrated product **38i**, catalytic amounts of KI, 0.62 g K_2CO_3 and 10 mL of DMF. After workup, 0.75 g (58%) of product were obtained as a brownish oil.

IR: (film)

$\tilde{v}$ (cm^{-1}) = 3138, 1640, 1649, 1581, 1329, 852 and 678.

^{1}H-NMR: (mixture or stereoisomers, 300 MHz, acetone-d$_6$)

Main Z-isomer:

δ (ppm): 1.91-2.01 (m, 2 H, CH$_2$), 2.28 (s, 6 H, N(CH$_3$)$_2$), 2.43 (t, J = 9 Hz, 2 H, NCH$_2$), 3.98 (t, J = 9 Hz, 2 H, NCH$_2$), 6.67 (s, 1 H, CH$_{olef}$), 7.30-7.48 (m, 8 H, CH$_{arom}$), 7.87 (d, J = 9 Hz, 1 H, CH$_{arom}$).

Minor E-isomer: quantity too low to assign peaks.

^{13}C-NMR: (mixture of stereoisomers, 75 MHz, CDCl$_3$)

Main E-isomer:

δ (ppm): 26.7 (t, 1 C, CH$_2$), 37.6 (t, 1 C, NCH$_2$), 45.5 (t, 2 C, N(CH$_3$)$_2$), 56.9 (t, 1 C, CH$_2$N), 110.4 (d, 1 C, CH$_{olef}$), 123.1 (d, 1 C, CH$_{arom}$), 123.2 (s, 1 C, Cq), 127.8 (d, 1 C, CH$_{arom}$), 128.7 (d, 1 C, CH$_{arom}$), 129.2 (d, 2 C, CH$_{arom}$), 129.6 (d, 1 C, CH$_{arom}$), 129.9 (s, 1 C, Cq$_{arom}$), 130.4 (d, 1 C, CH$_{arom}$), 131.4 (d, 1 C, CH$_{arom}$), 135.1 (d, 1 C, CH$_{arom}$), 135.4 (s, 1 C, Cq$_{arom}$), 136.4 (s, 1 C, Cq$_{arom}$), 166.7 (s, 1 C, C=O).

Minor E-isomer: quantity too low to assign peaks.

HRMS: (mixture of stereoisomers, ESI/MeOH)

m/z: calcd for $C_{20}H_{22}ON_2$ (M+Na)$^+$: 329.1624, found: 329.1624 ± 1 ppm.

8.3.5.3.23 Synthesis of 2-[3-(dimethylamino)propyl]-3-(4-fluorobenzylidene)-2,3-dihydro-1H-isoindol-1-one (39w) [Experiment 117]
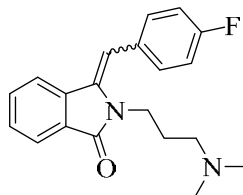
General procedure 12 was followed using 0.40 mL dimethylamine, 1.51 g dehydrated product **38j**, catalytic amounts of KI, 0.62 g K_2CO_3 and 10 mL of DMF. After workup, 0.75 g (55%) of product were obtained as a red brownish oil.

IR: (film)

$\widetilde{\nu}$ (cm^{-1}) = 3246, 1633, 1674, 1579, 1145, 843 and 674.

^{1}H-NMR: (mixture or stereoisomers, 300 MHz, CDCl$_3$)

Main Z-isomer:

δ (ppm): 1.92-1.97(m, 2 H, CH$_2$), 2.30 (s, 6 H, N(CH$_3$)$_2$), 2.55 (t, J = 9 Hz, 2 H, NCH$_2$), 3.97 (t, J = 9 Hz, 2 H, NCH$_2$), 6.57 (s, 1 H, CH$_{olef}$), 7.15-7.18 (m, 2 H, CH$_{arom}$), 7.22-7.27 (m, 1 H, CH$_{arom}$), 7.34-7.45 (m, 4 H, CH$_{arom}$), 7.89 (d, J = 9 Hz, 1 H, CH$_{arom}$).

Minor E-isomer: quantity too low to assign peaks.

^{13}C-NMR: (mixture of stereoisomers, 75 MHz, CDCl$_3$)

Main E-isomer:

δ (ppm): 26.4 (t, 1 C, CH$_2$), 38.6 (t, 1 C, NCH$_2$), 43.7 (t, 2 C, N(CH$_3$)$_2$), 55.4 (t, 1 C, CH$_2$N), 110.1 (d, 1 C, CH$_{olef}$), 120.4 (d, 1 C, CH$_{arom}$), 122.7 (s, 1 C, Cq), 127.7 (d, 1 C, CH$_{arom}$), 128.3 (d, 1 C, CH$_{arom}$), 129.1 (d, 2 C, CH$_{arom}$), 129.6 (d, 1 C, CH$_{arom}$), 129.8 (s, 1 C, Cq$_{arom}$), 130.3 (d, 1 C, CH$_{arom}$), 131.4 (d, 1 C, CH$_{arom}$), 135.4 (s, 1 C, Cq$_{arom}$), 135.9 (s, 1 C, Cq$_{arom}$), 157.9 (s, 1 C, Cq$_{arom}$), 166.7 (s, 1 C, C=O).

Minor E-isomer: quantity too low to assign peaks.

HRMS: (mixture of stereoisomers, ESI/MeOH)

m/z: calcd for $C_{20}H_{21}N_2OF$ (M+H)$^+$: 325.1711, found: 325.1708 ± 1 ppm.

calcd for $C_{20}H_{21}N_2OF$ (M+Na)$^+$: 347.1530, found: 347.1532 ± 1 ppm.

8.3.5.3.24 Synthesis of 2-[3-(dimethylamino)propyl]-3-(2-methylbenzylidene)-2,3-dihydro-1H-isoindol-1-one (39x) [Experiment 118]
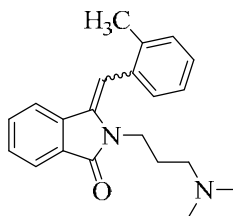
General procedure 12 was followed using 0.40 mL dimethylamine, 1.50 g dehydrated product **38o**, catalytic amounts of KI, 0.62 g K_2CO_3 and 10 mL of DMF. After workup, 0.71 g (53%) of product were obtained as a brownish oil.

IR: (film)

$\widetilde{v}$ (cm^{-1}) = 3142, 1687, 1644, 1560, 1280, 864 and 681.

^{1}H-NMR: (mixture or stereoisomers, 300 MHz, CDCl$_3$)

Main Z-isomer:

δ (ppm): 1.92-1.97 (m, 2 H, CH$_2$), 2.12 (s, 3 H, CH$_3$), 2.24 (s, 6 H, N(CH$_3$)$_2$), 2.44 (t, J = 6 Hz, 2 H, NCH$_2$), 3.90 (t, J = 6 Hz, 2 H, NCH$_2$), 6.50 (s, 1 H, CH$_{olef}$), 7.11-7.17 (m, 3 H, CH$_{arom}$), 7.35-7.45 (m, 4 H, CH$_{arom}$), 7.88 (d, J = 9 Hz, 1 H, CH$_{arom}$).

Minor E-isomer: quantity too low to assign peaks.

^{13}C-NMR: (mixture of stereoisomers, 75 MHz, CDCl$_3$)

Main E-isomer:

δ (ppm): 20.1 (q, 1 C, CH$_3$), 26.4 (t, 1 C, CH$_2$), 36.9 (t, 1 C, NCH$_2$), 45.4 (t, 2 C, N(CH$_3$)$_2$), 55.8 (t, 1 C, CH$_2$N), 110.1 (d, 1 C, CH$_{olef}$), 123.0 (d, 1 C, CH$_{arom}$), 123.3 (s, 1 C, Cq), 127.5 (d, 1 C, CH$_{arom}$), 128.7 (d, 1 C, CH$_{arom}$), 129.1 (d, 2 C, CH$_{arom}$), 129.2 (d, 1 C, CH$_{arom}$), 129.6 (s, 1 C, Cq$_{arom}$), 130.7 (d, 1 C, CH$_{arom}$), 131.4 (d, 1 C, CH$_{arom}$), 135.4 (s, 1 C, Cq$_{arom}$), 135.5 (s, 1 C, Cq$_{arom}$), 136.7 (s, 1 C, Cq$_{arom}$), 166.5 (s, 1 C, C=O).

Minor E-isomer: quantity too low to assign peaks.

HRMS: (mixture of stereoisomers, ESI/MeOH)

m/z: calcd for C$_{21}$H$_{24}$N$_2$O (M+H)$^+$: 321.1961, found: 321.1962 ± 1 ppm.

calcd for C$_{21}$H$_{24}$N$_2$O (M+Na)$^+$: 343.1781, found: 343.1784 ± 1 ppm.

8.3.6 Synthesis of AL12, AL5 and their analogues in flow

8.3.6.1 Solvent optimization for multistep continuous flow setup under batch conditions [Experiment 119-125]

This study was conducted to find a common solvent for all three reaction steps. Therefore, each step was conducted in acetone, acetonitrile and/or DMF, respectively, under batch conditions.

8.3.6.1.1 Synthesis of 3-benzyl-2-(2-bromoethyl)-3-hydroxy-2,3-dihydro-1H-isoindol-1-one (37a) [Experiment 119]
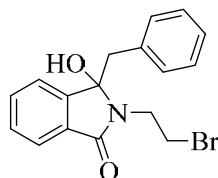
General procedure 10 was followed using 2.04 g of phenylacetic acid, 1.04 g of K$_2$CO$_3$, 1.27 g of N-bromoethyl phthalimide and 360 mL of acetonitrile/pH 7 buffer (1:1) and 3 hours of irradiation. After workup, 1.38 g (80%) of product were obtained as a colourless crystalline solid.

^{1}H-NMR: (300 MHz, CDCl$_3$)

Identical to Experiment 63.

8.3.6.1.2 Synthesis of 3-benzyl-2-(2-bromoethyl)-3-hydroxy-2,3-dihydro-1H-isoindol-1-one (37a) [Experiment 120]

General procedure 10 was followed using 2.04 g of phenylacetic acid, 1.04 g of K$_2$CO$_3$, 1.27 g of N-bromoethyl phthalimide and 360 mL of DMF/pH 7 buffer (1:1) and 3 hours of irradiation. After workup, 0.78 g (45%) of product were obtained as a off-white solid.

^{1}H-NMR: (300 MHz, CDCl$_3$)

Identical to Experiment 63.

8.3.6.1.3 Synthesis of 3-benzylidene-2-(2-bromoethyl)-2,3-dihydro-1H-isoindol-1-one (38a) [Experiment 121]
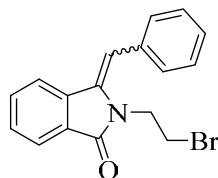
General procedure 11 was followed using 1.52 g of photoproduct **37a**, 3 drops of conc. H_2SO_4 and 30 mL of acetone. Reaction mixture was diluted with water (25 mL), concentrated to dryness and extracted with DCM (3 × 25 mL). After workup, 0.53 g (37%) of product were obtained as a yellowish solid.

^{1}H-NMR: (300 MHz, CDCl$_3$)

Identical to Experiment 79.

8.3.6.1.4 Synthesis of 3-benzylidene-2-(2-bromoethyl)-2,3-dihydro-1H-isoindol-1-one (38a) [Experiment 122]

General procedure 11 was followed using 1.52 g of photoproduct **37a**, 3 drops of conc. H_2SO_4 and 30 mL of DMF. After workup, 1.19 g (83%) of product were obtained as a brownish solid.

^{1}H-NMR: (300 MHz, CDCl$_3$)

Identical to Experiment 79.

8.3.6.1.5 Synthesis of 3-benzylidene-2-(2-bromoethyl)-2,3-dihydro-1H-isoindol-1-one (38a) [Experiment 123]

General procedure 11 was followed using 1.52 g of photoproduct **37a**, 3 drops of conc. H_2SO_4 and 30 mL of acetonitrile. After workup, 1.15 g (80%) of product were obtained as a yellowish oil.

^{1}H-NMR: (300 MHz, CDCl$_3$)

Identical to Experiment 79.

8.3.6.1.6 Synthesis of 3-benzylidene-2-[2-(diethylamino)ethyl]-2,3-dihydro-1H-isoindol-1-one (39a) [Experiment 124]
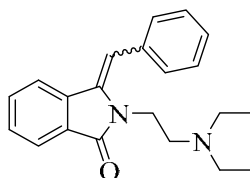
General procedure 12 was followed using 0.34 mL of diethylamine, 0.98 g dehydrated product **38a**, catalytic amounts of KI, 0.62 g K_2CO_3 and 10 mL of acetone. After workup, 0.45 g (46%) of product were obtained as an amorphous brown solid.

^{1}H-NMR: (300 MHz, CDCl$_3$)

Identical to Experiment 95.

8.3.6.1.7 Synthesis of 3-benzylidene-2-[2-(diethylamino)ethyl]-2,3-dihydro-1H-isoindol-1-one (39a) [Experiment 125]

General procedure 12 was followed using 0.34 mL of diethylamine, 0.98 g dehydrated product **38a**, catalytic amounts of KI, 0.62 g K_2CO_3 and 10 mL of acetonitrile. After workup, 0.52 g (53%) of product were obtained as a brownish solid.

^{1}H-NMR: (300 MHz, CDCl$_3$)

Identical to Experiment 95.

8.3.6.2 Photodecarboxylative addition of phenylacetates to *N*-alkylphthalimides under flow conditions [Experiments 126-135]

General procedure 13 (GP13): 20 mL of a degassed 2:1 mixture of the respective phenylacetic acid (3 eq.), K_2CO_3 (1.5 eq.) and *N*-(bromoalkyl) phthalimide (1 eq.) in a solvent:pH 7 buffer (2:1) was pumped through the in-house flow photoreactor equipped with a single 8 W UVB fluorescent tube. The reaction mixture and 20 mL of wash solvent were collected in a flask. The reaction mixture was concentrated to dryness at low temperature (<30°C) and extracted with CH_2Cl_2 (3 × 25 mL). The combined organic layer was dried over $MgSO_4$. The solvent was evaporated to dryness on a rotary evaporated at low temperature (<30°C) and the product was dried in vacuum.

8.3.6.2.1 Synthesis of 3-benzyl-2-(2-bromoethyl)-3-hydroxy-2,3-dihydro-1H-isoindol-1-one (37a) [Experiment 126]
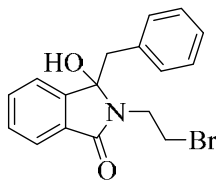
General procedure 13 was followed using 0.09 g of phenylacetic acid, 0.07 g of K_2CO_3, 0.083 g of *N*-bromoethyl phthalimide and 20 mL of acetone/pH 7 buffer (2:1) and a 20 minutes residence time (at a flow rate of 0.25 mL/min). After workup, 0.11 g (87%) of product were obtained as a yellowish solid.

^{1}H-NMR: (300 MHz, CDCl$_3$)

Identical to Experiment 63.

8.3.6.2.2 Synthesis of 3-benzyl-2-(2-bromoethyl)-3-hydroxy-2,3-dihydro-1H-isoindol-1-one (37a) [Experiment 127]

General procedure 13 was followed using 0.09 g of phenylacetic acid, 0.07 g of K_2CO_3, 0.083 g of *N*-bromoethyl phthalimide and 20 mL of acetonitrile/pH 7 buffer (2:1) and a 30 minutes residence time (at a flow rate of 0.16 mL/min). After workup, 0.09 g (83%) of product were obtained as a yellowish solid.

¹H-NMR: (300 MHz, CDCl₃)

Identical to Experiment 63.

8.3.6.2.3 Synthesis of 2-(2-bromoethyl)-3-hydroxy-3-(4-methoxybenzyl)-2,3-dihydro-1H-isoindol-1-one (37e) [Experiment 128]

General procedure 13 was followed using 0.14 g of *p*-methoxyphenylacetic acid, 0.07 g of K_2CO_3, 0.083 g of *N*-bromoethyl phthalimide and 20 mL of acetone/pH 7 buffer (2:1) and a 20 minutes residence time (at a flow rate of 0.25 mL/min). Workup and titruation with ethyl acetate (10 mL) and cyclohexane (~3 ml, dropwise) furnished 0.123 g (85%) of the product as a yellowish solid.

¹H-NMR: (300 MHz, CDCl₃)

Identical to Experiment 67.

8.3.6.2.4 Synthesis of 2-(2-bromoethyl)-3-hydroxy-3-(4-methoxybenzyl)-2,3-dihydro-1H-isoindol-1-one (37e) [Experiment 129]

General procedure 13 was followed using 0.14 g of *p*-methoxyphenylacetic acid, 0.07 g of K_2CO_3, 0.083 g of *N*-bromoethyl phthalimide and 20 mL of acetonitrile/pH 7 buffer (2:1) and a 30 minutes residence time (at a flow rate of 0.16 mL/min). Workup and titruation with ethyl acetate (10 mL) and cyclohexane (~3 ml, dropwise) furnished 0.123 g (85%) of the product as a yellowish solid.

¹H-NMR: (300 MHz, CDCl₃)

Identical to Experiment 67.

8.3.6.2.5 Synthesis of 3-benzyl-2-(3-bromopropyl)-3-hydroxy-2,3-dihydro-1H-isoindol-1-one (37i) [Experiment 130]
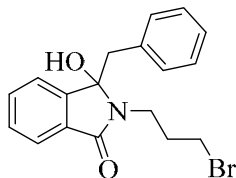
General procedure 13 was followed using 0.09 g of phenylacetic acid, 0.07 g of K_2CO_3, of 0.09 g of *N*-bromopropyl phthalimide and 20 mL of acetone/pH 7 buffer (2:1) and 20 minutes residence time (at a flow rate of 0.25 mL/min). After workup, 0.11 g (95%) of product were obtained as a colourless solid.

^{1}H-NMR: (300 MHz, CDCl$_3$)

Identical to Experiment 71.

8.3.6.2.6 Synthesis of 3-benzyl-2-(3-bromopropyl)-3-hydroxy-2,3-dihydro-1H-isoindol-1-one (37i) [Experiment 131]

General procedure 13 was followed using 0.09 g of phenylacetic acid, 0.07 g of K_2CO_3, of 0.09 g of *N*-bromopropyl phthalimide and 20 mL of acetonitrile/pH 7 buffer (2:1) and a 30 minutes residence time (at a flow rate of 0.16 mL/min). After workup, 0.1 g (91%) of product were obtained as a colourless solid.

^{1}H-NMR: (300 MHz, CDCl$_3$)

Identical to Experiment 71.

8.3.6.2.7 Synthesis of 2-(3-bromopropyl)-3-hydroxy-3-(4-methylbenzyl)-2,3-dihydro-1H-isoindol-1-one (37n) [Experiment 132]

General procedure 13 was followed using 0.11 g of *p*-methylphenylacetic acid, 0.07 g of K_2CO_3, of 0.09 g of *N*-bromopropyl phthalimide and 20 mL of acetone/pH 7 buffer (2:1) and a 20 minutes residence time (at a flow rate of 0.25 mL/min). After workup, 0.1 g (80%) of product were obtained as a colourless crystalline solid.

^{1}H-NMR: (300 MHz, CDCl$_3$)

Identical to Experiment 76.

8.3.6.2.8 Synthesis of 2-(3-bromopropyl)-3-hydroxy-3-(4-methylbenzyl)-2,3-dihydro-1H-isoindol-1-one (37n) [Experiment 133]

General procedure 13 was followed using 0.11 g of *p*-methylphenylacetic acid, 0.07 g of K$_2$CO$_3$, of 0.09 g of *N*-bromopropyl phthalimide and 20 mL of acetonitrile/pH 7 buffer (2:1) and a 30 minutes residence time (at a flow rate of 0.16 mL/min). After workup, 0.1 g (83%) of product were obtained as a colourless crystalline solid.

¹H-NMR: (300 MHz, CDCl$_3$)

Identical to Experiment 76.

8.3.6.2.9 Synthesis of 2-(3-bromopropyl)-3-hydroxy-3-(4-methylbenzyl)-2,3-dihydro-1H-isoindol-1-one (37n) [Experiment 134]

General procedure 13 was followed using 0.10 g of *p*-fluorophenylacetic acid, 0.07 g of K$_2$CO$_3$, of 0.09 g of *N*-bromopropyl phthalimide and 20 mL of acetone/pH 7 buffer (2:1) and a 20 minutes residence time (at a flow rate of 0.25 mL/min). After workup, 0.12 g (89%) of product were obtained as a yellowish solid.

¹H-NMR: (300 MHz, CDCl$_3$)
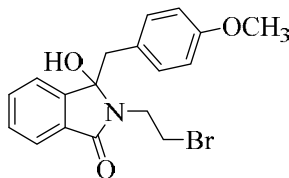
Identical to Experiment 72.

8.3.6.2.10 Synthesis of 2-(3-bromopropyl)-3-hydroxy-3-(4-methylbenzyl)-2,3-dihydro-1H-isoindol-1-one (37n) [Experiment 135]

General procedure 13 was followed using 0.10 g of *p*-fluorophenylacetic acid, 0.07 g of K$_2$CO$_3$, of 0.09 g of *N*-bromopropyl phthalimide and 20 mL of acetonitrile/pH 7 buffer (2:1) and a 30 minutes residence time (at a flow rate of 0.16 mL/min). After workup, 0.12 g (90%) of product were obtained as a yellowish solid.

¹H-NMR: (300 MHz, CDCl$_3$)

Identical to Experiment 72.

8.3.6.3 Coupled photodecarboxylative addition of phenylacetates to *N*-alkylphthalimides and dehydration of photoproducts under flow conditions [Experiments 136-140]

General procedure 14 (GP14): A degassed mixture of the respective phenylacetic acid (3 eq.), K_2CO_3 (1.5 eq.) and *N*-(bromoalkyl) phthalimide (1 eq.) in 10 mL of acetonitrile:pH 7 buffer (3:1) was pumped through the in-house flow photoreactor equipped with a single 8 W UVB fluorescent tube using a residence time of 30 min (at a flow rate of 0.16 mL/min). After 20 minutes, 20 mL of a 1:1 mixture of acetonitrile and 10 M H_2SO_4 were injected at a flow rate of 0.16 mL/min into the effluent stream in a T-junction. The combined reaction mixture was pumped through a 10 m capillary submerged in an ultrasonic bath. The final product was collected at the exit of the thermal capillary. The collected reaction mixture was diluted with water (25 mL) and extracted with CH_2Cl_2 (3 × 25 mL). The combined organic layers were washed with brine (25 mL) and dried over $MgSO_4$. Evaporation and drying furnished the desired product.

8.3.6.3.1 Synthesis of 3-benzylidene-2-(2-bromoethyl)-2,3-dihydro-1H-isoindol-1-one (38a) [Experiment 136]
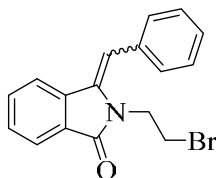
General procedure 14 was followed using 0.045 g of phenylacetic acid, 0.035 g of K_2CO_3, 0.042 g of *N*-bromoethyl phthalimide and 30 and 20 minutes residence times. After workup, 0.036 g (91%) of product were obtained as a yellowish solid.

**^{1}H-NMR:** (300 MHz, CDCl$_3$)

Identical to Experiment 79.

8.3.6.3.2 Synthesis of 2-(2-bromoethyl)-3-(4-methoxybenzylidene)-2,3-dihydro-1H-isoindol-1-one (38e) [Experiment 137]

General procedure 14 was followed using 0.055 g of *p*-methoxyphenylacetic acid, 0.035 g of K_2CO_3, 0.042 g of *N*-bromoethyl phthalimide and 30 and 20 minutes residence times. After workup, 0.036 g (90%) of product were obtained as a bright yellow oil.

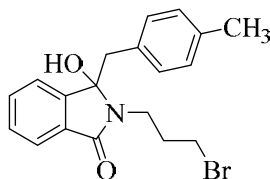**¹H-NMR:** (300 MHz, CDCl₃)

Identical to Experiment 83.

8.3.6.3.3 Synthesis of 3-benzylidene-2-(3-bromopropyl)-2,3-dihydro-1H-isoindol-1-one (38i) [Experiment 138]

General procedure 14 was followed using 0.045 g of phenylacetic acid, 0.035 g of K₂CO₃, 0.045 g of *N*-bromopropyl phthalimide and 30 and 20 minutes residence times. After workup, 0.035 g (83%) of product were obtained as a yellow oil.
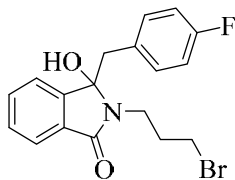
¹H-NMR: (300 MHz, CDCl₃)

Identical to Experiment 87.

8.3.6.3.4 Synthesis of 2-(3-bromopropyl)-3-(4-methylbenzylidene)-2,3-dihydro-1H-isoindol-1-one (38n) [Experiment 139]
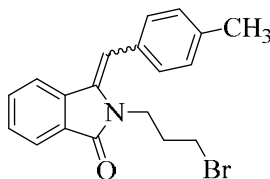
General procedure 14 was followed using 0.050 g of *p*-methylphenylacetic acid, 0.035 g of K₂CO₃, 0.045 g of *N*-bromopropyl phthalimide and 30 and 20 minutes residence times. After workup, 0.034 g (86%) of product were obtained as a yellow oil.

¹H-NMR: (300 MHz, CDCl₃)

Identical to Experiment 92.

8.3.6.3.5 Synthesis of 2-(3-bromopropyl)-3-(4-fluorobenzylidene)-2,3-dihydro-1H-isoindol-1-one (38j) [Experiment 140]

General procedure 14 was followed using 0.051 g of 4-fluorophenylacetic acid, 0.035 g of K$_2$CO$_3$, 0.045 g of *N*-bromopropyl phthalimide and 30 and 20 minutes residence times. After workup, 0.04 g (94%) of product were obtained as a yellow oil.

^{1}H-NMR: (300 MHz, CDCl$_3$)

Identical to Experiment 88.

8.3.6.4 In series multistep flow synthesis of AL12, AL5 and their analogues [Experiments 141-145]

General procedure 15 (GP15): A degassed mixture of the respective phenylacetic acid (3 eq.), K$_2$CO$_3$ (1.5 eq.) and *N*-(bromoalkyl) phthalimide (1 eq.) in 10 mL of acetonitrile:pH 7 buffer (3:1) was pumped through the in-house flow photoreactor equipped with a single 8 W UVB fluorescent tube at a residence time of 30 min (at a flow rate of 0.16 mL/min). Ater 20 minutes, 20 mL of a 1:1 mixture of acetonitrile and 10 M H$_2$SO$_4$ were injected at a flow rate of 0.16 mL/min into the effluent stream in a T-junction. The combined reaction mixture was pumped through a 10 m capillary submerged in an ultrasonic bath. The effluent from the thermal reaction was passed through a cartridge filled with ion exchange resin. After another 20 minutes, a mixture of 2 mL of diethylamine in 38 mL of acetonitrile was injected at a flow rate of 0.25 mL/min into the reaction stream in a T-junction. The combined reaction mixture is passed through a 10 m capillary submerged in a water bath at 100°C. The crude amination product was collected at the exit of the second thermal capillary. 50 mL of water were added to the collected reaction mixture and the solution was acidified using 1 M HCl. The solution was subsequently washed with ethyl acetate (50 mL). The aqueous layer containing the target compound was then basified to pH 10 using ammonia solution and extracted with CH$_2$Cl$_2$ (3 × 25 mL). The combined organic phase was collected, washed with brine (50 mL) and dried over MgSO$_4$. The organic layer was evaporated to dryness by rotary evaporation and further dried in vacuum.

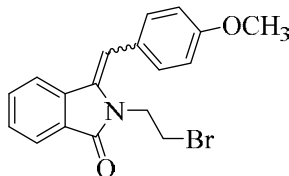### 8.3.6.4.1 Synthesis of 3-benzylidene-2-[2-(diethylamino)ethyl]-2,3-dihydro-1H-isoindol-1-one (39a) [Experiment 141]
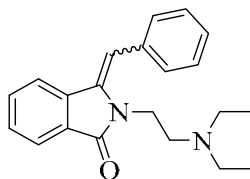
General procedure 15 was followed using 0.045 g of phenylacetic acid, 0.035 g of K_2CO_3, 0.042 g of *N*-bromoethyl phthalimide, 2 mL of diethylamine and 30, 20 and 20 minutes residence times. After workup, 0.039 g (75%) of product were obtained as a brownish solid.

^{1}H-NMR: (300 MHz, CDCl$_3$)

Identical to Experiment 79.

8.3.6.4.2 Synthesis of 2-[2-(diethylamino)ethyl]-3-(4-methoxybenzylidene)-2,3-dihydro-1H-isoindol-1-one (39e) [Experiment 142]
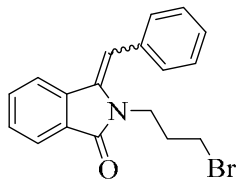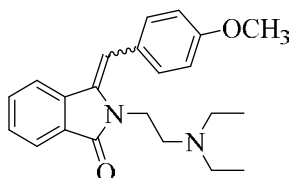

General procedure 15 was followed using 0.055 g of *p*-methoxyphenylacetic acid, 0.035 g of K_2CO_3, 0.042 g of *N*-bromoethyl phthalimide, 2 mL of diethylamine and 30, 20 and 20 minutes residence times. After workup, 0.042 g (73%) of product were obtained as a brownish oil.

^{1}H-NMR: (300 MHz, CDCl$_3$)

Identical to Experiment 83.

8.3.6.4.3 Synthesis of 3-benzylidene-2-[2-(diethylamino)propyl]-2,3-dihydro-1H-isoindol-1-one (39i) [Experiment 143]
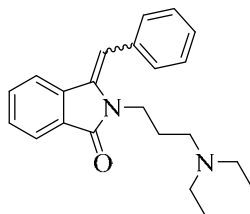
General procedure 15 was followed using 0.045 g of phenylacetic acid, 0.035 g of K_2CO_3, 0.045 g of *N*-bromopropyl phthalimide, 2 mL of diethylamine and 30, 20 and 20 minutes residence times. After workup, 0.042 g (75%) of product were obtained as a brownish oil.

^{1}H-NMR: (300 MHz, CDCl$_3$)

Identical to Experiment 87.

8.3.6.4.4 Synthesis of 2-[2-(diethylamino)propyl]-3-(4-methylbenzylidene)-2,3-dihydro-1H-isoindol-1-one (38n) [Experiment 144]
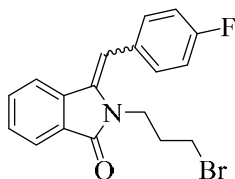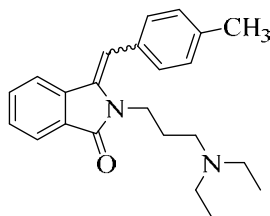

General procedure 15 was followed using 0.050 g of *p*-methylphenylacetic acid, 0.035 g of K$_2$CO$_3$, 0.045 g of *N*-bromopropyl phthalimide, 2 mL of diethylamine and 30, 20 and 20 minutes residence times. After workup, 0.047 g (77%) of product were obtained as a brownish oil.

^{1}H-NMR: (300 MHz, CDCl$_3$)

Identical to Experiment 92.

8.3.6.4.5 Synthesis of 2-[2-(diethylamino)propyl]-3-(4-fluorobenzylidene)-2,3-dihydro-1H-isoindol-1-one (39j) [Experiment 145]
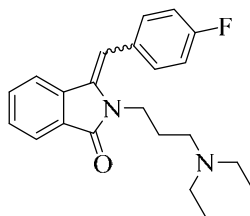
General procedure 15 was followed using 0.051 g of 4-fluorophenylacetic acid, 0.035 g of K$_2$CO$_3$, 0.045 g of *N*-bromopropyl phthalimide, 2 mL of diethylamine and 30, 20 and 20 minutes residence times. After workup, 0.046 g (75%) of product were obtained as a brownish solid.

^{1}H-NMR: (300 MHz, CDCl$_3$)

Identical to Experiment 88.

8.3.7 Synthesis of aristolactams [Experiments 146-156]

8.3.7.1 Synthesis of 3-hydroxy-3-(2-iodobenzyl)-2-methyl-2,3-dihydro-1H-isoindol-1-one (43) [Experiment 146]
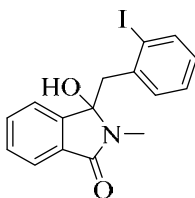
General procedure 10 was followed using 3.93 g of *o*-iodophenylacetic acid, 1.04 g of K_2CO_3, 1.27 g of *N*-methyl phthalimide and 60 mL of acetone/pH 7 buffer (1:1) and 3 hours of irradiation. After worup and column chromatography using 30% EtOAc in cyclohexane as eluent, 1.52 g (51%) of product were obtained as yellow crystals.

Melting point: 147-148°C.

¹H-NMR: (400 MHz, acetone-d₆)

δ (ppm): 3.00 (s, 3 H, NCH₃), 3.26 (d, J = 16 Hz, 1 H, CH₂Ar), 3.68 (d, J = 16 Hz, 1 H, CH₂Ar), 5.42 (s, 1 H, OH), 6.95 (ddd, J = 4, 8, 8 Hz, 1 H, CH$_{arom}$), 7.02-7.07 (m, 1 H, CH$_{arom}$), 7.25-7.30 (ddd, J = 4, 8, 8 Hz, 1 H, CH$_{arom}$), 7.35 (dd, J = 4, 8 Hz, 1 H, CHarom) 7.56-7.60 (m, 1 H, CH$_{arom}$), 7.76 (dd, J = 8, 8 Hz, 1 H, CH$_{arom}$).

¹³C-NMR: (100 MHz, acetone-d₆)

δ (ppm): 24.0 (s, 1 C, NCH₃), 47.7 (s, 1 C, CH₂Ar), 90.2 (s, 1 C, COH), 104.0 (s, 1 C, CH$_{arom}$), 122.8 (s, 1 C, CH$_{arom}$), 123.9 (s, 1 C, CH$_{arom}$), 128.5 (s, 1 C, CH$_{arom}$), 129.3 (s, 1 C, CH$_{arom}$), 129.6 (s, 1 C, CH$_{arom}$), 131.4 (s, 1 C, CH$_{arom}$), 131.8 (s, 1 C, CH$_{arom}$), 132.5 (s, 1 C, Cq$_{arom}$), 139.6 (s, 1 C, Cq$_{arom}$), 139.9 (s, 1 C, CH$_{arom}$), 147.7 (s, 1 C, Cq$_{arom}$), 166.5 (s, 1 C, C=O).

8.3.7.2 Synthesis of 2-(2-bromoethyl)-3-hydroxy-3-(2-iodobenzyl)-2,3-dihydro-1H-isoindol-1-one (44a) [Experiment 147]
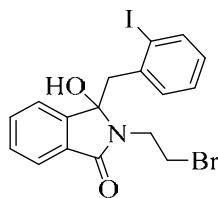
General procedure 10 was followed using 3.93 g of *o*-iodophenylacetic acid, 1.04 g of K_2CO_3, 0.81 g of *N*-bromoethyl phthalimide and 60 mL of acetone/pH 7 buffer (1:1) and 3 hours of irradiation. A yellowish solid precipitated during irradiation. Workup and further purification by column chromatography using 30% EtOAc in cyclohexane as eluent gave 1.0 g (67%) of product as yellow crystals.

¹H-NMR: (400 MHz, acetone-d₆)

δ (ppm): 3.34 (d, J = 18 Hz, 1 H, CH₂Ar), 3.75 (m, 2 H, CH₂Br), 3.84 (d, J = 18 Hz, 1 H, CH₂Ar), 4.10 (m, 2 H, NCH₂), 5.68 (s, 1 H, OH), 6.89 (d, 1 H, CH$_{arom}$), 6.99 (dd, 1 H, CH$_{arom}$), 7.31-7.50 (m, 3 H, CH$_{arom}$), 7.62 (dd, 1 H, CH$_{arom}$), 7.78 (d, 1 H, CH$_{arom}$).

¹³C-NMR: (100 MHz, CDCl₃)

δ (ppm): 41.8 (t, 1 C, NCH$_2$), 48.5 (t, 1 C, CH$_2$Ar), 55.2 (t, 1 C, CH$_2$Br), 90.3 (s, 1 C, COH), 124.2 (d, 1 C, CH$_{arom}$), 128.5 (d, 1 C, CH$_{arom}$), 129.5 (d, 1 C, CH$_{arom}$), 130.2 (d, 1 C, CH$_{arom}$), 131.5 (d, 1 C, CH$_{arom}$), 132.7 (d, 1 C, CH$_{arom}$), 138.0 (d, 1 C, Cq$_{arom}$), 140.2 (d, 1 C, CH$_{arom}$), 147.8 (s, 1 C, Cq$_{arom}$), 156.2 (s, 1 C, Cq$_{arom}$), 173.5 (s, 1 C, C=O).

HRMS: (ESI/MeOH)

m/z: calcd for C$_{17}$H$_{15}$NO$_2$BrI (M+Na)$^+$: 493.9223, found: 493.9242 ± 4 ppm.

8.3.7.3 Synthesis of 2-(3-bromopropyl)-3-hydroxy-3-(2-iodobenzyl)-2,3-dihydro-1H-isoindol-1-one (44b) [Experiment 148]
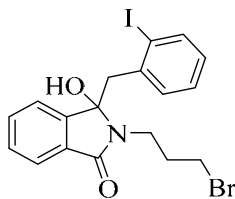
General procedure 10 was followed using 3.93 g of *o*-iodophenylacetic acid, 1.04 g of K$_2$CO$_3$, 1.34 g of *N*-bromopropyl phthalimide and 60 mL of acetone/pH 7 buffer (1:1) and 3 hours of irradiation. A yellowish solid precipitated during irradiation. After workup and further purification by column chromatography using 30% EtOAc in cyclohexane as eluent, 1.72 g (71%) of product were obtained as a yellowish solid.

¹H-NMR: (400 MHz, CDCl$_3$)

δ (ppm): 3.33 (d, J = 15 Hz, 1 H, CH$_2$Ar), 3.63-3.67 (m, 3 H, CH$_2$Ar), 3.85-3.97 (m, 2 H, CH$_2$Br, NCH$_2$), 5.63 (s, 1 H, OH), 6.89 (d, J = 9 Hz, 1 H, CH$_{arom}$), 7.02 (m, 1 H, CH$_{arom}$), 7.28-7.51 (m, 5 H, CH$_{arom}$), 7.64 (d, J = 9 Hz, 1 H, CH$_{arom}$), 7.81 (d, J = 9 Hz, 1 H, CH$_{arom}$).

¹³C-NMR: (100 MHz, CDCl$_3$)

δ (ppm): 32.3 (t, 1 C, CH$_2$), 33.4 (t, 1 C, CH$_2$Br), 38.6 (t, 1 C, NCH$_2$), 48.2 (t, 1 C, CH$_2$Ar), 91.2 (s, 1 C, COH), 115.0 (d, 1 C, CH$_{arom}$), 119.2 (d, 1 C, CH$_{arom}$), 120.7 (s, 1 C, CH$_{arom}$), 121.9 (s, 2 C, CH$_{arom}$), 123.8 (s, 1 C, Cq$_{arom}$), 128.7 (s, 2 C, CH$_{arom}$), 129.9 (s, 1 C, CH$_{arom}$), 131.5 (s, 1 C, CH$_{arom}$), 132.0 (s, 1 C, Cq$_{arom}$), 140.2 (s, 1 C, Cq$_{arom}$), 160.9 (s, 1 C, C=O).

HRMS: (ESI/MeOH)

m/z: calcd for C$_{18}$H$_{17}$NO$_2$BrI (M+Na)$^+$: 507.9380, found: 507.9365 ± 3 ppm.

8.3.7.4 Synthesis of 3-(2-iodobenzylidene)-2-methyl-2,3-dihydro-1H-isoindol-1-one (45) [Experiment 149]
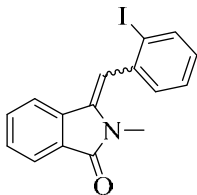
General procedure 11 was followed using 1.52 g of photoproduct **43**, 3 drops of conc. H_2SO_4 and 30 mL of CH_2Cl_2. After workup, 1.3 g (90%) of product were obtained as a yellow solid.

Melting point: 142-144°C.

^{1}H-NMR: (mixture of stereoisomers, 300 MHz, acetone-d_6)

Main *E*-isomer:

δ (ppm): 3.44 (s, 3 H, NCH$_3$), 6.65 (s, 1 H, CH$_{olef.}$), 7.02 (d, J = 8 Hz, 1 H, CH$_{arom}$), 7.26 (m, 1 H, CH$_{arom}$), 7.43 (ddd, J = 4, 8, 8 Hz, 1 H, CH$_{arom}$), 7.53-7.58 (m, 2 H, CH$_{arom}$), 7.64 (dd, J = 4, 8 Hz, 1 H, CH$_{arom}$), 7.81 (d, J = 8 Hz, 1 H, CH$_{arom}$), 8.10 (dd, J = 4, 8 Hz, 1 H, CH$_{arom}$).

Minor *Z*-isomer: quantity too low to assign peaks.

8.3.7.5 Synthesis of 2-(2-bromoethyl)-3-(2-iodobenzylidene)-2,3-dihydro-1H-isoindol-1-one (46a) [Experiment 150]
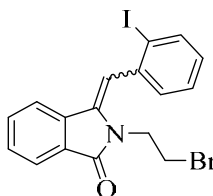
General procedure 11 was followed using 1.89 g of photoproduct **44a**, 3 drops of conc. H_2SO_4 and 30 mL of CH_2Cl_2. After workup, 1.63 g (90%) of product were obtained as a yellow oil.

^{1}H-NMR: (mixture of stereoisomers, 300 MHz, CDCl$_3$)

Main *E*-isomer:

δ (ppm): 3.68 (t, J = 6 Hz, 2 H, CH$_2$Br), 4.33 (t, J = 6 Hz, 2 H, NCH$_2$), 6.36 (s, 1 H, CH$_{olef}$), 7.02 (d, 1 H, CH$_{arom}$), 7.13 (dd, 1 H, CH$_{arom}$), 7.29-7.52 (m, 4 H, CH$_{arom}$), 7.86 (m, 1 H, CH$_{arom}$), 7.99 (d, 1 H, CH$_{arom}$).

Minor *Z*-isomer: quantity too low to assign peaks.

^{13}C-NMR: (mixture of stereoisomers, 75 MHz, CDCl$_3$)

Main *E*-isomer:

δ (ppm): 28.6 (t, 1 C, CH$_2$Br), 42.0 (t, 1 C, NCH$_2$), 110.9 (d, 1 C, CH$_{olef}$), 114.2 (d, 2 C, CH$_{arom}$), 120.6 (d, 1 C, CH$_{arom}$), 120.9 (s, 1 C, Cq), 123.8 (s, 1 C, Cq$_{arom}$), 123.9 (d, 1 C, CH$_{arom}$), 129.1 (d, 1 C, CH$_{arom}$), 130.6 (d, 2 C, CH$_{arom}$), 131.7 (s, 1 C, Cq$_{arom}$), 132.9 (d, 1 C, CH$_{arom}$), 136.9 (s, 1 C, Cq$_{arom}$), 140.0 (s, 1 C, Cq$_{arom}$), 170.4 (s, 1 C, C=O).

Minor Z-isomer: quantity too low to assign peaks.

HRMS: (mixture of stereoisomers, ESI/MeOH)

m/z: calcd for C$_{17}$H$_{13}$ONBrI (M+Na)$^+$: 475.9117, found: 475.9128 ± 2 ppm.

8.3.7.6 Synthesis of 2-(3-bromopropyl)-3-(2-iodobenzylidene)-2,3-dihydro-1H-isoindol-1-one (46b) [Experiment 151]
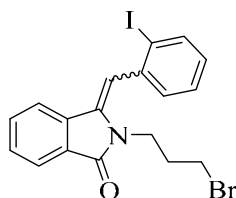
General procedure 11 was followed using 1.95 g of photoproduct **44b**, 3 drops of conc. H$_2$SO$_4$ and 30 mL of CH$_2$Cl$_2$. After workup, 1.56 g (83%) of product were obtained as a yellow liquid.

^{1}H-NMR: (mixture of stereoisomers, 300 MHz, CDCl$_3$)

Main E-isomer:

δ (ppm): 2.41-2.49 (quin, 2 H, CH$_2$), 3.53 (t, J = 9 Hz, 2 H, NCH$_2$), 4.25 (t, J = 9 Hz, 2 H, CH$_2$Br), 6.48 (s, 1 H, CH$_{olefin.}$), 7.18 (d, J = 9 Hz, 1 H, CH$_{arom}$), 7.16-7.22 (m, 1 H, CH$_{arom}$), 7.30-7.35 (m, 1 H, CH$_{arom}$), 7.42-7.49 (m, 2 H, CH$_{arom}$), 7.51-7.55 (m, 1 H, CH$_{arom}$), 7.85 (d, J = 9 Hz, 1 H, CH$_{arom}$), 8.03 (d, J = 9 Hz, 1 H, CH$_{arom}$).

Minor Z-isomer: quantity too low to assign peaks.

^{13}C-NMR: (mixture of stereoisomers, 75 MHz, CDCl$_3$)

Main E-isomer:

δ (ppm): 31.3 (t, 1 C, CH$_2$), 32.5 (t, 1 C, CH$_2$Br), 39.0 (t, 1 C, NCH$_2$), 110.4 (d, 1 C, CH$_{olef}$), 114.2 (d, 1 C, CH$_{arom}$), 120.4 (d, 1 C, CH$_{arom}$), 125.0 (d, 1 C, Cq), 128.7 (d, 1 C, CH$_{arom}$), 129.2 (d, 2 C, CH$_{arom}$), 130.9 (d, 2 C, CH$_{arom}$), 131.5 (d, 1 C, Cq$_{arom}$), 132.6 (d, 1 C, CH$_{arom}$), 135.5 (s, 1 C, Cq$_{arom}$), 137.1 (s, 1 C, Cq$_{arom}$), 140.1 (s, 1 C, Cq$_{arom}$), 167.5 (s, 1 C, C=O).

Minor Z-isomer: quantity too low to assign peaks.

HRMS: (mixture of stereoisomers, ESI/MeOH)

m/z: calcd for C$_{18}$H$_{15}$NOBrI (M+Na)$^+$: 489.9274, found: 489.9279 ± 1 ppm.

8.3.7.7 Photodehydrohalogenation reactions

General procedure 16 (GP16): 3 mmol of iodo-enamide were dissolved in 60 mL of dry benzene in a Pyrex Schlenk flask. The solution was degassed with nitrogen and irradiated in a Rayonet chamber reactor equipped with UVB light for 15 hours. The solvent was removed in vacuum and the crude product was purified by column chromatography using 20% EtOAc in cyclohexane as eluent.

8.3.7.7.1 Synthesis of 1-methyl-6,7-naphthyl[cd]indol-2(1H)-one (47) [Experiment 152]
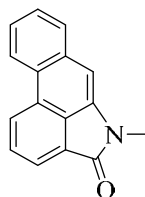
General procedure 16 was followed using 1.08 g of dehydration product **45**, 60 mL of benzene and 15 hours of irradiation. After workup, 0.17 g (24%) of **47** were obtained as a yellow amorphous solid.

¹H-NMR: (400 MHz, acetone-d₆)

δ (ppm): 3.47 (s, 3 H, NCH₃), 7.39 (s, 1 H, CH$_{arom}$), 7.62 (m, 2 H, CH$_{arom}$), 7.92 (t, J = 8 Hz, 1 H, CH$_{arom}$), 7.99 (d, J = 8 Hz, 1 H, CH$_{arom}$), 8.06 (d, J = 8 Hz, 1 H, CH$_{arom}$), 8.70 (d, J = 8 Hz, 1 H, CH$_{arom}$), 8.82 (d, J = 8 Hz, 1 H, CH$_{arom}$).

8.3.7.7.2 Synthesis of 1-(2-bromoethyl)-6,7-naphthyl[cd]indol-2(1H)-one (48a) [Experiment 153]
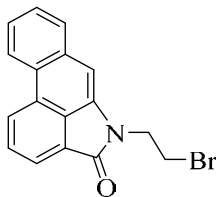
General procedure 16 was followed using 1.37 g of dehydration product **46a**, 60 mL of benzene and 15 hours of irradiation. After workup, 0.56 g (57%) of **48a** were obtained as a yellowish solid.

¹H-NMR: (400 MHz, CDCl₃)

δ (ppm): 3.74 (t, J = 8 Hz, 2 H, CH₂Br), 4.41 (t, J = 8 Hz, 2 H, NCH₂), 7.21 (s, 1 H, CH$_{arom}$), 7.61 (m, 1 H, CH$_{arom}$), 7.87 (m, 2 H, CH$_{arom}$), 8.13 (d, J = 8 Hz, 1 H, CH$_{arom}$), 8.55 (d, J = 8 Hz, 1 H, CH$_{arom}$), 8.64 (d, J = 8 Hz, 1 H, CH$_{arom}$).

¹³C-NMR: (100 MHz, CDCl₃)

δ (ppm): 29.1 (t, 1 C, CH$_2$Br), 43.1 (t, 1 C, NCH$_2$), 106.0 (d, 1 C, CH$_{olef}$), 114.2 (d, 2 C, CH$_{arom}$), 120.6 (d, 1 C, CH$_{arom}$), 123.8 (s, 1 C, Cq), 123.9 (s, 2 C, Cq$_{arom}$), 124.6 (d, 1 C, CH$_{arom}$), 126.6 (d, 1 C, CH$_{arom}$), 127.1 (d, 2 C, CH$_{arom}$), 128.7 (s, 1 C, Cq$_{arom}$), 130.0 (d, 1 C, CH$_{arom}$), 135.1 (s, 2 C, Cq$_{arom}$), 162.4 (s, 1 C, Cq$_{arom}$), 172.8 (s, 1 C, C=O).

HRMS: (ESI/MeOH)

m/z: calcd for C$_{17}$H$_{21}$NOBr (M+Na)$^+$: 347.9994, found: 347.9999 ± 1 ppm.

8.3.7.7.3 Synthesis of 1-(3-bromopropyl)-6,7-naphthyl[cd]indol-2(1H)-one (48b) [Experiment 154]
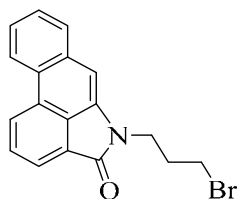
General procedure 16 was followed using 1.41 g of dehydration product **46b**, 60 mL of benzene and 15 hours of irradiation. Workup gave 0.56 g (55%) of **48b** as a yellow solid.

^{1}H-NMR: (400 MHz, CDCl$_3$)

δ (ppm): 2.43 (t, J = 6 Hz, 2 H, CH$_2$), 3.52 (t, 2 H, J = 6 Hz, 2 H, NCH$_2$), 4.17 (t, J = 6 Hz, 2 H, CH$_2$Br), 7.25 (s, 1 H, CH$_{olef}$), 7.58-7.63 (m, 2 H, CH$_{arom}$), 7.83-7.92 (m, 2 H, CH$_{arom}$), 8.11 (d, J = 9 Hz, 1 H, CH$_{arom}$), 8.55 (d, J = 9 Hz, 1 H, CH$_{arom}$), 8.62 (d, J = 9 Hz, 1 H, CH$_{arom}$).

^{13}C-NMR: (100 MHz, CDCl$_3$)

δ (ppm): 30.0 (t, 1 C, CH$_2$), 29.5 (t, 1 C, CH$_2$Br), 38.2 (t, 1 C, NCH$_2$), 105.7 (d, 1 C, CH$_{olef}$), 120.0 (d, 2 C, CH$_{arom}$), 121.1 (s, 1 C, Cq), 122.7 (s, 2 C, Cq$_{arom}$), 125.9 (d, 1 C, CH$_{arom}$), 126.0 (d, 2 C, CH$_{arom}$), 127.1 (d, 2 C, CH$_{arom}$), 127.7 (s, 1 C, Cq$_{arom}$), 129.3 (d, 1 C, CH$_{arom}$), 134.8 (s, 2 C, Cq$_{arom}$), 157.1 (s, 1 C, Cq$_{arom}$), 170.0 (s, 1 C, C=O).

8.3.7.8 Amination of aristolactams

8.3.7.8.1 Synthesis of 1-[2-(diethylamino)ethyl]-6,7-naphthyl[cd]indol-2(1H)-one (49a) [Experiment 155]
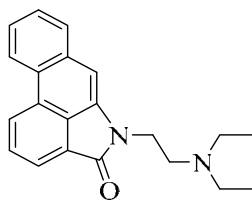
General procedure 12 was followed using 0.34 mL of diethylamine, 0.98 g dehydrated product **46a**, catalytic amounts of KI, 0.62 g K_2CO_3 and 10 mL of DMF. After workup, 0.678 g (71%) of product were obtained as a brownish oil.

¹H-NMR: (400 MHz, CDCl₃)

δ (ppm): 1.06 (t, 6 H, 2 × CH₃), 2.67 (q, 4 H, 2 × CH₂), 2.86 (t, 2 H, CH₂Br), 4.08 (t, 2 H, NCH₂), 7.15 (s, 1 H, CH_arom), 7.57 (m, 2 H, CH_arom), 7.85 (m, 2 H, CH_arom), 8.10 (d, 1 H, CH_arom), 8.53 (d, 1 H, CH_arom), 8.60 (d, 1 H, CH_arom).

¹³C-NMR: (100 MHz, CDCl₃)

δ (ppm): 13.1 (q, 2 C, CH₃), 39.9 (t, 1 C, CH₂N), 48.5 (t, 2 C, N(CH₂)₂), 63.1 (t, 1 C, NCH₂), 105.8 (d, 1 C, CH_olef), 119.1 (d, 1 C, CH_arom), 123.9 (s, 1 C,Cq), 124.4 (d, 1 C, CH_arom), 125.0 (s, 1 C, Cq_arom), 126.2 (d, 1 C, CH_arom), 126.9 (d, 1 C, CH_arom), 128.5 (d, 2 C, CH_arom), 130.2 (s, 1 C, Cq_arom), 135.1 (d, 1 C, CH_arom), 138.0 (s, 1 C, Cq_arom), 154.7 (s, 1 C, Cq_arom), 156.6 (s, 1 C, Cq_arom), 169.1 (s, 1 C, C=O).

HRMS: (ESI/MeOH)

m/z: calcd for $C_{21}H_{22}N_2O$ (M+H)⁺: 319.1805, found: 319.1810 ± 2 ppm.

  calcd for $C_{21}H_{22}N_2O$ (M+Na)⁺: 341.1624, found: 341.1633 ± 3 ppm.

8.3.7.8.2 Synthesis of 1-[2-(diethylamino)propyl]-6,7-naphthyl[cd]indol-2(1H)-one (49a) [Experiment 156]
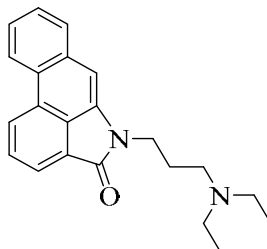
General procedure 12 was followed using 0.34 mL of diethylamine, 1.12 g dehydrated product **46b**, catalytic amounts of KI, 0.62 g K_2CO_3 and 10 mL of DMF. After workup, 0.82 g (75%) of product were obtained as a brownish yellow oil.

¹H-NMR: (400 MHz, acetone-d₆)

δ (ppm): 1.07 (t, J = 9 Hz, 2 H, N(CH₃)₂), 2.06 (m, 2 H, CH₂), 2.57-2.66 (m, 6 H, N(CH₃)₂), 2.43 (t, J = 9 Hz, 2 H, 3NCH₂), 4.08 (t, J = 6 Hz, 2 H, NCH₂), 7.22 (s, 1 H, CH_olef), 7.61-7.65 (m, 2 H, CH_arom), 7.86-7.92 (m, 2 H, CH_arom), 8.14 (d, J = 6 Hz, 1 H, CH_arom), 8.14 (d, J = 6 Hz, 1 H, CH_arom), 8.63 (d, J = 6 Hz, 1 H, CH_arom).

¹³C-NMR: (100 MHz, CDCl₃)

δ (ppm): 12.7 (q, 2 C, CH$_3$), 30.3 (t, 1 C, CH$_2$), 37.5 (t, 1 C, CH$_2$N), 41.4 (t, 2 C, N(CH$_2$)$_2$), 59.6 (t, 1 C, NCH$_2$), 106.9 (d, 1 C, CH$_{olef}$), 114.1 (d, 1 C, CH$_{arom}$), 119.9 (s, 1 C, Cq), 125.0 (d, 1 C, CH$_{arom}$), 125.2 (s, 1 C, Cq$_{arom}$), 125.9 (d, 1 C, CH$_{arom}$), 126.3 (d, 1 C, CH$_{arom}$), 128.7 (d, 2 C, CH$_{arom}$), 129.2 (s, 1 C, Cq$_{arom}$), 133.4 (d, 1 C, CH$_{arom}$), 137.9 (s, 1 C, Cq$_{arom}$), 148.7 (s, 1 C, Cq$_{arom}$), 150.5 (s, 1 C, Cq$_{arom}$), 167.6 (s, 1 C, C=O).

8.3.8 Tandem photochemical-thermal synthesis of 2-(4-hydroxybenzyl)-3-(2-phenyl-ethylidene)-2,3-dihydro-1H-isoindol-1-one, AKS186 (53) [Experiment 157]
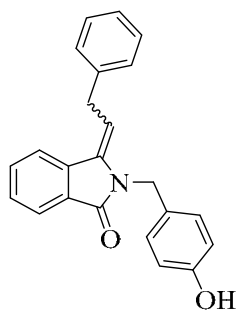
A solution of 0.033g (0.2 mmol) of 3-phenylpropanoic acid, 0.021 g (0.15 mmol) of K$_2$CO$_3$ and 0.0295 g (0.1 mmol) of *N*-(4-acetoxybenzyl) phthalimide in 10 mL of acetone/water (2:1) was pumped into the photochemical UV-150 loop of the Vapourtec easyPhotochem reactor at a flow rate of 0.1 ml/min. Neat TFA (20 mL) was injected into the effluent at a flow rate of 0.2 ml/min before entering the thermal reactor, which was kept at 50°C. The product was diluted with water (50 mL) and the acetone fraction was removed to dryness. The resulting reaction mixture was extracted with dichloromethane (3 × 50 mL), washed with saturated NaHCO$_3$ solution (3 × 50 mL) and brine (2 × 50 mL), dried over MgSO$_4$ and evaporated to dryness. Purification by column chromatography over SiO$_2$ using ethyl acetate:n-hexane (1:1) furnished 0.054 g (80%) of a *E/Z*-mixture of AKS-186 as a colourless solid.

^{1}H-NMR: (mixture of stereoisomers, 300 MHz, CDCl$_3$)

Main *E*-isomer:

δ (ppm): 3.96 (d, J = 9 Hz, 2 H, CH$_2$Ph), 4.95 (s, 2 H, NCH$_2$), 5.61 (t, J = 9 Hz, 1 H, CH$_{olef}$), 6.74 (d, J = 9 Hz, 2 H, CH$_2$), 7.11 (t, J = 9 Hz, 4 H, CH$_{arom}$), 7.22 (d, J = 9 Hz, 1 H, CH$_{arom}$), 7.29 (d, J = 9 Hz, 1 H, CH$_{arom}$), 7.51-7.58 (m, 3 H, CH$_{arom}$), 7.85 (d, J = 9 Hz, 1 H, CH$_{arom}$), 7.96 (d, J = 9 Hz, 1 H, CH$_{arom}$).

Minor *Z*-isomer: quantity too low to assign peaks.

^{13}C-NMR: (mixture of stereoisomers, 75 MHz, CDCl$_3$)

δ (ppm): 33.2 (s, 1 C, CH$_2$), 42.7(s, 1 C, CH$_2$), 111.3 (s, 1 C, COH), 115.5 (s, 1 C, CH$_{arom}$), 122.2 (s, 1 C, CH$_{arom}$), 123.7 (s, 1 C, CH$_{arom}$), 126.5 (s, 1 C, CH$_{arom}$), 128.1 (s, 1 C,

CH$_{arom}$), 128.4 (s, 1 C, CH$_{arom}$), 128.6 (s, 1 C, CH$_{arom}$), 128.9 (s, 1 C, CH$_{arom}$), 129.1 (s, 1 C, CH$_{arom}$), 130.4 (s, 1 C, Cq$_{arom}$), 132.1 (s, 1 C, Cq$_{arom}$), 135.6 (s, 1 C, Cq$_{arom}$), 139.5 (s, 1 C, Cq$_{arom}$), 154.8 (s, 1 C, Cq$_{arom}$), 166.6 (s, 1 C, C=O).

8.3.9 Solar addition of phenylacetates to *N*-alkylphthalimides [Experiments 158-167]

8.3.9.1 Solar addition of phenylacetates to *N*-alkylphthalimides under flow conditions

General procedure 17 (GP17): 4 mmol of the respective phthalimide in 180 mL of acetone was mixed with 60 mL of 8 mmol potassium carboxylate solution in pH 7 buffer. The solution was pumped into solar reactor with various residence times. Sunlight was refocused frequently on the microchannel by aligning the reactor's glass tube with the shadow of a retort stand, which was placed next to the reactor on the ground. Solar experiments were carried out between 12:00 and 4:00 pm. Most of the acetone was removed by rotary evaporation (water bath <35°C) and the resulting reaction mixture was extracted with dichloromethane (3 × 50 mL), washed with saturated NaHCO$_3$ solution (3 × 50 mL) and brine (2 × 50 mL), dried over MgSO$_4$ and evaporated to dryness. If necessary, the crude product was purified by column chromatography.

8.3.9.1.1 Synthesis of 3-benzyl-2-(2-bromoethyl)-3-hydroxy-2,3-dihydro-1H-isoindol-1-one (55) [Experiment 158]
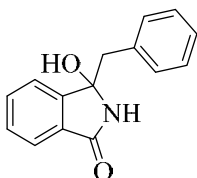
General procedure 17 was followed using 1.09 g of phenylacetic acid, 0.83 g of K$_2$CO$_3$, 0.59 g of phthalimide and 240 mL of acetone/pH 7 buffer (3:1) and a residence time of 40 min. The product precipitated as yellowish solid. After workup, 0.89 g (93%) of product were obtained as a colourless solid.

^{1}H-NMR: (300 MHz, acetone-d$_6$)

δ (ppm): 3.35 (d, J = 12 Hz, 1 H, CH$_2$Ph), 3.42 (d, J = 12 Hz, 1 H, CH$_2$Ph), 5.41 (s, 1 H, COH), 7.01-7.21 (m, 5 H, CH$_{arom}$), 7.31-7.70 (m, 4 H, CH$_{arom}$), 7.87 (s, 1 H, NH).

8.3.9.1.2   3-Benzyl-3-hydroxy-2-methylisoindol-1-one (56) [Experiment 159]
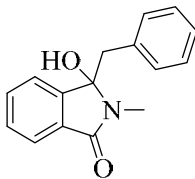
General procedure 17 was followed using 1.09 g of phenylacetic acid, 0.83 g of K_2CO_3, 0.64 g of *N*-methylphthalimide and 240 mL of acetone/pH 7 buffer (3:1) and a residence time of 53 min. The product precipitated as a yellowish solid. After workup, 0.84 g (84%) of product were obtained as a yellowish solid.

Melting point: 129-131°C.

IR: (film)

$\widetilde{v}$ (cm^{-1}) = 3280 br, 1666, 1623, 1450, 1433, 1160, 1069, 789 and 688.

^{1}H-NMR: (400 MHz, CDCl$_3$)

δ (ppm): 2.85 (s, 3 H, NCH$_3$), 3.08 (d, J =12 Hz, 1 H, CH$_2$Ph), 3.45 (d, J = 12 Hz, 1 H, CH$_2$Ph), 3.86 (s, 1 H, OH), 6.85 (dd, J = 3, 9 Hz, 2 H, CH$_{arom}$), 7.05-7.12 (m, 3 H, CH$_{arom}$), 7.25 (d, J = 9 Hz, 1 H, CH$_{arom}$).7.31 (dd, J = 3, 9 Hz, 1 H, CH$_{arom}$), 7.38 (d, J = 9 Hz, 1 H, CH$_{arom}$), 7.45 (ddd, J = 3, 9, 9 Hz, 1 H, CH$_{arom}$).

^{13}C-NMR: (100 MHz, CDCl$_3$)

δ (ppm): 24.2(s, 1 C, NCH$_3$), 42.7 (s, 1 C, CH$_2$), 90.9 (s, 1 C, COH), 123.0 (s, 1 C, OH$_{arom}$), 123.2 (s, 1 C, CH$_{arom}$), 127.3 (s, 1 C, CH$_{arom}$), 128.3 (s, 1 C, CH$_{arom}$),129.8 (s, 1 C, CH$_{arom}$), 130.3 (s, 1 C, CH$_{arom}$), 131.4 (s, 1 C, CH$_{arom}$), 132.0 (s, 1 C, Cq), 134.7 (s, 1 C, Cq), 146.5 (s, 1 C, Cq), 167.4 (s, 1 C, C=O).

8.3.9.1.3   Synthesis of 3-benzyl-2-(2-bromoethyl)-3-hydroxy-2,3-dihydro-1H-isoindol-1-one (37a) and isolation of 9b-benzyl-2,3-dihydro[1,3]oxazolo[2,3-a]isoindol-5(9bH)-one (57) [Experiment 160]
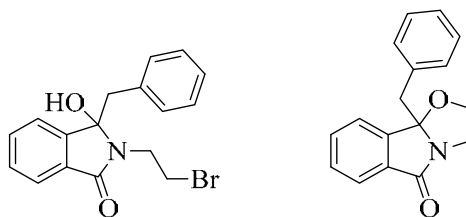
General procedure 17 was followed using 1.09 g of phenylacetic acid, 0.83 g of K_2CO_3, 1.02 g of *N*-bromoethylphthalimide and 240 mL of acetone/pH 7 buffer (3:1) and a residence time of 40 min. The product precipitated as a yellowish solid. After workup and further purification

by column chromatography using 20% EtOAc in cyclohexane as eluent, 1.45 g (74%) of product were obtained as a colourless solid.

3-Benzyl-2-(2-bromoethyl)-3-hydroxy-2,3-dihydro-1H-isoindol-1-one (37a):

^{1}H-NMR: (300 MHz, CDCl$_3$)

Identical to Experiment 63.

9b-Benzyl-2,3-dihydro[1,3]oxazolo[2,3-a]isoindol-5(9bH)-one (57):

^{1}H-NMR: (300 MHz, acetone-d$_6$)

δ (ppm): 3.14 (m, 1 H, NCH$_2$), 3.30 (d, J = 14 Hz, 1 H, CH$_2$Ph), 3.44 (d, J = 14 Hz, 1 H, CH$_2$Ph), 3.98 (dt, 3 H, J = 4, 5 Hz, 2 H, CH$_2$O), 4.17 (m, 1 H, NCH$_2$), 7.12-7.26 (m, 5 H, CH$_{arom}$), 7.47-7.72 (m, 4 H, CH$_{arom}$).

^{13}C-NMR: (75 MHz, acetone-d$_6$)

δ (ppm): 43.4 (t, 1 C, CH$_2$Ph), 44.5 (t, 1 C, NCH$_2$), 71.3 (t,1 C, CH$_2$O), 102.4 (s, 1 C, CqO), 125.2 (d, 1 C, CH$_{arom}$), 125.3 (d, 1 C, CH$_{arom}$), 128.5 (d, 1 C, CH$_{arom}$),129.7 (d, 2 C, CH$_{arom}$),131.9 (d, 1 C, CH$_{arom}$), 132.5 (d, 2 C, CH$_{arom}$),1234.0 (s, 1 C, CHq$_{arom}$), 134.7 (d, 1 C, CHarom), 137.6 (s, 1 C, CHq$_{arom}$), 148.7 (s, 1 C, Cqarom), 174.9 (s, 1 C, C=O).

8.3.9.1.4 Synthesis of 3-benzyl-2-(2-bromoethyl)-3-hydroxy-2,3-dihydro-1H-isoindol-1-one (37a) [Experiment 161]
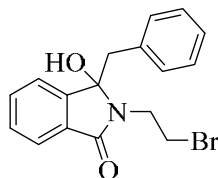
General procedure 17 was followed using 1.09 g of phenylacetic acid, 0.83 g of K$_2$CO$_3$, 1.02 g of *N*-bromoethylphthalimide and 240 mL of acetone/pH 7 buffer (3:1) and a residence time of 40 min. The collection flask was kept in an ice bath to avoid thermal reaction to (**57**). The product precipitated as a yellowish solid. After workup, 1.24 g (86%) of product were obtained as a colourless solid.

^{1}H-NMR: (300 MHz, CDCl$_3$)

Identical to Experiment 63.

8.3.9.1.5 Synthesis of 2-(2-bromoethyl)-3-hydroxy-3-(4-methoxybenzyl)-2,3-dihydro-1H-isoindol-1-one (37e) [Experiment 162]

General procedure 17 was followed using 1.32 g of *p*-methoxyphenylacetic acid, 0.83 g of K$_2$CO$_3$, 1.02 g of *N*-bromoethylphthalimide and 240 mL of acetone/pH 7 buffer (3:1) and a residence time of 40 min. The collection flask was kept in an ice bath to avoid thermal reaction to (**57**). The product precipitated as a yellowish solid. After workup, 2.55 g (83%) of product were obtained as a yellowish solid.

^{1}H-NMR: (300 MHz, CDCl$_3$)

Identical to Experiment 67.

8.3.9.1.6 Synthesis of 4-{[2-(2-bromoethyl)-1-hydroxy-3-oxo-2,3-dihydro-1H-isoindol-1-yl]methyl}phenyl acetate (37q) [Experiment 163]
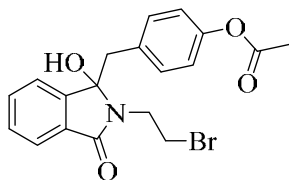
General procedure 17 was followed using 1.43 g of *p*-acetoxyphenylacetic acid, 0.83 g of K$_2$CO$_3$, 1.02 g of *N*-bromoethylphthalimide and 240 mL of acetone/pH 7 buffer (3:1) and a residence time of 40 min. The collection flask was kept in an ice bath to avoid thermal reaction to (**57**). The product precipitated as a yellowish solid. After workup, 2.59 g (80%) of product were obtained as a colourless solid.

^{1}H-NMR: (300 MHz, acetone-d$_6$)

δ (ppm): 2.05 (s, 3 H, CH$_3$), 3.25 (d, J = 14 Hz, 1 H, CH$_2$Ar), 3.44 (d, J = 14 Hz, 1 H, CH$_2$Ar), 3.54 (m, 2 H, CH$_2$Br), 3.73 (ddd, J = 6, 10, 14 Hz, 1 H, NCH$_2$), 3.94 (ddd, J = 6, 10, 14 Hz, 1 H, NCH$_2$), 6.72 (m, 2 H, CH$_{arom}$), 6.83 (m, 2 H, CH$_{arom}$), 7.33 (m, 3 H, CH$_{arom}$), 7.44 (m, 1 H, CH$_{arom}$), not observed (1 H, COH).

^{13}C-NMR: (75 MHz, acetone-d$_6$)

δ (ppm): 21.0 (s, 1 C, CH$_3$), 41.8 (s, 1 C, NCH$_2$), 42.8 (s,1 C, CH$_2$Ar), 91.8 (s, 1 C, COH), 121.9 (s, 2 C, CH$_{arom}$), 123.3 (s, 1 C, Cq), 130.2 (d, 2 C, CH),131.9 (s, 2 C, CH$_{arom}$),132.2 (s, 1 C, CH$_{arom}$), 132.7 (s, 1 C, Cq$_{arom}$),133.5 (s, 1 C, Cq$_{arom}$), 147.7 (s, 1 C, Cq$_{arom}$), 150.4 (s, 1 C, CH$_{arom}$), 167.2 (s, 1 C, O$_2$C), 169.6 (s, 1 C, C=O).

8.3.9.1.7 Synthesis of 3-benzyl-2-(3-bromopropyl)-3-hydroxy-2,3-dihydro-1H-isoindol-1-one (37i) [Experiment 164]
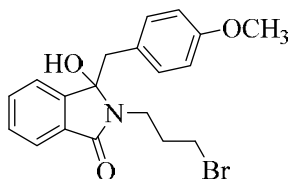
General procedure 17 was followed using 1.09 g phenylacetic acid, 0.83 g of K_2CO_3, 1.07 g of *N*-bromopropylphthalimide and 240 mL of ac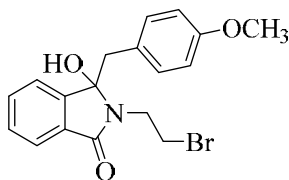etone/pH 7 buffer (3:1) and a residence time of 40 min. The collection flask was kept in an ice bath to avoid thermal cyclization. The product precipitated as a yellowish solid. After workup, 1.48 g (95%) of product were obtained as a colourless solid.

¹H-NMR: (300 MHz, CDCl₃)

Identical to Experiment 71.

8.3.9.2 Solar addition of phenylacetates to *N*-alkylphthalimides under batch conditions

8.3.9.2.1 Attempted synthesis of 3-benzyl-2-(2-bromoethyl)-3-hydroxy-2,3-dihydro-1H-isoindol-1-one (37a) [Experiment 165]
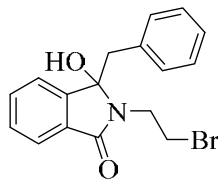
A solution of phenylacetic acid (3 eq.), K_2CO_3 (1.5 eq.) and *N*-bromoethylphthalimide (1 eq.) in acetone/pH 7 buffer (3:1) was exposed to sunlight in a round-bottom flask for 200 min. After usual work-up, the crude product was analyzed by NMR-spectroscopy.

¹H-NMR: (300 MHz, CDCl₃)

No conversion to detectable photoproducts was observed.

8.3.9.2.2 Attempted synthesis of 3-benzyl-2-(2-bromoethyl)-3-hydroxy-2,3-dihydro-1H-isoindol-1-one (37a) [Experiment 166]

A solution of phenylacetic acid (3 eq.), K_2CO_3 (1.5 eq.) and *N*-bromoethylphthalimide (1 eq.) in acetone/pH 7 buffer (3:1) was exposed to sunlight in a Schlenk flask for 200 min. After usual work-up, the crude product was analyzed by NMR-spectroscopy.

¹H-NMR: (300 MHz, CDCl₃)

No conversion to detectable photoproducts was observed.

8.3.9.2.3 Attempted synthesis of 3-benzyl-2-(2-bromoethyl)-3-hydroxy-2,3-dihydro-1H-isoindol-1-one (37a) [Experiment 167]

A solution of phenylacetic acid (3 eq.), K_2CO_3 (1.5 eq.) and *N*-bromoethylphthalimide (1 eq.) in acetone/pH 7 buffer (3:1) was split over two test tubes and exposed to sunlight in a solar float for 200 min. After usual work-up, the crude product was analyzed by NMR-spectroscopy.
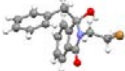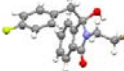
¹H-NMR: (300 MHz, CDCl₃)

No conversion to detectable photoproducts was observed.

8.4 X-ray crystallographic data

X-Ray crystallographic analyses were performed on a Bruker APEX-II CCD diffractometer. Key crystallographic data is compiled in **Table 8.1** [263]. Due to its poor crystallographic data, compound **27** has been excluded. Crystallographic data (excluding structure factors) for **37a**, **37b**, **E-38a** and **Z-39a** have been deposited with the Cambridge Crystallographic Data Centre as supplementary numbers CCDC1417120 (**37a**), CCDC1417119 (**37b**), CCDC1417121 (**E-38a**) and CCDC1417118 (**Z-39a**). Copies of the data can be obtained free of charge on application to CCDC, 12 Union Road, Cambridge, CB2 1EZ, UK (fax: +44 (0)1223 336033; email: deposit@ccdc.cam.ac.uk).

Table 8.1: Key crystallographic data.

Parameter	37a	37b	*E*-38a	*Z*-39a
Formular	$C_{17}H_{16}BrNO_2$	$C_{17}H_{15}BrFNO_2$	$C_{17}H_{14}BrNO$	$C_{21}H_{24}N_2O$
M_w (g/mol)	346.21	364.20	328.19	320.42
a (Å)	22.295(5)	22.456(5)	8.7086(18)	13.7086(19)
b (Å)	9.132(2)	9.0378(18)	8.8445(17)	14.571(2)
c (Å)	16.300(4)	16.536(3)	10.632(2)	19.447(3)
α (°)	90	90	75.519(4)	90
β (°)	104.525(4)	105.133(7)	70.336(4)	107.974(3)
γ (°)	90	90	71.145(4)	90
Volume (Å³)	3212.6(13)	3239.7(11)	720.5(2)	3694.9(9)
Z	8	8	2	8
δ_{calc} (g/cm³)	1.432	1.493	1.513	1.152
Crystal system	Monoclinic	monoclinic	triclinic	monoclinic

Space group	C 2/c	C 2/c	P -1	C 2/c
Reflections collected	3898	3932	3357	4173
Reflections unique	1772	2334	2376	2331
R_1	0.0757	0.0502	0.0462	0.0571
wR_2	0.2540	0.1544	0.1388	0.1654
Goodness of Fit	0.975	1.037	1.041	1.032

Chapter 9:

References

9. References

[1]   H. D. Roth *Ang. Chem. Int. Ed*. **1989**, *28*, 1193.

[2]   H. Trommsdorff *Ann. Chem. Pharm*. **1834**, *11*, 190.

[3]   S. E. Braslavsky *Pure Appl. Chem.* **2007**, *79*, 293.

[4]   J. D. Coyle *Photochemistry in Organic Synthesis*, Royal Society of Chemistry: London, UK, **1986**.

[5]   D. Frackowiak *J. Photochem. Photobiol. B: Biol*. **1988**, *2*, 399.

[6]   D. Rehm, A. Weller *Isr. J. Chem*. **1970**, *8*, 259.

[7]   D. Rehm, A. Weller *Ber. Bunsenges. Phys. Chem*. **1969**, *73*, 834.

[8]   V. Wintgens, P. Valat, J. Kossanyi, L. Biczok, A. Demeter, T. Berces *J. Chem. Soc., Faraday Trans.* **1994**, *90*, 411.

[9]   A. G. Griesbeck, H. Görner *J. Photochem. Photobiol. A: Chem*. **1999**, *129*, 111.

[10]   H. Hayashi, S. Nagakura, Y. Kubo, K. Maruyama *Chem. Phys. Lett.* **1980**, *72*, 291.

[11]   D. W. Leedy, D. L. Muck *J. Am. Chem. Soc*. **1971**, *93*, 4264.

[12]   G. Farnia, A. Romanian, G. Capobianco, F. Torzo *J. Electroanal. Chem*. **1971**, *33*, 31.

[13]   G. Capobianco, G. Farnia, F. Torzo *Ric. Sci*. **1968**, *38*, 842.

[14]   M. Oelgemöller, A. G. Griesbeck, J. Lex, A. Haeuseler, M. Schmittel, M. Niki, D. Hesek, Y. Inoue *Org. Lett*. **2001**, *3*, 1593.

[15]   M. Oelgemöller, A. Haeuseler, M. Schmittel, A. G. Griesbeck, J. Lex, Y. Inoue *J. Chem. Soc., Perkin Trans*. *2* **2002**, 676.

[16]   A. G. Griesbeck, S. Schieffer *Photochem. Photobiol. Sci*. **2003**, *2*, 113.

[17]   L. Biczok, H. Görner *Chem. Phy*. **2012**, *392*, 10.

[18]   Y. Sato, H. Nakai, T. Mizoguchi, M. Kawanishi, Y. Hatanaka, Y. Kanaoka *Chem. Pharm. Bull.* **1982**, *30*, 1262.

[19]   Y. Sato, H. Nakai, T. Mizoguchi, M. Kawanishi, Y. Kanaoka *Chem. Pharm. Bull.* **1973**, *21*, 1164.

[20]   A. Bartoschek, A. G. Griesbeck, M. Oelgemöller *J. Inf. Rec*. **2000**, *25*, 119.

[21]   M. Oelgemöller, A. G. Griesbeck *J. Photochem Photobiol. C: Photochem. Rev*. **2002**, *3*, 109.

[22]   W. Kramer, A. G. Griesbeck, F. Nerowski, M. Oelgemöller *J. Inf. Rec*. **1998**, *24*, 81.

[23]   G. McDermott, D. J. Yoo, M. Oelgemöller *Heterocycles* **2005**, *65*, 2221.

[24]   A. G. Griesbeck, W. Kramer, M. Oelgemöller *Synlett* **1999**, 1169.

[25]   Y. Takahashi, T. Miyashi, U. C. Yoon, S. W. Oh, M. Mancheno, Z. Su, D. F. Falvey, P. S. Mariano *J. Am. Chem. Soc*. **1999**, *121*, 3926.

[26]   U. C. Yoon, D. U. Kim, C. W. Lee, Y. S. Choi, Y.-J. Lee, H. L. Ammon, P. S. Mariano *J. Am. Chem. Soc*. **1995**, *117*, 2698.

[27]   U. C. Yoon, S. W. Oh, S. M. Lee, S. J. Cho, J. Gamlin, P. S. Mariano *J. Org. Chem*. **1999**, *64*, 4411.

[28]   U. C. Yoon, C. W. Lee, S. W. Oh *Tetrahedron* **1999**, *55*, 11997.

[29]   U. C. Yoon, C. W. Lee, S. W. Oh, P. S. Mariano *Tetrahedron* **1999**, *55*, 11997.

[30]   F. Qiu, D. L. Na, F. W. Hai *Sci. China Chem*. **2012**, *55*, 2090.

[31]   D. Budac, P. Wan *J. Photochem. Photobiol. A: Chem.* **1992**, *67*, 135.

[32]   Y. Yoshimi *J. Synth. Org. Chem. Jpn* **2013**, *71*, 935.

[33]   M. Martín-Flesia, A. Postigo *Curr. Org. Chem.* **2012**, *16*, 2379.

[34]   P. Wagner *J. Acc. Chem. Res*. **1983**, *16*, 461.

[35]   A. G. Griesbeck, F. Nerowski, J. Lex *J. Org. Chem*. **1999**, *64*, 5213.

[36]   A. G. Griesbeck, W. Kramer, M. Oelgemöller *Green Chem*. **1999**, *1*, 205.

[37]   M. Sohora, T. S. Ramljak, K. Mlinaric-Majerski, N. Basaric *Croat. Chem. Acta* **2014**, *87*, 431.

[38]   D. J. Yoo, E. Y. Kim, M. Oelgemöller, S. C. Shim *Heterocycles* **2000**, *54*, 1049.

[39]   D. J. Yoo, E. Y. Kim, M. Oelgemöller, S. C. Shim *Photochem. Photobiol. Sci*. **2004**, *3*, 311.

[40]   U. C. Yoon, C. W. Lee, S. W. Oh, H. J. Kim, S. J. Lee *J. Photosci*. **2000**, *7*, 143.

[41]   A. R. Kim, K. Lee, C. Lee, D. J. Yoo, F. Hatoum, M. Oelgemöller *Tetrahedran Lett*. **2005**, *46*, 3395.

[42]   Y. Lee, D. Ahn, K. Lee, A. R. Kim, D. J. Yoo, M. Oelgemöller *Tetrahedran Lett*. **2011**, *52*, 5029.

[43]   A. R. Kim, H. Cho, Y. Lee, D. J. Yoo *Bull. Korean Chem. Soc*. **2012**, *33*, 3477.

[44]   U. C. Yoon, S. J. Lee, S. W. Oh, D. W. Cho *J. Photosci*. **2001**, *8*, 99.

[45]   A. G. Griesbeck, M. Oelgemöller, J. Lex, A. Haeuseler, M. Schmittel *Eur. J. Org. Chem*. **2001**, 1831.

[46]   U. C. Yoon, Y. X. Jin, S. W. Oh, C. H. Park, J. H. Park, C. F. Campana, X. Cai, E. N. Duesler, P. S. Mariano *J. Am. Chem. Soc*. **2003**, *125*, 10664.

[47]   A. G. Griesbeck, T. Heinrich, M. Oelgemöller, A. Molis, A. Heidtmann *Helv. Chem. Acta* **2002**, *85*, 4561.

[48]   A. G. Griesbeck, W. Kramer, T. Heinrich, J. Lex *Photochem. Photobiol. Sci*. **2002**, *1*, 237.

[49]   A. G. Griesbeck, M. Oelgemöller *Synlett* **1999**, 492.

[50]   A. G. Griesbeck, M. Oelgemöller, J. Lex *Synlett* **2000**, 1455.

[51]   A. G. Griesbeck, M. S. Gudipati, J. Hirt, J. Lex, M. Oelgemöller, H. Schmickler, F. Schouren *J. Org. Chem.* **2000**, *65*, 7151.

[52]   A. G. Griesbeck, N. Nazarow, J. M. Neudörfl, M. Heffen *Green Chem.* **2012**, *14*, 3004.

[53]   M. Oelgemöller, P. Cygon, J. Lex, A. G. Griesbeck *Heterocycles* **2003**, *59*, 669.

[54]   A. G. Griesbeck, N. Maptue, S. Bondock, M. Oelgemöller *Photochem. Photobiol. Sci.* **2003**, *2*, 450.

[55]   A. G. Griesbeck, K. Warzecha, J. M. Neudörfl, H. Görner *Synlett* **2004**, 2347.

[56]   F. Hatoum, S. Gallagher, L. Baragwnath, J. Lex, M. Oelgemöller *Tetrahedran Lett.* **2009**, *50*, 6335.

[57]   V. Belluau, P. Noeureuil, E. Ratzke, A. Skvortsov, S. Gallagher, C. A. Motti, M. Oelgemöller *Tetrahedran Lett.* **2010**, *51*, 4738.

[58]   F. Hatoum, J. Engler, C. Zelmer, J. Wißen, C. A. Motti, J. Lex, M. Oelgemöller *Tetrahedran Lett.* **2012**, *53*, 5573.

[59]   S. Gallagher, F. Hatoum, N. Zientek, M. Oelgemöller *Tetrahedran Lett.* **2010**, *51*, 3639.

[60]   F. Hatoum, S. Gallagher, M. Oelgemöller *Tetrahedran Lett.* **2009**, *50*, 6593.

[61]   A. Soldevilla, A. G. Griesbeck *J. Am. Chem. Soc.* **2006**, *128*, 16472.

[62]   A. Soldevilla, R. Perez-Ruiz, Y. D. Miara, A. G. Griesbeck *Chem. Com.* **2010**, 3747.

[63]   K. Gilmore, P. H. Seeberger *Chem. Rec.* **2014**, *14*, 410.

[64]   M. Oelgemöller, N. Hoffmann, O. Shvydkiv *Aust. J. Chem.* **2014**, *67*, 337.

[65]   M. Oelgemöller *Chem. Eng. Technol.* **2012**, *35*, 1144.

[66]   M. Oelgemöller, O. Shvydkiv *Molecules* **2011**, *16*, 7522.

[67]   E. E. Coyle, M. Oelgemöller *Photochem. Photobiol. Sci.* **2008**, *7*, 1313.

[68]   O. Shvydkiv, S. Gallagher, K. Nolan, M. Oelgemöller *Org. Lett.* **2010**, *12*, 5170.

[69]   M. Oelgemöller, S. Gallagher, K. McCarthy *Process.* **2014**, *2*, 158.

[70]   O. Shvydkiv, K. Nolan, M. Oelgemöller *Beilstein J. Org. Chem.* **2011**, *7*, 1055.

[71]   S. Josland, S. Mumtaz, M. Oelgemöller *Chem. Eng. Technol.* **2016**, *39*, 81.

[72]   Y. Yoshimi, A. Nishio, M. Hayashi, T. Morita *J. Photochem. Photobiol. A: Chem.* **2016**, *331*, 17.

[73]   S. Gabriel *Ber. Dtsch Chem. Gesell.* **1887**, *20*, 2224.

[74]   G. Ding, B. Lu, Y. Li, J. Wan, Z. Zhang, X. Xiea *Adv. Synth. Catal.* **2015**, *357*, 1013.

[75]   G. Chen, Y. Wang, X. Hao, S. Mu, Q. Sun *Chem. Central J.* **2011**, *5*, 1

[76]   H. Schiff *Justus Liebigs Ann. Chem.* **1866**, *140*, 92.

[77]   S.-Y. Han, Y.-A. Kim *Tetrahedron* **2004**, *60*, 2447.

[78]   C. A. G. N. Montalbetti, V. Falque *Tetrahedron* **2005**, *61*, 10827.

[79]   Y. Okada *Curr. Org. Chem.* **2001**, *5,* 1.

[80]   T. Nishio, H. Yamamoto *J. Heterocycl. Chem.* **1995**, *32*, 883.

[81]   C. M. Taylor, R. Hardre, P. J. B. Edwards, J. H. Park *Org. Lett.* **2003**, *5*, 4413.

[82]   F. Hatoum, S. Gallagher, L. Baragwanath, J. Lex, M. Oelgemöller *Tetrahedron Lett*. **2009**, *50*, 6335.

[83]   J. Näsman *Org. Synth.* **1993**, *8*, 396.

[84]   F. Braude, H. G. Lindwall *J. Am. Chem. Soc.* **1933**, *55*, 325.

[85]   Q-B. Zhang, W.-L. Jia, Y.-L. Ban, Y. Zheng, Q. Liu, L.-Z. Wu *Chem. Eur. J.* **2016**, *22*, 2595.

[86]   R. K. Harris, E. D. Becker, S. M. Cabral de Menezes, R. Goodfellow, P. Granger *Pure Appl. Chem.* **2001**, *73*, 1795.

[87]   A. A. Vitale, A. E. Stahl, P. C. dos Santos Claro, M. A. F. Addato, R. P. Diez, A. H. Jubert *J. Mol. Struct.* **2008**, *881*, 167.

[88]   V. Belluau, P. Noeureuil, E. Ratzke, A. Skvortsov, S. Gallagher, C. A. Motti, M. Oelgemöller *Tetrahedron Lett*. **2010**, *51*, 4738.

[89]   Y. Jiang, C.-A. Chen, K. Lu, I. Daniewska, J. D. Leon, R. Kong, C. Forray, B. Li, L. G. Hegde, T. D. Wolinsky, D. A. Craig, J. M. Wetzel, K. Anderson, M. R. Marzabadi *J. Med. Chem.* **2007**, *50*, 3870.

[90]   A. Couture, E. Deniau, P. Grandclaudon *Tetrahedron* **1997**, *53*, 10313.

[91]   L. Castedo, E. Guitián, J. M. Saá, R. Suau *Heterocycles* **1982**, *19*, 279.

[92]   S. N. Pandeya, S. Smitha, M. Jyoti, S. K. Sridhar *Acta Pharm.* **2005**, *55*, 27.

[93]   K. Maruyama, K. Kubo *J. Photochem*. **1985**, *28*, 571.

[94]   G. Haucke, B. Seidel, A. Graness *J. Photochem*. **1987**, *37*, 139.

[95]   K. C. Joshi, R. T. Pardasani, A. Dandia, S. Bhagat *Heterocycles* **1991**, *32*, 1491.

[96]   C. Huang, M. Zheng, J. Xu, Y. Zhang *Molecules* **2013***, 18*, 2942.

[97]   M. D. Lainchbury *PhD Thesis*, University of Bristol, **2008**.

[98]   P. J. Wagner *Acc. Chem. Res.* **1983**, *16*, 461.

[99]   C. Galli, L. Mandolini *Eur. J. Org. Chem.* **2000**, 3117.

[100]   L. Capaldo, L. Buzzetti, M. Daniele, F. Maurizio, R. Davide *J. Org. Chem*. **2016**, *81*, 7102.

[101]   M. T. Silva, J. C. Netto-Ferreira *J. Photochem. Photobiol. A*. **2004**, *162*, 225.

[102] H. M. Meshram, N. N. Rao, N. S. Kumar, L. C. Rao *Der Pharma Chemica* **2012**, *4*, 1355.

[103] Q. Ren, J. Huang, L. Wang, W. Li, H. Liu, X. Jiang, J. Wang *ACS Catal.* **2012**, *2*, 2622.

[104] K. Maruyama, Y. Kubo *J. Org. Chem.* **1981**, *46*, 3612.

[105] K. Maruyama, T. Ogawa, Y. Kubo, T. Araki *J. Chem. Soc. Perkin Trans. 1* **1985**, 2025.

[106] D. Majhi, S. K. Das, P. K. Sahu, S. M. Pratik, A. Kumar, M. Sarkar *Phy. Chem. Chem. Phys.* **2014**, *16*, 18349.

[107] D. Noukakis, P. Suppan *J. Luminesc.* **1991**, *47*, 285.

[108] T. G. Kim, M. F. Wolford, M. R. Topp *Photochem. Photobiol. Sci.* **2003**, *2*, 576.

[109] T. Soujanya, R. W. Fessenden, A. Samanta *J. Phys. Chem.* **1996**, *100*, 3507.

[110] E. Krystkowiak, K. Dobek, A. Maciejewski *J. Photochem. Photobiol. A: Chem.* **2006**, *184*, 250.

[111] S. Aich, C. Raha, S. Basu *J. Chem. Soc. Faraday Trans.* **1997**, *93*, 2991.

[112] P. H Mazzochi, S. Minamikawa, M. J. Bowen *J. Org. Chem.* **1978**, *43*, 3079.

[113] A. Maciejewski, E. Krystkowiak, J. Koput, K. Dobek *Chem. Phys. Chem.* **2011**, *12*, 322.

[114] D. M. E. Davies, C. Murray, M. Berry, A. J. Orr-Ewing, K. I. Booker-Milburn *J. Org. Chem.* **2007**, *72*, 1449.

[115] K. Bowden, S. P. Hiscocks, A. Perjessy *J. Chem. Soc. Perkin Trans. 2* **1998**, 291.

[116] S. Wawzonek, H. A. Latinen, S. J. Kwiatkowski *J. Am. Chem. Soc.* **1944**, *66*, 830.

[117] I. R. Hardcastle, J. Liu, E. Valeur, A. Watson, S. U. Ahmed, T. J. Blackburn, K. Bennaceur, W. Clegg, C. Drummond, J. A. Endicott, B. T. Golding, R. J. Griffin, J. Gruber, K. Haggerty, R. W. Harrington, C. Hutton, S. Kemp, X. Lu, J. M. McDonnell, D. R. Newell, M. E. M. Noble, S. L. Payne, C. H. Revill, C. Riedinger, Q. Xu, J. Lunec *J. Med. Chem.* **2011**, *54*, 1233.

[118] A. Dalal, R. Khanna, D. Kumar, P. Jindal, A. Chaudhary, R. C. Kamboj *Curr. Org. Chem.* **2015**, *19*, 2156.

[119] P. J. Wagner *Acc. Chem. Res.* **1971**, *4*, 168.

[120] H. Koshima, M. Fukano, H. Uekusa *J. Org. Chem.* **2007**, *72*, 6786.

[121] K. Fujii, H. Uekusa, M. Fukano, H. Koshima *CrystEngComm* **2011**, *13*, 3197.

[122] U. Pischel, S. Abad, L. R. Domingo, F. Boscá, M. A. Miranda *Angew. Chem. Int. Ed.* **2003**, *42*, 2531.

[123]   F. Boscá, I. Andreu, I. M. Morera, A. Samadi, M. A. Miranda *Chem. Commun.* **2003**, 1592.

[124]   W. Ando, J. Suzuki, T. Migita *Bull. Chem. Soc. Jpn* **1971**, *44*, 1987.

[125]   G. Vermeersch, J. Marko, N. Febvay-Garot, S. Caplain, A. Couture, A. Lablache-Combier *Tetrahedron* **1978**, *34*, 2453.

[126]   A. Lewandowska-Andralojc, F. Kazmierczak, G. L. Hug, G. Hörner, B. Marciniak *Photochem. Photobiol.* **2013**, *89*, 14.

[127]   H.-G. Henning, R. Berlinghoff *Z. Chem.* **1981**, *21*, 150.

[128]   M. Sakamoto, N. Sekine, H. Miyoshi, T. Mino, T. Fujita *J. Am. Chem. Soc.* **2000**, *122*, 10210.

[129]   P. B. Jones, M. P. Pollastri, N. A. Porter *J. Org. Chem.* **1996**, *61*, 9455.

[130]   U. Lindemann, G. Reck, D. Wulff-Molder, P. Wessig *Tetrahedron* **1998**, *54*, 2529.

[131]   C.-E. Liu, Q. Han, N. Ma, Z.-S. Geng, R.-H. Zhang, Z.-Q. Jiang *Tetrahedron. Lett*. **2013**, *54*, 541.

[132]   A. G. Griesbeck, W. Kramer, J. Lex *Angew. Chem. Int. Ed. Engl.* **2001**, *40*, 577.

[133]   A. G. Griesbeck, W. Kramer, J. Lex *Synthesis* **2001**, 1159.

[134]   N. A. Romero, D. A. Nicewicz *Chem. Rev.* **2016**, *116*, 10075.

[135]   K. Nakajima, Y. Miyake, Y. Nishibayashi *Acc. Chem. Res.* **2016**, *49*, 1946.

[136]   J. Hu, J. Wang, T. H. Nguyen, N. Zheng *Beilstein J. Org. Chem.* **2013**, *9,* 1977.

[137]   S. Maity, N. Zheng *Synlett* **2012**, *23*, 1851.

[138]   Y. Miyake, K. Nakajima, Y. Nishibayashi *Chem. Comm*. **2012**, *48*, 6966.

[139]   E. Hasegawa, W. Xu, P. S. Marino, U. C. Yoon, J. U. Kim *J. Am. Chem. Soc*. **1988**, *110*, 8099.

[140]   E. Hasegawa, M. A. Brumfield, P. S. Marino *J. Org. Chem.* **1988**, *53*, 5435.

[141]   Y. T. Jeon, C. P. Lee, P. S. Marino *J. Am. Chem. Soc*. **1991**, *113*, 8847.

[142]   W. Xu, X. M. Zhang, P. S. Marino *J. Am. Chem. Soc*. **1991**, *113*, 8863.

[143]   U. C. Yoon, P. S. Marino *Acc. Chem. Res*. **1992**, *25*, 233.

[144]   Y. Miyake, K. Nakajima, Y. Nishibayashi *Chem. Comm*. **2013**, *49*, 7854.

[145]   A. Millet, Q. Lefebrve, M. Rueping *Chem. Eur. J.* **2016**, *22*, 13464.

[146]   S. Bertrand, N. Hoffmann, S. Humbel, J. P. Pete *J. Org. Chem.* **2000**, *65*, 8690.

[147]   X. Ju, D. Li, W. Li, W. Yu, F. Bian *Adv. Synth. Catal.* **2012**, *354*, 3561.

[148]   J. Tang, G. Grampp, Y. Liu, B.-X. Wang, F.-F. Tao, L.-J. Wang, X.-Z. Liang, H.-Q. Xiao, Y.-M. Shen *J. Org. Chem.* **2015**, *80*, 2724.

[149]   Z. Liang, S. Xu, W. Tian, R. Zhang *Beilstein J. Org. Chem.* **2015**, *11,* 425.

[150]   L. Chen, C. S. Chao, Y. Pan, S. Dong, Y. C. Teo, J. Wang, C.-H. Tan *Org. Biomol. Chem.*, **2013**, *11*, 5922.

[151]   Z. Song, A. P. Antonchick *Tetrahedron* **2016**, *72*, 7715.

[152]   A. K. Yadav, L. D. S. Yadav *Tetrahedron Lett.* **2016**, *57*, 1489.

[153]   D. Lenhart, T. Bach *Beilstein J. Org. Chem.* **2014**, *10*, 890.

[154]   P. Kohs, D. Jadhav, G. Pandey, O. Reiser *Org. Lett.* **2012**, *14*, 672.

[155]   G. H. Lovett, B. A. Sparling *Org. Lett.* **2016**, *18*, 3494.

[156]   D. W. Manley, A. Mills, C. O'Rourke, A. M. Z. Slawin, J. C. Walton *Chem. Eur. J.*, **2014**, *20*, 5492.

[157]   G. Gutenberger, E. Steckhan, S. Blechert *Angew. Chem. Int. Ed.* **1998**, *37*, 660.

[158]   N. Hoffmann *Tetrahedron: Asymm.* **1994**, *5*, 879.

[159]   O. Shvydkiv, A. Yavorskyy, S. B. Tan, K. Nolan, N. Hoffmann, A. Youssef, M. Oelgemöller *Photochem. Photobiol. Sci.* **2011**, *10*, 1399.

[160]   S. Bertrand, N. Hoffmann, J.-P. Pete *Eur. J. Org. Chem.* **2000**, 2227.

[161]   H. Siegermann In: *Techniques of Electroorganic Synthesis*, N. L. Weinberg (Ed.), John Wiley & Sons: New York, United States, **1975**, Vol. V, Part II, pp. 667.

[162]   N. L. Weinberg, H. R. Weinberg *Chem. Rev.* **1968**, *68*, 449.

[163]   L. Chu, C. Ohta, Z. Zuo, D. W. C. MacMillan *J. Am. Chem. Soc.* **2014**, *136*, 10886.

[164]   T. Koike, M. Akita *Synlett* **2013**, *24*, 2492.

[165]   T. Noël, X. Wang, V. Hessel *Chimica Oggi-Chem. Today* **2013**, *31*, 10.

[166]   M. B. Plutschack, C. A. Correia, P. H. Seeberger, K. Gilmore *Top. Organomet. Chem.* **2015**, *57*, 43.

[167]   A. Sugimoto, T. Fukuyama, Y. Sumino, M. Takagi, I. Ryu *Tetrahedron* **2009**, *65*, 1593.

[168]   A. Marsili *EP-0105131A1* **1982**.

[169]   J. D. Coyle, L. R. B. Bryant, J. E. Cragg, J. F. Challiner, E. J. Haws *J. Chem. Soc. Perkin Trans. 1* **1985**, 1177.

[170]   H. Görner, A. G. Griesbeck, T. Heinrich, W. Kramer, M. Oelgemöller *Chem. Eur. J.* **2001**, *7*, 1530.

[171]   H. Yokoi, T. Nakano, W. Fujita, K. Ishiguro, Y. Sawaki *J. Am. Chem. Soc.* **1998**, *120*, 12453.

[172]   D. D. M. Wayner, D. J. McPhee, D. Griller *J. Am. Chem. Soc.* **1988**, *110*, 132.

[173]   A. G. Griesbeck, H. Mauder, I. Müller, E.-M. Peters, K. Peters, H. G. von Schnering *Tetrahedron Lett.* **1993**, *34*, 453.

[174] T. Bousquet, J. F. Fleury, A. Daich, P. Netchitailo *Tetrahedron* **2006**, *62*, 706.

[175] B. E. Torian, L. L. Braun *J. Heterocycl. Chem.* **1984**, *21*, 293.

[176] C. J. Wharton, R. Wrigglesworth *J. Chem. Soc. Perkin Trans. 1* **1985**, 809.

[177] W. S. Ang, B. Halton *Aust. J. Chem.* **1971**, *24*, 851.

[178] T. Heine, C. Corminboeuf, G. Seifert *Chem. Rev.* **2005**, *105*, 3889.

[179] N. Kise, Y. Kawano, T. Sakurai *J. Org. Chem.* **2013**, *78*, 12453.

[180] Y. Chen, J. C. Sabio, R. L. Hartman *J. Flow Chem.* **2015**, *5*, 166.

[181] T. Horie, M. Sumino, T. Tanaka, Y. Matsushita, T. Ichimura, J. Yoshida *Org. Process Res. Dev.* **2010**, *14*, 405.

[182] P. van Male, M. H. J. M. de Croon, R. M. Tiggelaar, A. van den Berg *Internat. J. Heat Mass Transf.* **2004**, *47*, 87.

[183] B. E. Maryanoff, H.-C. Zhang, J. H. Cohen, I. J. Turchi, C. A. Maryanoff *Chem. Rev.* **2004**, *104,* 1431.

[184] L. M. Salonen, M. Ellermann, F. Diederich *Angew. Chem. Int. Ed.* **2011**, *50*, 4808.

[185] D. Webb, T. F. Jamison *Chem. Sci.* **2010***, 1*, 675.

[186] J. A. Glaser *Clean Technol. Environ. Policy* **2013**, *15*, 205.

[187] D. T. McQuade, P. H. Seeberger *J. Org. Chem.* **2013***, 78*, 6384.

[188] S. Fuse, Y. Mifune, N. Tanabe, T. Takahashi *Org. Biomol. Chem.* **2012**, *10*, 5205.

[189] V. D. Pinho, B. Gutmann, C. O. Kappe *RSC Adv.* **2014**, *4*, 37419.

[190] D. H. Drewry, D. M. Coe, S. Poon *Med. Res. Rev.* **1999**, *19*, 97.

[191] J. Eames, M. Watkinson *Eur. J. Org. Chem.* **2001**, 1213.

[192] Y. L. Choi, J. K. Kim, S.-U. Choi, Y.-K. Min, M.-A. Bae, B. T. Kim, J.-N. Heo *Bioorg. Med. Chem. Lett.* **2009**, *19*, 3036.

[193] V. Kumar, Poonam, A. K. Parsad, V. S. Parmar *Nat. Prod. Rep.* **2003**, *20*, 565.

[194] R. J. Olsen, S. R. Pruett *J. Org. Chem.* **1985**, *50*, 5457.

[195] A. Couture, E. Deniau, P. Grandclaudon, H. Rybalko-Rosen, S. Léonce, B. Pfeiffer, P. Renard *Bioorg. Med. Chem. Lett.* **2002**, *12*, 3557.

[196] P. A. Baguley, J. C. Walton *Angew. Chem. Int. Ed.* **1998**, *37*, 3072.

[197] K. B. Jørgensen *Molecules* **2010**, *15*, 4334.

[198] S. J. Blanksby, G. B. Ellison *Acc. Chem. Res.* **2003**, *36*, 255.

[199] L. T. Molina, M. J. Molina, F. S. Rowland *J. Phys. Chem.* **1982**, *86*, 2672.

[200] Y. Kato, M. Takemoto, K. Achiwa *Chem. Pharm. Bull.* **1999**, *44*, 529

[201] G. E. Batley *Anal. Chem.* **1984**, *56*, 2261.

[202] M. Montalti, A. Credi, L. Prodi, M. T. Gandolfi In: *Handbook of Photochemistry – 3rd Edition*, CRC Press: Boca Raton, United States, **2006**, Chapter 11, pp. 583.

[203] M. Oelgemöller *Chem. Rev.* **2016**, *116*, 9664.

[204] Q. Fu In: *Encyclopedia of Atmospheric Sciences*, J. Holton (Ed.), Academic Press: Amsterdam, The Netherlands, **2003**, pp. 1859.

[205] A. Fernández-García, E. Zarza, L. Valenzuela, M. Pérez *Renew. Sustain. Energy Rev.* **2010**, *14*, 1695.

[206] P. Esser, B. Pohlmann, H.-D. Scharf *Angew. Chem. Int. Ed. Engl.* **1994**, *33*, 2009.

[207] A. M. Braun, M. Maurette, E. Oliveros In: *Photochemical Technology*, Wiley: Chichester, UK, **1991**, pp. 148.

[208] (a) H. Harwood *Chem. Rev.* **1962**, *62*, 99. (b) R. H. Vekariya, H. D. Patel *Tetrahedron* **2014**, *70*, 3949.

[209] (a) C. Djerassi *J. Chem. Rev.* **1948**, *43*, 271. (b) R. E. Pearson, J. C. Martin *J. Am. Chem. Soc.* **1963**, *85*, 354.

[210] (a) R. C. Larock In: *Comprehensive Organic Transformations*, 3rd edition, VCH: New York, **1999**, pp 709. (b) A. W. Erin, S. M. Sherif, H. M. Gaber *Molecules* **2003**, *8*, 793. (c) U. Yunus, E. Winterfeldt *J. Chin. Chem. Soc.* **2007**, *54*, 1087. (d) C. Dogo-Isonagie, T. Bekele, S. France, J. Wolfer, A. Weatherwax, A. E. Taggi, D. H. Paull, T. Dudding, T. Lectka *Eur. J. Org. Chem.* **2007**, *7*, 1091.

[211] (a) J. Talegaonkar, S. Mukhija, K. S. Boparai *Talanta* **1982**, *29*, 327. (b) W. Zhang, D. P. Curran, C.H.T. Chen *Tetrahedron Lett.* **2002**, *58*, 3871.

[212] G. Arabaci, X-C Guo, K. D. Beebe, K. M. Coggeshall, D. Pei *J. Am. Chem. Soc.* **1991**, *121*, 5085.

[213] (a) E. W. Garbisch *J. Org. Chem.* **1965**, *30*, 2109. (b) C. Beachdel, D. H. Kalubert *Tetrahedron Lett.* **1998**, *39*, 4987.

[214] L. C. King, G. K. Ostrum *J. Org. Chem.* **1964**, *29*, 3459.

[215] S. J. Pasaribu, L. K. Williams *Aust. J. Chem.* **1973**, *26*, 1327.

[216] S. Kajigaeshi, T. Kakinami, T. Okamoto, S. Fujisaki *Bull. Chem. Soc. Jpn* **1987**, *60*, 1159.

[217] T. A. Salama, Z. Novak *Tetrahedron Lett.* **2011**, *52*, 4026.

[218] L. F. Fieser, M. Fieser In: *Reagents for Organic Synthesis*, John Wiley & Sons: New York, Vol. 1, **1967**, pp. 967.

[219] L. A. Yanovskaya, A. P. Terentev, L. I. Belen *J. Gen. Chem.* **1952**, *22*, 1594.

[220] F. Krohnke, K. Ellegast *Chem. Ber.* **1953**, *86*, 1556.

[221]   (a) J. C. Lee, Y. H. Bae *Synlett* **2003**, 507. (b) J. C. Lee, Y. H. Bae, S.-K. Chang *Bull. Korean. Chem. Soc.* **2003**, *24*, 407. (c) B. Das, K. Venkateswarlu, G. Mahender, I. Mahender *Tetrahedron Lett.* **2005**, *46*, 3041.

[222]   (a) K. Tanemura, T. Suzuki, Y. Nishida, K. Satsumbayashi, T. Horaguchi *Chem. Lett.* **2003**, *32*, 932. (b) A. C. Cope, E. P. Burrows, M. E. Derieg, S. Moon, W. D. Wirth *J. Am. Chem. Soc.* **1965**, *87*, 5452.

[223]   H. Schmid, P. Karrer *Helv. Chim. Acta* **1946**, *29*, 573.

[224]   (a) K. Tanemura, T. Suzuki, Y. Nishida, K. Satsumbayashi, T. Horaguchi *Chem. Commun.* **2004**, 470. (b) C. Ramesh, G. Mahender, N. Ravindranath, B. Das *Tetrahedron Lett.* **2003**, *59*, 1049.

[225]   S. K. Guha, B. Wu, B. S. Kim, W. Bail, S. Koo *Tetrahedron Lett.* **2006**, *47*, 291.

[226]   M. V. Adhikari, S. D. Samanat *Ultrason. Sonochem.* **2002**, *9*, 107.

[227]   S. S. Arbuj, B. Suresh, Waghmode, A. V. Ramaswamy *Tetrahedron Lett.* **2007**, *48*, 1411.

[228]   M. Jereb, M. Zupan, S. Stavber *Helv. Chimica Acta* **2009**, *92*, 555.

[229]   D. Sterk, M. Jukic, Z. Casar *Org. Process Res. Dev.* **2013**, *17*, 145.

[230]   N. Chowdhury, S. Dutta, S. Karthick, A. Anoop, S. Dasgupta, N. D. P. Singh *J. Photochem. Photobiol. B: Biol.* **2012**, *115*, 25.

[231]   D. Cantillo, O. de Frutos, J. A. Rincon, C. Mateos, O. Kappe *J. Org. Chem.* **2014**, *79*, 223.

[232]   S. Deshpande, B. Gadilohar, Y. Shinde, D. Pinjari, A. Pandit, G. Shankarling *Solar Energy* **2015**, *113*, 332.

[233]   S. Shimizu, Y. Imamura, T. Ueki *Org. Process Res. Dev.* **2014**, *18*, 354.

[234]   (a) F. L. Lambert, W. D. Ellis, R. Parry *J. Org. Chem.* **1965**, *30*, 304. (b) M. D. Carr, B. D. England *Proc. Chem. Soc.* **1958**, 350.

[235]   X.-Y. Guan, Z. Al-Misba'a, K. Huang *Arab. J. Chem.* **2015**, *8*, 892.

[236]   R. Becker, S. A. M. W. van den Broek, P. J. Nieuwland, K. Koch, F. P. J. T. Rutjes *J. Flow. Chem.* **2012**, *2*, 87.

[237]   S. Mayadevi *Indian J. Chem.* **2012**, *51A*, 1298.

[238]   Y. Nishiyama, K. Nakatani, H. Tanimoto, T. Morimoto, K. Kakiuchi *J. Org. Chem.* **2013**, *78*, 7186.

[239]   Y. Nishiyama, R. Mori, K. Nishida, H. Tanimoto, T. Morimoto, K. Kakiuchi *J. Flow Chem.* **2014**, *4*, 184.

[240]   A. Smakula *Z. Phy. Chem.* **1934**, *B25*, 90.

[241]   R. E. Buckles *J. Am. Chem. Soc.* **1955**, *77*, 1040.

[242] F. B. Mallory, C. S. Wood, J. T. Gordon *J. Am. Chem. Soc.* **1964**, *86*, 3094.

[243] F. B. Mallory, C. S. Wood *J. Org. Chem.* **1964**, *29*, 3374.

[244] F. B. Mallory, C. W. Mallory *Org. Reac.* **1984**, *30*, 1.

[245] W. H. Laarhoven *Rec. Trav. Chim. - J. Royal Netherl. Chem.* **1983**, *102*, 185.

[246] S. Hagen, H. Hopf In *Modern Routes to Extended Aromatic Compounds (Carbon Rich Compounds I)*, Springer-Verlag: Berlin, Germany, **1998**, Vol. 196, pp. 45.

[247] H. Meier *Angew. Chem. Int. Ed. Eng.* **1992**, *31*, 1399.

[248] Y. Tominaga, R. N. Castle *J. Heterocycl. Chem.* **1996**, *33*, 523.

[249] W. H. Laarhoven *Org. Photochem.* **1989**, *10*, 163.

[250] T. Mori, Y. Inoue *Mol. Supramol. Photochem.* **2005**, *12*, 417.

[251] R. I. Duclos Jr., J. S. Tung, H. Rapoport *J. Org. Chem.* **1984**, *49*, 5243.

[252] L. Liu, B. Yang, T. J. Katz, M. K. Poindexter *J. Org. Chem.* **1991**, *56*, 3769.

[253] A. Sudhakar, T. J. Katz *Tetrahedron Lett.* **1986**, *27*, 2231.

[254] A. Sudhakar, T. J. Katz, B. Yang *J. Am. Chem. Soc.* **1986**, *108*, 2790.

[255] F. B. Mallory, M. J. Rudolph, S. M. Oh *J. Org. Chem.* **1989**, *54*, 4619.

[256] M. Scholz, M. Mühlstädt, F. Dietz *Tetrahedron Lett.* **1967**, *8*, 665.

[257] Q. Lefebvre, M. Jentsch, M. Rueping *Beilstein J. Org. Chem.* **2013**, *9*, 1883.

[258] H. Okamoto, T. Takane, S. Gohda, Y. Kubozono, K. Sato, M. Yamaji, K. Satake *Chem. Lett.* **2014**, *43*, 994.

[259] M. Montalti, A. Credi, L. Prodi, M. T. Gandolfi In: *Handbook of Photochemistry – 3rd Edition*, CRC Press: Boca Raton, United States, **2006**, Chapter 3, pp. 83.

[260] K. Terao, Y. Nishiyama, S. Aida, H. Tanimoto, T. Morimoto, K. Kakiuchi *J. Photochem. Photobiol. A: Chem.* **2012**, *242*, 13.

[261] H. E. Gottlieb, V. Kotlyar, A. Nudelman *J. Org. Chem.* **1997**, *62*, 7512.

[262] A. A. Avetisyan, G. S. Melikyan, M. T. Dangyan *Armyanskii Khim. Zh.* **1971**, *24*, 1087.

[263] H. D. Flack *Acta Cryst. A* **1983**, *39*, 876.